

Downstream Fining of Sediments in the Meuse River

Rafael Eduardo Murillo-Muñoz

M.Sc. Thesis H.H. 341

May 1998

International Institute for Infrastructural
Hydraulic and Environmental Engineering

Hydraulic Engineering Department

Downstream Fining of Sediments in the Meuse River

Thesis submitted as a partial fulfilment
of the requirements for the degree of
Master of Science
in Hydraulic Engineering

By

Rafael Eduardo Murillo-Muñoz

Delft, The Netherlands
May, 1998

*To those who have
always given me their hands:*

My parents.

Examination Committee

Prof. Bela Petry

*International Institute for
Infrastructural, Hydraulic and
Environmental Engineering*

Ir. H. Don Duizendstra

*Rijkswaterstaat,
RIZA, River Department,
Arnhem, The Netherlands*

Ir. Gerrit J. Klaassen

*International Institute for
Infrastructural, Hydraulic and
Environmental Engineering*

Murillo-Muñoz, R. E. (1998). **Downstream Fining of Sediments in the Meuse River.** MSc thesis, N°. HH 341. International Institute for Infrastructural, Hydraulic and Environmental Engineering. 146 p, 70 Fig, 211 Ref.

Abstract

The Meuse River (Maas River), the second largest river in The Netherlands, enters the country as a gravel-bed river. Near the city of Roermond, in the so-called Roer Graben, an area where tectonics is known to be active, the river shows a sharp transition from a gravel-bed river with pronounced armouring to a sand-bed river with bedforms. During this transition the D_{50} of the bed material changes from about 16 to about 2.6 millimetres whilst the bed slope also decreases from about 0.48 to 0.10 m/km. Until now the cause of this transition is not known. The present study attempts to explain this gravel-sand transition by studying the different phenomena that can play a role. The following possible causes can be listed: i) abrasion and breakdown of the bed material particles; ii) vertical tectonic movements (uplift and subsidence) which will induce longitudinal sorting of the bed material within the Roer Graben Rift system; iii) the presence of ancient deposits; and iv) the input of fine sediments from a smaller tributary. The latter two were considered to be of minor importance.

To study the different phenomena it was necessary to link the prototype information on the present river characteristics to the limited available geological information of the area. In the first phase of the study a substantial effort was put in the elaboration of field data, whereby information on both changes in bed material (particle distribution and mineralogy) along the river and the sediment transport rates were collected, analysed and critically assessed. Also the available information on the geology of the region and on tectonic activity like subsidence was reviewed in this phase.

In a next phase the relevance of the different possible explanations was assessed. Abrasion rates for the different minerals were determined and an estimate of their importance was made. Also the effect of the subsidence and the induced deposition on sediment transport rates, longitudinal sorting and on the particle distribution was assessed. Moreover a numerical (1D morphological) model developed by Cui and Parker (1998) was used to verify the conclusions of the first assessment more quantitatively. Although the model is not completely applicable to the Meuse River, it provided additional support for the conclusions of the study.

From the study of the available field data and the tectonics of the region, the initial assessment and the numerical simulation of the different process involved, it is concluded that the subsidence in the Roer Graben provides an adequate environment of deposition triggering the selective transport of particles causing the coarse material to settle preferentially. The combined action of the selective transport and the abrasion of sandstone results in an increase of the sand content of the bed material in downstream direction. After some distance a threshold point is reached where the sand content starts to govern the behaviour of the sediment mixture. In combination this causes that the sand “overwhelms” the gravel and the river starts to behave as a sand-bed river; consequently the gravel-sand transition is formed.

The improved understanding of the morphological behaviour of the Meuse River and the possible explanation of the sharp transition, allowed to formulate some implications for future field data collection and for numerical modelling of the morphology of the complicated reach of the Meuse River where the transition takes place. It is clear however that the extensive human interference with the river in the 19th and 20th century (normalisation, reservoirs, barrages, and gravel mining) in combination with the complicated geological conditions in the area will never allow for a full understanding of the morphological behaviour of the river.

Key words: DOWNSTREAM FINING; MEUSE RIVER; SEDIMENTS; SELECTIVE TRANSPORT; ABRASION; SUBSIDENCE; NEOTECTONICS

Acknowledgements

Many people should be mentioned here, but it is hardly impossible to list all of them. Nevertheless, I am indebted by the constructive comments and help that H.D. Duizendstra (RIZA, The Netherlands) gave during the development of the project. I am also indebted to G.J. Klaassen (I.H.E, The Netherlands), because he gave the opportunity to work in this study and for supervise me during the project.

I would like to thank B. Petry (I.H.E) for the encouragement that he gave me during all my MSc. studies and E. Alaniz (National University of Cordoba, Argentina) because she gave me a strong support during my live in Delft; I will always remember it, many thanks.

I also want to express my gratitude to J.H. Van den Berg (Utrecht University, The Netherlands); E. Mosselman (Delft Hydraulics, The Netherlands) and Y. Kodama (Tottori University, Japan). Their comments and suggestions during the different phases of the study were timely and stimulating.

The use of the model Acronym5 was possible thanks to G. Parker and Y. Cui (St. Anthony Falls Laboratory, U.S.A.). They provided me with the model and related information, thanks to both of you.

I would also like to thank to the Civil Engineering Department of the University of Costa Rica for the support they gave me. I must mention also R. Oreamuno (DHICA, Costa Rica) for the encouragement he gave. I still hope to see you in the next generation of the Universe!.

Finally I would like to thank to H. Ikeda (University of Tsukuba, Japan); J. Gerretsen (Rijkswaterstaat, The Netherlands); T. Camelbeeck (Royal Observatory of Belgium); A.W. Burger and M.W. Van den Berg (Geological Survey of The Netherlands) and H.J.A. Berendsen (Utrecht University, The Netherlands). They provided me valuable information without which this study would not be completed successfully.

Many thanks to all of you.

This study was funded by the Ministry of Transport, Public Works and Water Management of the Netherlands (Directorate Limburg, Rijkswaterstaat), and administer through the Institute for Inland Water Management and Waste Water Treatment (RIZA). This study was carried out at the International Institute for Infrastructural, Hydraulic and Environmental Engineering (I.H.E.), Delft, The Netherlands.

*Rivers never forget,
sooner or later
we would have to pay back.*

Table of contents

| | |
|---|------|
| Abstract | i |
| Acknowledgements | ii |
| Table of contents | iii |
| List of figures | vii |
| List of tables | xi |
| List of symbols | xiii |
| | |
| Chapter 1 | |
| General description | 1 |
| 1.1 Introduction | 1 |
| 1.2 Problem description | 1 |
| 1.3 Justification of the study | 1 |
| 1.4 Objectives of the study | 2 |
| 1.5 Methodology | 2 |
| 1.6 Structure of the report | 3 |
| | |
| Chapter 2 | |
| Characteristics of the Meuse River Basin | 5 |
| 2.1 Introduction | 5 |
| 2.2 Catchment of the Meuse River | 5 |
| 2.3 Geology of the region | 5 |
| 2.3.1 <i>Geological setting of the region</i> | 5 |
| 2.3.2 <i>Tectonic of the region</i> | 8 |
| 2.3.3 <i>Sediments deposits of the Rhine River within the Roer Graben</i> | 10 |
| 2.3.4 <i>Geological conditions along the Meuse River</i> | 10 |
| 2.4 Hydrological conditions | 13 |
| 2.5 Morphology of the Meuse River | 14 |
| 2.5.1 <i>Geological times</i> | 14 |
| 2.5.2 <i>Present conditions</i> | 16 |
| 2.6 Human impact on the Meuse River | 19 |
| | |
| Chapter 3 | |
| Downstream fining with sediment mixtures | 25 |
| 3.1 Introduction | 25 |
| 3.2 Some observation on downstream fining | 25 |
| 3.3 Unsteady sediment transport within uniform material | 26 |

| | |
|---|----|
| Chapter 3 | |
| Downstream fining with sediment mixtures (continuation) | |
| 3.4 Abrasion process | 27 |
| 3.4.1 <i>Mechanisms of abrasion</i> | 27 |
| 3.4.2 <i>Laboratory experiments</i> | 28 |
| 3.4.3 <i>Mathematical description</i> | 32 |
| 3.5 Subsidence | 33 |
| 3.6 Selective transport of particles and exchange with the river | 36 |
| 3.7 Modelling of sediment mixtures | 37 |
| | |
| Chapter 4 | |
| Analysis of the bed material and sediment transport rates | 39 |
| 4.1 Introduction | 39 |
| 4.2 Bed material characterisation | 39 |
| 4.2.1 <i>Representatively of characteristic parameters</i> | 39 |
| 4.2.2 <i>Characteristic parameters</i> | 41 |
| 4.2.3 <i>Armour layer and substratum composition</i> | 42 |
| 4.2.4 <i>Bimodal composition of the bed material</i> | 44 |
| 4.2.5 <i>Median diameter of the bed material</i> | 45 |
| 4.2.6 <i>Gravel-sand content of the sediments</i> | 46 |
| 4.3 Sediment transport rates in the Meuse River | 47 |
| 4.3.1 <i>Bed level and bed slope in the Meuse River</i> | 48 |
| 4.3.3 <i>Sediment transport rates in the gravel-bed reach</i> | 50 |
| 4.3.4 <i>Sediment transport rates in the sandy-bed reach</i> | 57 |
| 4.3.5 <i>Comparison of gravel-bed and sandy-bed reach</i> | 59 |
| 4.3.6 <i>Dimensionless sediment transport rates in the Meuse River</i> | 60 |
| 4.3.7 <i>Discussion</i> | 62 |
| | |
| Chapter 5 | |
| Causes of downstream fining in the Meuse River and their contributions | 63 |
| 5.1 Introduction | 63 |
| 5.2 Causes of downstream fining in the Meuse River | 63 |
| 5.3 Relevance of the abrasion process | 65 |
| 5.3.1 <i>Characteristic particles</i> | 66 |
| 5.3.1.1 <i>Van Straaten's work</i> | 66 |
| 5.3.1.2 <i>Interpretation of the mineralogical information</i> | 67 |
| 5.3.2 <i>Assessment of the abrasion process</i> | 69 |
| 5.3.3 <i>Break down of particles</i> | 70 |

| | |
|---|-----|
| Chapter 5 | |
| Factors of downstream fining in the Meuse River and its contributions (continuation) | |
| 5.4 Relevance of the tectonic movements - simplified approach | 72 |
| 5.4.1 <i>Assessment of the relative importance</i> | 72 |
| 5.4.2 <i>Deposition width</i> | 76 |
| 5.5 Relevance of tectonic movements – using selective transport | 77 |
| 5.6 Relevance of the ancient deposits and the Roer River | 80 |
| 5.7 Change in bed slope | 80 |
| | |
| Chapter 6 | |
| Numerical modelling of the downstream fining of sediments | 83 |
| 6.1 Introduction | 83 |
| 6.2 Selection of the model | 83 |
| 6.3 The selected numerical model | 84 |
| 6.4 Results of the simulation | 85 |
| 6.4.1 <i>Model schematisation</i> | 85 |
| 6.4.2 <i>Results of the simulation</i> | 86 |
| 6.5 Sensitivity analysis | 88 |
| 6.6 Effect of river training in the 19 th century | 91 |
| | |
| Chapter 7 | |
| Discussion and implications of the results | 93 |
| 7.1 Introduction | 93 |
| 7.2 Limitations of the available field data | 93 |
| 7.3 On the cause of the downstream fining in the Meuse River | 94 |
| 7.4 On the used numerical modeld (Acronym5) | 97 |
| 7.5 Implications for collection of field data | 98 |
| 7.6 Implications for the morphological modelling of the Meuse River | 99 |
| | |
| Chapter 8 | |
| Conclusions and recommendations | 101 |
| 8.1 Conclusions | 101 |
| 8.2 Recommendations | 103 |
| | |
| Bibliography | 105 |

**Table of contents
(continuation)**

| | |
|--|-----|
| Appendix 1 | |
| Mathematical description of the abrasion process | 117 |
| Appendix 2 | |
| Some sediment predictor for mixtures of sediments | 127 |
| Appendix 3 | |
| Armour layer and substratum composition | 133 |
| Appendix 4 | |
| Bimodal composition of the bed material | 137 |
| Appendix 5 | |
| Variability of the D_m and D_{50} and D_m/D_{50} of sediments with bimodal composition | 143 |

List of figures

Figure

| | |
|---|----|
| 2.1 A). Catchment area of the Meuse River | 6 |
| B.) River chainage in Limburg province | 7 |
| 2.2 Geological setting of the area | 5 |
| 2.3 Classification of the different blocks | 8 |
| 2.4 Vertical velocities estimated in cm per century (cm/cy) | 9 |
| 2.5 Geological profile along the Meuse River | 11 |
| 2.6 Approximately vertical displacement rates (in mm/y) along the Meuse River | 12 |
| 2.7 Temporal distribution of discharges in the Meuse River at Borgharen | 13 |
| 2.8 Flow duration curve at Borgharen for the period 1911-1997 | 13 |
| 2.9 Geomorphological map of the Meuse Valley | 17 |
| 2.10 Planform of the Meuse River near Grevenbicht in 1849 (left) and 1905 (right) | 21 |
| 3.1 Roundness against distance of travel on a pebbly floor | 30 |
| 3.2 Loss of weight against roundness on a pebbly floor | 30 |
| 3.3 Abrasion weight losses for monolithologic clast populations | 31 |
| 3.4 Definition sketch for sediment conservation including tectonic movements | 34 |
| 3.5 Morphological effect of vertical tectonic movements | 35 |
| 3.6 Definition sketch for the three layers model | 37 |
| 4.1 Variation of the substratum in the Meuse River | 40 |
| 4.2 Variation of D_{50} (in mm) in the substratum along the Meuse River | 42 |
| 4.3 Geometric standard deviation of the substratum samples in the Meuse River | 43 |
| 4.4 Development of the bimodal composition in the bed material (substratum) | 44 |
| 4.5 Change in granulometric curves of the bed material in downstream direction | 45 |
| 4.6 Median diameter of the substratum material | 45 |
| 4.7 Gravel and sand content along the Meuse River | 46 |
| 4.8 Spatial variation of the D_{16} , the D_{50} and the D_{84} | 47 |

List of figures (continuation)

Figure

| | | |
|------|--|----|
| 4.9 | Average (minimal) sediment transport rates in the Meuse River | 48 |
| 4.10 | Thalweg elevation along the Meuse River | 49 |
| 4.11 | Trend of the thalweg elevation along the Meuse River | 50 |
| 4.12 | Frequency distribution of discharges at Borgharen for the period 1911-1997 | 54 |
| 4.13 | Sediment transport in function of the discharge | 54 |
| 4.14 | Relation between sediment transport and discharge | 54 |
| 4.15 | Average granulometric curves used in the tests for the gravel-bed reach | 56 |
| 4.16 | Results using MPM with hiding coefficient and the average grain size distribution of the substratum material for the gravel-bed reach | 56 |
| 4.17 | Results using the surface based predictor of Parker and an average grain size distribution of the armour layer for the gravel-bed reach | 56 |
| 4.18 | Frequency distribution of discharges at Borgharen for the period 1911-1997 | 58 |
| 4.19 | Sediment transport rate (MPM) as function of the discharge for the sandy-bed reach | 58 |
| 4.20 | Relation between sediment transport and discharge for the sandy bed reach | 58 |
| 4.21 | Average granulometric curve used in the tests for the sandy-bed reach | 57 |
| 4.22 | Results using MPM with hiding coefficient and the average grain size distribution of the substratum material for the sandy | 57 |
| 4.23 | Comparison of the sediment load in the gravel-bed and sandy-bed reach | 59 |
| 4.24 | Dimensionless results using MPM with hiding coefficient and the average grain size distribution of the substratum material for the gravel-bed reach | 61 |
| 4.25 | Dimensionless results using the surface based predictor of Parker and the average grain size distribution of the armour layer for the gravel-bed reach | 61 |
| 4.26 | Dimensionless results using MPM with hiding coefficient and the average grain size distribution of the substratum material for the sandy-bed reach | 61 |
| 4.27 | Dimensionless results in the Meuse River | 62 |
| 5.1 | Distribution of rock groups (in percentage) by size fraction according to Van Straaten (1946) | 68 |
| 5.2 | Distribution of the minerals groups along the river | 69 |

List of figures (continuation)

Figure

| | | |
|------|---|----|
| 5.3 | Fragmentation load cumulative curves of Moss' results | 71 |
| 5.4 | Summary of abrasion properties of andesite and chert particles | 72 |
| 5.5 | Definition sketch for the mass balance of sediments | 72 |
| 5.6 | Schematic representation of the influence of subsidence rates | 73 |
| 5.7 | Granulometric composition of the bed material at different locations, $B_d = 750$ m and $S_{t,u} = 35 \times 10^3$ m ³ /y | 74 |
| 5.8 | Granulometric composition of the bed material at km 110; $S_{t,u} = 35 \times 10^3$ m ³ /y. Original curve from Grevenbicht | 75 |
| 5.9 | Accumulated frequency distribution of occurrence of the D50 for different values of deposition width | 76 |
| 5.10 | Schematisation of wave-like aggradation of self-preserving form | 78 |
| 5.11 | Variation of the D_{50} in the bed material for a wave speed of 3.0 m/y | 80 |
| 5.12 | Relation between sediment load and bed slope in the sandy reach | 82 |
| 6.1 | Scheme of the model used in the simulations | 85 |
| 6.2 | Variation of the median diameter of the substratum according to the simulation | 86 |
| 6.3 | Water surface, bed elevation and Froude number computed | 87 |
| 6.4 | Channel bed slope (in m/km) | 87 |
| 6.5 | Gravel and sand transport rates (in m ² /s) | 87 |
| 6.6 | Effects on the D_m (substratum) due to variation in subsidence rate | 88 |
| 6.7 | Variation on the D_m (substratum) due to changes in sediment load | 89 |
| 6.8 | Influence of the deposition width in the values of D_m (substratum) | 89 |
| 6.9 | Variation of D_m (substratum) for different abrasion coefficient (β^*) | 89 |
| 6.10 | Changes in D_m due to changes in the hiding exponent (η) of the surface based sediment predictor of Parker (1990) | 90 |
| 6.11 | Sensitivity of the model to changes in the water discharge | 91 |
| 6.12 | Variation of the D_m (substratum) for the current conditions of the deposition width ($B_d = 100$ metres) | 91 |

**List of figures
(continuation)**

Figure

| | |
|--|----|
| 7.1 Changes in mobility, dune profiles and sedimentary structures as functions of the sand: gravel ratio of bed-load | 95 |
| 7.2 Trend of the bed slope at the beginning of the 19 th century | 96 |
| 7.3 Grain size distribution of the substratum at different depths | 96 |

List of tables

Table

| | | |
|-----|---|----|
| 2.1 | Average vertical displacement due to tectonics in the area of study | 10 |
| 2.2 | Main geological characteristics along the Dutch reach of the Meuse River | 12 |
| 2.3 | Summary of the geomorphological-sedimentary changes and their ages in the Meuse basin at the transition from Wichselian Pleniglacial to the Holocene | 15 |
| 2.4 | Values of sinuosity for two different periods of time | 19 |
| 2.5 | Bank erosion rates in the Meuse River | 19 |
| 2.6 | Overview of human activities that have affected the Meuse River | 20 |
| 2.7 | Some characteristic of the reservoirs in the tributaries of the Meuse River | 22 |
| 2.8 | Catchment area of the Meuse River for some locations along the river | 22 |
| 3.1 | Main features of gravel-sand transitions in some rivers | 25 |
| 3.2 | Abrasion of pebbles: summary of its nature and rounding effects processes | 29 |
| 3.3 | Abrasion durability scale | 31 |
| 3.4 | Value of the coefficient β^* in percentage per kilometre | 33 |
| 4.1 | Sources of field data | 41 |
| 4.2 | Values of D_{50} (in mm) of the armour layer and substratum at different locations | 44 |
| 4.3 | Comparison between bed-load measurements and predicted values | 52 |
| 4.4 | Values of discharges and sediment load at different percentiles of time | 53 |
| 4.5 | Comparison of the sediment transport rates in the Meuse River according to MPM predictor | 60 |
| 5.1 | Effects of the different factors in the characteristics of the Meuse River | 64 |
| 5.2 | Fraction by grain size used by Van Straaten (1946) | 66 |
| 5.3 | Location of the samples | 67 |
| 5.4 | Probable rock fragments present in the Meuse deposits according to different approaches | 69 |
| 5.5 | Rates of subsidence considered in the analysis | 74 |

**List of tables
(continuation)**

Table

| | |
|--|----|
| 5.6 Predicted values of D_{50} at km 110 using the simplified approach for different deposition widths and $S_{t,u} = 35 \times 10^3 \text{ m}^3/\text{y}$ | 75 |
| 5.7 Values of D_{50} at km 110 for different wave speed | 79 |
| 6.1 Characteristics of the models | 83 |
| 7.1 Characteristic of the transitions in the Meuse River | 93 |

List of symbols

| | | |
|---------------|--|-----------------------------|
| \tilde{A}_j | : abrasion rate for the grain size j ; | $[\text{m}^3/\text{sm}^2]$ |
| A_j | : coefficient of Ackers and White predictor; | [-] |
| a | : meander amplitude; | [m] |
| B | : channel width; | [m] |
| B_b | : bank-full width; | [m] |
| B_c | : channel width in Acronym5 model; | [m] |
| B_d | : deposition width; | [m] |
| B_v | : valley width; | [m] |
| C | : Chézy coefficient; | $[\text{m}^{1/2}/\text{s}]$ |
| C_g | : grain roughness; | $[\text{m}^{1/2}/\text{s}]$ |
| C_j | : coefficient of Ackers and White predictor; | [-] |
| D | : grain size in terms of equivalent diameter ($D = 2^{-\phi}$); | [m] |
| D_a | : can be the average grain size for which no exposure correction is necessary, or the grain size of the mixture which no needs no correction; | [m] |
| D_c | : cut-off grain size; | [m] |
| D_{gr} | : coefficient of Ackers and White predictor; | [-] |
| D_j | : characteristic grain size of size fraction j ; | [m] |
| D_m | : geometric mean diameter; | [m] |
| D_{mf} | : geometric mean diameter of the sediment load; | [m] |
| D_{mp} | : geometric mean diameter of the surface layer; | [m] |
| D_o | : coefficient of Ackers and White predictor; | [-] |
| D_{35} | : particle size at which 35% of the particles are smaller than D_{35} ; | [-] |
| D_{50} | : particle size at which 50% of the particles are smaller than D_{50} ; | [m] |
| D_{90} | : particle size at which 90% of the particles are smaller than D_{90} ; | [m] |
| F_{ae} | : equivalent areal content density of grains exposed on surface; | $[\text{m}^2]$ |
| F_{gr} | : mobility number; | [-] |
| f_j | : percentage of the size fraction j available in the bed load; | [-] |
| $G(\chi)$ | : function of the surface based predictor of Parker; | [-] |
| G_j | : dimensionless transport rate; | [-] |
| g | : acceleration due to gravity; | $[\text{m}^2/\text{s}^2]$ |
| h | : mean water depth; | [m] |
| I | : fraction of time of any given year; | [-] |
| i | : mean slope of energy; | [m/m] |
| i_b | : mean slope of the river bed; | [m/m] |
| j | : size fraction; | [-] |
| L_a | : thickness of the active layer; | [m] |
| m | : empirical coefficient for the sediment transport formula; | [-] |
| m_j | : exponent of Ackers and White predictor; | [-] |
| n | : empirical exponent for the sediment transport formula; | [-] |
| n_j | : exponent of Ackers and White predictor; | [-] |
| p_j | : percentage of the size fraction j available in the active layer; | [-] |
| p_{oj} | : percentage of the size fraction j available in the substratum; | [-] |
| p_{jo} | : percentage of the size fraction j in the interface; | [-] |
| Q_b | : bank-full discharge; | $[\text{m}^3/\text{s}]$ |
| q | : water discharge per unit width; | $[\text{m}^2/\text{s}]$ |
| R | : hydraulic radius; | [m] |
| \tilde{S} | : sinuosity of the channel; | [-] |
| S_t | : bed material transport (including both bed and suspended load); | $[\text{m}^3/\text{s}]$ |
| $S_{t,d}$ | : downstream sediment transport; | $[\text{m}^3/\text{s}]$ |

**List of symbols
(continuation)**

| | | |
|-------------------|--|------------|
| $S_{t,u}$ | : upstream sediment transport; | $[m^3/s]$ |
| S_b | : volume bed-load transport rate/width/time; | $[m^2/s]$ |
| S_{bj} | : bed-load transport for the size fraction j per unit of width; | $[m^2/s]$ |
| S_t | : total sediment transport per unit width (bed and suspended load); | $[m^2/s]$ |
| S_{tj} | : total sediment transport per unit width in the grain fraction j ; | $[m^2/s]$ |
| t | : time coordinate; | $[s]$ |
| u | : mean water velocity; | $[m/s]$ |
| u^* | : shear velocity; | $[m/s]$ |
| V | : volume of material deposited; | $[m^3]$ |
| W^* | : dimensionless bed-load of Parker and Klingeman predictor; | $[-]$ |
| w | : straining parameter; | $[-]$ |
| w_o | : parameter of the surface based predictor of Parker; | $[-]$ |
| x | : coordinate in flow direction; | $[m]$ |
| z_b | : bed level above some datum of reference; | $[m]$ |
| z_o | : thickness of the substratum layer; | $[m]$ |
| α | : coefficient; | $[-]$ |
| β^* | : particle abrasion coefficient; | $[m^{-1}]$ |
| χ | : dummy variable; | $[-]$ |
| Γ | : elevation of a material line of the earth's crust directly underneath the river; | $[m]$ |
| Δ | : submerged specific density of the gravel; | $[-]$ |
| Δt | : interval of time; | $[s]$ |
| Δx | : length of the reach; | $[m]$ |
| Δz_d | : thickness of deposition layer; | $[m]$ |
| ε | : porosity of the bed material; | $[-]$ |
| ξ_j | : hiding coefficient; | $[-]$ |
| η | : exponent; | $[-]$ |
| φ_{op} | : dimensionless shear stress in the surface based predictor of Parker; | $[-]$ |
| μ | : ripple factor; | $[-]$ |
| ν | : kinematic viscosity of the water; | $[m^2/s]$ |
| θ_s | : Shields parameter in the surface based predictor of Parker; | $[-]$ |
| ρ | : density of the water; | $[kg/m^3]$ |
| σ_g | : standard deviation of the bed material distribution; | $[-]$ |
| σ_ϕ | : standard deviation of the surface size distribution on ϕ -scale; | $[-]$ |
| $\sigma_{\phi o}$ | : parameter of the surface based predictor of Parker; | $[-]$ |
| τ | : shear stress; | $[N/m^2]$ |
| τ_c | : dimensionless critical shear stress; | $[-]$ |
| τ_j^* | : dimensionless Shields stress; | $[-]$ |
| τ_{tj}^* | : reference stress ($\tau_{tj}^* = 0.0386$); | $[-]$ |
| τ'_j | : grain shear stress; | $[N/m^2]$ |
| ϕ | : grain size on logarithmic ϕ -scale in the bed load ($\phi = -\log_2(D)$); and | $[-]$ |
| ϕ' | : grain size on logarithmic ϕ -scale in the surface layer. | $[-]$ |

Chapter 1

General description

1.1 Introduction

Gradual downstream fining in gravel-bed rivers is a well-known feature. The rate of fining depends upon the specific influence of abrasion or size selective transport and the reduction in grain size diameters can take tens of kilometres down to 1 km. In contrast to gradual downstream fining, examples of sudden gravel-sand transitions has been reported as well typically involving a reduction in grain size diameter of some orders of magnitude over a few hundred to a few kilometres, often with an associated break in channel slope. The present study “Downstream fining of Sediments in the Meuse River” focuses on the gravel-sand transition that takes place in the Dutch part of the Meuse River (Maas River). In doing this, not only abrasion and break down are considered but also selective transport triggered by basin subsidence is taken into account and the influence of each of these three processes in the downstream fining is assessed.

1.2 Problem description

The Meuse River enters The Netherlands in Southern Limburg near the village of Eijsden. It flows to the North and it forms the border between Belgium and The Netherlands in the reach approximated by villages of Borgharen and Maasbracht. Near the city of Roermond, the river shows a sharp transition from a gravel-bed to a sand-bed river. Over this transition, which takes places within a few tens of kilometres, the D_{50} of the bed material changes from about 16 to 2.6 millimetres whilst the slope also decreases from about 0.48 m/km to about 0.10 m/km.

Several possible explanations can be proposed for this sudden change in the granulometric composition of the bed material. Most of them centre around three possible causes: abrasion, break down and selective transport. Authors like Holly and Rahuel (1990b), Parker (1991a,b), Hoy and Ferguson (1994) among others have studied these phenomena and they reported that downstream fining of sediments is linked to aggradation. However, aggradation has not been observed in the Meuse River in the past; on the contrary, the riverbed seems to have been stable. This seeming contradiction might be explained by subsidence due to tectonics. Hence, there might be a close relation between aggradation and tectonic movement in the area. It is explored in this study that in the past downstream fining of sediments was taking place in an aggrading river, while this aggradation of the bed is counteracted by vertical tectonic movements of the area. When these two phenomena would balance, the riverbed would appear to be stable. This might explain the fining situation observed in the field.

1.3 Justification of the study

Gravel-sand transitions imply that there is a sudden change in the grain size distribution of the bed material and usually, but not always, there is also a change in bed slope. Hence, the continuity of sediment is not fulfilled for all size fractions of the bed material along the transition and deposition must occur. Since the Meuse River has a gravel-sand transition, the sediment continuity per grain fraction is not fulfilled and consequently the sediment transport is affected, making it difficult to interpret field measurements of the sediment load. Furthermore, this also limits the possibilities of mathematically modelling the morphological behaviour of the river, unless the relevant phenomena are taken into account.

In view of these, an explanation of this sudden change in the river characteristic taking into account the three processes (abrasion, break down and selective transport triggered by subsidence) is needed

and it will contribute to a better understanding of the morphological behaviour of the Meuse River. It will also allow to assess the implications that the results have will for future data collection as well as the possibilities of modelling the morphological behaviour of the river.

1.4 Objectives of the study

The aim of the study is to investigate the transition from a gravel-bed to a sand-bed river that takes place in the Meuse River and its implications. Two different, but related topics will be studied: first, the role that selective transport and abrasion plays in the change of the granulometry of the bed material, and second, the relationship between aggradation and tectonic movements that might induce the selective sorting.

In order to achieve the above aim, the following objectives were defined for this study:

- ◆ to elaborate the available data on bed material characteristics, on sediment transport and on slopes in the Meuse River in more detail to get a more consistent picture than presently available.
- ◆ to investigate the causes that have produced the transition from a gravel-bed river to a sand-bed river;
- ◆ to study the implications that the phenomena causing the gravel-sand transition has for field measurements and their interpretation; and
- ◆ to assess the implications that the phenomena causing the gravel-sand transition has for the modelling of the Meuse River.

1.5 Approach of the study

To initiate the study “Downstream fining of sediment in the Meuse River” the available information regarding the setting of the basin and the river was collected and when required further elaborated. This information includes the geology and the tectonic of the region as well as along the river course. Hydrological and morphological data on the river were also studied and, in addition, the anthropological activities (human-induced changes) in or in the neighbourhood of the river were taken into account. Furthermore, a literature review on downstream fining and related topics like abrasion, selective transport and subsidence was performed.

The description of the bed material and its characteristics were subsequently studied using the available information. In doing this, different characteristic parameters like D_{50} , D_m and geometric standard deviation were determined. Typical features of gravel-sand transitions like the development of bimodal composition and changes in gravel-sand content were also considered. Later on, different sediment transport predictors were tested against available bed-load measurement and the most suitable of them were selected for the subsequent steps of the study.

Once the general framework was set and the field data processed, not only was the relevance of each one of the processes involved in the downstream fining of sediments assessed but also the combined effect was studied via mathematical modelling. In the case of the Meuse River abrasion, break down and selective transport of particles induced by basin subsidence were considered.

The results of the different assessment were interpreted and discussed in the light of: i) future collection of field data and, ii) morphological modelling of the Meuse River. Finally, conclusions and recommendations for future studies are drawn.

1.6 Structure of the report

This report is divided into eight chapters in order to present clearly the results and findings of the study. Each chapter deals with a separated but related topic. Chapter 1 deals with the description of the problem and the objectives of the study while Chapter 2 presents some characteristics of the Meuse River Basin like the catchment area, geology of the region, hydrology and morphology of the river. Chapter 3 introduces the necessary theoretical background to study gravel-sand transitions and in Chapter 4 the analysis of the field data and the estimation of sediment transport rates in the Meuse River are carried out. Chapter 5 deals with the individual assessment for the relevance that each one of the possible causes of downstream fining in the Meuse River could have whilst in Chapter 6 the combined effects of the possible causes are assessed via numerical modelling. Chapter 7 contains the discussion of the results and the implications that these results have for future data collection and numerical simulations of the Meuse River. Finally, Chapter 8 gives the conclusions and recommendations of this study.

Chapter 2

Characteristics of the Meuse River Basin

2.1 Introduction

This chapter briefly describes the principal characteristics of the Meuse River Basin. It starts with the description of catchment and its geological setting as well as the geological conditions along the river course. Subsequently, the hydrological conditions in the Meuse River and its morphology are briefly introduced. Finally, the human activities in the river banks are discussed.

2.2 Catchment of the Meuse River

The Meuse River drains an area of about 33,000 km² distributed over four countries in the following way: about 10,000 km² in France; about 13,000 km² in Belgium; 6,000 km² in The Netherlands and 4,000 km² in Germany. It has a length of 891 km, 496 of them in France, 183 in Belgium and the remaining length in The Netherlands. The maximum altitude goes up to about 500 m (+NAP). Figure 2.1A shows the catchment area of the Meuse River while Figure 2.1B presents the river chainage in the Limburg province of The Netherlands.

2.3 Geology of the region

The watershed of the Meuse covers several geological formations and therefore, it is a complex combination of morpho-tectonic units. It is not the intention to describe here in great detail each one of these units, but rather to provide some general information on the geology of the Meuse River Basin. Interested readers are referred to more specialised references like Geluk et al (1994), Camelbeeck & Meghraoui (1996), and Van den Berg (1996) among others for a more extensive description of the geological setting of the Meuse River.

2.3.1 Geological setting of the region

The area of interested is localised in the Lower Rhine Embayment (white area in Figure 2.2A approximately). The Lower Rhine Embayment belongs to part of Germany and The Netherlands, and it is a tectonic depression localised between the southern North Sea Basin, the uplifting areas of Ardennes and Rhenish Shield and the London-Brabant Massif (see Figure 2.2B).

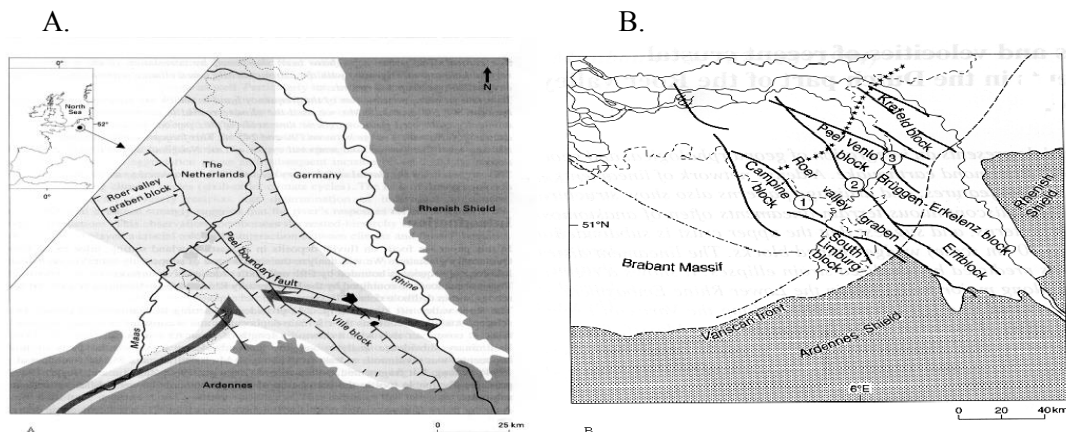


Figure 2.2 Geological setting of the area.
Source: Van den Berg (1996).

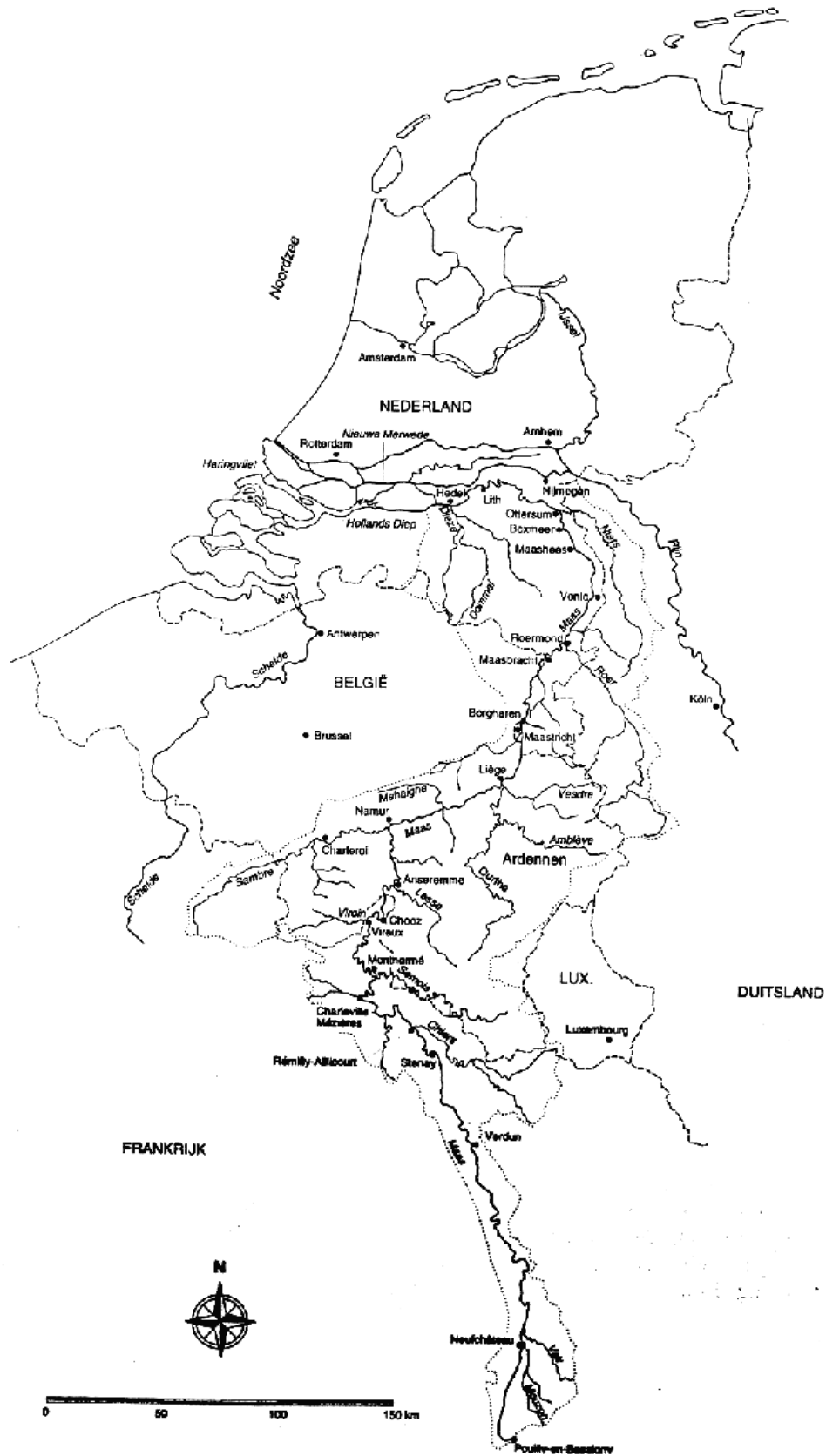


Figure 2.1 A) Catchment area of the Meuse River.

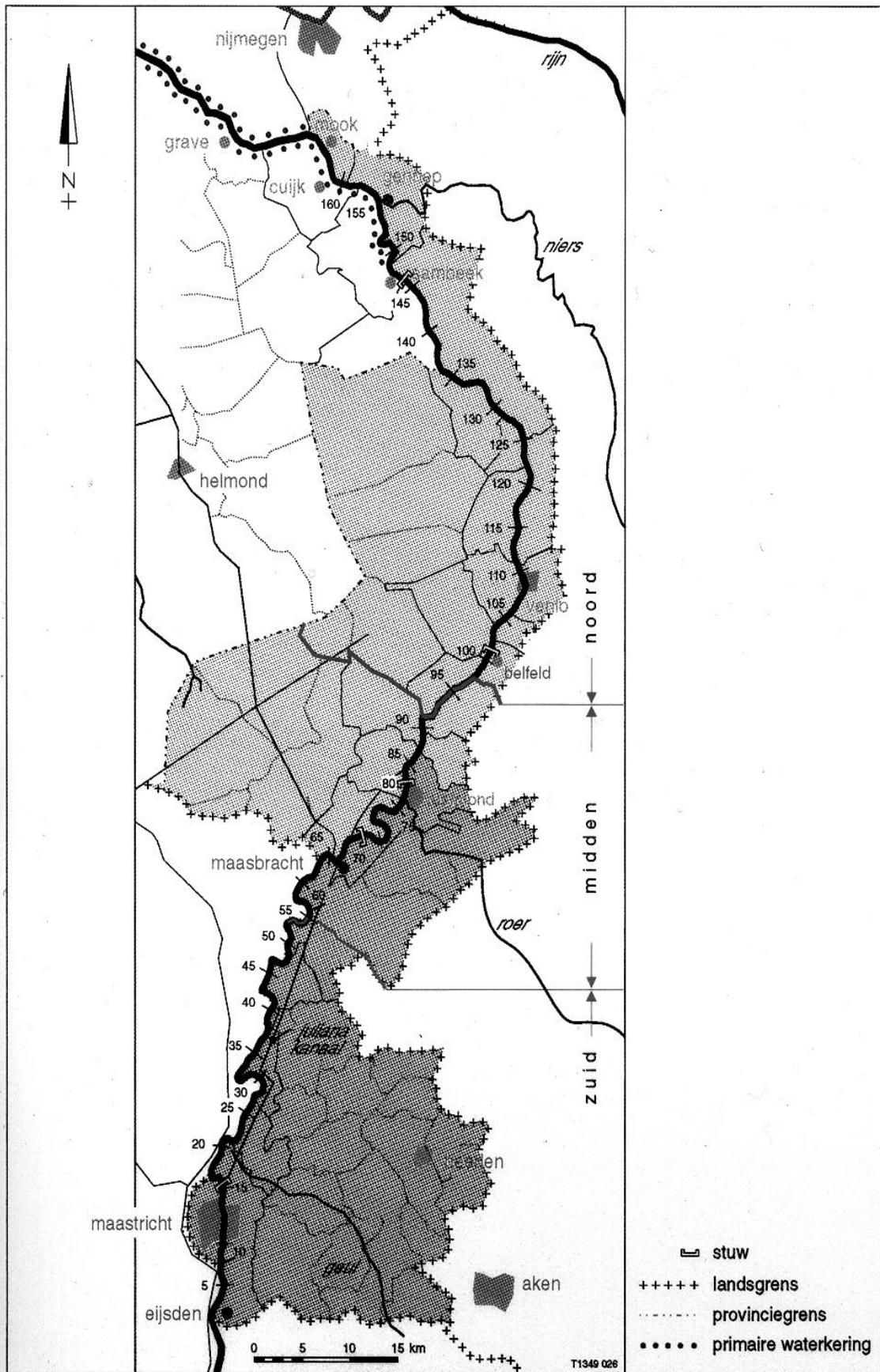


Figure 2.1 B) River chainage in the Limburg province.

This depression is composed of several north-eastward tilted blocks, among others, the Roer Valley Graben block and the Ville block. Fluvial sediments appear in the Southeast of the Embayment since the Middle Miocene and they have been supplied by precursors of the Rhine and Meuse rivers and they pass to full marine ones in the Northwest part of the Embayment.

2.3.2 Tectonic of the region

In the study region, there is a set of faults with NW-SE orientation that determine several north-eastward tilted blocks. Based on the tectonic movements during the Cenozoic, Geluk et al (1994) classified these blocks in five different areas (see Figure 2.3):

1. The Krefeld Block: relative high block which borders the subsiding area in the North.
2. The Venlo, Peel and Köln Blocks: areas of intermediate subsidence.
3. The Roer Valley Graben and the Erft Block: areas of strong subsidence.
4. The Campine and South Limburg Blocks: areas of intermediate subsidence.
5. The Brabant Massif: bordering the subsiding area in the South.

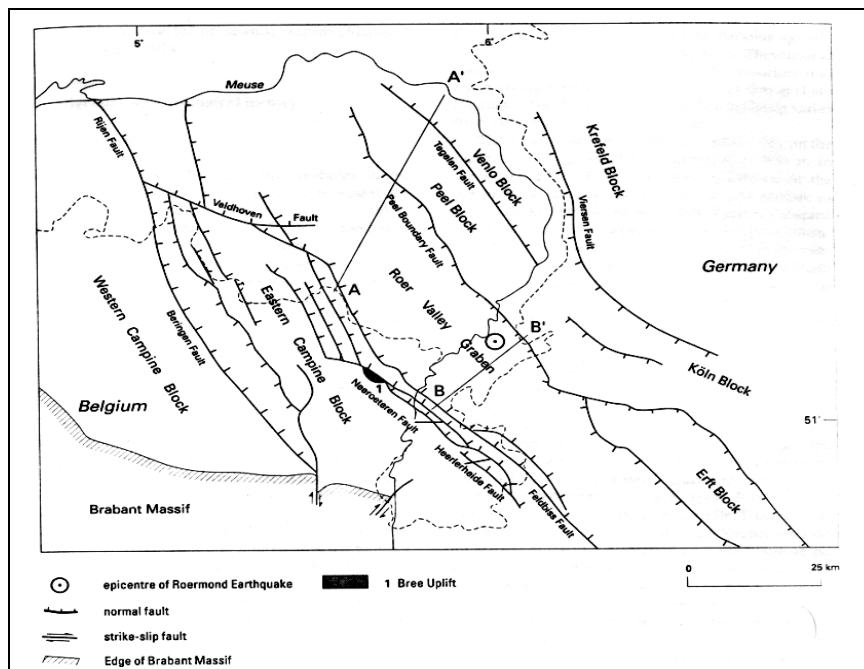


Figure 2.3 Classification of the different blocks.
Source: Van den Berg (1996).

The Venlo Block, the Peel Block (or Peel Horse), the Roer Valley Graben and the South Limburg Block are of particular importance for this study. From South to North, the Feldbiss fault divides the South Limburg Block from the Roer Valley Graben; the latter is divided from the Peel Horse by the Peel fault and between the Peel Horse and the Venlo Block the Tegelen fault forms the boundary. Van den Berg et al (1994) studied these units and estimated, based on the Dutch ordinance system, the vertical velocities within them. According to their findings, there are differential movements in each one of the four units; Table 2.1 and Figure 2.4 summarises the differential movements in the different sectors as defined by the faults of the zone.

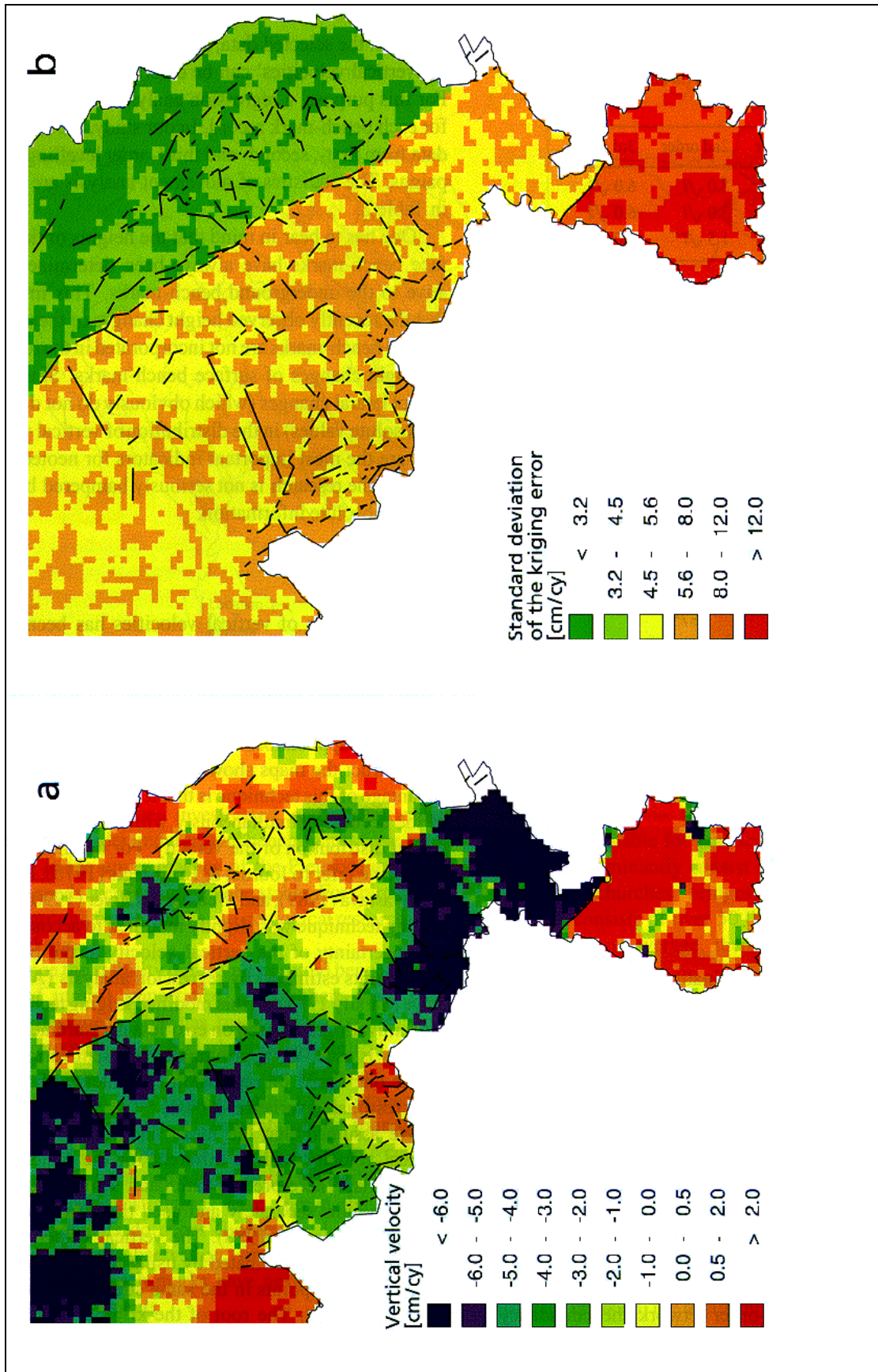


Figure 2.4. Vertical velocities estimated in cm per century (cm/cy).
Source: Van den Berg et al (1994)

Table 2.1
Average vertical displacement due to tectonics in the of study area.

| River reach | River chainage (km) | Vertical rate (mm/y) | Standard deviation (mm/y) | Type of movement |
|-------------------------|---------------------|----------------------|---------------------------|------------------|
| ← - Geulle | 0.0 – 26.0 | 0.05 – 0.20 | 0.80 – 1.20 | Uplift |
| Geulle – Feldbiss | 26.0 – 45.0 | > 0.20 | 0.80 – 1.20 | Uplift |
| Feldbiss – Stevensweert | 45.0 – 63.5 | -0.60 – -0.50 | 0.45 – 0.56 | Subsidence |
| Stevensweert – Beegden | 63.5 – 75.0 | -0.30 – -0.20 | 0.45 – 0.56 | Subsidence |
| Beegden – Peel | 75.0 – 88.0 | -0.30 – -0.20 | 0.45 – 0.56 | Subsidence |
| Peel – Tegelen | 88 – 102.5 | -0.10 – 0.00 | < 0.32 | Subsidence |
| Tegelen – Velden | 102.5 – 112.0 | 0.00 – 0.05 | < 0.32 | Uplift |
| Velden - → | 112.0 - → | -0.10 – 0.00 | < 0.32 | Subsidence |

Source: Van den Berg et al (1994).

2.3.3 Sediment deposits of the Rhine River within the Roer Graben

Fluvial sediments appear in the Southeast of the Lower Rhine Embayment since the Middle Miocene. The rivers Rhine and Meuse have supplied them, but the positions of these rivers have repeatedly changed in space and time.

During the early Pleistocene, fault activity in the South-eastern part of the Lower Rhine Embayment led to replacement of local river sedimentation in the Roer Graben (Formation Kedichem) by sediments of the Rhine River which are represented by the Formation Sterksel (see Figure 2.5). The “Weert” mineral zone distinguishes this formation and its spatial distribution shows that the Rhine occupied a wide depositional plain with a mid-graben area of non-deposition. The Formation Sterksel is characterised by gravel and coarse sand; according to the geological profile along the Meuse River (see Figure 2.5), it is not localised near enough to the river bed at shallow depth to represent a lithological control on the bed material transition of the Meuse River.

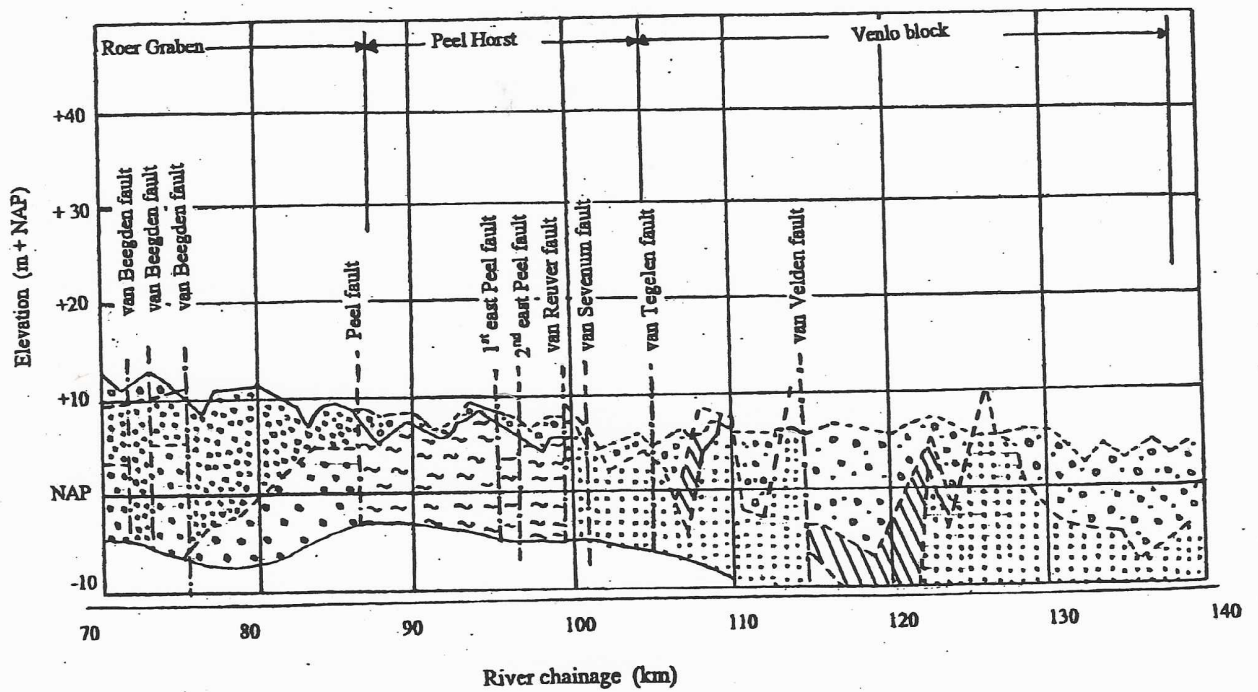
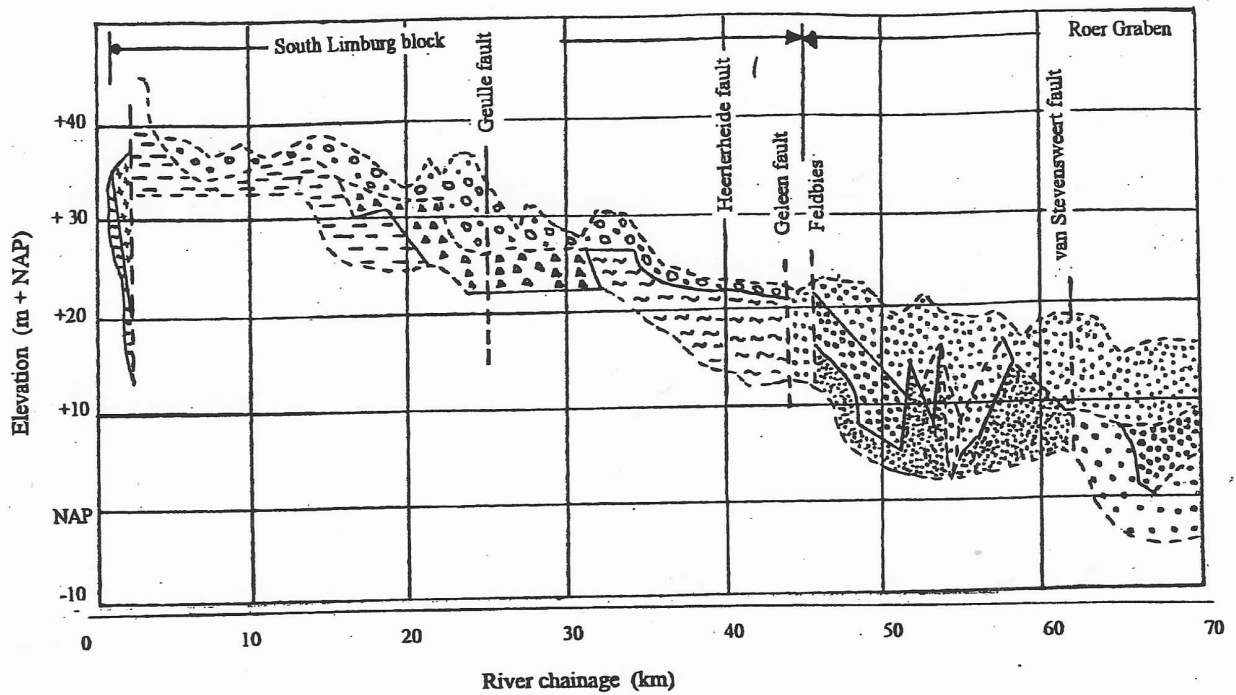
After the period of strong fault activity during which the Formation Sterksel was deposited, the Rhine River no longer took a North-western course through the central part of the Roer Graben, but flowed northward from Bonn in its present valley. It was replaced by the Meuse River (the Rosmalen mineral zone). Since then (middle Pleistocene) the Meuse River is, within the Roer Graben, mainly flowing over its own Holocene and Late Pleistocene deposits.

Beyond the hinge line of the North Sea Basin (see Figure 2.2) sediments from both the Meuse and the Rhine River have built the Holocene lowland floodplain.

2.3.4 Geological conditions along the Meuse River

Following the river course from the its source in France to its mouth in The Netherlands, the Meuse River sequentially flows over permeable Jurassic rocks in eastern France, the impermeable Hercynian Ardennes Massif in Belgium and permeable Cretaceous to Tertiary deposits in The Netherlands.

Within The Netherlands, several geological features along the course of the Meuse River can be distinguished (see Figure 2.5). Each one of these features is characterised by a different environment of deposition and has its own attributes. Of particular interest for this study is the type of material that is associated to each feature. Table 2.2 summaries this information by giving the name of the geological feature, the period in which it was deposited and a description of the type of deposition.



- | | | | | | |
|--|----------------------------|--|---------------------------|--|------------------------|
| | Carboniferous | | Miocene | | Van Veghel formation |
| | Vaalser formation | | Pliocene | | Van Sterksel formation |
| | Meuse terrace | | Van Kreftenheye formation | | Kalksteen formation |
| | Oligocene | | Practigica Formation | | Van Tegelen formation |
| | Van Grubbervorst formation | | | | |

Figure 2.5 Geological profile along the Meuse River.

Table 2.2
Main geological characteristics
along the Dutch reach of the Meuse River

| Geological feature | Period | Type of material |
|------------------------|--------------------|-------------------------------|
| Formation Vaalser | Mesozoic | Green sand, shale, quartzite |
| Formation Kalksteen | Cretaceous | Limestone |
| Meuse terraces | Holocene | Gravel and sands |
| Oligocene deposits | Oligocene | Sandy clays |
| Miocene deposits | Miocene | Loamy sands |
| Pliocene deposits | Pliocene | Gravel, clayey sand, clay |
| Formation Kreftenheye | Late Pleistocene | Gravel, coarse sand |
| Formation Praetiglien | Early Pleistocene | Gravel, fine sand, clay, coal |
| Formation Veghel | Middle Pleistocene | Gravel, coarse sand |
| Formation Sterksel | Early Pleistocene | Gravel, coarse sand |
| Formation Grubbenvorst | Holocene | Gravel, coarse sand |
| Formation Tegelen | Early Pleistocene | Coarse sand, clay |

Source: Waterloopkundig Laboratorium (1981).

From this brief geological description, we can, broadly speaking, infer that the Meuse River is flowing in The Netherlands over old deposits of its own sediments, and that they mainly are constituting of gravel and coarse sand, though from different periods of time and probably from different lithological origins.

The influence of tectonics is represented by the set of faults that the river crosses along its course. More important, however, is the differential movement between two adjacent blocks; Figure 2.6 shows a schematic representation of the vertical displacement rates along the river course. From this figure, it is clear that the movements are not uniform. In the South Limburg Block (upstream km 45) uplift is taking place, which encourages an incision of the river (degradation). Within the Roer Graben (km 45 to 88), on the contrary, subsidence is taking place at significant rates.

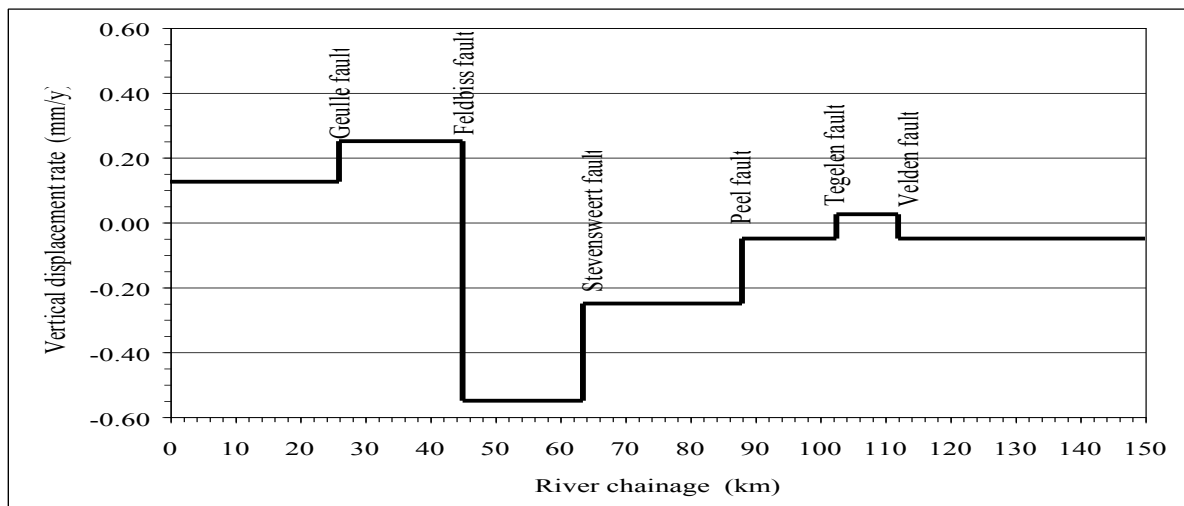


Figure 2.6 Approximate vertical displacement rates (in mm/y) along the Meuse River.
(Negative values indicate subsidence).
Data source: Van den Berg et al (1994).

2.4 Hydrological conditions

The Meuse River is characterised by a fast response to precipitation in its catchment; this is mainly due to the presence of large tributaries together with relative impervious subsoil (Hercynian Ardennes Massif) in Belgium. Available data includes discharges and water levels since 1911 onwards. On the long term, the average discharge in the Meuse River at Borgharen is about 250 m³/s, but records go from less than 70 m³/s in 1976 up to 3047 m³/s in 1993, indicating that the river has a great variation in its flows. Figure 2.7 shows the temporal distribution of discharges in the Meuse River at Borgharen (km 16.0) while Figure 2.8 gives the flow duration curve at the same location for the period 1911 to 1997.

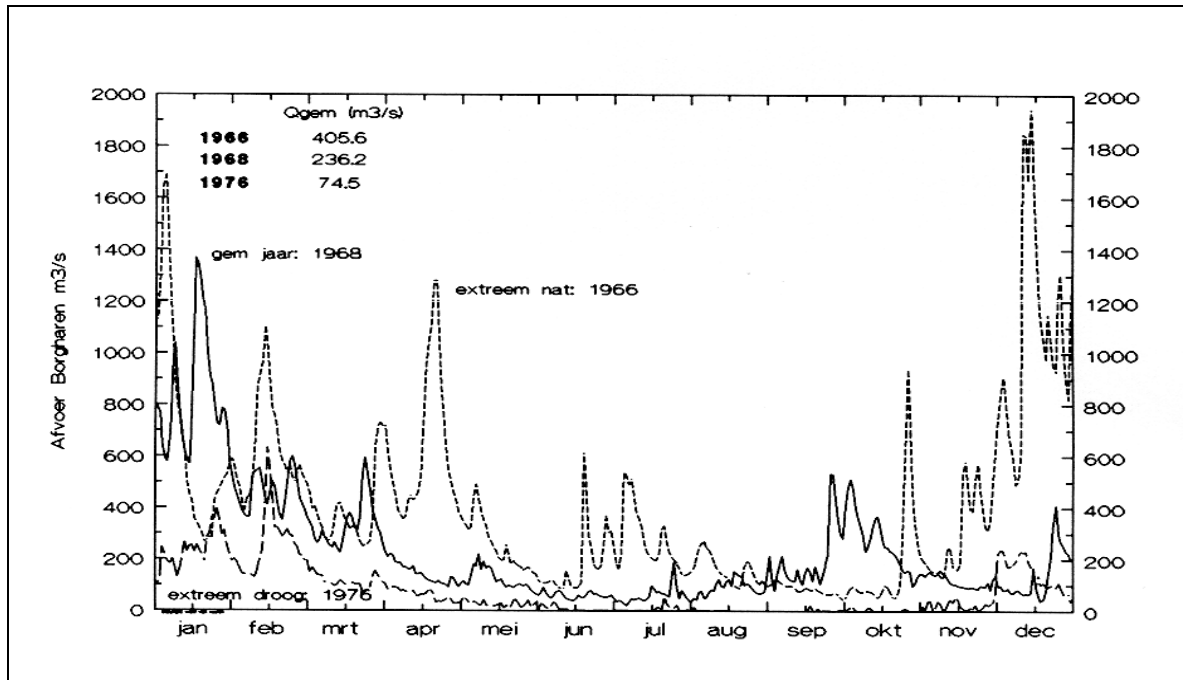


Figure 2.7 Temporal distribution of discharges in the Meuse River at Borgharen.

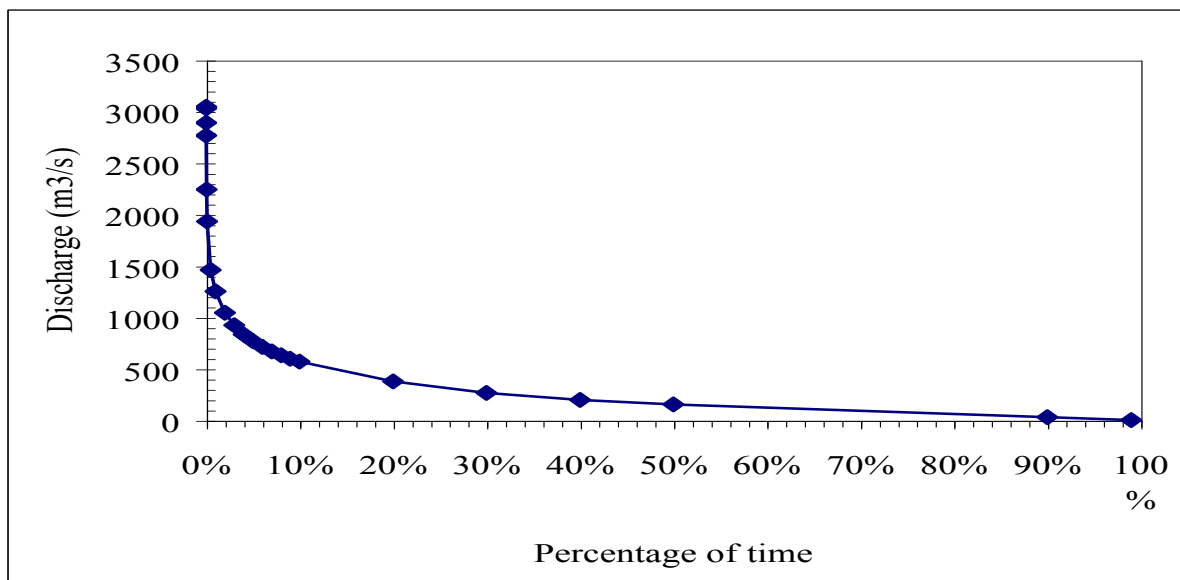


Figure 2.8 Flow duration curve at Borgharen for the period 1911-1997.

Source: Rijkswaterstaat.

2.5 Morphology of the Meuse River

The morphological description of the Meuse River presented hereafter is divided in two parts. The first part deals with the morphological evolution of the Meuse in geological times, whilst the second part is devoted mainly to the present conditions of the Meuse River. Nevertheless, both descriptions presented here are simplified ones and for a more complete description the interested readers are referred to specialised references like Paulissen (1973), Vandenberghe et al (1994) and Törnqvist (1993a) or Sloff & Barneveld (1996) among others.

2.5.1 Geological times

In the case of the Meuse River, climate is interpreted as the initial driving force for changes in the river pattern. Incision phases have been recorded at the beginning of warmer periods (Bølling and Preboreal) linked to vertical erosion due to the over-capacity of the river to transport the sediment entering the system. On the contrary, cool periods caused a reduction in the mean discharge of the Meuse River and an increase in the sediment supply. This increase in sediment supply can be understood mainly because of the denudation processes as the vegetation belt shifted to lower latitudes and the flora did also change to probably mainly tundra. During the geological evolution of the Meuse River, cycles of warm and cool periods have produced transformations from a typical braided to single channel meandering patterns; these transformations have occurred gradually over quite a long time and not instantaneously in a single step. These transformations can be summarised as follows.

During the Weichselian Late Pleniglacial, a braided river plain with straight branches characterised the Meuse River. In the next phase, during the Bølling, the river system changed from aggradation to degradation and the morphology from straight to sinuous branches. The individual channels were generally deeper than the channels during the Pleniglacial; this was probably due to the increasing of soil cohesion (by pedogenesis), the higher soil humidity and the development of the vegetation cover. In the younger parts of this period tendencies has been found to more curved and wider forms and therefore this period has been interpreted as transitional.

In the Allerød period, the river was characterised by high sinuosity with large, wide meanders that eroded the deposits of the previous phase and this new phase in the Meuse River was hence, of the single-channel type. The scars of the meanders of this period show asymmetric cross sections while point-bars reveal well-developed fining-upward sequences. According to the infillings found in the large meanders (Vandenberghe et al, 1994) the initiation of this meandering system is dated to *c.* 11,800 BP while the end is dated to *c.* 10,900 BP. Hence, this phase of large meanders stopped at the Allerød-Younger Dryas transition.

During the Younger Dryas the Meuse River transformed into a braided system. The colder conditions during this period resulted in more open vegetation, which induced the delivery of greater quantities of sediment and coarser grain sizes to the river as well as more pronounced peak discharges. This phase is separated from the previous one by its straight edges and it is characterised by a multiple system of shallow, straight to slightly curved channels. Bars in this floodplain are locally covered by river dune sand and the width-depth ratio of the channels is high. Vandenberghe et al (1994) suggest that the colder climatic conditions of this period, resulted in the crossing of the thresholds (in river peak discharges and bed load) for river adaptation in the Meuse Valley. At the beginning of the Holocene, the Younger Dryas floodplain was incised and also transformed into a terrace. The Meuse River changed to a single channel with straight to slightly curved alignment. Table 2.3 summarises the evolution of the Meuse Valley and indicates the principal mechanisms and fluvial styles during each geological period.

Table 2.3

Summary of the geomorphological-sedimentary changes and their ages in the Meuse basin at the transition from the Weichselian Pleniglacial to the Holocene.

| Stratigraphy / ¹⁴ C-age | Fluvial process | Fluvial pattern / sedimentation |
|--|--|--|
| Holocene ———— 10,250 ———— | Slight lateral movement [Slight incision] | Side bars, levees (?) One channel, Straight to slightly curved |
| Younger Dryas ———— 10,900 ———— | Lateral erosion | Braided: channels + bars |
| Allerød 11,850 | | Large meanders |
| Bølling ———— 13,000 ———— | Incision | Transitional: multichannel, Slightly curved |
| Late Pleniglacial (Weichselian) c. 18 – 25,000 | Aggradation / stability Incision Aggradation | Braided: straight branches Braided |

Source: Vandenberg et al (1994).

In the delta area (beyond the hinge line) the geological evolution is shared with the Rhine River. The basement sediments that underlie the Holocene Rhine-Meuse Delta were deposited during the Weichselian; this basement mainly consists of a package of sand and gravel. During the Pleistocene-Holocene transition, climatic changes produced a period of incision presumably by meandering rivers until the relatively rapid rise of the sea level that took place during the Holocene. This increase in sea level produced two channel patterns in the Rhine-Meuse Delta. In areas with low gradients as well as high bank stability anastomosing systems developed. In zones where ones of these two conditions were not fulfilled, intermediate but essentially meandering systems developed. Moreover, these two styles alternated in time, especially in the West-central part of the Rhine-Meuse Delta. A final remark on the geological evolution of the delta area is that during all of the Holocene period, areas located to the East of Leerdam remained outside of direct influence of the sea level changes (Van Dijk et al, 1991).

2.5.2 Present conditions

This description of the present morphological conditions in the Meuse River is a summary of the findings reported by Paulissen (1973). It is not the intention to give a comprehensive overview of all his findings; some limited information of the morphological characteristics of the river. More complete morphological descriptions can be found in Paulissen (1973), Waterloopkundig Laboratorium (1981) and Sloff & Barneveld (1996) among others.

The natural Meuse River of the last centuries, used to be a typical island river, with mainly a single channel and many stream divergences (at least 100 islands). The actual existing islands have evolved very little over the last 200 years and the main part of these islands has disappeared since 1850 due to river training measures.

The thalweg profile shows in the well-developed meander bends a multiple development of the pool-riffle system, caused by a secondary sinuosity of the thalweg. It seems also, as Paulissen reports, that the relation between the curvature radius and the maximal depth of the river bed depends on the stream pattern. The riffles are higher in the straight channel at the inflection point of the meanders than in the meander bends.

The evolution of the gravel bed is the consequence of two processes: the evolution of a meander bend and of a straight channel. The evolution of a meander bend is caused mainly by the formation of point bars, which have a very great extension and are characterised by a graded bedding structure of low angle. The evolution of straight channels is caused by the construction of an important gravel bar and the shifting of the thalweg in the river bed.

The alluvial plain, constantly 4 km width, is formed by lateral and vertical erosion of the Meuse River in its own terraces. The gravel surface in the alluvial plain is always a few meters lower than in the terraces and the top of the gravel deposits shows identical characteristics as the point bars and the channel lag deposits in the actual stream. The limit between the alluvial plain and the terraces is formed by a series of abandoned channels, which coincides with an abrupt limit between coversands and alluvium.

The alluvial plain is also characterised by a very high number of abandoned channels (see Figure 2.9), all of the chute cut-off and the avulsion type. Stream migrations only occur during inundation periods and the formation of ice barriers in the river bed could cause important stream avulsions. It is suggested by Paulissen that stream migration and accretion of the alluvial plain still occurred during late historical time and that a large number of morphological old channels were abandoned in recent times. The rate of accumulation in the abandoned channels was not only function of time, but also of the distance between the abandoned and the active channel.

In the alluvial plain there is a lack of morphological pronounced natural levees, both along the actual Meuse and along the abandoned channels. This is the result of the frequent and fast migration of the stream which prevents the deposition of important levee deposits, and, in a further stage of evolution, of the sedimentation of overbank deposits above the levee deposits, causing a flattening of the initial morphological differences.

Paulissen divided the sediments of the alluvial plain into 2 units, namely sediments of vertical and of lateral accretion. The lateral accretion consists predominantly of gravel with mean size between 15 and 20 centimetres approximately. Coarse sand is deposited only in the gravel pores and a mantle of fine alluvium (silt) covers all deposits of lateral accretion. The material of vertical accretion has a very poor sorting. The channel lag and the overbank deposits have identical granulometric curves and they are mainly fine sediments.

LEGENDE - LEGEND

I. MORFOGRAFIE EN MORFOMETRIE
MORPHOGRAPHY AND MORPHOMETRY

GEANALYSEERDE VORMEN - ANALYSED FORMS

Vlakken (helling < 1%) - Flat surfaces (inclination < 1%)

Erosief - Erosive
Sedimentair - Sedimentary

Hellingen - Slopes

| | Paralleel (1) Parallel | | Divergerend (2) Divergent |
|----------------------------|---------------------------|----------------------------|------------------------------|
| | erosief errosive | sedimentair sedimentary | sedimentair sedimentary |
| Rechtlijnig Rectilinear | | | |
| Concaaf Concave | | | |

Interval der tekens
Signi interval

32' - 1mm
16' - 2mm
8' - 3mm
4' - 4mm
2' - 5mm
1' - 6mm

- (1) De hellinggraad wordt aangegeven door het interval der hellingstekens.
The inclination is indicated by the interval of the slope lines.
(2) Het interval bij het breedste uiteinde geeft de gemiddelde hellinggraad aan.
The interval at the largest end indicates the mean inclination.

Hellingsconcessiteiten, - concaviteiten en lineaire knikken (1)
Slope concavities, - concavities and linear breaks of slope (1)

Convexe knik - Convex break of slope
Convexiteit - Convexity
Concaviteit - Concavity

- (1) Het hellingverschil wordt aangegeven door het interval der tekens.
The difference in inclination is indicated by the signs interval.

GESCHEMATISEERDE VORMEN - SCHEMATIZED FORMS

| | Dwaarsprofiel Cross Section | Erosief Erosive | Sedimentair Sedimentary | Kaart- breuk Image |
|---|--------------------------------|-----------------------------|----------------------------|------------------------------------|
| Valleien en Depressies Valleys and Depressions (1) | Vlak dal Flat valley | V-gegdal V-shaped valley | Boogdal Trough valley | Vlakbodemdal Flat bottom valley |
| Ruggen - Elevations | | | | |

(1) Het interval der dwarsprofielen geeft het verval aan van het lengteprofiel.
The interval of the cross sections indicates the inclination of the longitudinal profile.

GESYMBOLISEERDE VORMEN - SYMBOLIZED FORMS

Hellingen en Bermen - Slopes and Escarpments (1) (2)

Rechtlijnig - Rectilinear
Concaaf - Concave
Convex - Convex

- (1) Gemiddelde hellinggraad - door interval der hellingstekens
Mean inclination - indicated by the interval of the slope signs
(2) Barm- en hellingshoogte - Height of the escarpment and of the slope

< 2 m < 6 m < 18 m

Valleien, Depressies en Ruggen - Valleys, Depressions and Elevations (1)

Vlakbodemdal - Flat bottom valley
Boogdal - Trough valley
Vleugelval - V-shaped valley
Depressie - Depression
Rug - Elevation

- (1) Aangegeven door combinatie van 2 gesymboliseerde hellingen
Indicated by combination of 2 symbolized slopes

SYMBOLEN - SYMBOLS

Vorm - Form

Dalen - Valleys
vleugelvalen - V-shaped valleys
hoogdal - trough valleys

Duinen - Dunes
niet gedifferentieerd - not differentiated
paraboolduinen - parabolic dunes

Fluviatiel - Fluvatile
verlaten stroomgeulen - abandoned channels

Antropogeen - Antropogeneous
berm - escarpment

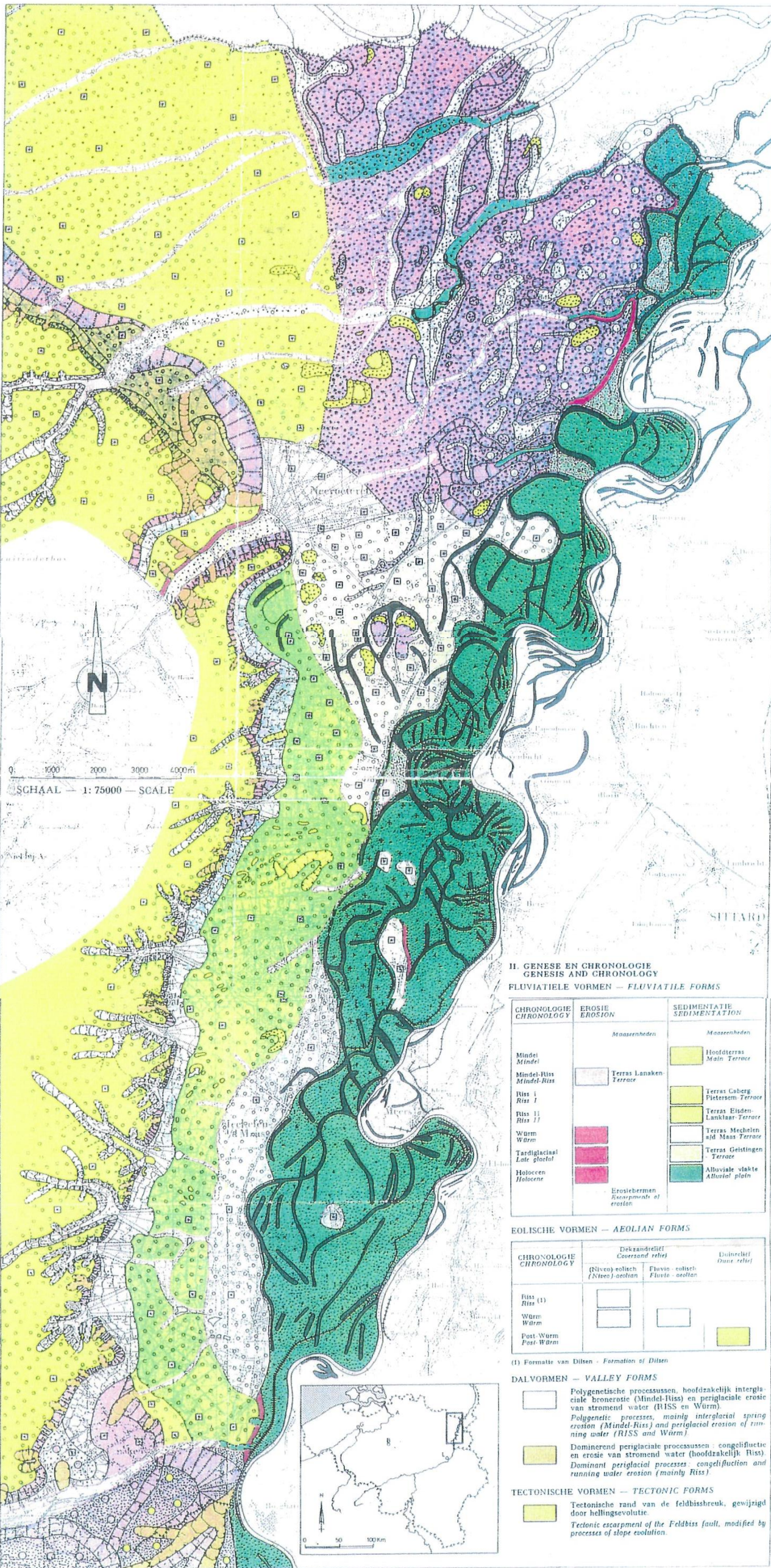
dijk 0.5 m-1.5 m
dike 1.5 m-2.5 m
2.5 m-3.5 m
3.5 m-4.5 m

kunstmatig afgesneden bedding - artificial cutted channel

Sedimenten - Sediments (1)
Grind
Zand
Leem
Klei

(1) Slechts aangegeven op vlakken - Only indicated on flat surfaces

- N.H. 1. Benaderende morfografische en/of genetische en/of sedimentologische grens.
2. Onderliggende genetische eenheden.
3. Vervalrichting.



II. GENESE EN CHRONOLOGIE
GENESIS AND CHRONOLOGY

FLUVIATIELE VORMEN - FLUVIATILE FORMS

| CHRONOLOGIE CHRONOLOGY | EROSIE EROSION | SEDIMENTATIE SEDIMENTATION |
|-------------------------------|--|------------------------------------|
| Mindel Mindel | | Moasenterras Maine Terrace |
| Mindel-Riss Mindel-Riss | Terras Lanaken Terrace | Terras Caberg Pieterson Terrace |
| Riss I Riss I | | Terras Elden- Lanklaar Terrace |
| Riss II Riss II | | Terras Mechten and Maas Terrace |
| Wurm Wurm | | Terras Geltingen Terrace |
| Tardiglaciaal Late glacial | | Alluviale vlakke Alluvial plain |
| Holoceen Holocene | Erosiehermen Escarpments of erosion | |

EOLISCHE VORMEN - AEOLIAN FORMS

| CHRONOLOGIE CHRONOLOGY | Deksandrelief (Niveo) eolisch (Niveo) aeolian | Duindrelief Dune relief |
|---------------------------|---|----------------------------|
| Riss (1) Riss (1) | | |
| Wurm Wurm | | |
| Post-Wurm Post-Wurm | | |

(1) Vormsatie van Dijken - Formation of Dikes

DALVORMEN - VALLEY FORMS

Polygenetische processussen, hoofdzakelijk interglaciale bronneroste (Mindel-Riss) en periglaciale erosie van stromend water (Riss en Wurm).
Polygenetic processes, mainly interglacial spring erosion (Mindel-Riss) and periglacial erosion of running water (Riss and Wurm).

Dominerend periglaciale processussen - conglufluente en erosie van stromend water (hoofdzakelijk Riss).
Dominant periglacial processes - conglufluente and running water erosion (mainly Riss).

TECTONISCHE VORMEN - TECTONIC FORMS

Tectonische rand van de feldbissbreuk, gewijzigd door hellingevoluitie.
Tectonic escarpment of the Feldbiss fault, modified by processes of slope evolution.

Figure 2.9 Geomorphological map of the Meuse Valley.
Source: Paulissen (1973).

Currently, the Meuse River presents a low sinuosity in its Belgium part, which is in sharp contrast to the sinuosity in the Dutch area. Paulissen (1973) reported that the global sinuosity of the Meuse River is 1.46; but this value depends on the river reach. As an example of this, Table 2.4 shows values of the sinuosity during the 19th century for five different reaches.

Table 2.4
Values of sinuosity for two different periods of time.

| River reach | Period of time | |
|------------------------|----------------|---------|
| | 1805/06 | 1846/47 |
| Lixhe – Borgharen | 1.09 | 1.11 |
| Borgharen – Cotem | 1.19 | 1.25 |
| Cotem – Grevenbricht | 1.72 | 1.56 |
| Grevenbricht – Walburg | 1.52 | 1.66 |
| Walburg – Maasbracht | 1.30 | 1.34 |

Source: Faessen (1993).

Bank erosion rates in the common Meuse River are reported by Kramer (1997); Table 2.5 presents the estimated values. As can be observed, there is a difference in the rate of bank erosion between both banks of the river.

Table 2.5
Bank erosion rates in the Meuse River.

| Period | Border | |
|-------------|-----------------|----------|
| | The Netherlands | Belgium |
| 1964 – 1986 | 0.04 m/y | 0.03 m/y |
| 1986 – 1994 | 0.19 m/y | 0.05 m/y |

Source: Kramer (1997)

From the 19th century onwards, the Meuse River has been trained in order to improve the navigation conditions of the river. Since that time, the river planform has been fixed and continuous human interference has been taking place. In the following section, this human interference is reviewed briefly.

2.6 Human impact on the Meuse river

In this Section a brief review is given of human activities that have affected the Meuse River. In view of the framework of the present study the review is limited to those activities that probably have had an impact the bed material composition, the sediment transport and/or the morphological characteristics of the river.

The main purpose of this review is to show that already over a long period human activities must have had an impact on the river, and that the physical effects of these activities are still developing. In this respect it is relevant to underline that in river morphological sense the Meuse River is a slow river. The morphological time scale of the Meuse River, defined by de Vries (1975) as the response time to a change to the downstream base level, is (depending on estimates of the sediment transport rates in the Meuse River, see also Chapter 4) about 400 centuries. The Meuse River is still an order of magnitude slower than even the Rhine River, which is already one of the slower rivers in the world (Jansen et al, 1994). The implication of this very long time scale is that the Meuse River responds very slowly to changes and should not be considered to be “in equilibrium”. Even without further human interference, for a long period to come the river will continue to adjust to changes in the past. Hence equilibrium considerations (e.g. incoming sediment = outgoing sediment) are probably not relevant for the Meuse River.

Human impact on the Meuse River has been multiple. Table 2.6 gives a summarised overview of these activities.

Table 2.6
Overview of human activities that have affected the Meuse River

| Type of human activity | Specific human impact |
|------------------------------------|---|
| Agriculture | <ul style="list-style-type: none"> ▪ Land use changes in the catchment (forest clearing) (since 11th century?) ▪ Removal of floodplain forest and change of floodplains to pastures (do) ▪ Land reclamation in the river via small-scale river training works (since 15th century?) |
| Housing | <ul style="list-style-type: none"> ▪ Development of villages and towns in floodplains with subsequent reduction of floodplain extent (also due to roads and railroads) (since 13th century?) ▪ Increased urbanisation and subsequent pavement of large areas of the catchment resulting in quicker drainage of catchment (19th and 20th century) |
| Water supply and power production | <ul style="list-style-type: none"> ▪ In total 9 reservoirs in Belgium (20th century) ▪ Low-head hydropower stations in Belgium and Netherlands (20th century) ▪ Diversion of drinking water (Antwerp, Brussels, Rotterdam, The Hague, ..) (20th century) |
| Navigation | <ul style="list-style-type: none"> ▪ Construction of barrages in France, Belgium and Netherlands (19th and 20th century) ▪ Narrowing of the main channel of the river in combination with closing of secondary channels (second half of 19th century) ▪ Construction of a number of parallel canals (20th century) ▪ Deepening of Meuse River in Belgium upstream of Namur |
| Flood control | <ul style="list-style-type: none"> ▪ Levee construction along the lower Meuse River (since 13th century) ▪ New mouth for the Meuse River (early 20th century) ▪ Cut-offs of bends in the lower Meuse River (after 1926) ▪ Lowering of floodplain of lower Meuse River (after 1926) ▪ Closing of “green rivers” (flood diversions) in lower Meuse River (after 1926) ▪ Levees around villages and towns in Meuse floodplains (20th century) |
| Sand, gravel, clay and coal mining | <ul style="list-style-type: none"> ▪ Sand and gravel mining from the main channel (20th century) ▪ Deep mining of sand and gravel from pits in the floodplain of the Meuse River (20th century) ▪ Limited clay mining in the floodplains (for brick production) ▪ Deep coal mining which has resulted in subsidence |
| Other uses (pm) | <ul style="list-style-type: none"> ▪ Cooling water ▪ Waste discharge ▪ Recreation |

Not all these activities must have had a major impact on the river. The most important activities with probably a large impact on the morphology of the Meuse River are described hereafter in some detail:

◆ *Normalisation in the 19th century*

In the 2nd half of the 19th century the Meuse River was “normalised” in an attempt to improve the sailing conditions in the river. This was done for the whole river reach in The Netherlands including the common Meuse River. The normalisation included narrowing of the river and the closure of secondary channels. Figure 2.10 shows the change in river planform of the Meuse River near Grevenbicht (km 43.6) as realised via river training works, mainly groynes and closures. The main impact of these normalisation works was a reduction of the width of the river, which has resulted in degradation of the main channel over several meters. At the same time the normalisation has fixed the planform of the river. Where in the past the river migrated and meandered within its valley (see Section 2.5 and Figure 2.9) nowadays the river has no freedom in lateral sense. This might have consequences for its alluvial fan formation near the transition from a steep gravel bed river to a gentler sand-bed river.

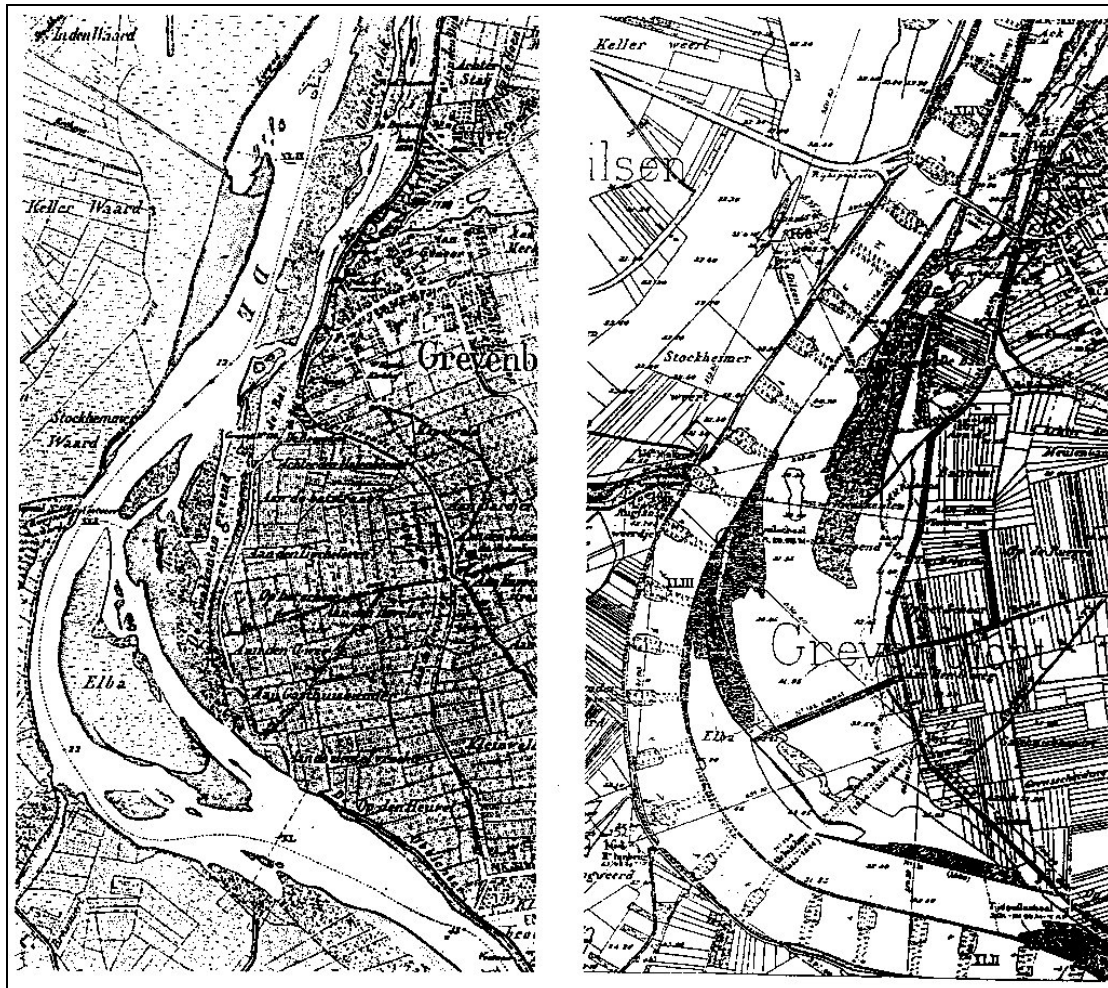


Figure 2.10 Planform of the Meuse River near Grevenbicht in 1849 (left) and 1905 (right)
 Source: Helmer, Klaassen and Silva (1991)

◆ *Flood control measures in the Lower Meuse River*

After the 1926 flood a number of flood control measures were taken in The Netherlands. In the lower Meuse River (downstream of Grave) a number of bends were cut-off, which has resulted in upstream degradation of about 2 metres.

◆ *Reservoirs in Belgium*

Mostly in the 20th century a number of reservoirs were built in tributaries of the Meuse River in Belgium. Table 2.7 provides an overview of these reservoirs. Also the extent of the upstream catchment and the total volume of these reservoirs is listed. The total volume of the reservoirs is about $110 \times 10^6 \text{ m}^3$. The average discharge of the Meuse River at Borgharen is about $250 \text{ m}^3/\text{s}$, which corresponds to a total volume of $8000 \times 10^6 \text{ m}^3$. The total reservoir volume is only about 1% of the yearly flow, but the effect of the reservoir will be larger. The number of floods in a year is in the order of ten (see Figure 2.7), hence the reservoir do have some effect on the hydrograph downstream. This effect is not very pronounced though. The impact of this control on the morphology of the river is most probably negligible. Similarly the reduction sediment supply can be considered. Assuming that the sediment supply is linearly related to the catchment area, the relative reduction in catchment area can be considered ($1.5 \times 10^3 \text{ km}^2$ reduction versus a total catchment area of $21.3 \times 10^3 \text{ km}^2$ at Borgharen, see Table 2.8). Assuming that all sediment settles

in the different reservoirs, it may be concluded that the reduction in sediment supply to the Meuse River due to these reservoirs is between 5 and 10%. Probably however only a part of this sediment will settle in the reservoirs, as apparently the reservoirs are relatively small.

Table 2.7
Some characteristics of the reservoirs in the tributaries of the Meuse River

| Reservoir name | Year of completion | Tributary | Upstream catchment area (km ²) | Volume of the reservoir (10 ⁶ m ³) |
|-------------------------|--------------------|-------------|--|---|
| La Gileppe | 1876 | Gileppe | 54.0 | (13.3) |
| | 1971 | Gileppe | 54.0 | 26.4 |
| La Vesdre | 1949 | la Vesdre | 106.0 | 25.0 |
| L'Ourthe | 1958 | l'Ourthe | 740.0 | 3.0 |
| Le Ry de Rome | 1974 | Ry de Rome | 10.1 | 2.2 |
| L'Eau d'Heure | 1978 | Eau d'Heure | 79.0 | 14.8 |
| La Warche (Robertville) | 1929 | La Warch | 118.0 | 11.0 |
| La Warche (Butgenbach) | 1932 | La Warche | 72.0 | 7.7 |
| La Vierre | 1965 | La Vierre | 242.0 | 1.3 |
| L'Ambleve | 1970 | L'Ambleve | - | 17.0 |
| <i>Total</i> | - | - | 1421.1 | 108.4 |

Source: Ministry of Public Works, Belgium (1985)

Table 2.8
Catchment area of Meuse River for some locations along the river

| | Distance to source (km) | River chainage (km) | Catchment area (10 ³ km ²) |
|-----------|-------------------------|---------------------|---|
| Borgharen | 631 | 16 | 21.3 |
| Lith | 812 | 200.8 | 29.4 |

Source: Breukel et al (1992)

◆ *Barrages in the Meuse River*

In the 19th but in particular in the 20th century many barrages were built in the Meuse River. In The Netherlands in total 7 barrages are present, one in Borgharen (upstream from the Grensmaas) and six downstream of the Grensmaas (Linne, Roermond, Belfeld, Sambeek, Grave and Lith). Though these barrages will induce upstream sedimentation during low-flow conditions, their overall effect on the morphology of the river will be small. They might have a substantial effect on the sediment transport pattern though.

◆ *Gravel mining and subsidence due to coal mining*

In the past substantial gravel mining has taken place in the main channel of the Meuse River, in particular in the area near Roermond and in the Grensmaas. In 1970 this mining was stopped and at present gravel and sand mining is only taking place in pits in the floodplain separate from the main channel. The effect of the gravel mining however has been serious and is most noticeable as degradation of the main channel over the last decades. Similarly subsurface coal mining has resulted in subsidence of a reach of considerable length of the Grensmaas near Meers (km 30). Also this will have resulted in upstream degradation. The total effect at Borgharen is a fall in water level of several metres.

◆ *Recent river improvements in Belgium*

Over the last decades additional works have been carried out in Belgium to upgrade the navigation route. Within this framework the Meuse River upstream of Namur was deepened by about 3 m, allowing now for ships up to 2000 ton. The effect however is that this river reach is now acting as a sediment trap, reducing the amount of sediment entering the downstream reaches.

In summary it can be stated that the overall effect of human interference has resulted in the Meuse River being an incised river which only floods occasionally its floodplain. At the same time the sediment supply to the downstream river reaches has been reduced considerably to the extent that the river hardly transport any bed material load across the border at Eijsden. At the same time though the wash load content of the river has increased substantially (Micha and Brolee, 1989). Due to the reduced upstream sediment supply and the degradation of the river over the last century the armouring of the river might have increased. For this, however, no evidence is available.

Chapter 3

Downstream fining of sediments

3.1 Introduction

This chapter discusses different processes contributing to downstream fining of sediments, in particular the mathematical description of them. It begins with an overview of a number of gravel-sand transitions from all over the world. In addition some information on the processes including comments on the different phenomena involved is given. Subsequently the equations relevant for unsteady sediment transport with uniform material are summarised. Next, the abrasion process, local level controls and selective transport of particles are discussed in some detail. Finally, the mathematical modelling of sediment mixtures is discussed to some extent but solution techniques are not included.

3.2 Some observation on downstream fining

Downstream fining is the term used to describe the gradual reduction, in downstream direction, of the mean size of bed material in gravel-bed rivers (Hoey and Ferguson, 1994). It is an almost universal feature of rivers and in many cases it is followed by an abrupt change to a sand bed. Table 3.1 shows some examples of rivers with downstream fining of sediments and the associated main features.

Table 3.1
Main features of gravel-sand transitions in some rivers.

| River | Country | Median Grain Size Before / After (mm) | River Chainage Before / After (km) | Slope Before / After (m/km) |
|--------------------|------------------|---------------------------------------|------------------------------------|-----------------------------|
| Siret | Romania | 5.0 / 0.3 | 566 / 578 | 0.10 / 0.020 |
| Bollin | England | 7.4 / 1.1 | 26 / 35 | ? |
| Ok Tedi-Fly | Papua New Guinea | 31.0 / 0.2 | 140 / 150 | 1.0 / 0.10 |
| Milk | Canada | 12.3 / 0.3 | 214 / 273 | ? |
| Lower Fraser | | 42.0 / 0.4 | 84 / 125 | 0.48 / 0.05 |
| Sunwapta | | 8.2 / 0.3 | 21 / 22 | 4.5 / 0.6 |
| Beauty Creek | | 6.0 / 0.3 | 7.7 / 8.0 | 4.0 / 0.05 |
| North Saskatchewan | | 7.2 / 0.3 | 888 / 909 | 0.19 / 0.35 |
| South Saskatchewan | | 7.9 / 0.2 | 940 / 965 | 0.10 / 0.10 |
| Red Deer | | 37.4 / 0.3 | 524 / 549 | 0.35 / 0.30 |
| Kinu | | Japan | 17.0 / 0.9 | 53 / 58 |
| Nagara | 25.0 / 1.1 | | 14 / 16 | 0.5 / 0.2 |
| Sho | 27.0 / 1.8 | | 19 / 24 | 2.0 / 0.5 |
| Kiso | 37.0 / 0.6 | | 19 / 20 | 1.0 / 0.2 |
| Watarase | 28.0 / 0.7 | | 20 / 22 | 1.0 / 0.6 |
| Allt Dubhalg | Scotland | | 14.6 / 0.5 | 2.6 / 2.8 |
| Endrick | | 6.6 / 0.6 | 34 / 35 | 0.16 / 0.03 |
| Tulla | | 13.9 / 0.6 | 14.5 / 14.9 | 3.0 / 0.4 |
| Meuse | The Netherlands | 16.0 / 2.6 | 90 / 105 | 0.48 / 0.10 |

Source: Sambrook Smith and Ferguson (1995).

Downstream fining can occur due to three different mechanisms or a combination of them: abrasion and break down, local level controls and selective transport of particles. In the abrasion process, particles are reduced in size by wear either during transport or by in situ conditions. It can be

produced by chemical or physical actions; in the former the reduction in size is due to the reaction of the minerals present in the grain with the chemical agents diluted in the water or introduced in the bed due to the activity of plants. The latter, the physical abrasion is caused in general terms by the collision of bed-load gravel particles with a gravel bed.

Local level control occurs by human action or by natural conditions. An example of downstream fining due to human action is the pattern of deposition in a reservoir, where coarse sediments are deposited in the tail of the reservoir and finer sediments are transported further downstream near the dam. In nature, downstream fining can be produced in rivers when the main channel induced a water level control in its tributaries. Tectonic movement (uplift or subsidence) can also induce downstream fining by means of changes in the bed slope inducing the selective transport of particles. However the presence of tectonic movement is not a necessary condition for the downstream fining as suggest the examples of the Red Deer River and the Milk River among others.

Selective transport of sediments produces two different phenomena, deposition and armouring. Deposition is typically the case for aggrading systems where the coarse sediments are settling; this sedimentation in the downstream direction is due to the natural change of slope produced by the concave profile generally present in rivers. Armouring is generally related to degrading systems and it is produced when the finer sediments are being transported whilst the coarse ones remain in the bed. Hoey and Ferguson (1994) also mention that recent investigations into the development of coarse surface layers in gravel bed rivers have suggested that the degree of surface coarsening is inversely related to the rate of sediment supply from upstream. They extended this argument to a river reach, suggesting that the degree of downstream fining may also decrease as the input sediment feed rate increases and reduce the degree of size selectivity in the bed load transport process.

Each of these mechanisms mentioned above is discussed in more detail manner hereafter. First, however it is convenient to look at unsteady sediment transport phenomena in the particular case of uniform material.

3.3 Unsteady sediment transport with uniform material

Sediment transport in rivers in unsteady conditions is a difficult task of fluvial hydraulics. The essential difficulty of dealing with this phenomenon is the present limitation in making a satisfactory quantitative description of the sediment transport process. However, the set of equations of motion is a useful tool to describe this process and they are confronted to three factors: sediment transport and friction factor formulas give notoriously unreliable predictions; sediment transport mechanisms are often quite simplified in modelling systems; and numerical solution algorithms are often quite crude, introducing errors and possibly leading to marginally stable results. In the case of one-dimensional modelling in a wide channel with small gradient, the equations of motion in conservative form are (Jansen, 1994):

$$\frac{\partial h}{\partial t} + \frac{\partial (uh)}{\partial x} = 0 \quad (3.1)$$

$$\frac{\partial (uh)}{\partial t} + \frac{\partial}{\partial x} \left(u^2 h + \frac{gh^2}{2} \right) + gh \frac{\partial z_b}{\partial x} + gh i = 0 \quad (3.2)$$

$$\frac{\partial z_b}{\partial t} + \frac{\partial s_t}{\partial x} = 0 \quad (3.3)$$

where:

| | |
|-------|--|
| g | : acceleration due to gravity; |
| h | : mean water depth; |
| i | : mean slope of energy slope; |
| s_t | : total sediment transport per unit width (bed material load); |
| t | : time coordinate; |
| u | : mean water velocity; |
| x | : coordinate in flow direction; |
| z_b | : bed level above some datum of reference; and |

Equation (3.1) and (3.2) are the continuity and momentum equations of water, respectively, and Equation (3.3) represents the continuity equation for the sediment. In this Equation (3.3), the sediment discharge may be estimated by any sediment transport formula. Sometimes it advantageous to simplify these sediment transport equations to an empirical power function of the flow velocity with the form:

$$s_t = m u^n \quad (3.4)$$

where m and n are empirical constants for which the values depend on the sediment properties. Sediment predictor formulas like Engelund-Hansen or Meyer-Peter & Müller can be fitted into Equation (3.4).

Equations (3.1) through (3.3) are a set of non-linear hyperbolic partial differential equations and closed-form solutions are available only for idealised cases. They are solved by numerical schemes in either uncoupled or coupled form. Several examples of the solutions and applications of this set of equations can be found in the literature (Cunge et al, 1980; Abbott and Cunge, 1982; Bhallamudi and Chaudry, 1991; Jansen, 1994 among others).

3.4 Abrasion process

Abrasion can be produced by physical or chemical actions. Different mechanisms are involved in these actions and some of them are discussed. Moreover, the results of the some laboratory experiments are discussed hereafter.

3.4.1 Mechanisms of abrasion

The reduction in size of an individual particle along the length of a river can be explained by means of the abrasion process. Our understanding of this process has been notably improved during the last five decades; nevertheless, there is still a lack in knowledge on the different mechanisms involved in it. Authors like Krumbein (1941), Plumley (1948) and Kuenen (1956) in the forty's and fifty's, or more recently Parker (1991a), Mikoš (1993) and Gölz (1986) in the ninety's, have studied these mechanisms in different ways. Kuenen (1956) distinguishes seven different mechanisms. They are discussed hereafter:

1. *Splitting or breaking*. Refers to the breaking of a particle into two or three parts of roughly equal size; the two or more new pieces will fall approximately in the same size class as the original one. Kuenen considered it highly improbable that splitting occurs during the transport of particles in natural streams.

2. *Crushing*. Small particles caught between two large ones are likely to be pulverised during fluvial transport. This action is denominated crushing and it produces material of an entirely different size class.
3. *Chipping*. The loss of small flakes from sharp edges is named chipping. In this process, only the original large particle remains as a pebble (or a sand grain). Chips from pebbles become part of the sand fraction and chips from sand part of the silt or clay sizes. Chipping is predominantly present in the first kilometres of the river and occurs when particles are rolling over a pebbly floor; after the most protruding edges have been chipped off, the process must gradually come to an end. Experiment shows that all sharp-edge pieces of whatever type of rock tend to chip.
4. *Cracking*. This is related to the development of small cracks on the surface of particles that have rolled on a pebbly floor. These cracks are due to the knocks sustained by the pebbles as they roll over the bottom; in contrast with the chipping process, the cracks die out in the body of the pebble and hence, they cannot loosen a flake. However, small wedges become detached between neighbouring cracks and drop out producing loss of weight, but much more slowly than by chipping. Cracking continues as long as the pebble rolls on pebbles.
5. *Grinding*. It is the rubbing of particles as they roll over each other, are pressed together, or are pushed completely along other ones. The result is the production of impalpable dust (wash load) and slow change in size and shape of the rubbing particles. There may or may not be small particles involved as abrasive; if so, these will frequently be crushed in the process.
6. *Chemical attack*. This corresponds to the weathering and solution of particles when they are in or outside the streambed. Chemical attack is favoured by a warm sub-humid climate and it could be an important process as Bradley (1970) showed in his study.
7. *Sandblasting*. In this mechanism the pebbles are stroke by sand particles flowing in suspension at high velocities. Sandblasting is not significant for pebble sizes; only boulders can remain stationary in a current with sufficient velocity to produce sandblasting.

Naturally, the relative importance of each of these mechanisms varies according to the circumstances. For instance, no crushing and little grinding can occur when only rounded particles are present, leaving cracking as the dominant agent. Adding sand to the flow, there will be some crushing and grinding as well, but less intensive cracking. The case of chipping is limited to the first kilometres of rolling (2-10 km roughly).

3.4.2 Laboratory experiments

Two different research devices have been used so far for abrasion experiments of river sediments in a laboratory: the tumbling mill and the circular flume. Krumbein (1941), Abbott and Peterson (1978), Kodama (1992), Mikoš (1993) and Schröter (1995) among others have used the former and specially Kuenen (1956) has used the latter. Discussions are still going on about which device better represents the conditions of fluvial abrasion. The principal objection to the tumbling mill is the precise determination of the real distance that the particle travels inside the mill. However, Mikoš (1994) argues that this has already been solved and preference should be given to the tumbling mill. Hereafter, two different results will be presented: first, Kuenen's results from a circular flume and second, Abbot and Peterson's results from a tumbling mill.

Kuenen did his experiments in a revolving current as he denominated his laboratory facility. He found that the lost of weight for quartzite, quartz porphyry and vein quartz, on an average, is only 0.021 percent per kilometre when they roll over a sand bed. However, when they are rolled on a pebbly floor (or on a gravel floor), it is 0.12 percent per kilometre. This limited abrasion on a sandy bed, is one of the most important results of his experiments. It shows that measurements in nature of

the degree of rounding over a given distance are of limited value if the nature of the bed, either sandy or gravelly, is not determined at the same time. Moreover, he mentioned that if the same clast were rolled over a gravel bed and over a sand bed, the abrasion on the gravel bed would be about five times greater than on the sand bed. He also studied the relevance of different parameters like weight, velocity and some other. Table 3.2, extracted from Kuenen's paper, summarises his observations.

Table 3.2
A) Importance of different abrasion mechanisms.

| Mechanism | Sandy bed | Pebbly bed | Floodplain |
|------------------------------------|-------------------------|------------------------------------|------------------------------|
| Splitting | | Very rare | Occasional (frost, chemical) |
| Crushing | | Small grains between large ones. | |
| Chipping | Minor over first few km | Dominant over first 2-10 km. | Insignificant |
| Surface cracking | | Major | |
| Grinding | Major | Minor | |
| Sandblasting | Insignificant | Minor and only at high velocities. | |
| Chemical (solution and weathering) | Slight (limestone) | Slight (limestone) | Significant |

B) Importance of different factors in the abrasion process

| FACTORS | |
|------------|--|
| Weight | Major influence on pebbly bed, small on sandy bed. |
| Velocity | Minor influence on medium to large pebbles; more influence on small pebbles. |
| Rock type | Major influence; chert is highly resistant; quartz, quartzite, quartz porphyry are resistant; graywacke, plutonic rocks, dense volcanics, some limestones are less resistant; other limestone, sandstone, lava, gneiss, schist, glass have small resistance. |
| Roundness | Great loss shown by angular material on pebbly bed (chipping); increase of roundness slows down all types of abrasion. |
| Sandy bed | Slight abrasion. |
| Pebbly bed | Strong abrasion, addition of sand reduces by 10-15 percent. |

Source: Kuenen (1956).

Striking features in Kuenen's results are that the clast's weight is not an important parameter on a sand bed and that the velocity has a slight influence too. On a pebbly floor the inclusion of sand produces a reduction on the abrasion of about 10 to 15 percent. The rounder the particle is, the slower it moves. Figure 3.1 and 3.2 show Kuenen's result on a pebbly floor for a number of angular rock fragments.

In contrast with Kuenen, Abbott and Peterson (1978) did their experiments in a tumbling mill and the dominant mechanisms in their experiments were chipping, cracking and grinding. They performed tests for a dozen of different rock types; Figure 3.3 shows their results. Based on these results, they developed an abrasion durability scale, which is presented in Table 3.3.

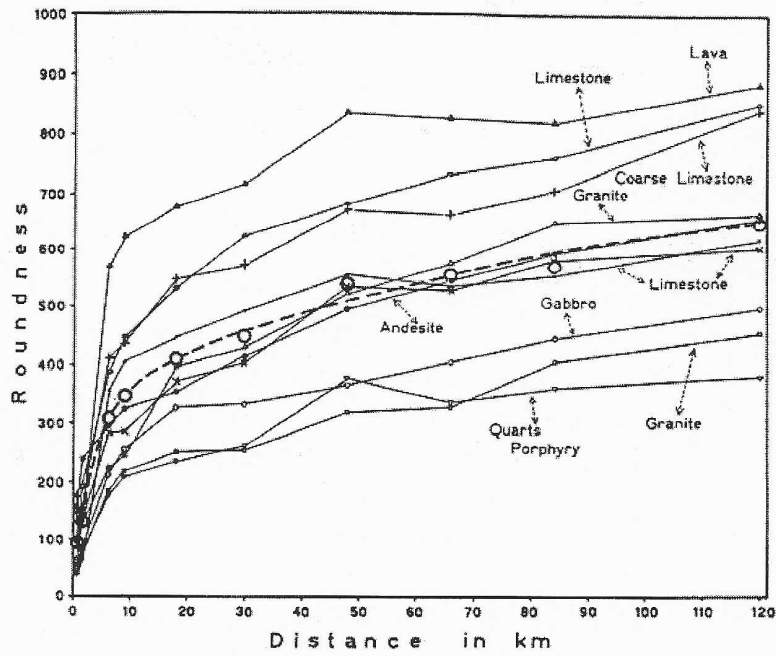


Figure 3.1 Roundness against distance of travel on a pebbly floor.
Source: Kuenen (1956).

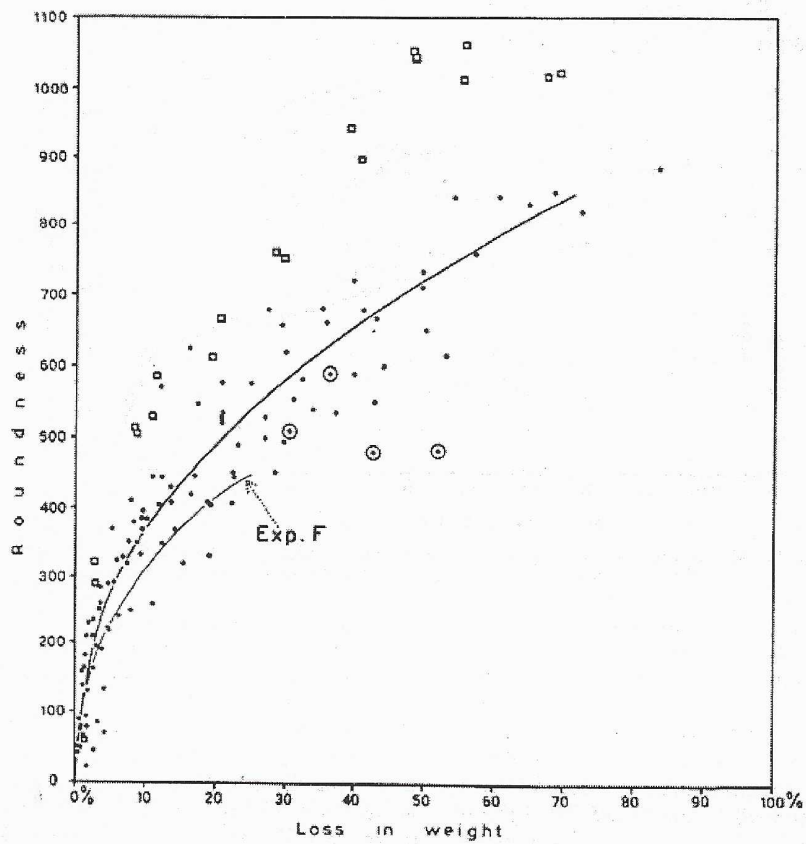


Figure 3.2 Loss of weight against roundness on a pebbly floor.
Source: Kuenen (1956).

Table 3.3
Abrasion durability scale

| ↑ Increasing durability | Clast type | Durability |
|--|--------------------------------------|--------------|
| | Chert Quartzite Poway Rhyolite | Ultradurable |
| Metabreccia Obsidian Metasandstone | Durable | |
| Gneiss Granodiorite Gabbro Basalt | Moderately durable | |
| Marble Schist | Weakly durable | |

Source: Abbott and Peterson (1978).

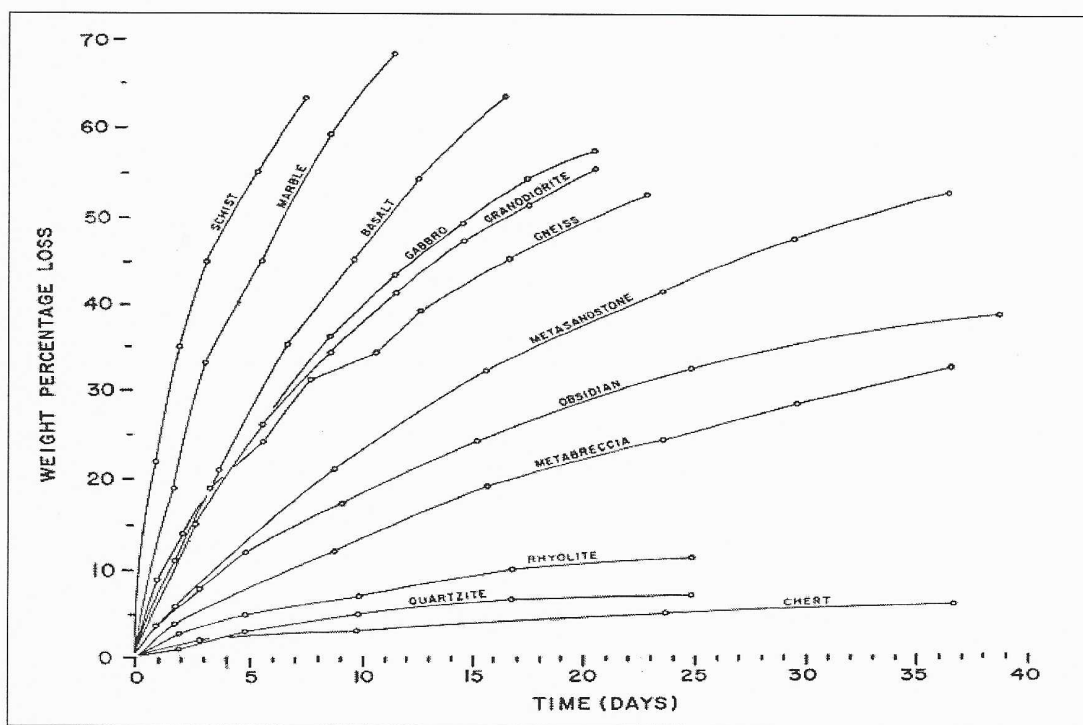


Figure 3.3. Abrasional weight losses for monolithologic clast populations.

Source: Abbot and Peterson (1978).

Abbott and Peterson (1978) also evaluated changes in rates of weight loss due to abrasion occurring when the pebbles are tumbled with rock fragments of different durability. They concluded the following:

- ◆ When rock types of different abrasional durability are tumbled (or transported) together, those with weaker durability are eliminated more quickly, and, conversely, those with greater durability are transported farther than if they would have travelled in a population of clasts with the same durability.

- ◆ In a population of mixed clast types tumbled for a short time (equivalent to a short distance of transport), the resulting clast assemblage resembled the original population (equivalent to source area composition).
- ◆ Conversely, in a population of mixed clast types tumbled for a long time (equivalent to a long distance of transport), the resulting clast becomes different from the original. Thus, the most durable rock types, forming only a small proportion of the original population, predominated to a marked degree in the final assemblage.

A final remark concerns the work of Plumley (1948). In his field study on the Black Hills terraces, he found the following order of resistance to abrasion in gravel streams: chert, quartz, and quartzite, metamorphic, limestone, and sandstone as least resistant. This scale is in accordance with the rock type and as the reader can infer, it follows the same sequence as the two scales mentioned before.

Adding up, in principle these two set of experiments give a good impression of the influence that abrasion has in the reduction of clast size and allow us to assess the relative importance that it could have in a specific case. According to Kuenen (1956), however, the travel distance required for the same degree of abrasion in nature is about four times that in the experiments. He argued that this is probably caused by the presence of a sandy bottom in the rivers. Apparently, still some uncertainties remain.

3.4.3 Mathematical description of abrasion

Until now fluvial abrasion has not been measured directly in the field. As a substitute, typically gravel has been placed either in a tumbling mill or in a circular flume. Based on tumbling mill results, Parker (1991a) developed a mathematical framework for the abrasion process in order to incorporate it into a mathematical model of downstream fining.

He assumed that the dominant mode of bed-load transport is saltation. He also considered quasi-equilibrium conditions where the flow and sediment transport fields may vary in time and in space, but the respective scales of variation are very much larger than the time and length interval associated with a single saltation.

In the case of a single rock type, two modes of abrasion were considered; abrasion of bed-load particles as they strike the bed, and in-situ abrasion of bed-surface particles as they are struck, in other words, he only considered the grinding process. Under the above conditions and for particle in the grain size class j , he derived to the following expression (see Appendix 1 for more details):

$$\tilde{A}_j = s_b \left[\frac{1}{3 \ln(2)} \frac{\partial}{\partial \phi} (\beta^* f_j) + \beta^* f_j \right] + s_b \left[\int \beta^*(\phi') f_j(\phi') d\phi' \right] \left[\frac{1}{3 \ln(2)} \frac{\partial F_{ae}}{\partial \phi} + F_{ae} \right] \quad (3.5)$$

where:

- \tilde{A}_j : abrasion rate for the grain size j in terms of volume of material lost to abrasion/time/bed area/ ϕ ;
- D : grain size in terms of equivalent diameter = $2^{-\phi}$;
- F_{ae} : equivalent areal content density of grains exposed on surface;
- s_b : volume bed-load transport rate/width/time;
- β^* : particle abrasion coefficient;
- f_j : percentage of the size fraction j available in the bed load;
- ϕ : grain size on logarithmic ϕ -scale in the bed load ($\phi = -\log_2(D)$); and
- ϕ' : grain size on logarithmic ϕ -scale in the surface layer.

In Equation (3.5), the first term, on the right hand side represents the abrasion rate for bed-load particles and the second term represents the abrasion rate that bed surface particles suffer due to striking grains of the bed-load.

The abrasion coefficient β^* gives an indication of how quickly particles abrade and it has been estimated by several authors, Table 3.4 shows the values of β^* obtained by Kuenen (1956) in his experiments.

Table 3.4
Value of the coefficient β^* in percentage per kilometre.

| Rock type | Sandy floor | Pebbly floor |
|-------------|-------------|--------------|
| Flint | 0.007 | 0.07 |
| Radiolarite | 0.007 | 0.05 |
| Quartzite | 0.017 | 0.06 |
| Quartz | 0.026 | -- |
| Graywacke | 0.056 | 0.38 |
| Gneiss | -- | 0.65 |
| Limestone | 0.090 | 0.95 |
| Obsidian | 0.081 | 1.00 |

Source: Kuenen (1956).

Gölz et al (1995) developed an exponential equation for the coefficient β^* in the upper part of the Rhine River. The equation takes into account the fact that abrasion is higher during the first kilometres of travelling and allows for a better representation of the phenomena; unfortunately, the equation is only for the case of quartzite and similar expressions for different rock types have not been derived yet.

Finally, including the effect of abrasion in Equation (3.3), we get the following expression:

$$\frac{\partial z_b}{\partial t} + \frac{\partial s_t}{\partial x} + \Sigma \tilde{A}_j = 0 \quad (3.6)$$

for the continuity of sediments where \tilde{A} is considered as the loss of material, which is supposed to contribute to the wash load and which does not anymore have relevance for morphological changes of the river. Loss of material does however affect the downstream bed material load and hence the morphological process downstream.

3.5 Subsidence

Subsidence is a special case of local level control. Local level controls, as previously mentioned, can be produced by human action or by the nature, and they can be induced in the water slope or in the bed slope. Local level controls that affect the water slope are normally taken into consideration as boundary or internal conditions, and have been discussed in many books. Contrary to this, local level controls that affect the bed slope are not often found in books and especially not those related to tectonic movements.

The tectonic movements considered in this study are produced by vertical displacements of the crust plate, either subsidence or uplift; therefore, the local level controls will be referred as vertical tectonic movements herein.

Tectonic movements can be due to tilting, due to uplift or subsidence and due to earthquakes. The formers are usually gradual processes with vertical velocities in the order of millimetres per year or less, but movements due to earthquakes occur quite sudden and can be in the order of meters. These

movements are introduced in the mathematical formulation as changes in the elevation of the bed. In the formulation of Equation (3.3), z_b is used to represent the elevation of the river bed above some datum. Let z_b be divided in two components: the component Γ from the datum up to the layer 1; and the component z_o , from layer 1 up to the river bed as is shown in Figure 3.4.

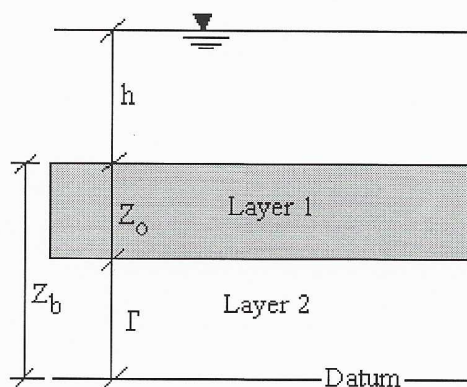


Figure 3.4 Definition sketch for sediment conservation including tectonic movements.

Now, Equation (3.3) can be rewriting in the form:

$$\frac{\partial \Gamma}{\partial t} + \frac{\partial z_o}{\partial t} + \frac{\partial s_t}{\partial x} = 0 \quad (3.7)$$

The first term in Equation (3.7) can be interpreted as the variation in time of the river bed elevation due to vertical movements produced by geological process, either subsidence or uplift. When we neglected this term, Equation (3.7) becomes again equal to Equation (3.3) where $z_o = z_b$ and the reference level is now set up exactly underneath layer 1.

The introduction of vertical movements in Equation (3.3) is not new; one of the first works was done by Parker (1991a). He defined Γ as follows: “ $\Gamma(x,t)$ denotes the ‘elevation’ (distance from the centre of the earth) of a material line of the earth’s crust directly underneath the river”. However, the reference level can be taken in a deep layer where it can be assumed that changes in elevation do not take place. Parker (1991a) also mentions that the variation in time of Γ allows for uplift or subsidence, and the variation of Γ in space allows for differential tectonism, and thus an impose change in river slope. Consequently, the river bed slope “ i_b ” is given by the relationship

$$i_b(x,t) = - \frac{\partial \Gamma}{\partial x} - \frac{\partial z_o}{\partial x} \quad (3.8)$$

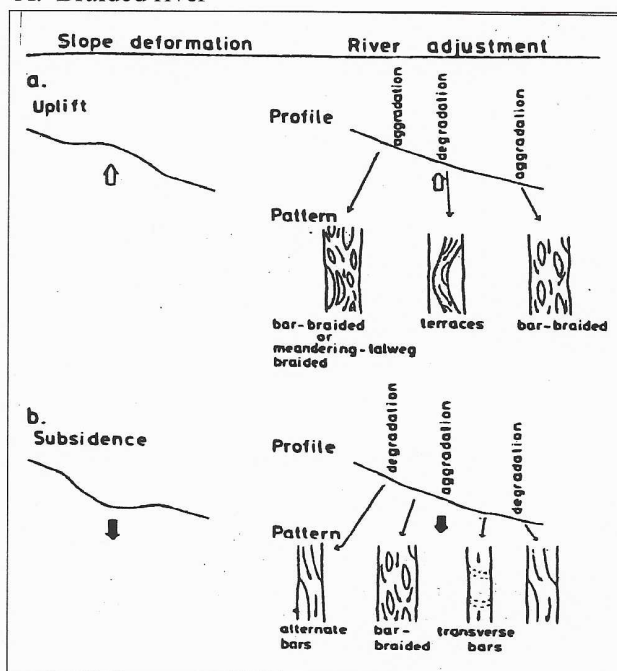
where the function of Γ must be specified independently from the fluvial process. Parker suggest that the effect of tectonism does not enter directly into the relation for mass balance, arguing that the bed slope must be known in order to compute the sediment transport parameters.

Tectonic movements do have an effect on the river planform as well. Uplift and subsidence produce different effects on the morphology of the river. A distinction is made between meandering and braided rivers. Figure 3.5 shows in a simplified way the effects of uplift and subsidence in the river pattern. In summary, changes in slope imposed on the longitudinal profile of a river are compensated initially by changes in sinuosity, so that the slope remains constant. Thus, an increase in slope (subsidence) leads to an increase in sinuosity, and a decrease in slope (uplift) leads to a decrease in

sinuosity. There are limits to the ability of rivers to change in this way. At high sinuosity the incidence of chute and neck cut-offs increase (reducing sinuosity again), and bank erosion and incision ensue. Reduction of slope may lead to meandering rivers experiencing more frequent flooding and developing anastomosed patterns. At both sides of the uplift area aggradation occurs whilst degradation takes place in both sides of the subsiding zone.

Furthermore, Paola (1986) mentions that subsidence induces deposition, while deposition causes downstream fining by selectively removing the coarsest clasts from the flow; and thus areas of rapid subsidence are areas of rapid downstream fining. In general basins that subside slowly near their source areas, transport gravels over relatively long distances compared with basins that subside rapidly near their source areas. In basin with asymmetric subsidence (more rapid at the upstream end and zero at the downstream end) the rate of downstream fining is much greater than in the case of a basin with uniform subsidence (symmetric case). In this latter case, the deposition of gravel is more sensitive to abrasion rate (Paola, 1986).

A. Braided river



B. Meandering river

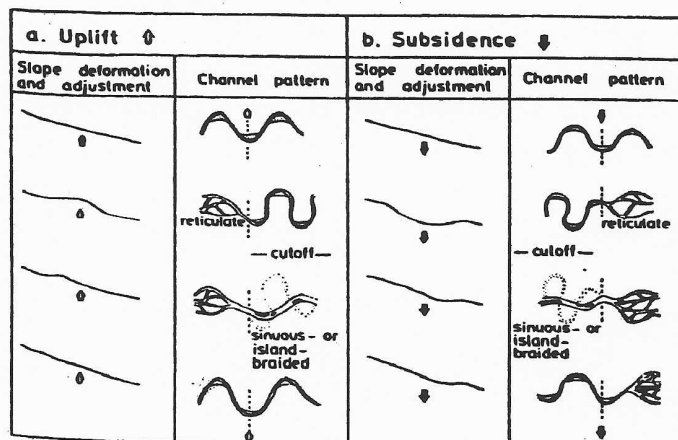


Figure 3.5 Morphological effect of vertical tectonic movements

Source: Miall (1996)

3.6 Selective transport of particles and exchange with the river bed

In the literature, many different sediment transport formulas are available for uniform material. They are used to determine the potential carrying capacity of a specific flow, and they require information on the hydraulic parameters and on the sediment size, represented by one characteristic particle (D_{50} , D_m or another). Since these formulas depend on the particle diameter, it can be inferred that under the same hydraulic conditions, the transport capacity of a smaller particle would be higher than the capacity of a large one.

Therefore, not all the particles present in a river bed will be transported at the same time, but selective transport will take place where the smaller particles are transported first and the bigger ones later. Similar with this, under different hydraulic conditions, big particles are deposited first whilst small ones remain in movement. This selective transport of sediment sizes in a mixture of particles is responsible for the phenomenon that is known as hydraulic sorting. In the case of one-dimensional modelling, it is called longitudinal sorting.

In problems dealing with sediment mixtures, it is essential to take into account the possibility of longitudinal sorting and associated phenomena's like armouring of the bed; therefore, the available sediment transport formulas should be applied to the different size fractions separately. Nevertheless, their application by size fractions cannot be done in a straightforward manner because not all the particles are equally exposed on the river bed. For instances, fine grains in a coarse mixture will be nested in between the coarse grains, so the coarse grains "hide" the finer fractions. On the contrary, coarse grains in a fine mixture will be more "exposed" relative to the flow.

To take into account this "hiding/exposure" of the grains in the uniform sediment transport formulas, researchers have developed correction factors or hiding coefficient. Most of these corrections are in the form of:

$$\xi_j = f\left(\left(\frac{D_j}{D_a}\right)^\eta\right) \quad (3.9)$$

where

- ξ_j : hiding coefficient;
- D_j : characteristic grain diameter of size fraction j;
- D_a : can be the average grain size for which no exposure correction is necessary, or the grain size of the mixture which no needs no correction;
- η : exponent; and
- j : size fraction.

Laguzzi (1993) presents a summary of the different available expressions for the hiding coefficient and she mentioned that most of them have been developed for a specific sediment transport formula. For the case of mixtures of sediments, Appendix 2 shows three different sediment transports predictors, whereby the hiding/exposure effect is taken care in different ways.

Another important aspect in the selective transport of sediments is the interaction among the different size fractions. This interaction is described by means of the mass balance within a thin "active", "surface" or "mixing" layer in which the exchange between the bed and the sediment transport over the bed takes place. Figure 3.6 shows a sketch of it.

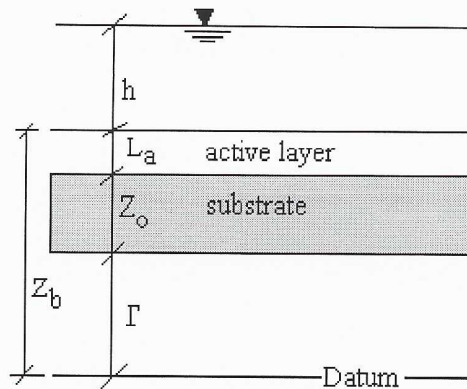


Figure 3.6 Definition sketch for the three layers model.

The so-called “sorting equation” represents the mass balance by grain sizes in this active layer. This equation has the following form:

$$\frac{\partial}{\partial t} (p_j L_a) + \frac{\partial}{\partial x} (s_b f_j) + \frac{\partial}{\partial t} (p_{j0} z_o) = 0 \quad (3.10)$$

where

- L_a : thickness of the active layer;
- s_{bj} : bed-load transport for the size fraction j per unit of width;
- p_j : percentage of the size fraction j available in the active layer;
- p_{oj} : percentage of the size fraction j available in the substratum;
- p_{j0} : percentage of the size fraction j in the interface; and
- f_j : percentage of the size fraction j available in the bed load.

In this equation, the exchange of size fractions occurs through a thin layer called the interface. This interface is located between the active layer and the substratum, while, during degradation there is a direct incorporation of some substratum material into the surface and therefore $p_{j0} = p_{oj}$.

During aggradation, the situation is less clear. Parker (1990, 1991a) suggests the alternatives $p_{j0} = p_j$ and $p_{j0} = f_j$. The former case may be appropriate when low sediment transport rates and slow aggradation provide conditions favouring perfect mixing prior to deposition. The latter, where the value of p_{j0} is set equal to the fraction f_j of the bed load, could occur if the bed load were to be buried as an avalanche face bar migrating downstream. As Parker (1991b) shows, these two alternatives produce very different estimates of downstream fining, with the assumption $p_{j0} = f_j$ preventing any downstream fining during continuous aggradation.

Finally, in gravel-bed rivers the thickness of the active layer L_a is in the order of magnitude of the elements' roughness, generally $L_a = 1-3 D_{90}$; in dune-covered beds, it can be assumed to be half the dune height. In certain cases it can also be estimated as a function of the water depth or as a function of bed shear stress and the median grain diameter. Further information on the dynamics of the active layer can be found in Ribberink (1987), Hoey and Ferguson (1994, 1997) and Armanini (1995) among others.

3.7 Modelling of sediment mixtures

In the previous section, it is mentioned that sediment mixtures should be treated by size fractions. Therefore, the different equations previously presented should be rewritten in order to handle this and

to include the possibility of tectonic movements and abrasion process. Hereafter, the relevant set of equations is presented:

Continuity equation of water

$$\frac{\partial h}{\partial t} + \frac{\partial (uh)}{\partial x} = 0 \quad (3.11)$$

Momentum equation of water

$$\frac{\partial (uh)}{\partial t} + \frac{\partial}{\partial x} \left(u^2 h + \frac{gh^2}{2} \right) + gh \frac{\partial z_b}{\partial x} + gh i = 0 \quad (3.12)$$

Continuity equation of sediments

$$\frac{\partial \Gamma}{\partial t} + \frac{\partial z_o}{\partial t} + \sum \left(\frac{\partial s_{bj}}{\partial x} \right) + \sum \tilde{A}_j = 0 \quad (3.13)$$

Sorting equation of the bed material

$$\frac{\partial}{\partial t} (p_j L_a) + \frac{\partial}{\partial x} s_b f_j + \frac{\partial}{\partial t} (p_{j0} z_o) + \tilde{A}_j = 0 \quad (3.14)$$

Equation (3.11) and (3.12) are the conventional equations for unsteady one-dimensional flow (conform Section 3.2). In the context of movable beds, it is important to notice that the area and the conveyance depends on the variable thalweg elevation, as well as the conveyance dependence on a variable alluvial friction factor as evaluate by an appropriate empirical expression. The density dependence on suspended sediment concentration has been neglected.

Equation (3.13) is the equation for bed material conservation writing by size fraction, but with separate recognition of the roles of tectonic movements, bed-load gradient and abrasion process. This equation can be relaxed through a bed loading law in order to take into account the spatial bed-load delay compared to its equilibrium value. Some of the applicable sediment transport predictors for mixtures are presented in Appendix 2.

Equation (3.14) is the so-called “sorting equation”, it can be recognised as another form of Equation (3.13), but written for each size class j and for an “active layer” control volume of thickness L_a below the bed surface. In this expression, the abrasion process has also been included.

In line with the Equations (3.1) to (3.3), the set of equations defined by (3.11) trough (3.14) can be solved by numerical schemes in either uncoupled or coupled form. A remark should be made regarding the number of size fraction to be used, because increasing the number of size fraction, the computational effort increase also in noticeable amount. Therefore, the user should specify the number of fractions according with the characteristics of the mixture and the aims of the model. See also Khin Ni Ni (1989).

Finally, in the set of Equations defined by (3.11) trough (3.14) the transport of suspended sediment is not considered. To represents this, the advective-diffusive transport equation of suspended sediment for each size class j should be added. Holly and Rahuel (1990a) present the complete set of equation of motion where the role of suspended sediments and its delayed adaptation is considered as well.

Chapter 4

Analysis of the bed material and sediment transport rates

4.1 Introduction

This chapter presents the results of a further elaboration of data on the bed material and on the sediment transport along the Dutch part of the Meuse River, in particular for the reach between kilometres 0 to 145. The analysis is based on the determination of characteristic parameters like D_{50} , median diameter and standard deviations at different locations along the river. The compositions of the armour layers and of the bed material are also studied as well as the development of bimodal composition in downstream direction. Finally, different sediment transport predictors are tested against the available field measurement in order to obtain a suitable tool to predict the sediment transport rates in the Meuse River. The results of this Chapter are needed for later use in Chapter 5 and 6.

4.2 Bed material characterisation

In this section the analysis of the available field data is presented. Different statistical parameters are determined as well as characteristic conditions present in rivers with a gravel-sand transition.

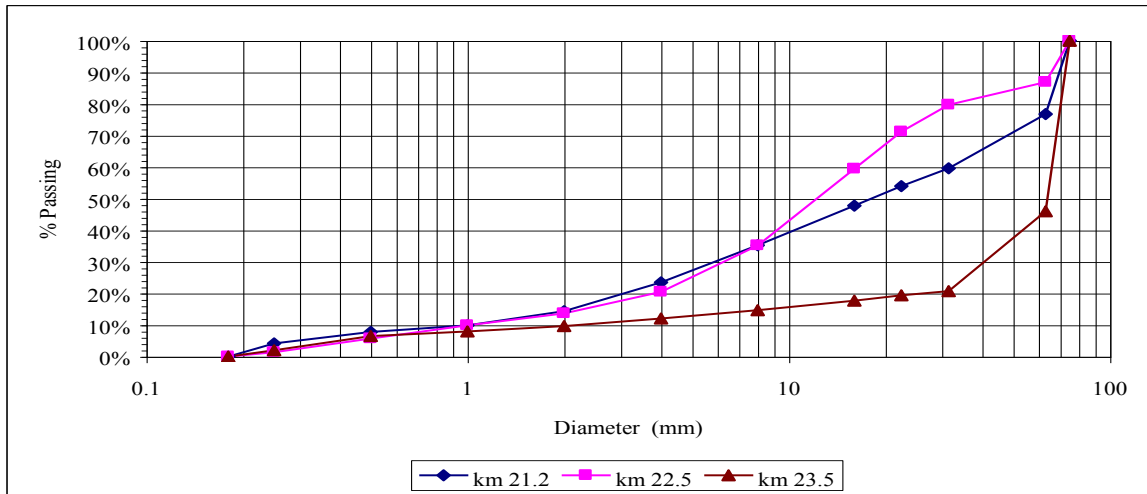
4.2.1 Representatively of parameters used for characterisation

Gravel-bed rivers are not easy to characterise by the few statistical parameters normally used, notably median diameter, standard deviation and D_{50} . Spatial and temporal variation of the sediments deposited may be important. In dry periods, this type of rivers normally present an armour layer while during floods, this armour layer becomes unstable and the underlying material is mobilised. Depending on when and where the samples are taken and the frequency of the sampling, the characterisation could lead to substantially different results. Moreover, due to the geological and morphological evolution of the basin, there may be different lithological conditions along the river. These changes may be present in downstream direction over short distances, and in vertical direction into the river bed. Even along both river banks could also have different type of material. As an example of the spatial variability, Figure 4.1 shows granulometric curves for the bed material (substratum) at different along the Meuse River.

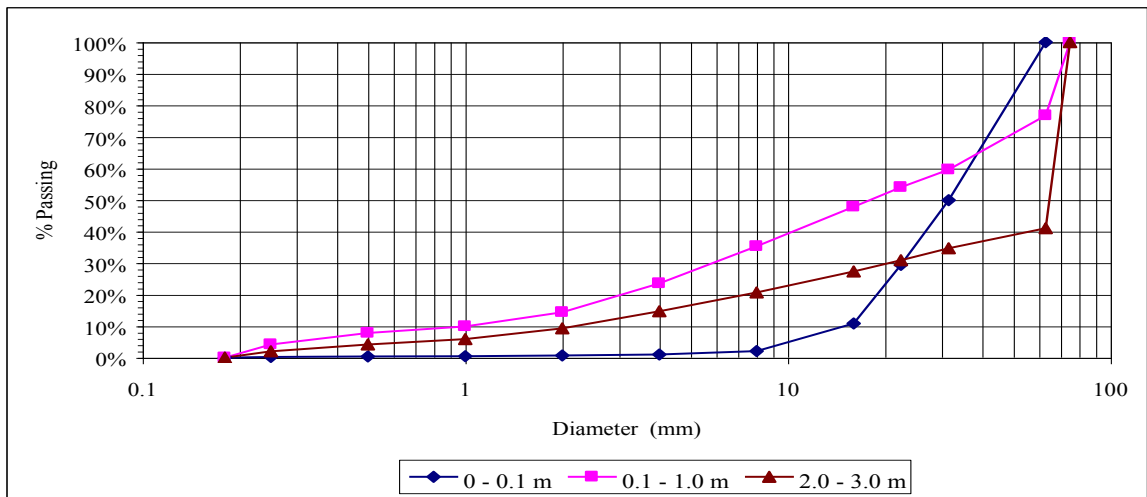
In this figure, it is possible to observe that the bed material presents important variations in the three directions. Figure 4.1A shows the variability of the bed material composition in longitudinal direction (from km 21.2 to 23.5) while Figure 2.1B gives granulometric curves at three different depths (the armour layer and two substrate layers), all of them different and thus providing an example for the variability in vertical direction. Finally, in Figure 2.1C, it is possible to observe the variation in lateral direction. At each location the four curves right, middle, left and average are quite different. These three examples clearly show the longitudinal, vertical and lateral variation of the sediments characteristics and emphasise the difficulty of representing accurately the field conditions as well as the different phenomena involved.

Besides, the difficulty increases when the river has been trained (like is the case with the Meuse River) and the reworking of the bed material has been important. Hence, to characterise a river such as the Meuse River by means of few parameters is not achieved easily and the derived parameters are perhaps not really representative of the real conditions in the field. Probably, a better representation of the field conditions could be achieved by means of the average gravel-sand content of the sediments; in which the percentage of the gravel and sand is presented along

A. Variation of the substratum in downstream direction



B. Variation of the bed material in vertical direction at km 22.2



C. Variation of the substratum in lateral direction at km 110

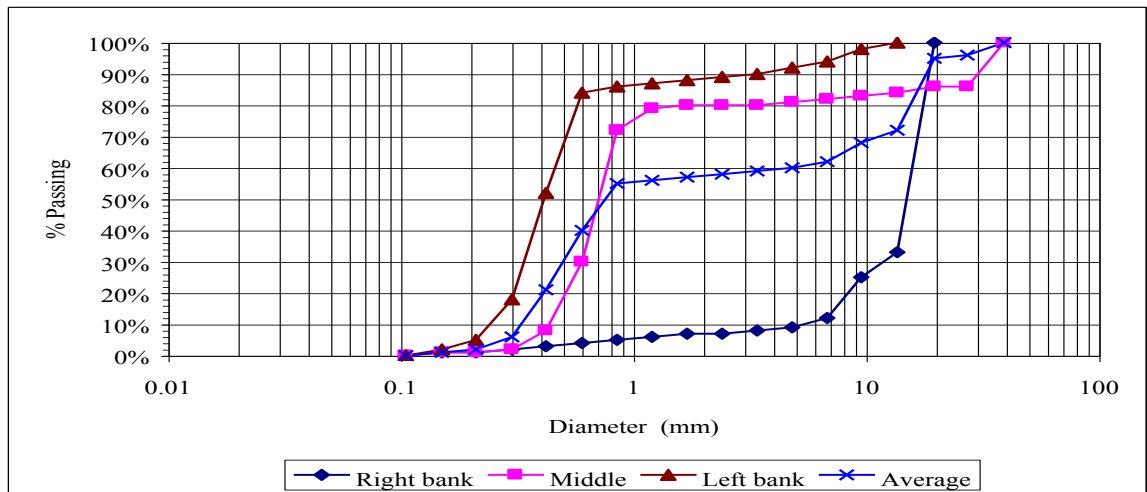


Figure 4.1 Spatial variation of the substratum in the Meuse River.
Data source: Rijkswaterstaat (1983) and Thijssen Comp. (1995).

the river. The reader should be aware of the large variability and while reading this report should keep in mind that dealing with gravel bed rivers, the representatively of the parameters is not as good as in the case of beds with uniform materials.

Nevertheless, the characterisation of the bed material by statistical parameters has been attempted in this study. However, no complete description of the Meuse sediments could be obtained. This would require a separate study, during which also additional field data might have to be collected. In the present characterisation the sources shown in Table 4.1 were used.

Table 4.1
Sources of field data

| Source | Year | Reach (km) | Spacing of Samples | Location of Samples | Sampling Method |
|----------------------|------|----------------------------|--------------------|---------------------|-------------------------|
| Waterloopkundig Lab. | 1981 | Various | 5.0 km | Point bars | Various |
| Rijkswaterstaat. | 1983 | 6.0 – 16.0 54.0 – 226.0 | 1.0 km | Summer bed | Bucket sample from boat |
| Van Manen et al. | 1994 | 15.5 – 52.7 | Specific points | Point bars | Bulk sample |
| Sorber et al. | 1995 | 15.5 – 52.7 | Specific points | Point bars | Bulk sample |
| Thijssen Comp. | 1995 | 20.0 – 25.0 | 200 m | Summer bed | Bore holes |
| Fugro Comp. | 1996 | 84.7 – 98.2 | 400 m | Summer bed | Bore holes |
| Wilkens and Lambeek. | 1997 | Various | Specific points | Summer bed | Field measurements |

Waterloopkundig Laboratorium (1981) present in graphical form information about the sediment characteristics based on data collected during the seventies. The results include some samples collected by the bulk sampling method as well as by the Wolman's method. The Rijkswaterstaat reference (1983) has the most complete spatial distribution of samples, however, the technique employed is not so accurate because it is likely that sediments from both, the armour layer and the substratum, were mixed during the process of taking the samples. The method used is dragging a bucket over the river bed and in this way the depth of sampling cannot be controlled. Here in, it is considered that these samples belong to the substratum material, which might not be correct.

The data presented by Van Manen et al (1994) and Sorber et al (1995) includes separate granulometric curves for the armour layer as well as for the substratum at two different depths. The samples were taken according to the well-known method of bulk samples. Following their nomenclature, in the present study only the (upper) layer 1 of the substratum is considered. The bore hole data given by Thijssen Comp. (1995) and Fugro Comp. (1996) appear to be an adequate representation of the substratum material although the samples can be biased to the finer material. In this study the upper layer reported by them are considered as representative of the substratum material. Finally, Wilkens and Lambeek (1997) present an overview of all available sediment transport measurements in the Meuse River using different devices and represent an extension of the work presented by Duizendstra et al (1994).

4.2.2 Characteristic parameters

The variation of the D_{50} in the bed material (substratum) and its geometric standard deviation are show in Figure 4.2 and 4.3. It is possible to observe that the D_{50} until the km 90 approximately is mainly in the coarse gravel range, the average value of the D_{50} is approximately equal to 16 mm and it is shown in Figure 4.2 with a straight line. There are a few points in this reach which are in the medium sand range but they may be due to problems related to the sampling. From about km 105 onwards, the D_{50} is significant smaller and the average value is about 2.6 mm. In this zone,

there is a lot of scatter in the data and this is reflected by higher values in the geometric standard deviation, probably produced by the bimodality in combination with the lateral sorting. Between km 90 and km 105 approximately, there is a gradual transition in the values of D_{50} . The study of this transition is one the objectives of this study.

An important point is the large values of the geometric standard deviation of the bed material (see Figure 4.3), especially from km 90 onwards. This implies that the correct collections of samples is particularly important in this reach of the river and indicates the necessity of more samples although increasing sampling will not reduce the variability. Rather a better estimate of the average values is better on the basis of more data. It may very well be that the large variation is caused by physical phenomena and is inherent to this type of mixed gravel-sand bed river.

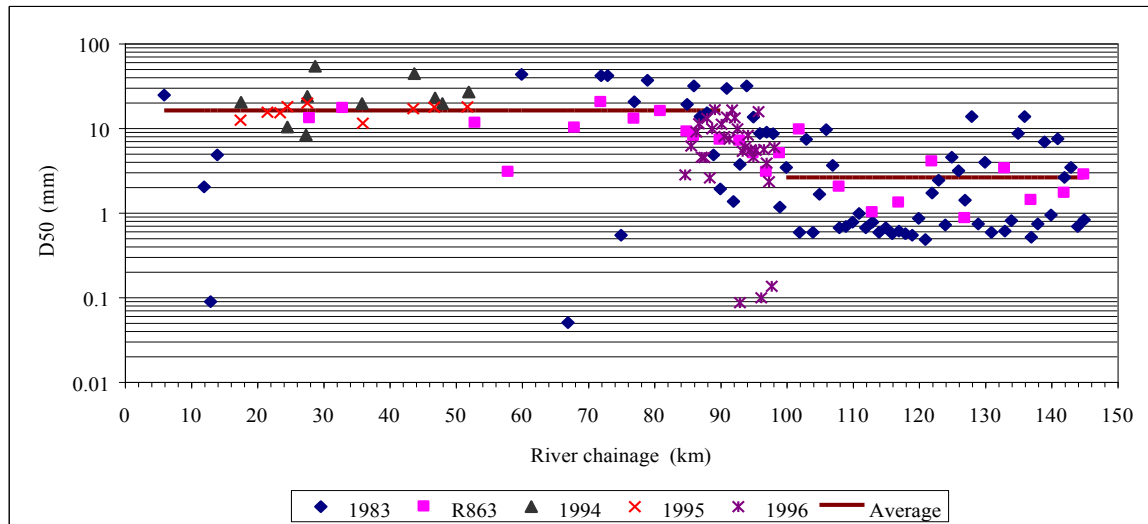


Figure 4.2. Variation of D_{50} (in mm) in the substratum along the Meuse River.
Source: see table 4.1 and legend.

4.2.3 Armour layer and substratum composition

The Meuse River is characterised by armour layers in its upper reaches. This may be linked to the fact that sediment supply from upstream is insufficient and that the river is degrading. It may also be a natural phenomenon inherent to gravel-bed reaches. In Table 4.2, the values of D_{50} for the armour layer and for the substratum (or bed material) obtained during the campaign of Van Mannen et al (1994) and Sorber et al (1995) are shown. It is possible to observe in this table that along this reach the D_{50} of the armour layer is higher than the D_{50} of the substratum. This condition suggests that the river is actually armoured. Appendix 3 contains the granulometric curves for both armour layer and substratum from some locations and in those figures, it can be observed that the active layer is coarser than the substratum. The only two exceptions are Gevenbricht and Koeweide (see Table 4.2, data of 1994). In these two locations the armour layer has a lower value of D_{50} than the substratum. The spatial and temporal variation of these samples is considerable and hence, this different behaviour may be due to problems during sampling or with the samples itself.

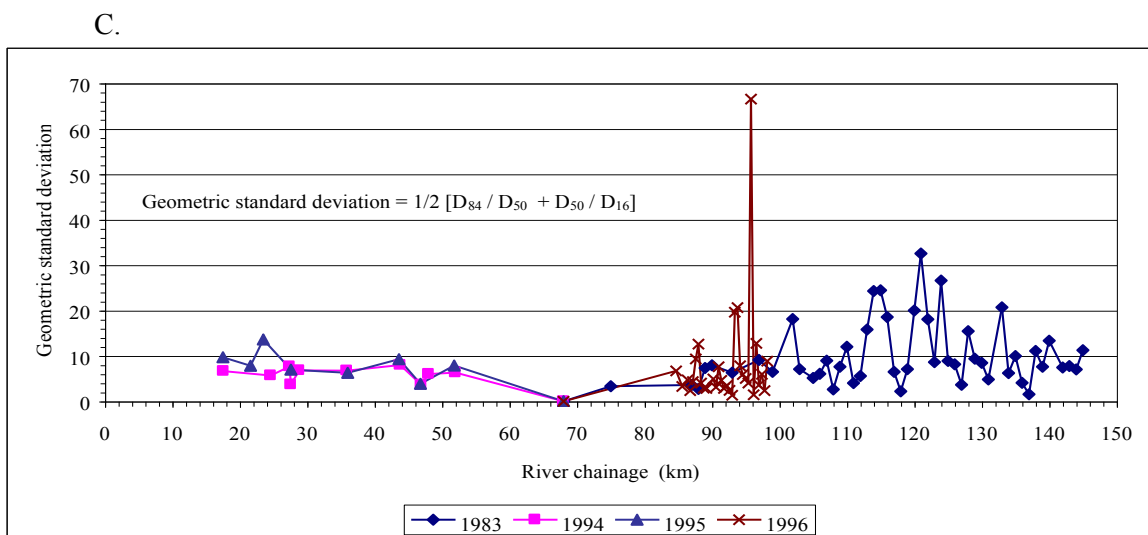
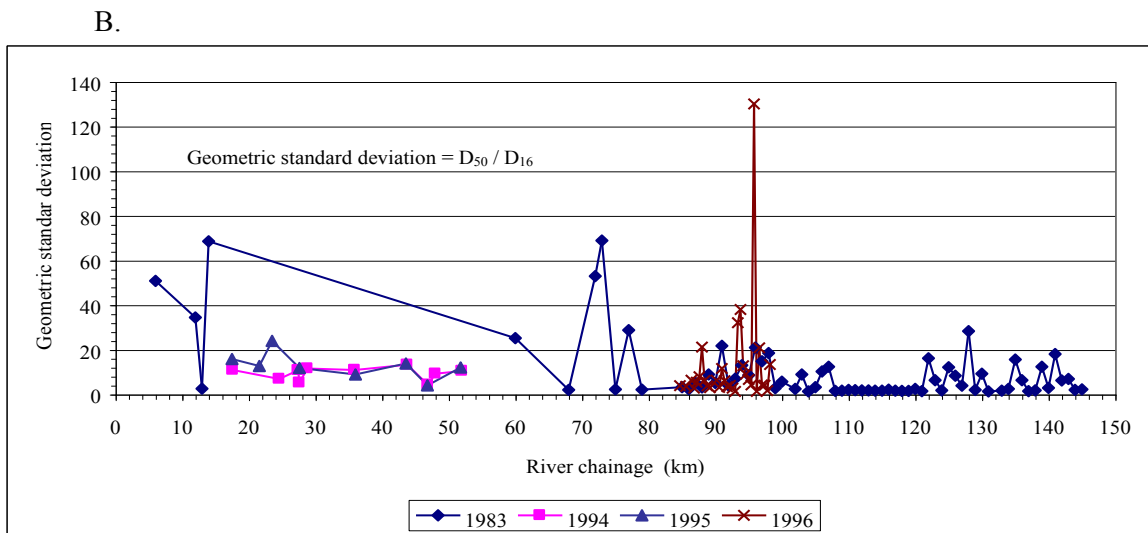
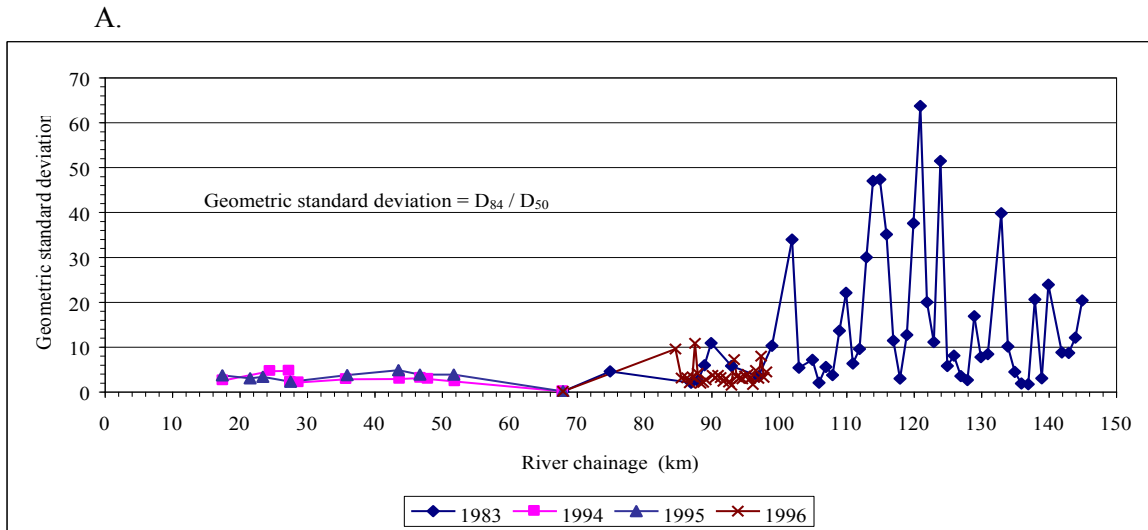


Figure 4.3. Geometric standard deviation of the substratum samples in the Meuse River.
Data source: see Table 4.1 and legend.

Table 4.2.
Values of D_{50} (in mm) of the armour layer and substratum at different locations.

| Location | Van Manen et al (1994) | | | Sorber et al (1995) | | |
|--------------------|------------------------|---------------------------|------------|---------------------|--------------|------------|
| | Reach (km) | Armour layer | Substratum | Reach (km) | Armour Layer | Substratum |
| Borgharen | 17.5 | 33.2 ± 1.6 ⁽¹⁾ | 20.1 ± 6.6 | 17.5 | 29.2 ± 1.9 | 12.3 ± 9.7 |
| Geulle aan de Maas | 24.7 | 56.6 ± 1.6 | 10.2 ± 5.7 | 24.6 | 35.5 ± 1.9 | 17.8 ± 8.6 |
| Elsloo | 27.4 | 30.2 ± 1.6 | 23.5 ± 3.7 | 27.6 | 28.7 ± 2.0 | 19.7 ± 7.0 |
| Leut | 35.7 | 37.2 ± 1.8 | 19.4 ± 6.8 | 36.0 | 36.4 ± 2.2 | 11.4 ± 6.2 |
| Grevenbricht | 43.8 | 39.5 ± 2.2 | 43.8 ± 8.0 | 43.6 | 48.2 ± 3.0 | 16.8 ± 9.2 |
| Koeweide | 46.9 | 20.5 ± 1.8 | 22.5 ± 3.7 | 46.8 | 22.0 ± 2.1 | 17.6 ± 3.9 |
| Roosteren | 51.8 | 32.0 ± 1.8 | 26.4 ± 6.3 | 51.8 | 52.6 ± 2.2 | 17.6 ± 7.8 |

⁽¹⁾ Geometric standard deviation = $\frac{1}{2} (D_{84}/D_{50} + D_{50}/D_{16})$

Source: Wilkens and Lambeek (1997).

4.2.4 Bimodal composition of the bed material

One of the characteristics observed in many transitions from gravel to sand-bed rivers is the development of a bimodal composition of the bed material (i.e. Yatsu, 1955; Sambrook Smith and Ferguson, 1995; Seal and Paola, 1995). The Meuse River is no exception; Figure 4.4 shows the development of a bimodal composition of the bed material with a gap between size 1 and 5 millimetres approximately. This gap in size material has been related to the break down of gravel particles into sand; this specific issue will be covered later on. In Appendix 4, figures similar to 4.4 are presented for other points along the river; the data from which they were derived from coming different sources.

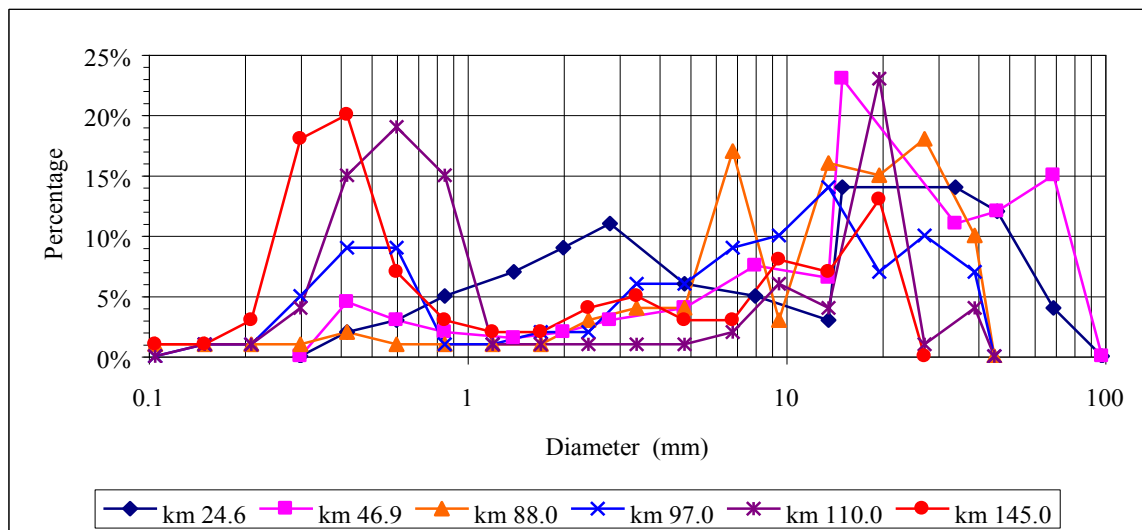


Figure 4.4. Development of the bimodal composition in the bed material (substratum).
Data source: Rijkswaterstaat (1983) and Van Manen et al (1994).

It is also important to notice the transformation of the grain size distribution in downstream direction. In Figure 4.5 the cumulative distribution of the grain sizes at some points is plotted. It is possible to observe that in downstream direction the distributions are shifting towards smaller diameters together with a change in the curve shape, from roughly uniform distribution to a bimodal one represented by the flat area between diameter 1 to 5 approximately.

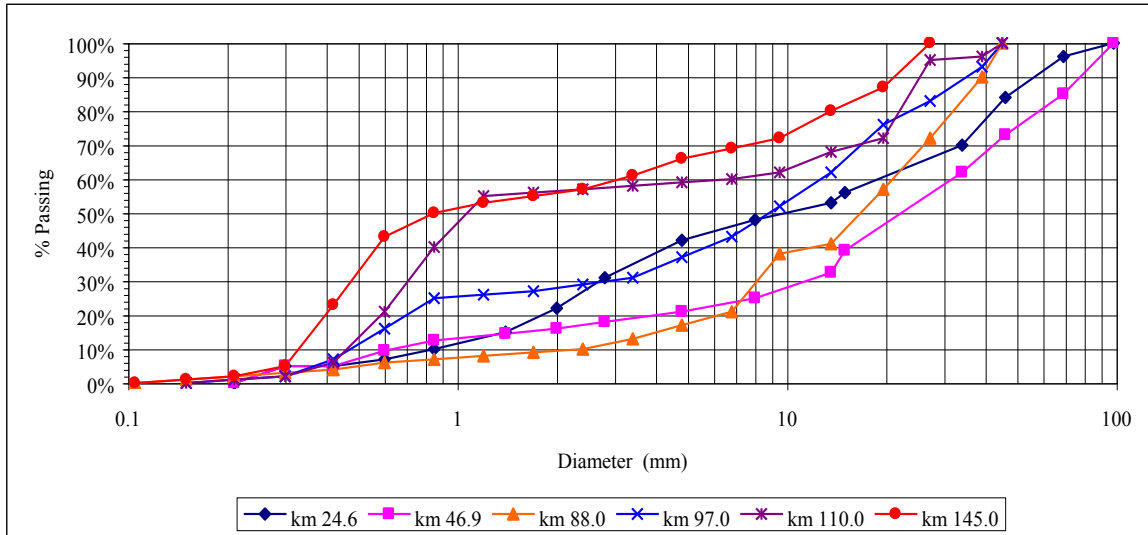


Figure 4.5. Change in granulometric curves of the bed material in downstream direction.
Data source: Rijkswaterstaat (1983) and Van Manen et al (1994).

4.2.5 Median diameter of the bed material

The presence of bimodal composition in the bed material (substratum) makes the D_{50} a sensitive parameter in the characterisation of the sediments of the Meuse River, especially if the D_{50} is within the flat zone of the granulometric curve ($1 \leq D_j \leq 5$ approximately). In Appendix 5 a theoretical analysis of this particular issue is presented and it is possible to observe there that depending on the content of fine sediment the D_{50} could change abruptly with small changes in the gravel-sand content. In such cases of a bimodal composition, the mean diameter (D_m) is more representative for the bed material. However, it is not always possible to determine the values of D_m from the available information; only the data from Van Manen et al (1994), Sorber et al (1995) and Fugro Comp. (1996) could be used. Figure 4.6 shows the computed median diameter for this data. The picture is less complete than Figure 4.2 but appears to be more consistent.

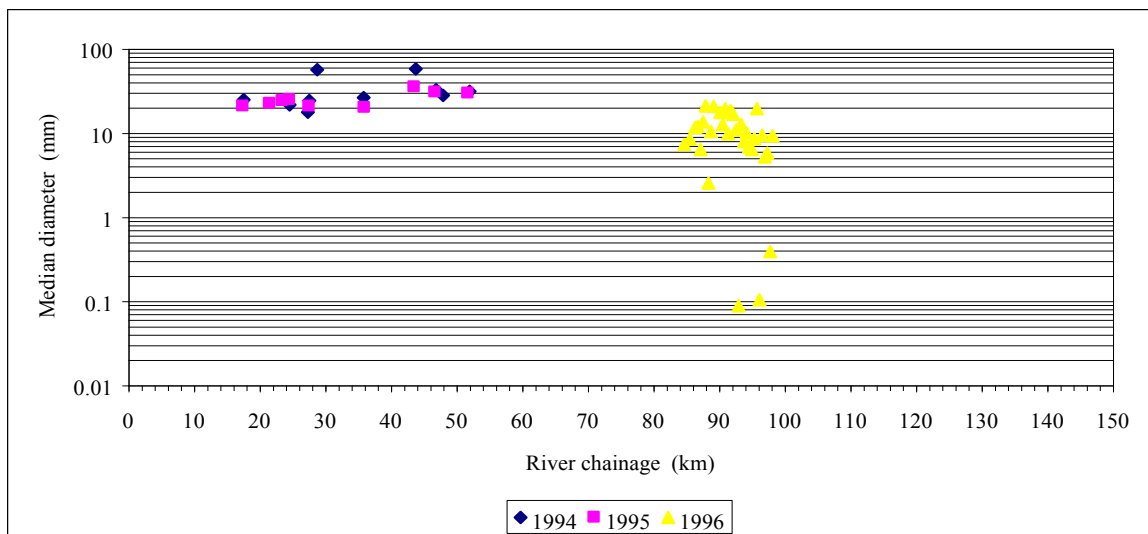


Figure 4.6 Median diameter of the substratum material.
Data source: Van Manen et al (1994), Sorber et al (1995)
and Fugro Comp. (1996).

In view of the impossibility to describe complete the transitions in terms of D_m , the relation between D_{50} and D_m was studied in order to take advantage of the other sources of information. In doing so, two different values of the relation D_m/D_{50} were computed, one for the gravel reach and one for the transition zone.

In the gravel reach the data from Van Manen et al (1994), Sorber et al (1995) were used and the average of the 19 values of D_m/D_{50} analysed was 1.51 with a standard deviation of 0.35. In the transition zone, the average value was 1.53 with a standard deviation of 0.55. The 31 possible relations from the data of Fugro Comp. (1996) were used for this zone.

Considering the total set of relations (50 in total) the average value is 1.52 with a standard deviation of 0.42, which can be a good approximation in the gravel reach and the transition zone. Hence, in principle knowing one the parameters of the substratum material, either D_{50} or D_m , the other one can be computed by the relation $D_m/D_{50} = 1.52 \pm 0.42$ allowing us to utilise all the available information. Nevertheless, the value of the standard deviation is high though, and use of the relation $D_m/D_{50} = 1.52$ will not help in removing the deficiencies of the plot of D_{50} versus the chainage.

4.2.6 Gravel-sand content of the sediments

The gravel-sand content of the sediment is another way to represent the spatial variation of the sediments. Figure 4.7 gives the percentage of gravel ($D_j \geq 2$ mm) and sand ($D_j < 2$ mm) content along the Meuse River. In this figure is possible to notice that the average sand content exceeds the 50% around the kilometre 100 approximately, where is also the reach where the gravel-sand transition occurs.

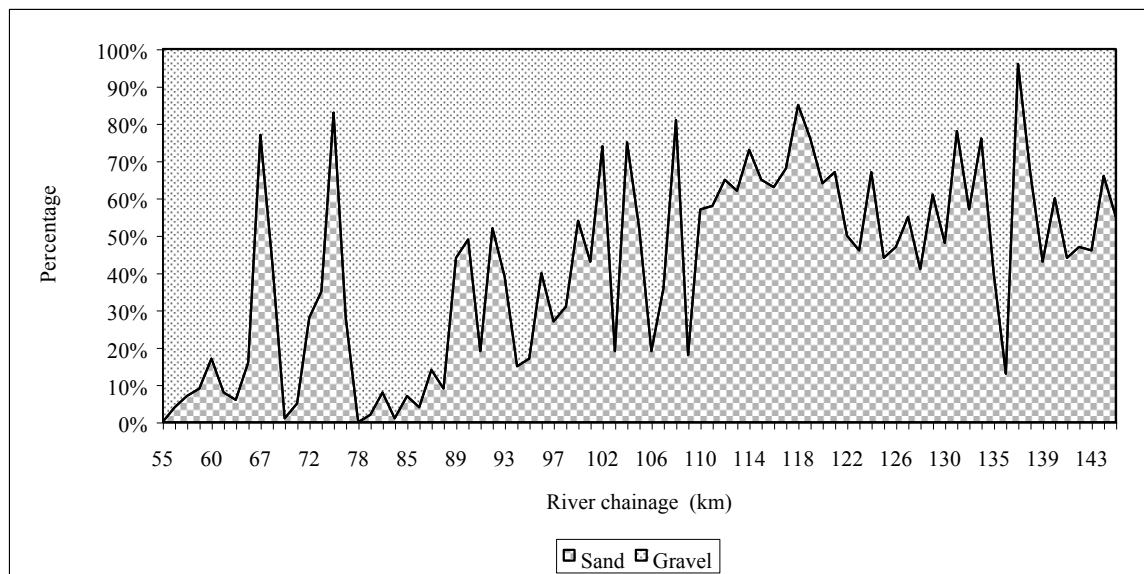


Figure 4.7. Gravel and sand content along the Meuse River.
Data source: Rijkswaterstaat (1983).

In Figure 4.7, two locations (notably around kilometres 67 and 75) two peaks in the sand content can be observed over short distances. These peaks may be produced because of the presence of the barrages of Linne and Roermond respectively, which induce sedimentation during low flow conditions. This however must be confirmed in the field. It is interesting to inspect the spatial variation of the D_{16} , the D_{50} and the D_{84} , since these characteristic diameters give an idea of the gravel-sand content in the bed material, Figure 4.8 presents this information. It is clearly shown in this figure that a sand content of the bed material of 50% is reached around kilometre 100.

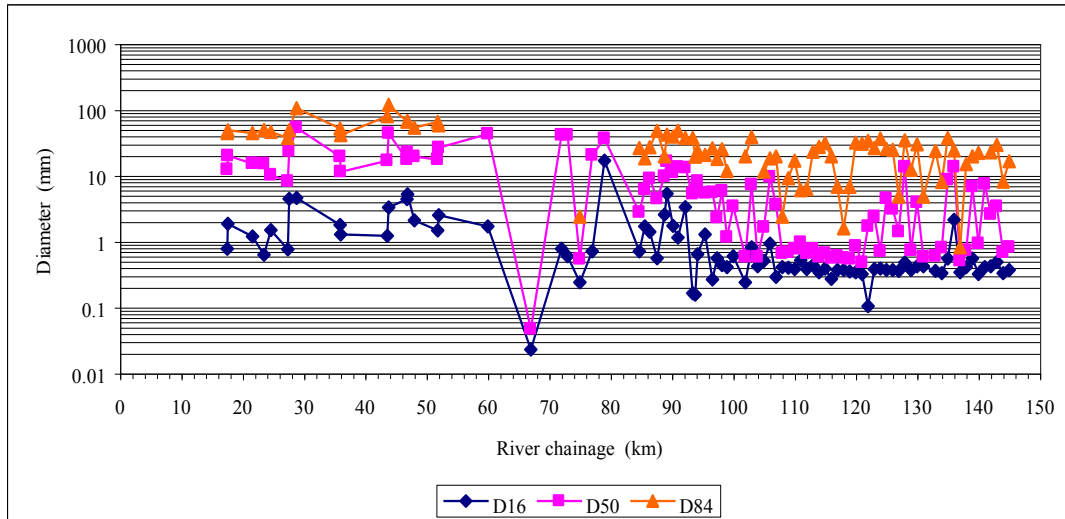


Figure 4.8 Spatial variation of the D_{16} , the D_{50} and the D_{84} .
 Data source: Rijkswaterstaat (1983), Van Manen et al (1994), Sorber et al (1995) and Fugro Comp. (1996)

4.3 Sediment transport rates in the Meuse River

In this section, different sediment transport predictors are tested against the available field measurement. The tests are performed for both reaches of the Meuse River: the gravel-bed and the sandy bed reach. The sediment transport predictors includes the case of the those formulas based in only one characteristic diameter as well as those based on the full grain size distribution which incorporate the hiding coefficient. The results of this section will be used in the next two Chapters of this study.

Regarding the sediment transport rates the Meuse River is not easy to characterise, because there is a great variety of data reported in the relevant literature. Waterloopkundig Laboratorium (1994) reports that the average sediment transport rate of the Meuse River is approximately $35 \times 10^3 \text{ m}^3/\text{y}$; but at Linne it is reported to be about $26 \times 10^3 \text{ m}^3/\text{y}$; $19 \times 10^3 \text{ m}^3/\text{y}$ at Kessel and $70 \times 10^3 \text{ m}^3/\text{y}$ at Ravenstein. Wilbers (1996) presents along the river course the average (minimal) sediment transport rates; this information is shown in Figure 4.9. This information is based on a further analysis of cross-sections of the Meuse River, which were sounded in the years 1978, 1987 and 1995. In preparing Figure 4.9 it was assumed that the sediment transport entering into the common Meuse from upstream is zero (see also section 2.6). According to this information the average sediment transport at Maasbracht over the period 1978-1995 is (at least) $50 \times 10^3 \text{ m}^3/\text{y}$. About half of this transport originates from bank erosion (see Section 2.5).

Furthermore, it has been observed in the Meuse River that the sediment load transported depends on whether or not the armour layer has been mobilised during a flood. If the armour layer remains stable when the flood is passing, then little sediment is transported. Once the armour layer is mobilised the substratum material is available and the sediment load increase rapidly. This phenomenon has been estimated to occur at discharges higher than $1250 \text{ m}^3/\text{s}$, a value, which coincide with the estimated bank-full discharge. During the recessing part of the flood the armour layer is built up once again but at lower level, and on the eroded layer sediments are deposited. These deposited sediments are available and therefore after a flood period this material can be transported at smaller discharges until the armour layer is exposed once again. The coarseness of the armour layer is a function of the magnitude of previous floods. A high flood will give a finer armour layer and more eroded sediment on top of the restored armour layer after the flood. The observations in the field correspond to flume experiments of Klaassen (1986) (see also Klaassen et al, 1988).

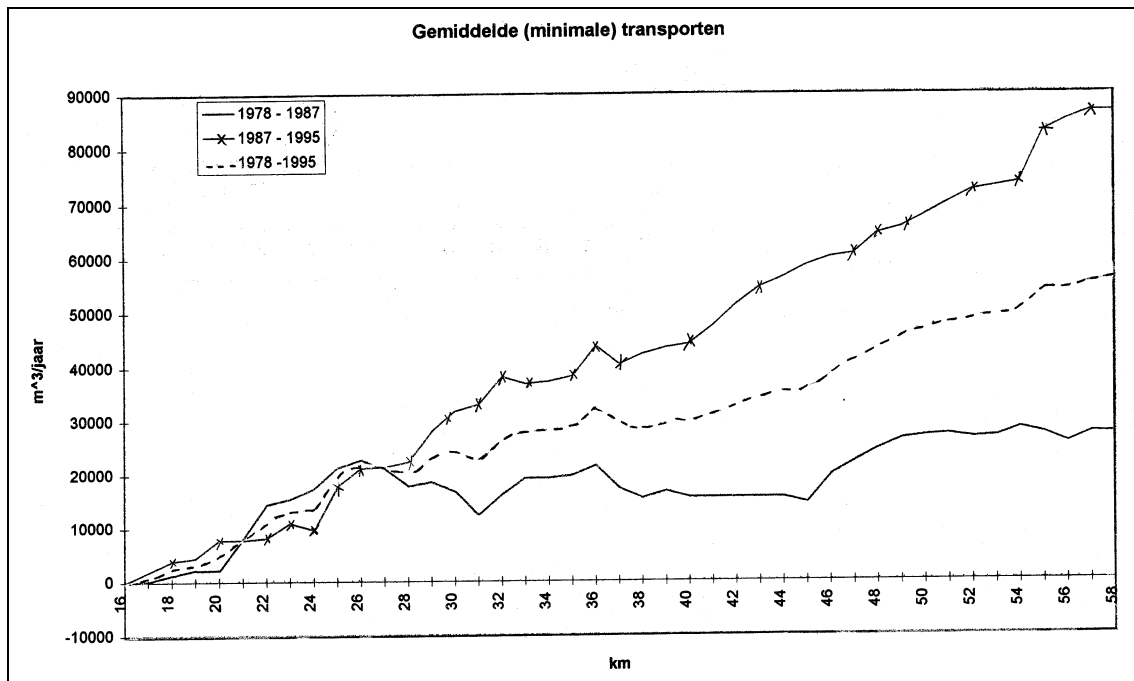


Figure 4.9 Average (minimal) sediment transport rates in the Meuse River.
Source: Wilbers (1996).

This behaviour of the sediment load is particularly important when sediment load rates in the Meuse River will be estimated. The key point is the fact that none of the available sediment transport predictors takes into account explicitly whether the armour layer has been mobilised or not.

In the next subsections separate assessments of the sediment rates in the gravel and in the sandy reach are presented. The results of these subsections will be used in the next chapters to estimate the relevance of the different processes involved in the downstream fining. However, first an estimation of the bed slope will be carried out in order to use the uniform flow approximation for the prediction of the sediment load.

4.3.1 Bed level and bed slope in the Meuse River

Bed levels along the Meuse River are represented here through the average bed level of a part of the river bed with a limited width (40 metres) on both sides of the thalweg. The thalweg elevation was selected as a representative elevation mainly because within one section of the river, the variation in elevation can be important and the difficulty to determine the division between main channel and floodplain. The data used in doing this are from survey sheets done by Rijkswaterstaat as well as the values reported in Rijkswaterstaat (1995), Fugro Comp. (1996) and Sloff and Barneveld (1996). Figure 4.10 shows the results obtained by Rijkswaterstaat over the period 1909 – 1995 and the striking feature is the impressive degradation process that the river bed has suffered. As explained in Section 2.6 the Meuse River has suffered serious degradation due to narrowing, downstream bend cut-off, dredging and subsurface mining. In the area near Maasband this has resulted in degradation of some 5 metres; in other reaches the degradation has been less severe but still is considerable. Only in the reach between kilometres 110 and 125 hardly any degradation has been observed. In the detailed data presented in Figure 4.10 it is possible to observe that in the period 1978 – 1995 the river bed degraded whilst in other ones aggradation did occur, which can be linked to the dynamic process of pools and riffles formation.

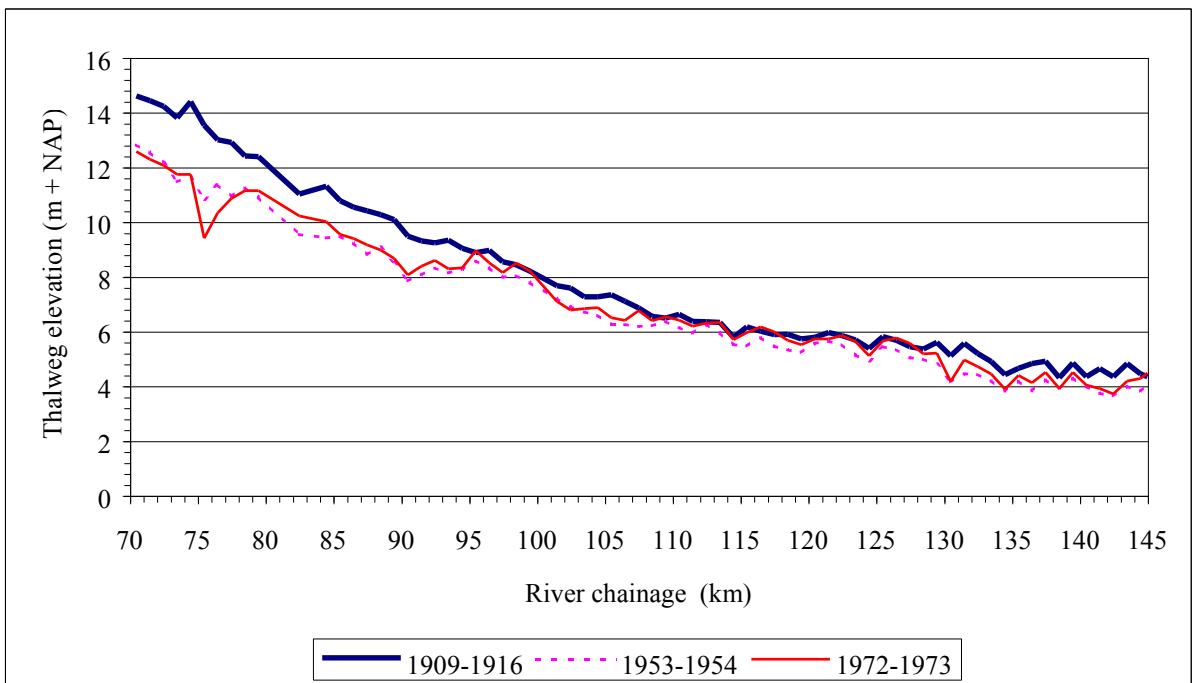
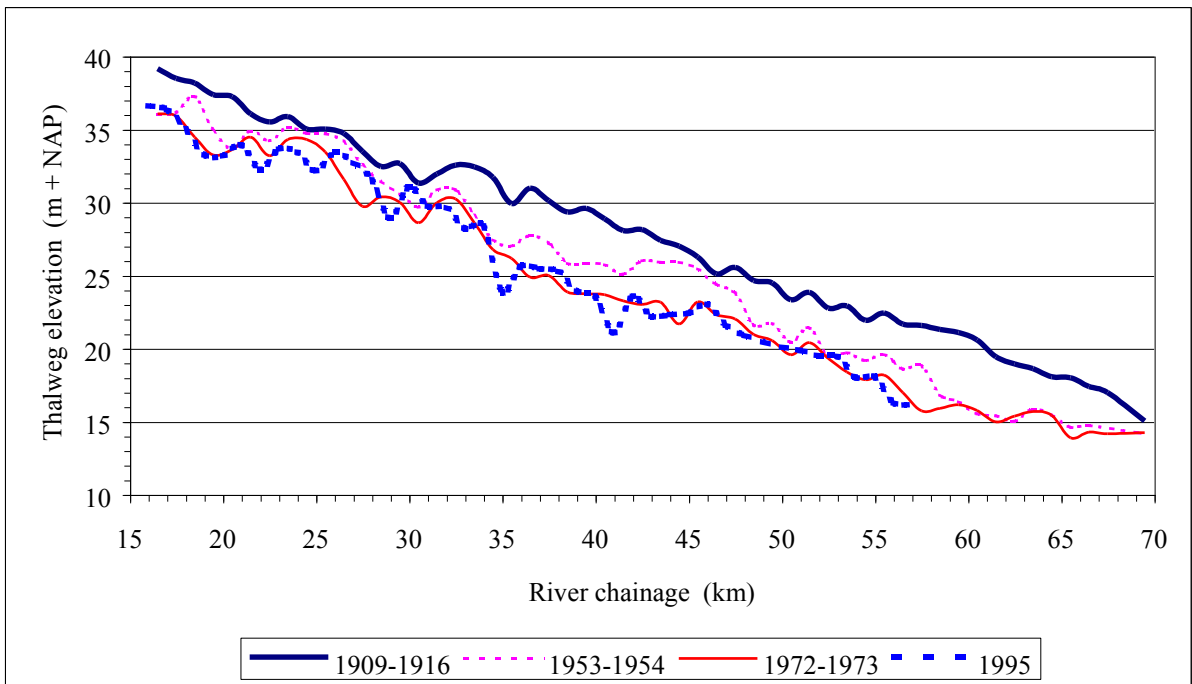


Figure 4.10 Thalweg elevation along the Meuse River.
Source: Rijkswaterstaat (1968) updated.

Moreover, in Figure 4.11 the slope of the river bed is estimated (using the more recent surveys) and the resulting lines represent the trend of the bed elevation. The trend of the data in the upper part of the river indicates a slope of 0.48 m/km whilst for the lower one a value of 0.10 m/km is found. It is possible to observe also that the change in the slope occurs between km 60 and 80. However, a close inspection of the bed levels from the surveys (see figure 4.10) indicates that in the period 1909 - 1916 the change in slope was more gradual with a shaper transition near the kilometre 95 (where probably the gravel-sand transition was formed). This suggests that the current location of the transition in the bed slope is probably the result of the intensive degradation process induced by the human interference in the system.

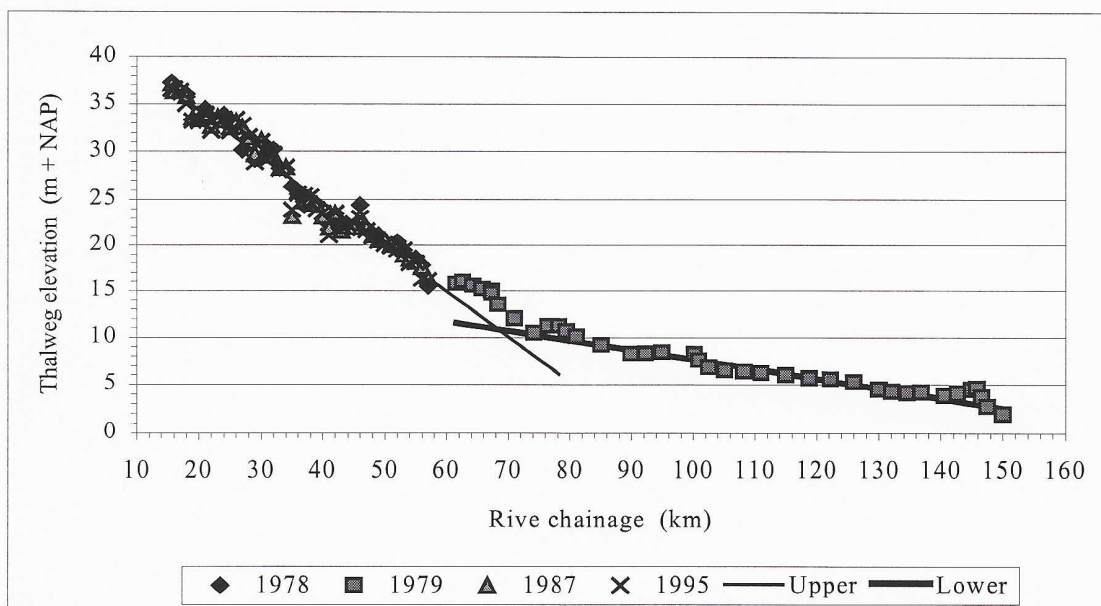


Figure 4.11 Trend of the thalweg elevation along the Meuse River.

4.3.3 Sediment transport rates in the gravel-bed reach

The sediment transport rates in the gravel-bed reach of the Meuse River were estimated using sediment predictors based on the use of only one representative diameter as well a sediment predictor based on the use of the full grain size distribution and hiding coefficients. Hereafter, the result of these two types of predictors are presented. The predictors were tested versus available field data, published in Duizendstra et al (1994) and Wilkens & Lambeek (1997).

◆ Sediment transport predictor based on one diameter

In the case where only one representative diameter is was used, three sediment transport predictors were tested, notably the modified Parker & Klingeman predictor (Parker, 1990), the Meyer-Peter & Müller predictor (Jansen, 1994) and the Graf-Suzka predictor (Sieben, 1993).

The Parker & Klingeman predictor was initially proposed by Parker et al (1982) and later on Parker (1990) modified it. This predictor is suitable for coarse bed material and in particular the formula intents to simulate the sediment transport on a paved bed. The sediment transport is given by

$$s_t = \frac{1}{1 - \epsilon} \frac{W^*}{\Delta} \sqrt{g} \left(\frac{u^2}{C^2} \right)^{3/2} \quad (4.1)$$

in which:

- s_t : sediment bed-load per unit of width;
- Δ : relative density of the sediments;
- u : average velocity in the main channel;
- C : Chézy coefficient; and
- ε : porosity of the bed material.

The value of the dimensionless bed load (W^*) depends on the ratio:

$$\omega = \frac{\theta_s}{\theta_r} \quad (4.2)$$

where θ_s is the Shields parameter and θ_r is a constant. Notably:

$$\theta_s = \frac{h i}{\Delta D_{50}} \quad \theta_r = 0.0876 \quad (4.3)$$

Here the D_{50} refers to the bed material (substratum). A distinction is made between three regions according to the value of ω :

$$W^* = 0.0025 \omega^{14.2} \quad \omega < 1.00 \quad (4.4a)$$

$$W^* = 0.0025 e^{[14.2(\omega - 1) - 9.28(\omega - 1)^2]} \quad 1.00 \leq \omega \leq 1.59 \quad (4.4b)$$

$$W^* = 0.0025 \left[5474 \left(1 - \frac{0.853}{\omega} \right)^{4.5} \right] \quad \omega > 1.59 \quad (4.4c)$$

The Meyer-Peter & Müller (Jansen, 1994) bed load predictor for use for sediments with $D_m > 0.4$ mm and $D_{max} < 29$ mm. The sediment predictor reads as follows:

$$s_t = \sqrt{g \Delta (D_m)^3} \frac{8}{1 - \varepsilon} \left(\mu \frac{h i}{\Delta D_m} - 0.047 \right)^{3/2} \quad (4.5)$$

where μ is the ripple factor given by

$$\mu = \left(\frac{C}{C_{90}} \right)^{3/2} \quad C_{90} = 18 \log_{10} \left(\frac{12h}{D_{90}} \right) \quad (4.6)$$

Applying the Meyer-Peter & Müller (MPM) predictor to the Meuse River, D_m was considered to be equal to the D_{50} of the substratum material. This provides a slight over-prediction of the sediment load.

Finally, Graf & Suzka proposed their sediment predictor based on flume experiments with coarse material ($D_{50} = 12.2$ mm and 23.5 mm). The sediment transport for the case of wide channels is predicted as follows

$$s_t = 10.4 \frac{\sqrt{g}}{\Delta} (hi)^{3/2} (\theta_s)^{3/2} \left(1 - \frac{\tau_c}{\theta_s} \right) \quad \theta_s \leq 0.068 \quad (4.7a)$$

$$s_t = 10.4 \frac{\sqrt{g}}{\Delta} (hi)^{3/2} \theta_s \quad \theta_s > 0.068 \quad (4.7b)$$

The dimensionless critical shear stress (τ_c) in Equation (4.7a) can be estimated by the empirical formulation suggested also by Graf & Suzka:

$$\tau_c = 0.042 e^{(5.06 i)} \quad (4.8)$$

In applying the above sediment predictors to the gravel reach of the Meuse River the following values of the different parameters which have to be entered, were assumed:

| | | | |
|-----------------|--------------------------|---|---------|
| i | : 0.486 m/km | B | : 100 m |
| C | : 46 m ^{1/2} /s | ε | : 0.40 |
| D ₅₀ | : 16 mm | Δ | : 1.65 |

Table 4.3 presents the comparison between predicted and measured values at three locations. In this table it is noticeable that the sediment predictors of Parker & Klingeman as well as Graf & Suzka are not suitable for predicting the sediment load in the Meuse River at lower discharges; the Meyer-Peter & Müller predictor, on the contrary, gives fair results at Maaseik although not at Eijsden.

Table 4.3
Comparison between bed-load measurement and predicted values.

| Date | Water Discharge (m ³ /s) | Bed-load Measurement (m ³ /day) x 10 ³ | Parker & Klingeman (m ³ /day) x 10 ³ | MPM (m ³ /day) x 10 ³ | Graf & Suzka (m ³ /day) x 10 ³ |
|-------------------|-------------------------------------|--|--|---|--|
| Eijsden (km 6.5) | | | | | |
| 19/Feb/90 | 710 | 0.02 | 0 | 0.1 | 0 |
| 10/Jan/91 | 1050 | 0.3 | 0 | 1.4 | 1.7 |
| 11/Jan/91 | 1066 | 0.2 | 0 | 1.5 | 1.7 |
| 09/Jan/91 | 1200 | 0.1 | 0 | 2.2 | 2.1 |
| 08/Jan/91 | 1550 | 0.3 | 0.3 | 4.1 | 3.2 |
| Maaseik (km 52.4) | | | | | |
| 02/Feb/94 | 700 | 0.5 | 0 | 0.1 | 0 |
| 30/Dec/94 | 1300 | 1.4 | 0 | 2.7 | 2.4 |
| 30/Jan/95 | 2770 | 5.1 | 7 | 11.4 | 8.3 |
| Maaseik (km 54.0) | | | | | |
| 18/Jan/91 | 580 | 0.3 | 0 | 0 | 0 |
| 21/Feb/90 | 710 | 0.2 | 0 | 0.1 | 0 |
| 17/Jan/91 | 720 | 0.3 | 0 | 0.1 | 0.9 |
| 16/Jan/91 | 800 | 0.7 | 0 | 0.4 | 1.0 |
| 15/Jan/91 | 900 | 0.5 | 0 | 0.6 | 1.3 |

Source: Wilkens and Lambeek (1997).

Moreover, the annual sediment load was also using the predictors for uniform material. The flow duration curve at Borgharen for the period 1911 – 1997 (Figure 2.8) was used in doing this. Table 4.4 gives the value of discharge at different percentiles of time. Also the predicted sediment load using the different predictors is given. The predicted total bed material load is 1.4x10³ m³/y; 24x10³ m³/y and 30x10³ m³/y for the Parker & Klingeman formula, MPM formula and Graf & Suzka formula respectively.

Table 4.4
Values of discharges and sediment load at different percentiles of time.

| Discharge (m ³ /s) | Probability of occurrence (% of time) | Sediment transport predictor | | |
|----------------------------------|---|---|---|--|
| | | Parker & Klingeman (x10 ³ m ³ /day) | MPM (x10 ³ m ³ /day) | Graf & Suzka (x10 ³ m ³ /day) |
| 3046 | 0.0001 | 9.6 | 13.1 | 9.8 |
| 3032 | 0.001 | 9.4 | 13.0 | 9.7 |
| 2891 | 0.005 | 8.1 | 12.2 | 8.9 |
| 2769 | 0.01 | 7.0 | 11.4 | 8.3 |
| 2245 | 0.05 | 3.2 | 8.2 | 5.9 |
| 1933 | 0.1 | 1.5 | 6.3 | 4.6 |
| 1460 | 0.5 | 0.2 | 3.6 | 2.9 |
| 1253 | 1.0 | 0.0 | 2.4 | 2.2 |
| 1046 | 2.0 | 0.0 | 1.4 | 1.6 |
| 925 | 3.0 | 0.0 | 0.9 | 1.3 |
| 836 | 4.0 | 0.0 | 0.5 | 1.1 |
| 768 | 5.0 | 0.0 | 0.3 | 1.0 |
| 715 | 6.0 | 0.0 | 0.1 | 0.1 |
| 670 | 7.0 | 0.0 | 0.0 | 0.0 |
| 632 | 8.0 | 0.0 | 0.0 | 0.0 |
| 600 | 9.0 | 0.0 | 0.0 | 0.0 |
| 572 | 10 | 0.0 | 0.0 | 0.0 |
| 377 | 20 | 0.0 | 0.0 | 0.0 |
| 266 | 30 | 0.0 | 0.0 | 0.0 |
| 199 | 40 | 0.0 | 0.0 | 0.0 |
| 154 | 50 | 0.0 | 0.0 | 0.0 |
| 31 | 90 | 0.0 | 0.0 | 0.0 |
| 3 | 99 | 0.0 | 0.0 | 0.0 |
| Total | | 1.4x10 ³ m ³ /y | 24x10 ³ m ³ /y | 30x10 ³ m ³ /y |

The results of computing the annual sediment load are summarised in Figure 4.12 to 4.14. Figure 4.13 shows the relation between sediment transport and discharge, it can be noticed that Parker & Klingeman is quite sensitive to high discharges while MPM and Graf & Suzka present a smoother behaviour. Moreover, Parker & Klingeman might be used to represent the sediment transport in the Meuse River after a long dry period, since it starts to produce sediment load after the necessary discharge to mobilise the armour layer. On the contrary, MPM and Graf & Suzka might be used to predict the sediment transport after floods, when the armour layer has already been mobilised. On the other hand, Figure 4.14 presents the percentages of time and of sediment transport in function of the discharge. In this figure, it possible to see that the higher sediment load is produce when the discharge is between 1000 and 1500 m³/s for the MPM and Graf & Suzka predictors.

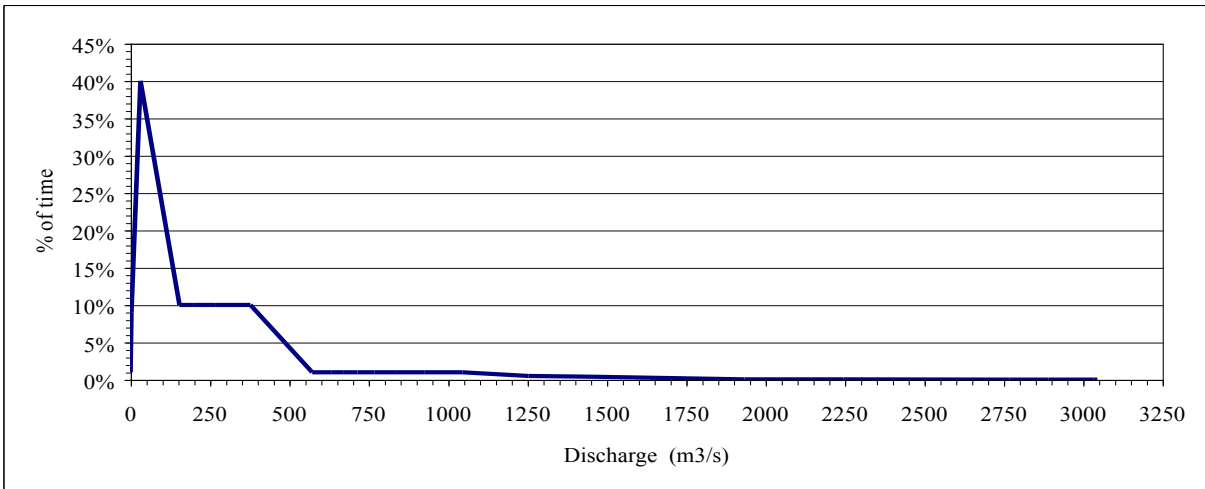


Figure 4.12 Frequency distribution of discharges at Borgharen for the period 1911-1997.
Source: Rijkswaterstaat.

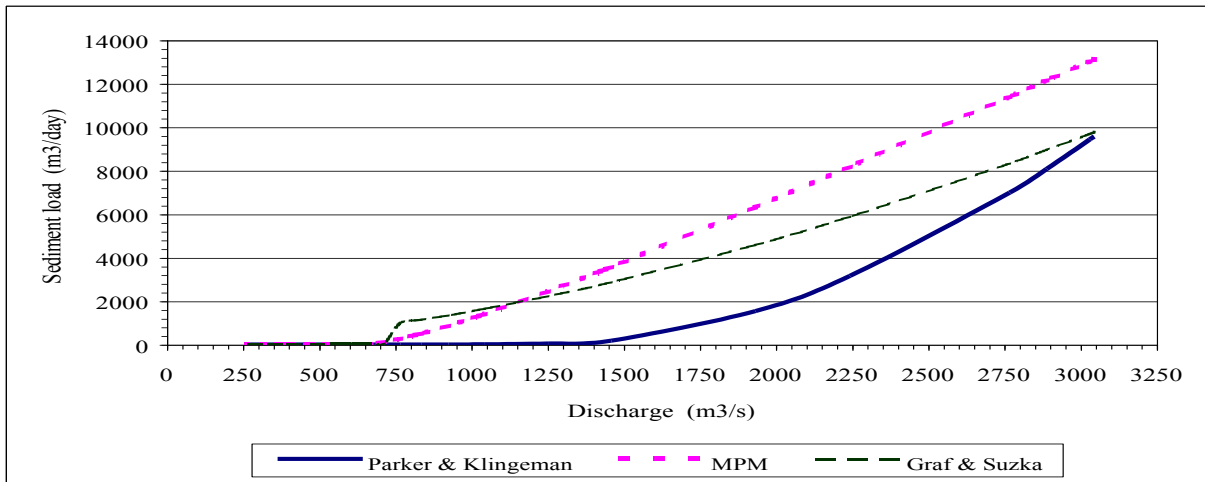


Figure 4.13 Sediment transport in function of the discharge for the gravel-bed reach.

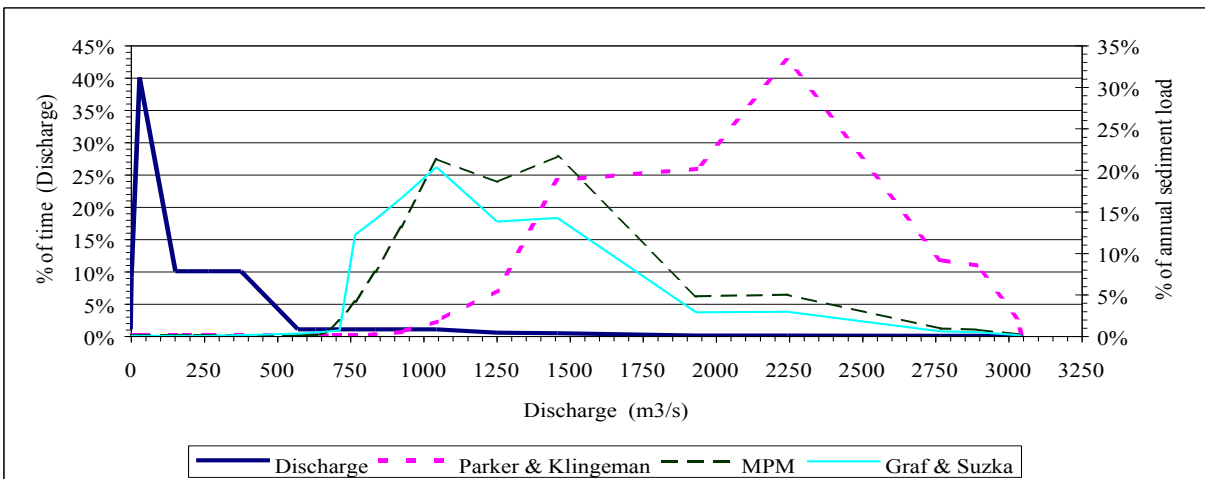


Figure 4.14 Relation between sediment transport and discharge for the gravel-bed reach.

◆ Sediment transport predictor for mixtures of sediments

In the case of mixtures of sediments it is preferable to consider the complete grain size distribution of the bed-load and to compute the transport for each fraction separately. This type of predictor has the advantage that the selective transport can be taken into consideration through the use of hiding coefficients. In the present study two predictors were tested, the Meyer-Peter & Müller and the surface based predictor of Parker (1990). In Appendix 2 the equations employed in their predictors are given in more detail; also information on the Ackers & White (1973) predictor is added, which has not been employed in this study though.

The Meyer-Peter & Müller predictor for mixture of sediments uses the grain size distribution of the bed-load, which can be approximated by the grain size distribution of the substratum. Moreover the hiding factor of Egiazaroff (improved by Ashida and Michiue) is employed and this factor reads as follows:

$$\xi_j = \left[\frac{\log_{10}(19)}{\log_{10}\left(19 \frac{D_j}{D_m}\right)} \right]^2 \quad D_j/D_m \geq 0.4 \quad (4.9)$$

$$\xi_j = 0.85 \frac{D_m}{D_j} \quad D_j/D_m < 0.4 \quad (4.10)$$

In the case of the surface base predictor of Parker (1990), the grain size distribution of the surface layer is employed and the hiding factor is

$$\xi_j = \alpha \left(\frac{D_j}{D_m} \right)^{-\eta} \quad (4.11)$$

where the coefficient α is equal to 1.048 and the exponent η is equal to 0.0951 for the Oak Creek data. The complete expression of both sediment transport predictors is presented in Appendix 2.

For testing both sediment predictors the same values for the parameters C , i , B , ϵ and Δ as used in Section 4.3.2 were also applied here. The granulometric curves (substratum and armour layer) used for the predictions are shown in Figure 4.15 and they were obtained by averaging the data reported by Van Manen et al (1994). The field measurements used in the testing were taken between 1969 and 1981 using the BTMA (Bodem Transport Meter Arnhem) and the DF2 (Delftse Fles op slede). The data reported by Wilkens and Lambeek (1997) only includes the sediment load (in m^3/day). Figure 4.16 gives the result using MPM whilst Figure 4.17 does for the case of the surface based formula of Parker (1990). The lines indicate the relation for the perfect agreement and the dots are the actual computed values.

As can be observed the MPM predictor tends to over-estimate the sediment load, while the Parker predictor consistently under-estimate the sediment loads. The MPM predictor does not explicitly take armouring into account and this might explain the large difference. The Parker predictor is based on data from Oak Creek, and apparently the armour layer characteristics (in relation to the substratum composition) is quite different for the Meuse River.

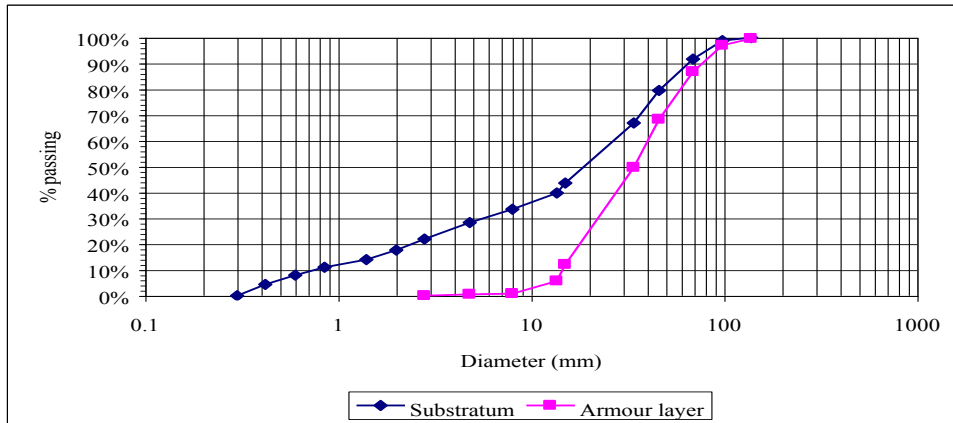


Figure 4.15 Average granulometric curves used in the tests for the gravel-bed reach.
Data source: Van Manen et al (1994)

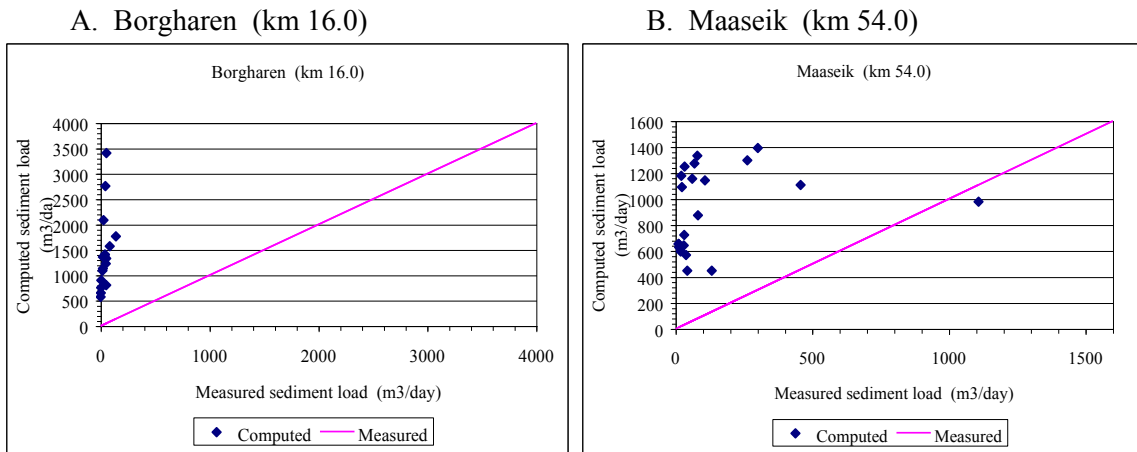


Figure 4.16 Results using MPM with hiding coefficient and the average grain size distribution of the substratum material for the gravel-bed reach.
Source data: Wilkens and Lambeek (1997).

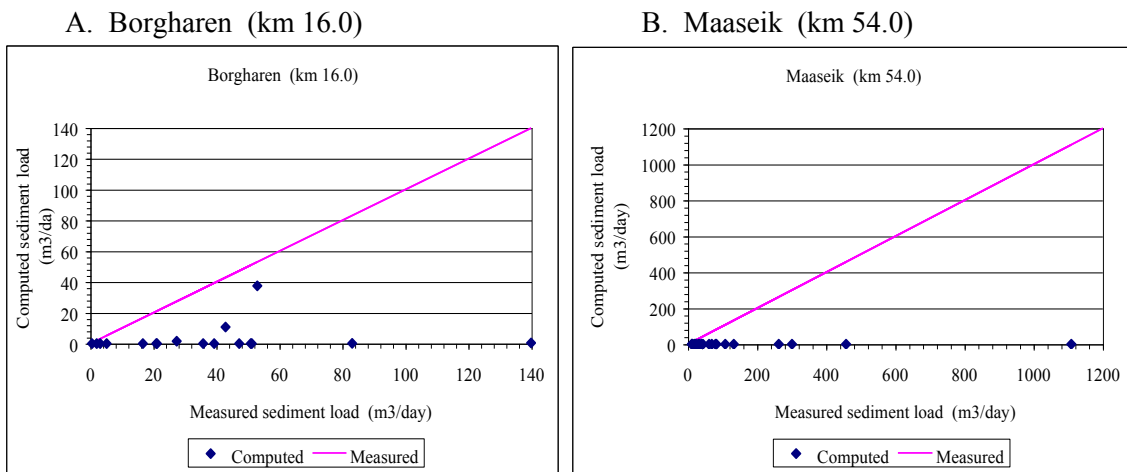


Figure 4.17 Results using the surface based predictor of Parker and the average grain size distribution of the armour layer for the gravel-bed reach.
Source data: Wilkens and Lambeek (1997).

4.3.4 Sediment transport rates in the sandy-bed reach

Similar to the case of the gravel-bed reach, both types of sediment predictor were used for the sandy-bed reach. Hereafter the results are presented.

◆ Sediment transport predictor based on one diameter

In the estimation for the sandy-bed reach only the MPM formula has been used. The Parker & Klingeman and the Graf & Suzka were especially developed for gravel-bed rivers and therefore must be less suitable. Moreover the principal aim here is to show the differences in behaviour between both reaches. In the present case the following values has been utilised: $i = 0.10$ m/km; $C = 55$ m^{1/2}/s (Sloff and Barneveld, 1996); $\Delta = 1.65$; $\varepsilon = 0.40$ and $D_{50} = 2.6$ millimetres. Figures 4.18 to 4.20 give the results.

◆ Sediment transport predictor for mixtures of sediments

Also a sediment transport predictor for a mixture of sediments considering all fraction separately were also used in the sandy-bed reach. Figure 4.21 shows the granulometric curve used in the tests whilst Figure 4.22 shows the results at two locations. Similar to the obtained results for the gravel-bed reach, the MPM formula with hiding coefficient is giving higher values of sediment load in the sandy-bed reach.

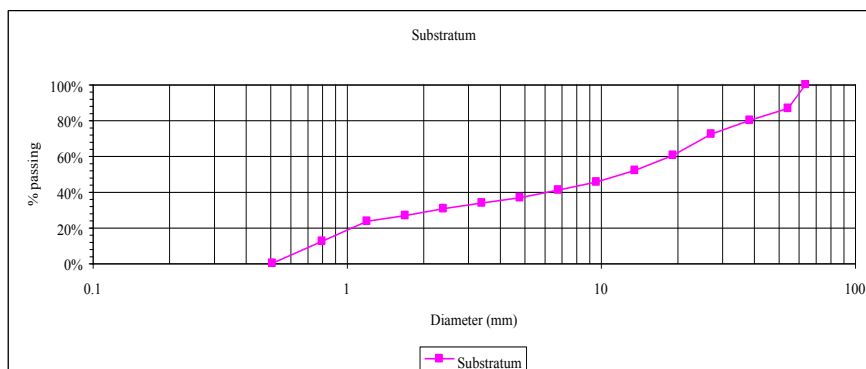
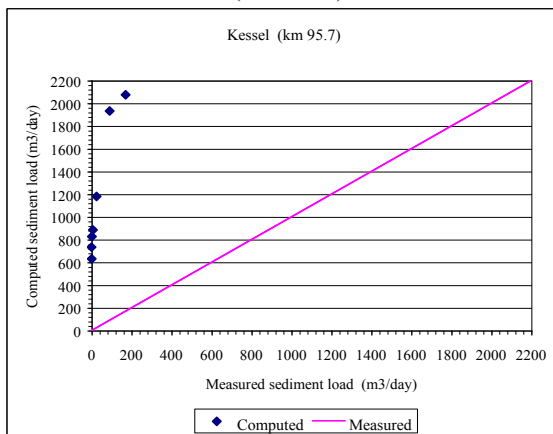


Figure 4.21 Average granulometric curve used in the tests for the sandy-bed reach. Data source: Rijkswaterstaat (1983)

C. Kessel (km 95.7)



D. Venlo (km 110.0)

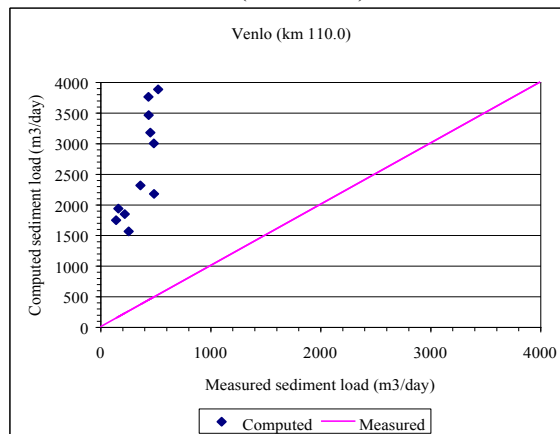


Figure 4.22 Results using MPM with hiding coefficient and the average grain size distribution of the substratum material for the sandy-bed reach.

Source data: Wilkens and Lambeck (1997).

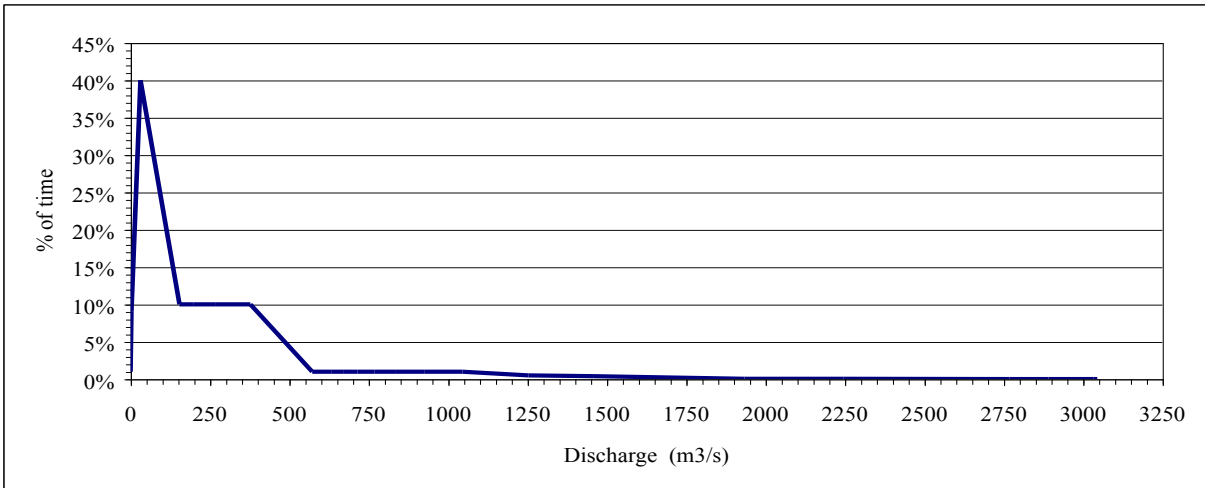


Figure 4.18 Frequency distribution of discharges at Borgharen for the period 1911-1997.
Source: Rijkswaterstaat

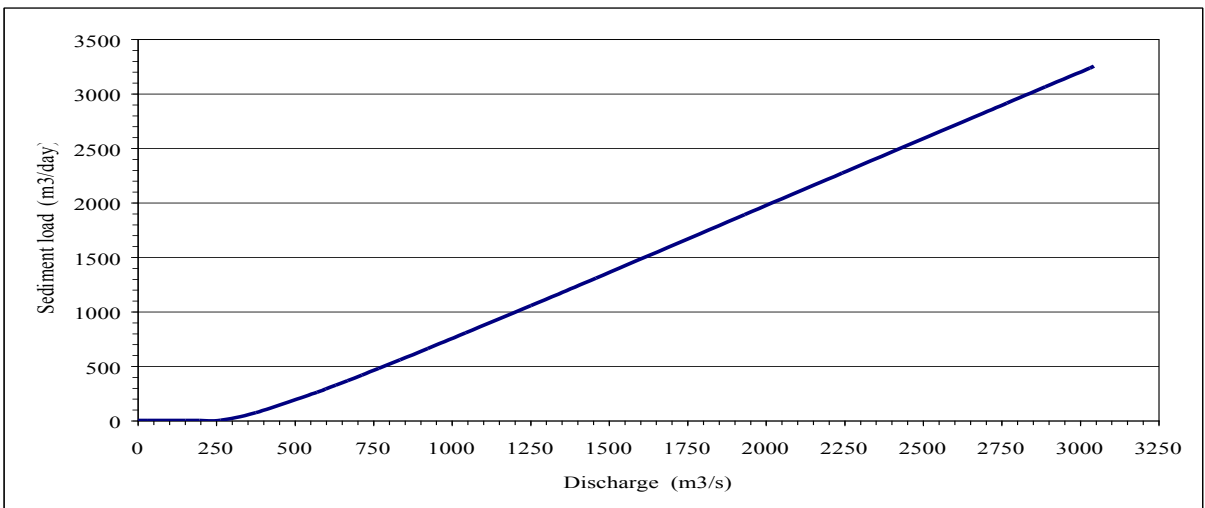


Figure 4.19 Sediment transport rate (MPM) as function of the discharge for the sandy-bed reach.

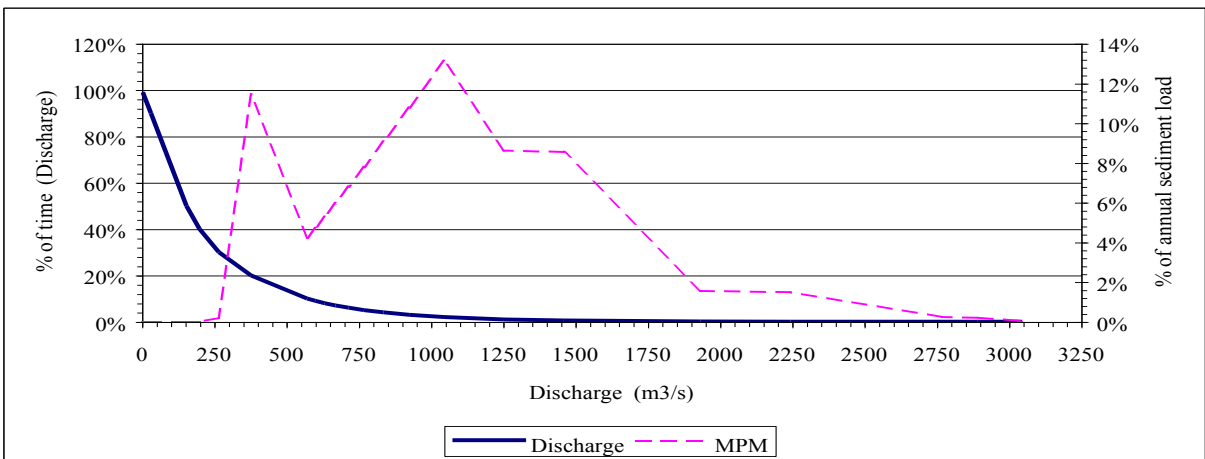


Figure 4.20 Relation between sediment transport and discharge for the sandy-bed reach.

4.3.5 Comparison of gravel-bed and sand-bed reach

In section 4.3.3 and 4.3.4 some data and predictions on two reaches are given. In this section a mutual comparison is made. Two main aspects:

- A. Total sediment load, and
- B. Sediment load over the year (as function of water discharge).

A) Total sediment load

In Figure 4.23 the distribution of the total sediment load as function of discharge is presented. In this figure it is clear that the sediment transport in both reaches is different. In the sandy-bed reach sediment transport occurs gradually along almost all the values of discharges, whilst in the case of the gravel-bed reach the sediment transport is displaced towards higher values of discharges. This phenomenon suggests that both reaches must have different morphological behaviour.

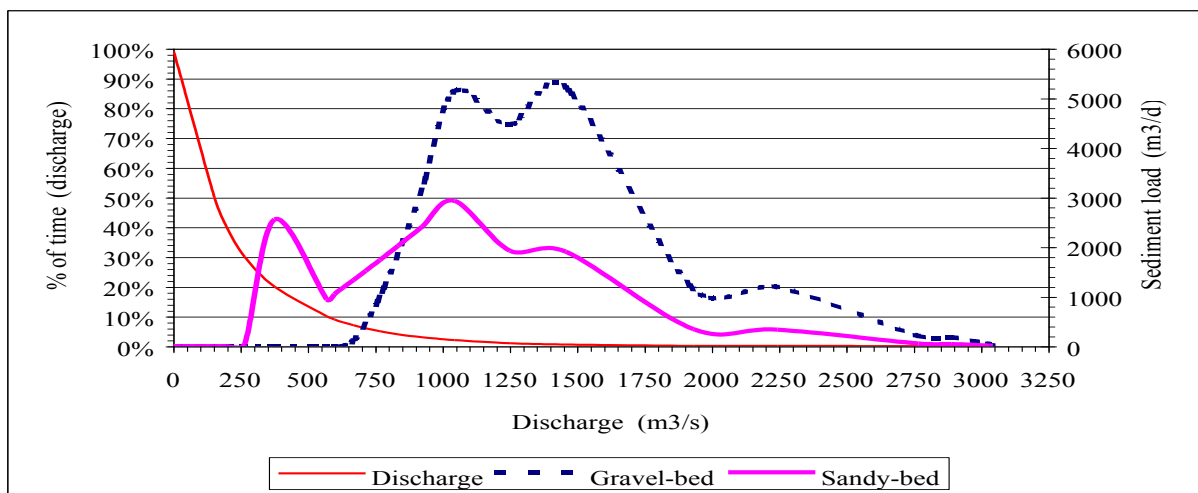


Figure 4.23 Comparison of the sediment load in the gravel-bed and sandy-bed reach.

Furthermore, Table 4.5 gives the values of the sediment load at different discharges. For high values of discharge the sediment loads are lower in the sandy-bed reach than in the gravel-bed reach, although in annual terms the average sediment load is fairly similar. This can be probably due to the presence of the armour layer in the gravel-bed reach, the effects that might have the subsidence of the area (see Chapter 5) or due to the human interference in the system. However, it is important to remember that the sediment transport predictors tested in this studied showed not to be too representative for the Meuse River.

B) Sediment load over the year

Figure 4.23 suggests that major part of the sediment load in the sandy-bed reach occur at lower values of discharge than in the case of the gravel-bed reach. Therefore, both reaches present a different morphological behaviour and this should be taken into consideration for modelling proposes. In addition, this behaviour implies that the sediment transport process in the Meuse River is an unsteady phenomenon and should be studied in such a way. None of the available sediment predictors have been developed in such conditions and therefore they represent a serious limitation for predicting sediment load in the Meuse River and modelling its morphological behaviour.

Table 4.5
Comparison of the sediment transport rates
in the Meuse River according to MPM predictor

| Discharge (m ³ /s) | Probability of occurrence (% of time) | Gravel-bed Reach (m ³ /day) | Sandy-bed reach (m ³ /day) |
|----------------------------------|---|--|---|
| 3046 | 0.0001 | 13.1 | 3.2 |
| 3032 | 0.001 | 13.0 | 3.2 |
| 2891 | 0.005 | 12.2 | 3.1 |
| 2769 | 0.01 | 11.4 | 2.9 |
| 2245 | 0.05 | 8.2 | 2.3 |
| 1933 | 0.1 | 6.3 | 1.9 |
| 1460 | 0.5 | 3.6 | 1.3 |
| 1253 | 1.0 | 2.4 | 1.1 |
| 1046 | 2.0 | 1.4 | 0.8 |
| 925 | 3.0 | 0.9 | 0.7 |
| 836 | 4.0 | 0.5 | 0.6 |
| 768 | 5.0 | 0.3 | 0.5 |
| 715 | 6.0 | 0.1 | 0.4 |
| 670 | 7.0 | 0.0 | 0.4 |
| 632 | 8.0 | 0.0 | 0.3 |
| 600 | 9.0 | 0.0 | 0.3 |
| 572 | 10 | 0.0 | 0.3 |
| 377 | 20 | 0.0 | 0.1 |
| 266 | 30 | 0.0 | 0.0 |
| 199 | 40 | 0.0 | 0.0 |
| 154 | 50 | 0.0 | 0.0 |
| 31 | 90 | 0.0 | 0.0 |
| 3 | 99 | 0.0 | 0.0 |
| Total | | 24x10 ³ m ³ /y | 22x10 ³ m ³ /y |

4.3.6 Dimensionless sediment transport rates in the Meuse River

Looking at the results obtained using the different sediment predictors, there are considerable doubts whether any of these formulas is suitable for the Meuse River; in some of the cases MPM predictor may give a better representation. The discrepancy between predicted and observed values can be linked to the sediment load behaviour previously mentioned or to the fact those average grain size distributions were used that perhaps are not representative of the field conditions. Moreover, Iseya and Ikeda (1987) reported that longitudinal sorting of sediment produces a rhythmic fluctuation of the bed-load when the gravel fraction represents the majority of the sediment. This implies that sediment load in a gravel-bed river is not always a direct function of hydraulic parameters as many of the available predictors assume and therefore, their application is rather doubtful. The most probably cause might be that none of these predictors is suitable, and that for the Meuse River a dedicated sediment transport predictor should be developed.

In view of the above, in Figure 4.24 to 4.26 the results are presented in dimensionless form. These figures clearly show the discrepancy between observed and predicted values. In Figure 4.24, the MPM predictor gives higher values than the observed whilst the surface based predictor of Parker (figure 4.25) gives lower values. For the case of the sandy-bed reach (Figure 4.26), MPM also gives higher values of sediment load.

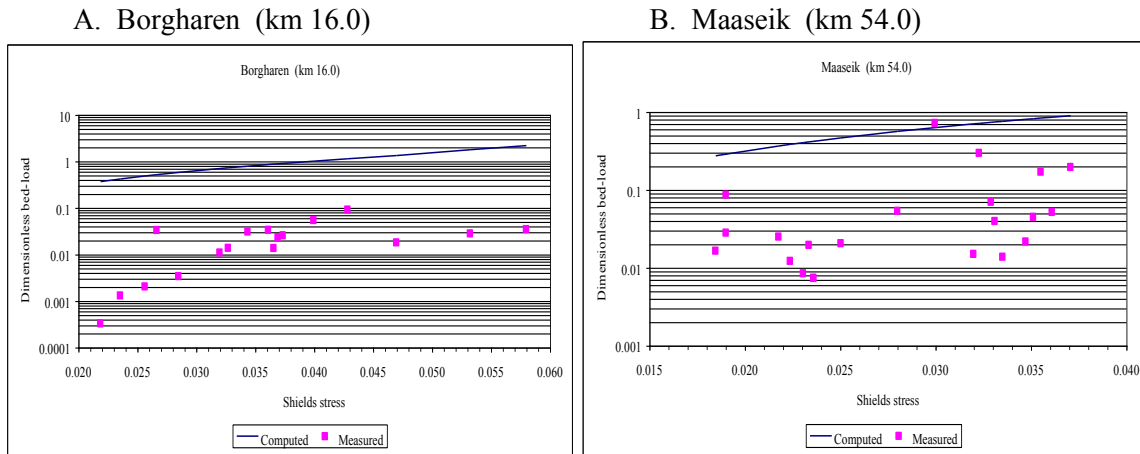


Figure 4.24 Dimensionless results using MPM with hiding coefficient and the average grain size distribution of the substratum material for the gravel-bed reach. Source data: Wilkens and Lambeek (1997).

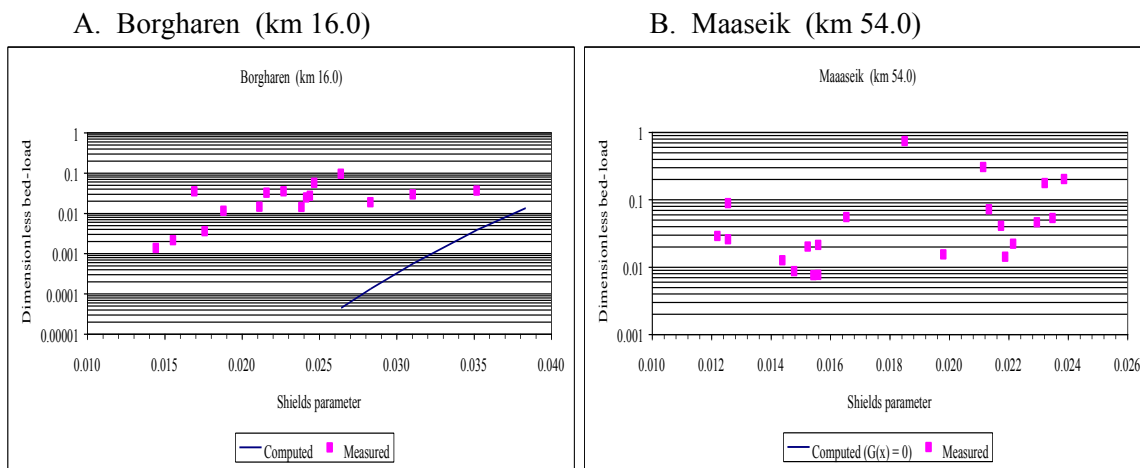


Figure 4.25 Dimensionless results using the surface based predictor of Parker and the average grain size distribution of the armour layer for the gravel-bed reach. Source data: Wilkens and Lambeek (1997).

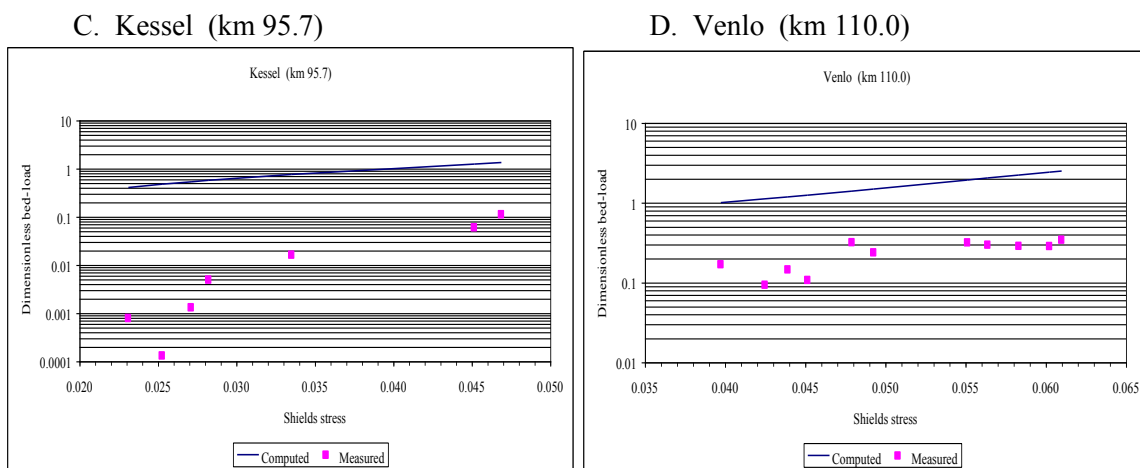


Figure 4.26 Dimensionless results using MPM and the average grain size distribution of the substratum material for the sandy-bed reach. Source data: Wilkens and Lambeek (1997).

Furthermore, Figure 4.27 present all the dimensionless values previously reported. This figure could be used to derive a sediment transport predictor for both reaches of the Meuse River. However, the derivation of this predictor is beyond of the scope of this project and should be carried out in a separate project. Moreover, similar graphs like Figure 4.27 but based on transport by grain fractions could also be made in the future allowing to derive a sediment transport predictor based on grain fractions. It is clear though that, in view of the scatter in Figure 4.27, for the time being even improved predictors will yield a poor prediction of the local and momentary bed loads. The best one might achieve is a predictor that on the average will give a better estimate that the existing sediment load predictors do.

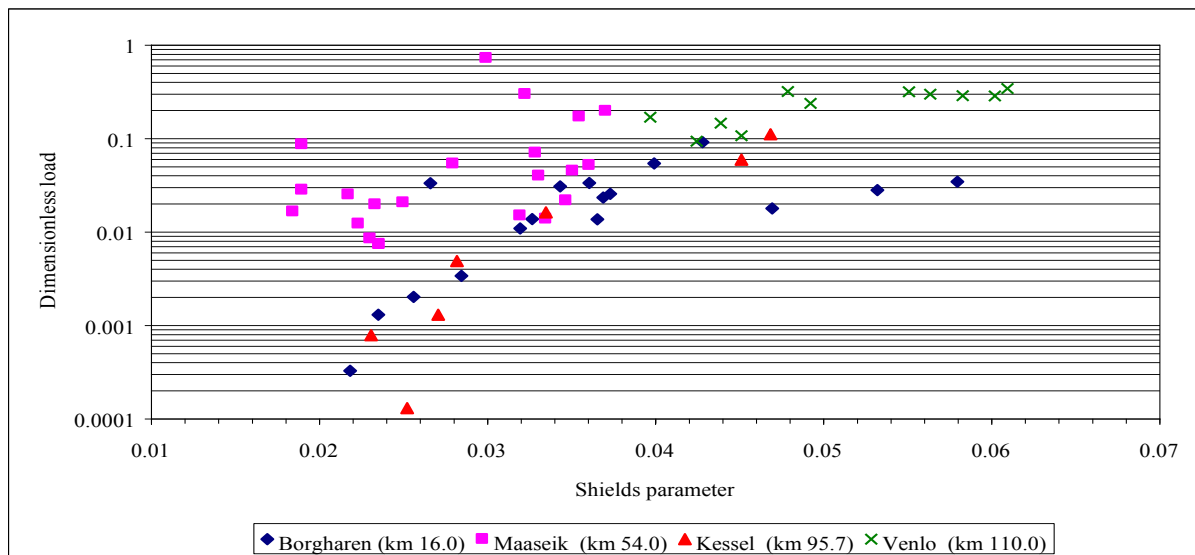


Figure 4.27 Dimensionless results in the Meuse River.
Source data: Wilkens and Lambeek (1997).

4.3.7 Discussion

The analysis of the field data reveals that there is a large variability both in space and probably in time, of the particle distribution of the bed material in the Meuse River. This variability can be linked to the physical processes in the Meuse River but also to the transient phenomena induced by human interference in the system since the 19th century. However, it is hardly impossible to determine which one has the major influence. Furthermore, the bed material in the Meuse River shows a development of a bimodal grain size distribution of the substratum material. This bimodal composition shows a gap between diameters of 1 and 5 millimetres approximately.

Regarding the sediment transport processes in the Meuse River it is possible to mention that they are quite complicated and difficult to understand because there are many factors involved. Notably: the presence of armour layers; the occurrence of a transition from a gravel-bed to a sand-bed river near Roermond; the effect of human interference which has induced transient phenomena and the limited availability of field data on bed material and sediment transport among others. According to Section 4.3 there is no sediment transport predictor that can, with a reasonable accuracy, predict the sediment transport in the Meuse River. Hence, such predictor should be developed in the near future and it should be based on the available sediment transport data, but conceptually should also take the complicated physical phenomena into account.

Finally, the sediment transport in the gravel-bed reach and in the sand-bed reach are taking place at different discharges. Most sediment in the sand-bed reach is taking place at lower discharges than in the gravel-bed reach. This suggests that the full hydrograph should be used in modelling and not one dominant discharge.

Chapter 5

Causes of downstream fining in the Meuse River and their contribution

5.1 Introduction

As discussed in the previous chapters, the Meuse River is characterised by a transition from a gravel bed to a sand bed river between kilometres 90 and 105. Over the length of this transition, the D_{50} of the bed material changes from about 16 to 2.6 millimetres and the slope shifts from about 0.48 m/km to 0.10 m/km. The fact that the transition in slope is now near kilometre 70 might be caused by human interference. About 100 year ago it was more gradual and located more downstream (see Subsection 4.3.1). These features could explain by means of the downstream fining of sediments and its associated processes.

Moreover, in the past the Meuse River had probably a relative stable bed profile and any aggradation that could explain the downstream fining was not very pronounced. For the time being, it is supposed here as a working hypothesis, that nevertheless downstream fining is caused by aggradation whereas, vertical tectonic movements (uplift and subsidence) of the area counteracted this aggradation of the bed and might have been in a sort of dynamic equilibrium with it.

In view of the above, in this Chapter an assessment of the relative importance of two different processes that are linked to the downstream fining is made. First, an assessment of the relative importance of the abrasion process is carried out; and second, the tectonic movements and their relationship with the bed stability are discussed. Moreover, an assessment of the causes of the change in the bed slope is also presented at the end of this Chapter. The selective transport of particles, the third process involved in the downstream fining, is considered in Chapter 6 via numerical modelling.

This Chapter discussed the various causes of downstream fining in a fairly qualitative way. Simply analytical assessments are added to get a feeling about the relative importance of the different causes. In Chapter 6 a numerical model is used to quantify the effect of the combined occurrence of abrasion, break down and subsidence. It builds on the understanding obtained in this chapter.

5.2 Causes of downstream fining in the Meuse River

Along the river course the Meuse sediments are subjected to different influences that contribute to the overall fining in downstream direction. Here these influences are called causes and these causes are: abrasion process, break down of particles, subsidence, selective transport, old deposits and the input of finer sediments from the Roer River. The principal effects that these causes have on the Meuse River characteristics are summarised in Table 5.1, where a distinction between a river with and without fixed planform is made. Furthermore a distinction is made between primary effects (on sediment load and bed material characteristics) and secondary effects (on deposits, slope and planform).

The abrasion process causes a slow reduction (the rate depends on the rock type) in the particle size and produces mainly sands and silts, thus the sand content and the wash load increase while the total bed-bed load decrease. The abrasion of particles can cause a concave profile in the river bed as Sinha and Parker (1996) pointed out.

Table 5.1
Effects of the different factors in the characteristics of the Meuse River

| Causes | Primary effects | | | | | Secondary effects | | | |
|--|---|------------------------------------|------------------------------------|--|----------------------------------|-----------------------------------|--|------------------------------------|--|
| | Sediment load | | Wash load | Bed material characteristics | | Floodplain deposits | Slope | Planform | |
| | Total bed material load | Sand content | | Size | Rock type | | | | Shape |
| Abrasion | - Slow reduction in downstream direction | - Increase in downstream direction | - Increase in downstream direction | - Slow reduction | - Determines the reduction rate | - Rounded particles suffer less | - Sand deposited in gravel pores | - Slow reduction (concave profile) | - No effect |
| Break down | - No changes - Development of bimodal composition | - Increase in downstream direction | - Slight increment | - Gravel particles smaller than the cut-off size are not present - Gradual discontinuity in the grain size distribution | - Affect its occurrence | - Production of angular particles | - Sand deposited in gravel pores | - Slow reduction (concave profile) | - No effect |
| Subsidence & selective transport (freely meandering river) | - Gradual reduction - Inferential deposition of gravel (downstream fining) | - Increase in downstream direction | - Slow increment | - Reduction by downstream fining | - No effect | - No effect | - Deep layers of gravel (floodplain and main channel) - Upward fining sequences | - Slow reduction of bed slope | - Anastomosed and braided patterns |
| Subsidence & selective transport (fixed river system) | - Slow reduction - Inferential deposition of gravel (downstream fining) | - Increase in downstream direction | - Gradual increase | - Reduction by downstream fining | - No effect | - No effect | - Deep layers of gravel (main channel) - vertical accretion with fine sediments in floodplain | - Slow reduction of bed slope | - Fixed by river training works - Propagation of the gravel-sand transition |
| Old deposits | - Determine the availability of material to be transported | - Might change | - Might change | - Determine grain size of available material | - Induce changes in rock type | - Likely to change | - No effect | - Might affect | - Might change by rock outcrop |
| Roer River | - Increase the load | - Increase | - Increase | - Sudden change in particle distribution | - Changes in rock type available | - Might change | - No effect | - May influence | - Might influence |

On the other hand, break down although a part of the abrasion process, produces a discontinuity in the grain size of the bed-load material but it does not affect the total load. It occurs spontaneously when the particles reach a certain cut-off diameter and this happens along the river course rather than at certain location. The cut-off diameter depends on the rock type. Break down and other phenomena abrasion have the same effect on the sand content, wash load and bed slope.

Subsidence and selective transport are linked. Subsidence provides the necessary depositional environment that triggers the selective transport and therefore aggradation by coarse particles and downstream fining of sediments. The deposition creates layers of gravel that are slowly subsiding and therefore producing deep gravel deposits. However, the combined action of the meandering process and the subsidence cause sequences of layers which usually present an upward fining. Subsidence and selective transport produce also a concave profile and therefore a gradual reduction of the bed slope. This is caused by a reduction of the sediment load and the bed material becoming finer in line with Lane's Balance (see Section 5.6).

In a river with a fixed planform, the combined action of subsidence and selective transport can produce more frequent inundation or even avulsion of the river (by aggradation of the bed); the location of the gravel-sand transition can also be affected and it might propagate in downstream direction.

The old deposits determine the type and size of particles available to be transported. Hence, it can produce changes in the sand content, wash load and the lithology of the transported material. If the old deposits form important rock outcrops, they can influence the planform of the river. Finally, the Roer River, a tributary of Meuse, may have also effects in the downstream fining of sediments in the Meuse River. The Roer River can increase the bed material load and introduce important amount of sand and wash load to the Meuse. If this happens, the grain size distribution can be affected and perhaps the lithology of the bed-load could also be affected as well.

In Table 5.1 also the effect of the different causes on the planform of the river is indicated. This is in particular based on Figure 3.5. In the present study the effect on the planform was not studied. It should be stated that from an inspection of Figure 2.9 it does seem to be very pronounced either.

5.3 Relevance of the abrasion process

In Section 3.4 it was mentioned that abrasion depends directly on particle size, particle velocity, and hardness of the bed and is inversely related to particle roundness and quantity of sand moving with the gravel. Experimental results and the mathematical description of the process were also discussed, but the findings were not linked to the specific case of the Meuse River. This is done in this section.

The relative importance of abrasion in the downstream fining of sediments depends on the characteristics of the specific case considered. For example, Cui et al (1996) cite cases in geologically young environments where abrasion appears to dominate the process; moreover, Seal and Paola (1995) report a strong downstream fining in a geologically young environment, but over a rapidly aggrading reach that is too short for significant abrasion. On the other hand, Hoey and Ferguson (1994) have documented downstream fining in a geologically old environment where the clasts are sufficiently durable to exclude abrasion.

Hereafter, an assessment of the characteristic particles of the Meuse River sediments is presented first. Later the relevance of the abrasion process is studied and finally the possibility of break down of Meuse particles is discussed.

5.3.1 Characteristic particles

The composition of the Meuse sediments was assessed by two different approaches. The first one is based on the PhD. thesis of Van Straaten (1946) “Grindonderzoek in Zuid-Limburg”, whilst the second one is based on the interpretation of the mineralogical information reported by Edelman and Van Baren (1935). Each of these approaches is summarised as hereafter.

5.3.1.1 Van Straaten’s work.

Van Straaten (1946) provides a general classification of the rock fragments present in the South Limburg area; it is based on the analysis of several samples, 107 in total, taken in the entire zone of South Limburg. He performed petrographical as well as size fraction analysis in order to find areas with similar characteristics.

The area of interest for the present study “Downstream fining of sediment in the Meuse River” corresponds with the region or group VI defined in Van Straaten’s work. This area matches with the valley bottom of the Meuse River (current floodplain area) and it is composed of sediments that are not arranged higher in terraces. In this zone Van Straaten took in total 5 samples.

The petrographical classification employed by Van Straaten is based on the thin layer analysis carried out for the different samples. Van Straaten classified the rocks in four groups, notably:

- A. *Quartz group*. This group includes all the rock fragments containing quartz, which are associated with common sedimentary deposits or metamorphic process.
- B. *Flint group*. Includes all the angular flints originate directly from the Cretaceous.
- C. *Sandstone group*. In this group is included the common sandstones: arkose, quartzite and phyllite.
- D. *Remaining rocks group*. Different kinds of rocks, which are present in minor quantities, are included in this group. These rocks are granite, conglomerates and silexite among others.

On the other hand, the analysis by size fractions used by Van Straaten considered six different grain sizes, as shown in Table 5.2. The fractions range from very coarse gravel to ultra coarse sand and although they do not match perfectly with the normal terminology, this description has also been included in Table 5.2 as a guideline.

Table 5.2
Fraction by grain size used by Van Straaten (1946).

| Fraction | Size (mm) | Description |
|----------|-------------|--------------------------------------|
| I | 22.5 – 30.0 | Very coarse gravel (16 – 63 mm) |
| II | 15.0 – 22.5 | Very coarse gravel |
| III | 9.0 – 15.0 | Moderate coarse gravel (5.6 – 16 mm) |
| IV | 4.0 – 9.0 | Moderate coarse gravel |
| V | 2.0 – 4.0 | Fine gravel (2.0 – 5.6 mm) |
| VI | 1.5 – 2.0 | Ultra coarse sand (0.42 – 2.0) |

Source: Van Straaten (1946).

In the area of interest (the present floodplain) Van Straaten took five samples, notably the samples 101 to 105 of his work. Table 5.3 gives the location of each of these samples whilst, Figure 5.1 shows the distribution (in percentage) of the four mineralogical groups in each sample analysed.

Table 5.3
Location of the samples.

| Sample | Location | Approximate river Chainage |
|--------|------------------|----------------------------|
| 101 | Gronsveld W. | 10.5 km |
| 102 | Gronsveld Maas | 10.0 km |
| 103 | Borgharen | 16.5 km |
| 104 | Groot Meers N. | 30.5 km |
| 105 | Groot Meers Maas | 32.0 km |

Source: Van Straaten (1946).

It is possible to infer from Figure 5.1 that the dominant group in the gravel fractions is the sandstone group and it is followed by the quartz group, although clearly of lesser importance. In the finer groups (V and VI), the percentage of the quartz is increasing in downstream direction until it reaches approximately the same importance as sandstone. However, since this tendency is in the finer fractions, it is not relevant for the downstream fining of sediments and can be interpreted as the result of abrasion suffered by the gravel particles. Generalising, it is possible to classify the gravel fraction of the four groups in order of decreasing importance as follows: sandstone group, quartz group, flint group and the remaining group.

Considering this, the most abundant rock fragments in the Meuse sediments correspond with those of the sandstone group and they are common sandstones: arkose, quartzite and phyllite. The sandstone and/or arkose are sedimentary rocks whilst quartzite and phyllite are metamorphic rocks. The rocks of the quartz group are of second order importance according to Van Straaten's work; these rocks are typical sedimentary rocks like sands and gravel and typical metamorphic rocks like the gneiss.

5.3.1.2 Interpretation of mineralogical information

Edelman and Van Baren (1935) studied the petrographical composition of the deposits of the Meuse River and they classified the minerals in heavy and light ones giving its percentage at different locations. However, the minerals reported by Edelman and Van Baren can also be classified in three groups. Tourmaline, zircon, and augite form the first group and they are typically related to igneous rocks. Similarly, chloritoid, garnet, staurolite, epidote and hornblende form the second group; they are related to metamorphic rocks. Finally, minerals that could be related to both types of rocks compose the third group. Figure 5.2 shows the distribution of this classification along the river length.

In accordance with this petrographical data and the regional geology, it is possible to infer that rock fragments from the gravel and coarse sand deposits are present in the whole area. These fragments are probably "igneous rock fragments" and "metamorphic rock fragments", although the first one is less abundant. It is also possible to infer that the "igneous rock fragments" probably come from acid to intermediate igneous rocks like granite, granodiorite, rhyolite and sianite among others. In similar way, the "metamorphic rock fragments" present in the deposits probably come from gneiss and schist.

The acid and intermediate igneous rocks are hard rocks and therefore, very resistant to weathering. On the other hand, metamorphic rocks like gneiss and schist are moderately resistant to weathering because they have planes of weakness in their internal structure. Hence, in decreasing order of resistance to weathering we have: acid igneous rocks, intermediate igneous rocks, gneiss and schist.

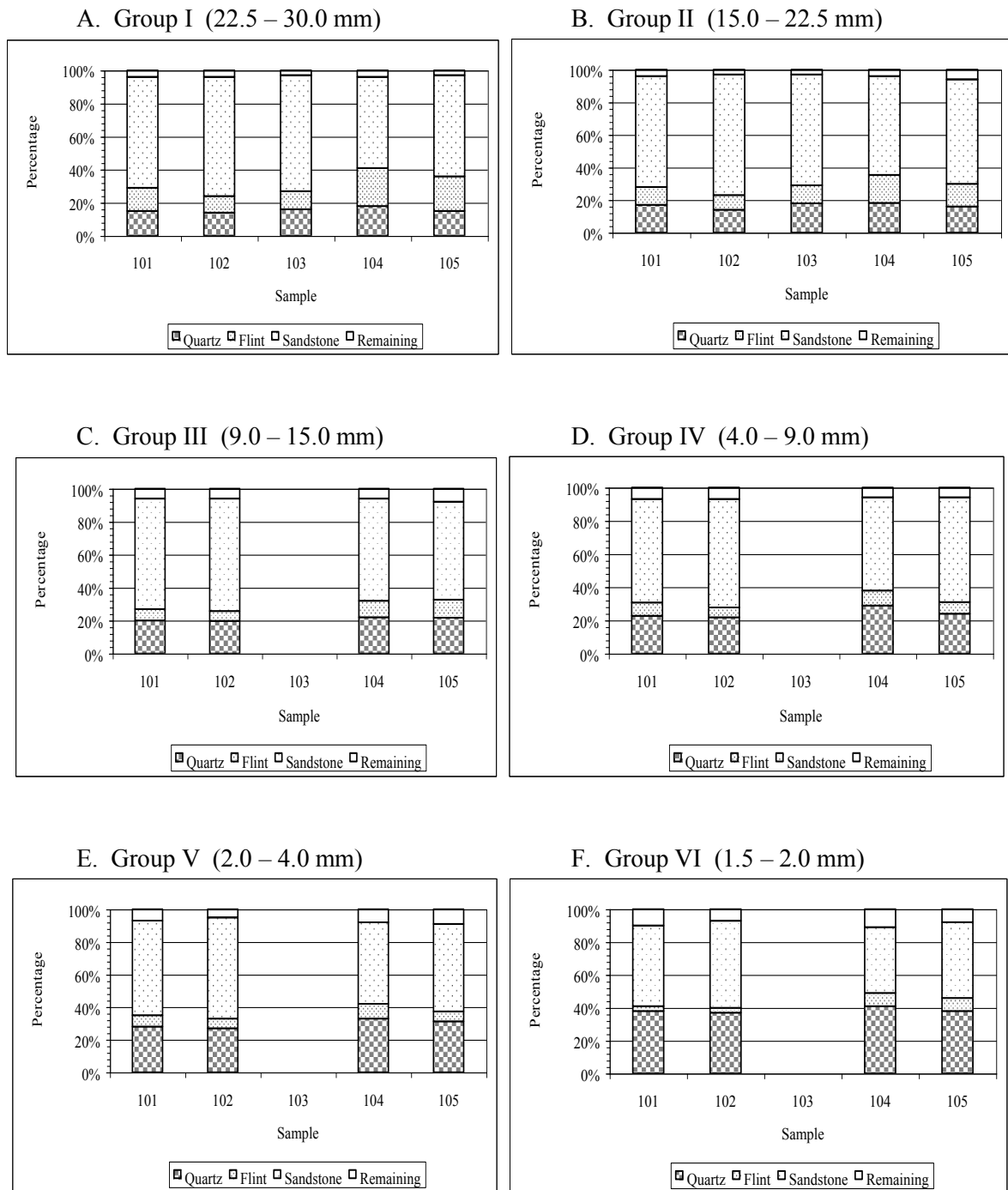


Figure 5.1 Distribution of rock groups (in percentage) by size fraction according to Van Straaten (1946).
Source data: Van Straaten (1946).

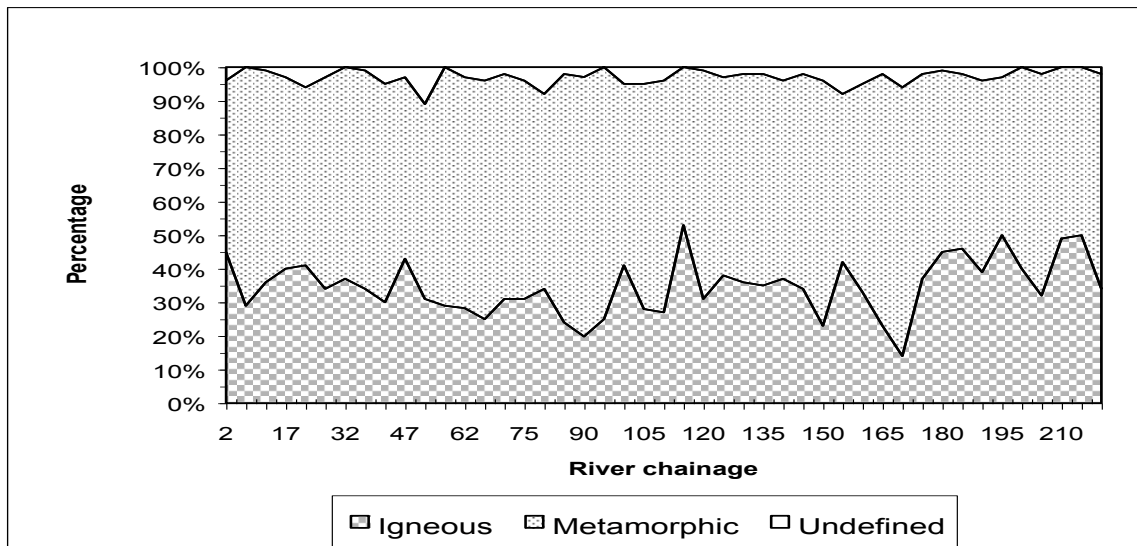


Figure 5.2 Distribution of the minerals groups along the river.
Source: data from Edelman and Van Baren (1935).

5.3.2 Assessment of the abrasion process

The relevance of the abrasion process is investigated on the basis of the results reported by Abbott and Peterson (1978) which have been already mentioned in Chapter 3. They performed, in a tumbling mill, tests for a dozen of different rock types. To assess the relative importance of the abrasion process, the different rock fragments suggested in the previous sections as principal elements of the Meuse sediments should be analysed. To do this and to clarify the situation, the suggested rock fragments are presented again in Table 5.4.

Table 5.4
Probable rock fragments present in the
Meuse deposits according to different approaches.

| Rock type | Approach | |
|--------------------------------|---------------------------------|-------------------------------------|
| | Van Straaten (1946) | Edelman and Van Baren (1935) |
| Igneous (intermediate to acid) | | Granite Granodiorite Rhyolite |
| Sedimentary | Sandstone Arkose | |
| Metamorphic | Quartzite Phyllite Gneiss | Gneiss Schist |

According to the abrasion durability scale of Abbott and Peterson (see Table 3.3 and Figure 3.3), the most resistant rock is the quartzite and the less resistant one is the phyllite. The complete order can be:

1. Quartzite
2. Rhyolite
3. Arkose
4. Sandstone
5. Granite
6. Gneiss
7. Granodiorite
8. Schist
9. Phyllite

To determine the importance of the abrasion process the less resistant rock should be employed in the assessment; however, there are no experimental data for the phyllite in the results of Abbott and

Peterson. Phyllite and schist have similar internal structure though and also similar resistance to weathering; but it is impossible to determine with the information available, which is the percentage of phyllite present in the deposits. In view of this and considering the fact that Van Straaten work is based on field data, here travelling over a distance of 15 km (which corresponds to the length of the transition in particle diameter in the Meuse River, notably from km 90 to km 105) is analysed.

Once the rock type is selected, it is necessary to estimate the time that the particles need to cover the 15 km of transition. Rijkswaterstaat has filmed the movement of the bed-load particles using a video camera attached to the Helley-Smith sampler (Duizenstra et al, 1994). From these movies, it is possible to observe the stochastic transport process of the sediment transport. The particles are not moving for quite some time and then suddenly they move at velocities that easily would reach about one meter per second approximately. If this velocity is considered, the loss of weight over the 15 km of transition is about 5% (using the metasandstone's curve in Figure 3.3). This reduction of weight can be transformed into a reduction of diameter and doing so, the particle diameter decreases from 16 mm to 15.7 mm approximately.

Furthermore, if particles travel at lower velocities they would suffer more abrasion (they reaming addressed) and therefore the reduction in diameter would be higher. If the velocity of the particles were 3 cm/s the loss of weight over the 15 km of transition would be about 15% (according to Figure 3.3). So, the diameter would decrease from 16 mm to 15.2 mm; situation that does not explain also the formation of the gravel-sand transition in the Meuse River. Application of other experimental results, like those of Kuenen (1956), would produce similar small reductions in grain diameter.

A remark relevant for both previous estimates is the fact that it is supposed that abrasion occurs only when the particle is moving, which is not true indeed. When the particle is at rest at a certain location, it suffers abrasion by the blows of other particles, by sandblasting and even by chemical attack. However, with the available methodologies, it is quite difficult to take all the mechanisms into consideration.

Summarising, in the case of the Meuse River, it is concluded that the abrasion process does not dominate the reduction of size in the bed material. It has a slight influence, but its contribution cannot explain the sudden reduction in the D_{50} from 16 to 2.6 mm. Since the principal rocks are sandstone, quartzite and phyllite, the main product of the abrasion process will be sand and perhaps some gravel that was glued by the matrix of the rocks. Hence, due to abrasion the gravel and sand content will change gradually in favour of the sand.

5.3.3 Break down of particles

The break down of particles is part of the abrasion process; nevertheless, it works in a slightly different way. Break down refers to the breaking of a particle into two or more parts of roughly equal size and therefore is presented here separately. It has been proposed in some cases as the mechanism for the transition from gravel to sand-bed. Yatsu (1957) was one of the firsts researchers to point out the potential relevance of this process. He argued that in some of the Japanese rivers that he studied the gravel-sand transition is caused by the tendency for 2 – 4 mm materials to be break down into smaller individual grains. He also mentioned that differences in rock characteristics, such as mineral size and hardness, may cause that the discontinuity of size varies in some degree.

Parker and Cui (1998), giving reference to Yatsu's hypothesis, mention that the process of abrasion of gravel or coarser particles continues until a size on the order of 10 mm is reached. When the particle size is reduced to about an order of magnitude larger than the characteristic size of the component crystalline structure the particle is subjected to shattering. This combination of processes causes the characteristic bimodality of the grain size distribution and the transition to sand. Additional evidence is given by Sambrook Smith and Ferguson (1995) who reported upon some Canadian rivers in which according to Shaw and Kellerhal the transition occurs due to the 1 – 4 mm material being readily

crushed to produce finer material that can be carried in suspension. They added that when the energy is insufficient to carry these medium sands in suspension they are deposited, forming a sandier (bimodal) bed.

Moss (1972) and Kodama (1992, 1994) give some physical evidence of the breakdown process. Moss did tests in a modified unconfined compression test machine using weathered granitic quartz. He assumed that if weaker particles are eliminated from the river first, then the average stress to fracture the remaining population of particles increases. Hence, if there is considerable break down of any size then the fragmentation stress should increase in downstream direction, because only the strongest particles are left in the channel.

Moss' results show that the 2 – 4.76 mm fractions showed an increased fragmentation stress more downstream, with the total number of these particles decreasing downstream. The opposite applied to the finest fractions. As an example, Figure 5.3 shows Moss' results using grains of 4.0 – 4.76 mm. The granite curve G, in this figure, corresponds to a composed data of five soil C horizon samples; curve S1 is for 100 grains taken half a kilometre from the stream source and; curve S2 is for the same quantity of material but collected 10 km downstream. Moss argues, that if the granite curve G is representative, curves S1 and S2 show that breakage took place and the weaker grains were eliminated. Following these results, Moss thus concludes that the 2 – 4.76 mm material is more readily broken, yielding additional fine sediment, which accumulates in the channel.

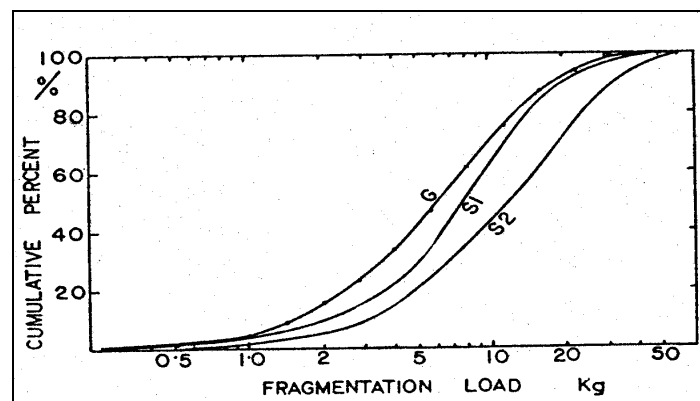


Figure 5.3 Fragmentation load cumulative curves of Moss' results.
Source: Moss (1972).

Kodama (1992, 1994) did experiments in a tumbling mill and he tried to reproduce flood conditions. He used in his test andesite and chert collected in the Watarase River in Japan and he found that when a mixture of gravel sizes was tumbled, the finer ones broke much faster than the coarser ones. He found also that chert tends to break down to smaller and angular gravel particles that constitute its principal elements; on the other hand, andesite produces fine particles like sand and silt while the particles get rounded. Figure 5.4 shows schematically the abrasion process of these two types of rocks.

Certainly, the experiments of Kodama show that break down of particles occurs and mainly depend on the lithology of sediments. In the case of the Meuse River sediment are quartzite, sandstone and phyllite. Quartzite has an internal structure, which is compact, and there are no defined structural planes of weakness and therefore, break down is unlikely to occur as principal mechanism of the abrasion process although it will produce big quantities of sand. On the other hand, sandstone may have planes of weakness depending on the environment of deposition and the degree of cementing between grains; thus sandstone might suffer break down. Finally, the elements of phyllite are grouped in plates (or in laminar layer) and therefore the phyllite is more likely to break down and produce fine gravel and sand. However, there are no sufficient field evidences to reject or to accept the break down as an important process in the case of the Meuse River. Field surveys are needed to further study the importance of break down in the Meuse River.

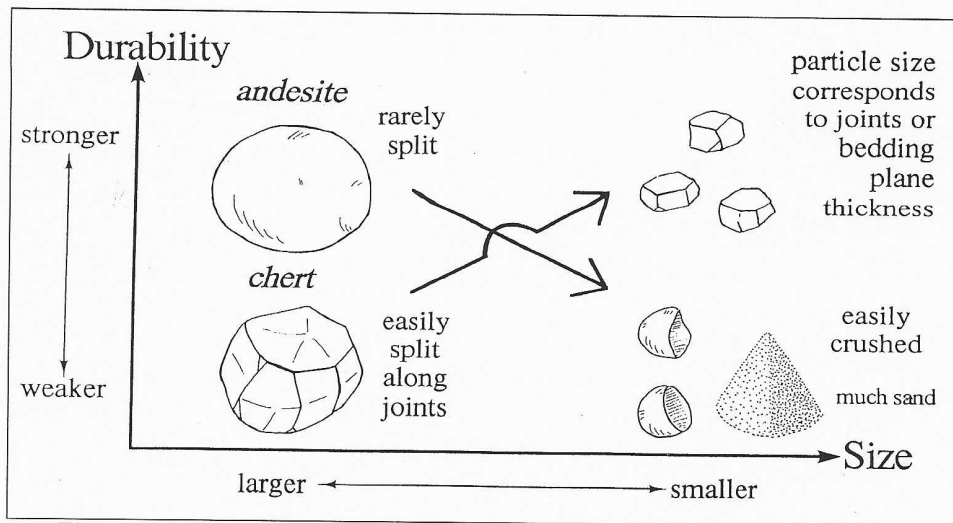


Figure 5.4 Summary of abrasion properties of andesite and chert particles.
Source: Kodama (1994).

5.4 Relevance of the tectonic movements-simplified approach

In this and the next section, an assessment is made of the importance that tectonic movements have in the downstream fining in the Meuse River is made. The influence of different variables is explored as well. In this section this is done by assuming that the coarser particles are depositing only. In the next section longitudinal sorting is included in the analysis.

5.4.1 Assessment of the relative importance

To assess the relative importance of the tectonic movements in the process of downstream fining a mass balance can be used. This balance is based on the equation of continuity for the sediment:

$$B \frac{\partial z_b}{\partial t} + \frac{\partial S_t}{\partial x} = 0 \quad (5.1)$$

where the term B represents the channel width and S_t the bed material transport (including both bed load and suspended bed material load).

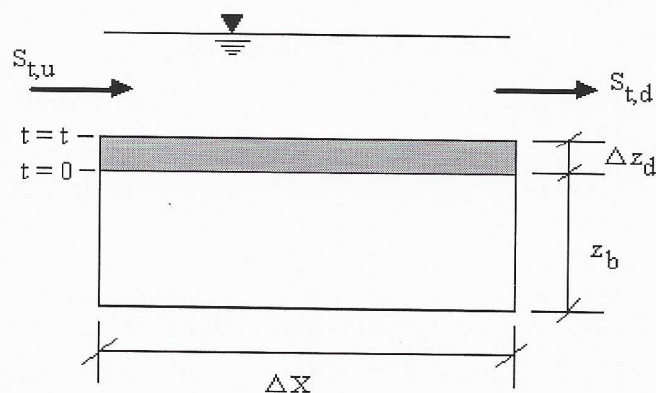


Figure 5.5 Definition sketch for the mass balance of sediments.

Assuming that aggradation is taking place ($\partial z_b / \partial t > 0$), Equation (5.1) can be transformed in terms of finite differences (see Figure 5.5):

$$B_d \Delta Z_d \Delta x = -(S_{t,d} - S_{t,u}) \Delta t \quad (5.2)$$

where

- B_d : deposition width;
- $S_{t,d}$: downstream sediment transport;
- $S_{t,u}$: upstream sediment transport;
- Δt : interval of time;
- Δx : length of the reach; and
- Δz_d : thickness of deposited layer.

It is implicitly assumed in Equation (5.2), that uniform deposition occurs in all the reach. Now, if subsidence is taking place in the area it may be assumed that the thickness of the deposition layer correspond to subsidence that happens in the time interval Δt . This implies that the bed elevation remains invariable during the time step. Considering this Equation (5.2) can also be written in the following way:

$$S_{t,d} = S_{t,u} - B_d \Delta x \frac{\Delta \Gamma}{\Delta t} \quad (5.3)$$

where the term $(\Delta z_d / \Delta t)$ was substituted been change by the subsidence rate $(\Delta \Gamma / \Delta t)$ in the area. The second term in the right hand side of Equation (5.3) represents the volume of material "V" that is deposited in the reach during the interval of time Δt . This volume "V" depends on the length of the subsidence reach, on the rate of subsidence and on the assumed deposition width. Moreover, under the above assumptions, Equation (5.3) shows that the sediment transport balance within the reach of interest depends on the sediment coming from upstream, the deposition width, and the subsidence rate.

Figure 5.6 presents one example of the application of Equation (5.3). If the curve "A" is considered to be entering the subsidence zone, it might be assumed that the volume of material "V" deposited is from the coarser fractions of the curve. The remaining grain sizes of curve "A" represent a complete new granulometric curve (curve "B"), applicable downstream of the subsidence zone and therefore, allowing us to assess the effect of subsidence.

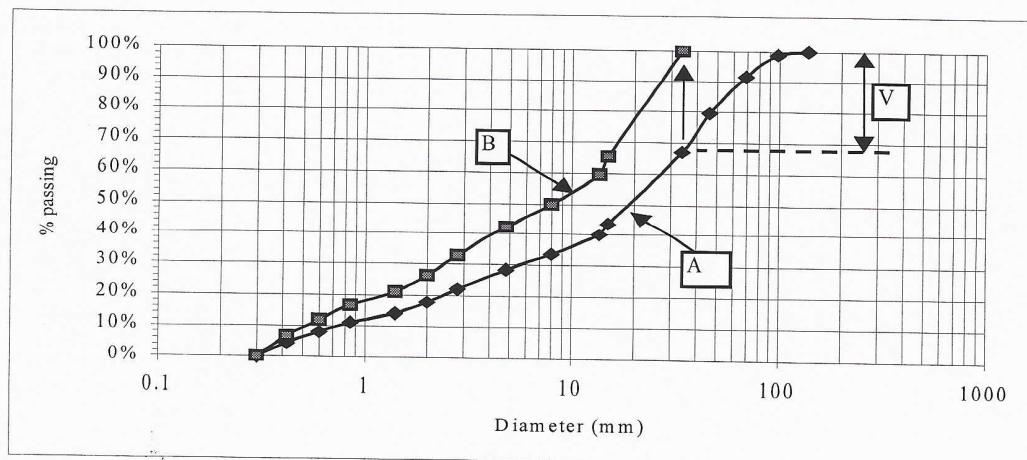


Figure 5.6 Schematic representation of the influence of subsidence rates.
See text for explanation.

As already mentioned Equation (5.3) was used to estimate the relevance of the vertical displacement on the basis of the conditions that prevails in the area. The conditions are discussed hereafter.

According to Van den Berg et al (1994), it might be assumed that there are two different rates of tectonic movements taking place in the area, though both are associated to subsidence. The first one is between the Feldbiss and Stevensweert faults and the second one is between the Stevensweert and Tegelen faults. Table 5.5 shows the approximate subsidence rates in these two sections (see also Figure 2.6).

Table 5.5
Rates of subsidence considered in the analysis.

| River reach | River chainage (km) | Subsidence rate (mm/y) |
|-------------------------|---------------------|------------------------|
| Feldbiss – Stevensweert | 45.0 – 65.0 | 0.60 |
| Stevensweert – Tegelen | 65.0 – 110.0 | 0.30 |

Equation (5.3) was applied to an average granulometric curve obtained from Sorber et al (1995) and since the length of the subsidence reach and the rates of subsidence are known the degree of fining depends only on the assumed deposition width. Applying Equation (5.3), it was assumed that the curve is representative at km 45 and it can produce the imposed sediment transport. Initially, the deposition width was set equal to the current channel width (100 m) and the sediment entering at km 45 was assumed to be equal to $35 \times 10^3 \text{ m}^3/\text{y}$. These conditions did not produce an appreciable change in the granulometric curve and therefore in the D_{50} . Hence after rethinking the conditions in the Meuse River it was decided to increase the deposition width in order to increase its influence. Values of B_d between 100 and 2,500 meters were tested. Since the subsidence rates were kept constant, this increment in the deposition width can be interpreted as an increment in the rate of deposition. As example Figure 5.7 shows the case of $B_d = 750$ metres.

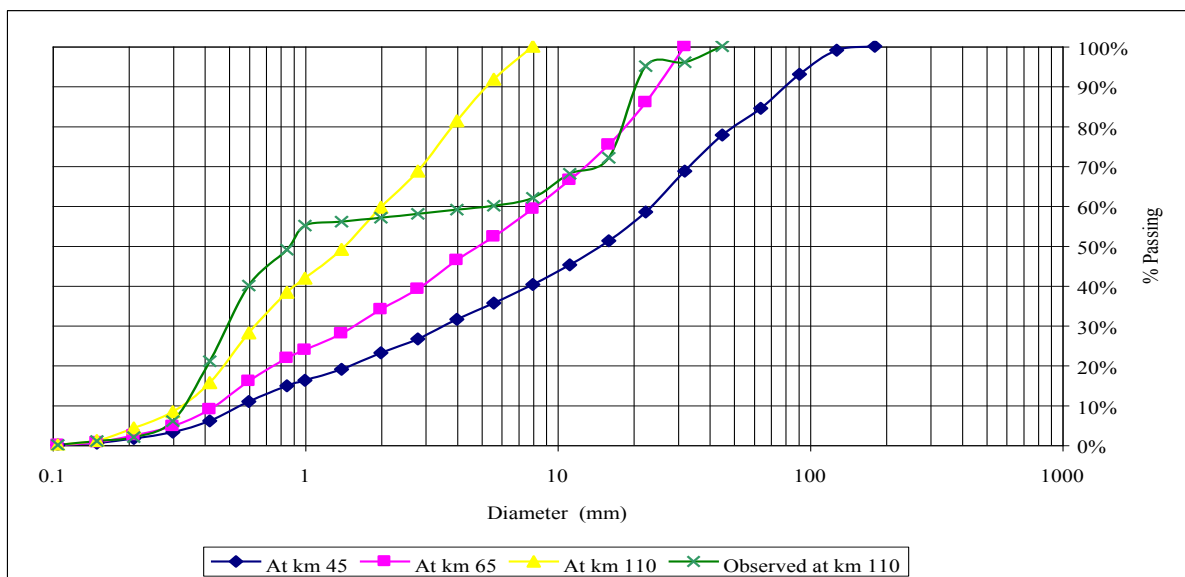


Figure 5.7 Granulometric composition of the bed material at different locations, $B_d = 750$ m and $S_{t,u} = 35 \times 10^3 \text{ m}^3/\text{y}$.

Figure 5.7 shows that there is a fair agreement in the fine part of the curves at km 110. The correspondence can be improved by selecting other value of B_d . It is also possible to observe that at this location, the bed material has a bimodal composition with a gap between the values of 1 and 5 mm approximately. This bimodal composition, as mentioned in Chapter 4, is a characteristic observed in the transition from a gravel-bed to a sand-bed of many rivers (Sambrook Smith and Ferguson, 1995). The coarse part of the bimodal composition at km 110 is not correctly represented

by the procedure utilised here. There might be several explanations for this: 1) break down is not included in this approach; 2) probably not only the coarser fraction is depositing but also part of the finer bed material. The latter can be investigated only when selective transport and the subsequent longitudinal sorting are taken into account. An approach using selective transport of particles is used in Section 5.5 to study whether more realistic assumption results in the development of bimodal distributions.

Moreover, three different granulometric curves reported by Sorber et al (1995) were also tested under the above assumptions. The curves at Borgharen (km 17.5), Grevenbicht (km 43.6) and Roosteren (km 51.8) were selected. Table 5.6 presents the summary of the results using these curves. Figure 5.8 shows the results using the curve at Grevenbicht for the cases of $B_d = 750$ and $B_d = 1,000$ m.

Table 5.6
Predicted values of D_{50} at km 110 using the simplified approach for different deposition widths and $S_{t,u} = 35 \times 10^3 \text{ m}^3/\text{y}$.

| Deposition width (m) | Original curve | | |
|----------------------|----------------|-------------|-----------|
| | Borgharen | Grevenbicht | Roosteren |
| 100 | 8.0 mm | 11.2 mm | 11.2 mm |
| 250 | 5.6 mm | 8.0 mm | 10.0 mm |
| 500 | 1.9 mm | 3.4 mm | 3.9 mm |
| 750 | 0.8 mm | 1.4 mm | 1.9 mm |
| 1,000 | 0.4 mm | 0.6 mm | 0.4 mm |
| 1,500 | 0.0 mm | 0.0 mm | 0.0 mm |
| 2,000 | 0.0 mm | 0.0 mm | 0.0 mm |

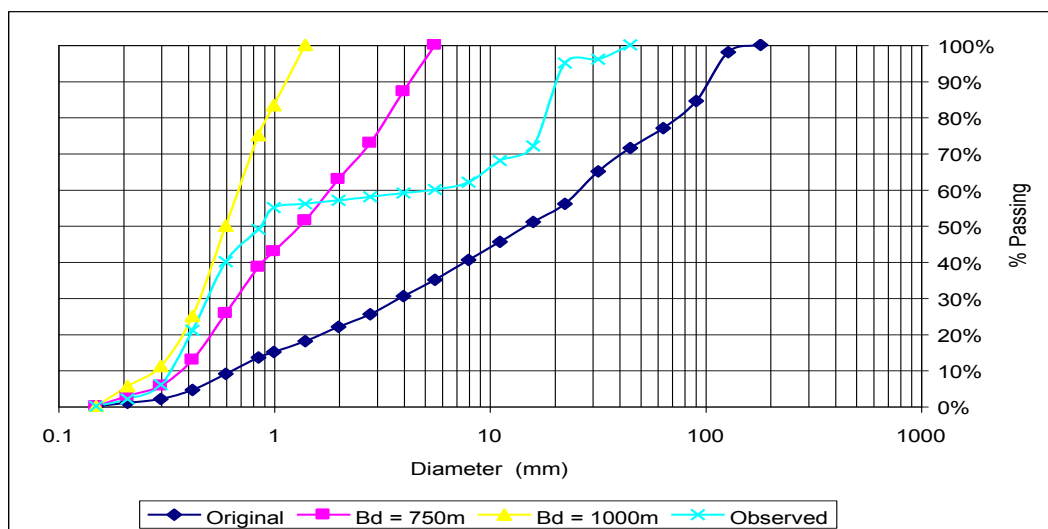


Figure 5.8 Granulometric composition of the bed material at km 110; $S_{t,u} = 35 \times 10^3 \text{ m}^3/\text{y}$. Original curve from Grevenbicht.

In addition, the imposed sediment transport at km 45 was also varied from 15×10^3 up to $75 \times 10^3 \text{ m}^3/\text{y}$ and tested in combination with several deposition widths ($100 \leq B_d \leq 2,500$ m) and the three granulometric curves mentioned above. The analysis of the possible combinations suggests that in order to get at km 110 similar diameters to those reported ($2.0 \leq D_{50} \leq 3.0$ mm), the deposition width should be between 500 and 750 meters approximately.

The results of this Section allow to conclude that the aggradation process which accompanies the downstream fining can be effectively counteracted by a similar subsidence rate preserving always the bed elevation and the reduction in size of the bed material. The reduction in size depends on the

sediment transport entering the reach and on the deposition width, the latter parameter being the more important one. The deposition width is discussed hereafter in more detail.

5.4.2 Deposition width

In the past, the Meuse River was a free meandering system. This allowed the river to meander within its floodplains, and adjust itself to the variable hydraulic conditions and sediment yields (by means of meanders, cut-off, etc.). Therefore the deposition of the sediments probably took place in wider zone than the channel width. This wider zone might correspond to the meander amplitude “a” of the river. To show this, four different relations for the meander amplitude in alluvial rivers can be applied:

| Relation | Bank-full discharge (Q_b) | Bank-full width (B_b) | Meander amplitude (a) |
|------------------------|----------------------------------|------------------------------|--------------------------|
| $a = 18.4 B_b^{0.99}$ | 900 m ³ /s | 120 m | 2.1 km |
| $a = 11.4 B_b^{1.04}$ | 900 m ³ /s | 120 m | 1.7 km |
| $a = 14 B_b$ | 900 m ³ /s | 120 m | 1.7 km |
| $a = 18.5 Q_b^{0.505}$ | 900 m ³ /s | 120 m | 0.6 km |

This manifests that although the total width of the meander belt is about 4.0 km (see Figure 2.9); the river adjusts itself to the different conditions in a width of about 1.5 kilometre. Consequently, there is a major probability that the sediments were also deposited over this width. Of course the previous relations are not for gravel-bed rivers but they can be interpreted as a rough approximation.

Here, the deposition width was also studied by means of an accumulated frequency distribution curve. In this, all the cases reported in Table 5.6 were considered and accumulated frequency curves were constructed (Figure 5.9).

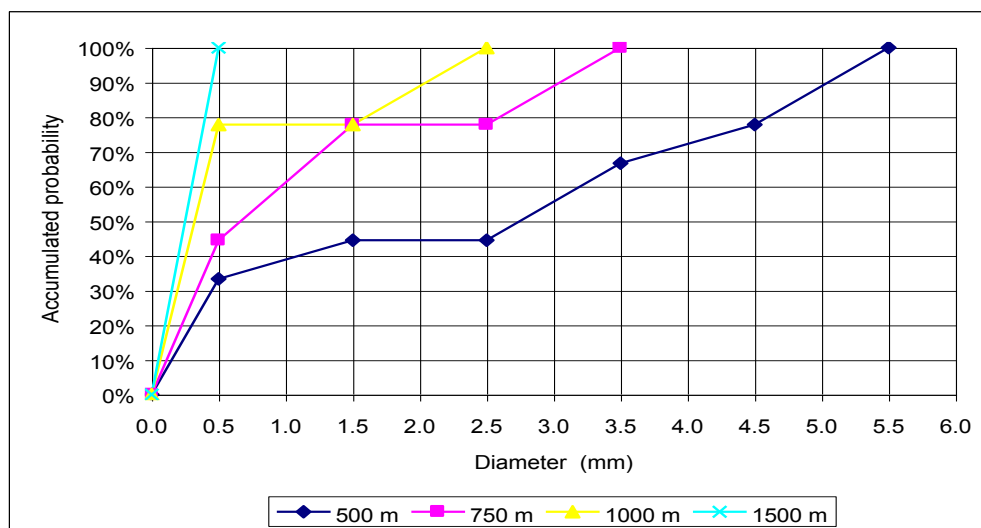


Figure 5.9 Accumulated frequency distribution of occurrence of the D_{50} for different values of deposition width.

Figure 5.9 should be interpreted as the probability that the D_{50} at km 110 would be within certain values and for a certain deposition width. As an example, there is a 22 percent of probability that the D_{50} would be between 4.5 and 5.5 when the deposition width is 500 meters. Following this, the higher probability that the D_{50} would be within 2.0 and 3.0 occurs when the deposition width is 500

higher probability that the D_{50} would be within 2.0 and 3.0 occurs when the deposition width is 500 metres. However, the combined inspection of Figures 5.8 and 5.9 suggests that a deposition width of 750 and 1,000 metres are also associated to a high probability of occurrence and therefore, could be considered too.

The relation between considered deposition width, meandering process and the fining of sediment could be interpreted as follows. Let consider that sedimentation of coarse grains only occurs in the main channel of the river and that the depth of the deposited sediment is equal to the average subsidence in the area, thus the bed level remains constant. If the river is meandering bank erosion occurs and the main channel would shift slowly its position. Considering this lateral movement, the location where sedimentation occurs is governed by the meandering process and therefore is shifting slowly together with the position of the meander; nevertheless the volume of deposited sediments is constant. The meandering of a river is a time dependent process and therefore according to the time scale we are looking at, should be the deposition width that we have to consider. In this study, we are looking at the long-term average conditions and consequently, we should consider the total deposition width over which sedimentation has occurred during a whole meander cycle, that is in all locations where the main channel has been due to the meandering process. According to the present findings in the Meuse River this deposition width seems to be between 500 and 1000 metres.

From Figure 2.9 it can be observed that the actual meandering width is about 4 km. This corresponds well with twice the meander amplitude as previously estimated. The meander width should be considered as extreme locations. The river is more frequently found within the belt. This might explain the discrepancy between the actual meander belt width and the values between 500 and 1000 metres found earlier. However, also the sequences of uplift and subsidence of the different blocks as well as the tilting processes present in the area could explain this discrepancy and might be interpreted as an external factor in the process of downstream fining.

These two conditions, morphology of the river and geological evolution of the area, are not accounted for in the equations. They might show up in the meander belt as horizontal discontinuities in the gravel layers. But this could be checked by collecting appropriate field data on the geology and the morphological evolution of the river itself through a complete geomorphological study.

5.5 Relevance of tectonic movements – using selective transport

Selective transport processes are most typical for gravel bed rivers, because of the rather wide size distribution of the bed material. In the case of study, the geological profile shows that the river is mainly flowing over gravel and coarse sand and therefore selective transport may play an important role. In this section the selective transport of particles is included into the assessment of the relevance that tectonic movement may have in the case of the Meuse River. It is an improve method of the approach used in Section 5.4 since it takes into account the behaviour of each grain size as well as the subsidence rate of the area, however, it only accounts for longitudinal sorting.

In this Section the methodology introduced by Parker (1991b) was employed. The methodology assumes that the profile of bed elevation is of the self-preserving form, and it propagates in downstream direction at a very slow horizontal wave speed c . If we consider that the river bed profile remains at the same level this horizontal wave speed can be related to the subsidence rate by expression (see Figure 5.10):

$$\frac{d\Gamma}{dt} = -c \frac{dz}{dx} = c i_b \quad (5.4)$$

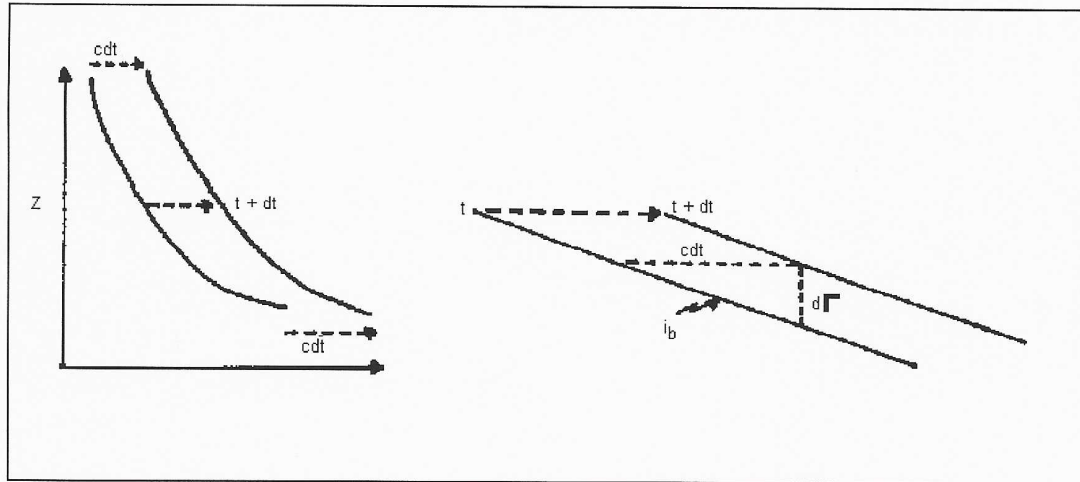


Figure 5.10 Schematisation of wave-like aggradation of self-preserving form.

Considering this, Equation (3.10) can be transformed in the following expression:

$$\frac{d}{dx} \left[\frac{s_b f_j}{(1 - \varepsilon)} - c L_a p_j \right] = -c p_{j0} i_b \quad (5.5)$$

where the term f_j represent the percentage of the grain size j in the bed load. To apply Equation (5.5) the composition of the bed load (f_j), of the surface layer (p_j), and of the exchange layer (p_{j0}) should be known and an appropriated sediment transport formula and thickness of the mixing layer should be selected.

In aggrading situations, the composition of the exchange layer can be set equal to the composition of the surface layer as was previously mentioned in Chapter 3. Similarly, the thickness of the surface layer can be set equal to its D_{90} . Selection of the sediment transport formula is not straightforward because it will affect the number of steps to solve Equation (5.5).

Considering the above and the aim of this Section, the formula of Parker (see Appendix 2) based on the composition of the surface layer was selected. This allows us to compute the sediment transport based on the parameter p_j . The formula consists of three parts and they match smoothly, and the overall relationship is consistent with other studies.

Parker (1990), in common with most recent approaches, assumes that different size fractions follow the same functional relationships between (s_j^* / p_j) and (τ_j^* / τ_{*j}) . The dimensionless bed load transport rate is defined as

$$s_{bj}^* = \frac{s_{bj}}{\sqrt{\Delta g D_j^3}} \quad (5.6)$$

where Δ is the submerged specific density of the gravel and the dimensionless Shields stress for a given size fraction is

$$\tau_j^* = \frac{hi}{\Delta D_j} \quad (5.7)$$

where $\alpha = 1.048$ and $\eta=0.0951$ for Oak Creek data (Parker, 1990); η is referred to as the hiding parameter and lies in the range from 0 (perfect equal mobility) to 1 (purely size selective transport). For the present assessment the value of Oak Creek data was utilised.

Finally, Equation (5.5) is solved with a forward explicit scheme following the procedure presented by Parker (1991b). Readers are referred to the work of Parker (1991a,b) for further details of the calculations. The granulometric curves at Koeweide (km 46.9) and at Roosteren (km 51.8) presented by Van Manen et al (1994) were used as upstream boundary condition and as initial condition ($x = 0$) respectively. In all the computations uniform flow and a Chézy coefficient of $46 \text{ m}^{1/2}/\text{s}$ were assumed.

Performing the calculations, different values of c were used ($1.0 \leq c \leq 3.5 \text{ m/y}$) in order to reproduce the observed downstream fining. Table 5.7 shows the values of D_{50} at km 110 obtained in this analysis.

Table 5.7
Values of D_{50} at km 110 for different wave speed.

| Wave speed (mm/y) | D_{50} (mm) | Equivalent subsidence rate (mm/y) |
|----------------------|------------------|--------------------------------------|
| 1350 | 5.0 | 0.60 |
| 1500 | 4.8 | 0.67 |
| 2000 | 4.2 | 0.89 |
| 2500 | 3.5 | 1.11 |
| 3000 | 2.8 | 1.34 |

From Table 5.7 is possible to infer that the value of $c=3.0 \text{ m/y}$ gave the best representation of the Meuse case. Figure 5.11 presents the variation in D_{50} of the bed material along the river reach under study.

From Figure 5.11, it is clear that the applied assumptions regarding subsidence rates and selected parameters are not able to reproduce accurately the observed pattern in D_{50} but they give a better estimation of the observed curves at km 110. In fact, Hoey and Ferguson (1997) present a sensitivity analysis where the influence of the different parameters is explored, suggesting that a carefully selection of parameters should be done. An inspection of the same figure reveals though that in an overall way the inclusion of the selective transport of particles allows to reproduce the sudden transition in grain size diameter that occurs in the Meuse River. Furthermore, the break down of particles has not been included yet in the different assessments and therefore the results can be improved ones the break down is also taken into consideration. In Chapter 6, a complete assessment including abrasion, break down, subsidence and selective transport is presented through the use of a numerical model.

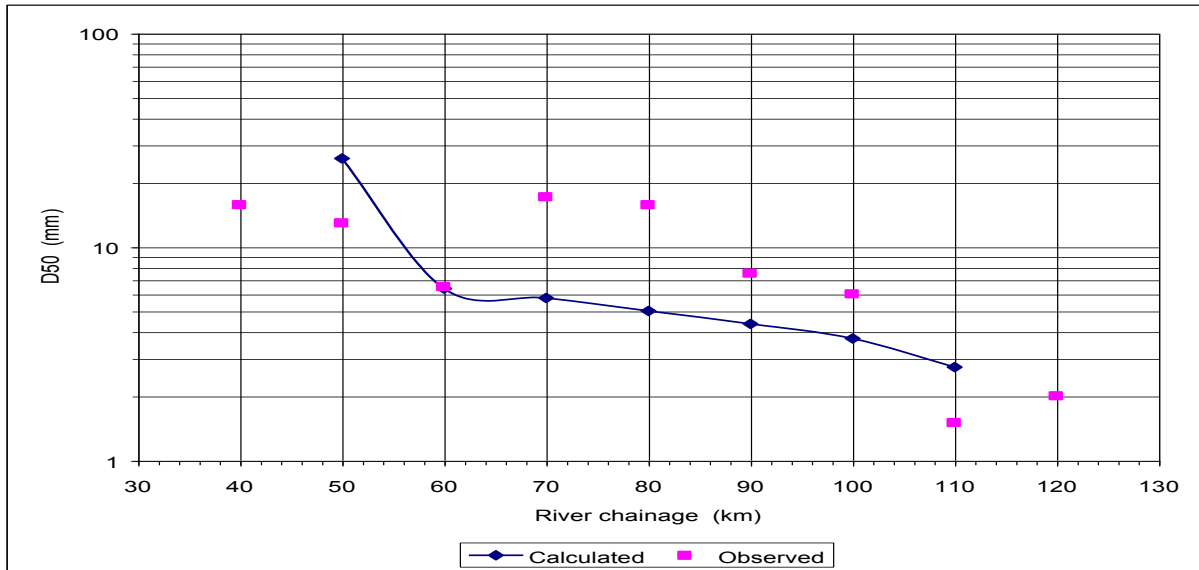


Figure 5.11 Variation of the D₅₀ in the bed material for a wave speed of 3.0 m/y.

5.6 Relevance of the ancient deposits and the Roer River.

It was mentioned in Section 2.3 that the Meuse River is flowing over its own deposits. These deposits were formed in different environment of deposition and they might represent a lithological control on the bed material. This is particular important in the delta area where could be a combination of fluvial a marine sediment. One way of estimating the importance of the ancient deposits is to compute the time needed to replace all ancient deposits from the active layer. Assume that the active layer thickness is as a maximum 0.5 metres. The volume of ancient deposits to be replaced is 0.5 (thickness) x 100 (width) x 200000 (length) = 10x10⁶ m³. Using a sediment rate of about 50x10³ m³/y about 200 year would be needed to replace all ancient deposits. Even considering that instead of the channel width possibly the deposition width should be used, still the conclusion might be that ancient deposits play only a minor role.

Another possible cause is the sediment input from the Roer River. The Roer River is one of the more important tributaries of the Meuse River. This river introduces sediment into the Meuse and can cause, in principle, one of the peaks in the gravel-sand content of the bed material (see Figure 4.7 at km 75). In view of the limited catchment size and the presence of barrages the effect of the Roer River is probably limited.

Both possible causes, old deposits and the Roer River, have not been studied in sufficient detail due to limitations in time and because they probably are not so important. Further studies are needed to determine their influence on the downstream fining of sediment in the Meuse River.

5.7 Change in bed slope

Sediment transport rates are directly linked to the bed slope if uniform flow is assumed and therefore changes in sediment load can lead to changes in bed slope. Moreover, if the diameter of the sediments were also changing it would affect also the bed slope. This can be observed in a qualitative way from Equation (5.9), which is known as the Lane balance:

$$S D^p B^{(n-3)/3} \propto Q^{n/3} i^{n/3} \quad (5.9)$$

Although Equation (5.9) cannot be applied in a straightforward manner to the Meuse case (as n and p are not really constant), it is clear from this equation that the slope depends directly on both the sediment load (S) and the diameter (D) of the particles. Thus, changes in either sediment load or grain diameter can produce changes in slope. According to Table 5.1 the sediment load can change due to abrasion and/or subsidence. The particle diameter can change due to abrasion, break down, subsidence, the ancient deposits and the input of sediments from the Roer River. This implies that, in principle, the observed change in slope can be used to understand more about the possible causes of the downstream fining.

Hence, to assess the change in bed slope all these factors should be considered. However in the present analysis only the changes in sediment load and in the particle diameter were taken into consideration. Furthermore, Table 5.6 gives values of D_{50} in the sandy reach (at km 110) and indicates that the grain diameter in the sandy reach not only depends on the initial grain size distribution (in the gravel reach) but also on the sediment load. In view of this complexity, in the present analysis the grain size distribution in the sandy reach was represented by only one diameter, that is 2.6 millimetres. A better approximation of this problem is presented in Chapter 6.

The assessment is based on the use of the Meyer-Peter & Müller sediment predictor, which is expressed as follows:

$$s_{ti} = \sqrt{g \Delta (D_m)^3} \frac{8}{1 - \varepsilon} \left(\mu \frac{h_i}{\Delta D_m} - 0.047 \right)^{3/2} \quad (5.10)$$

and the water depth by the expression:

$$Q = C B h^{3/2} i^{1/2} \quad (5.11)$$

Combining Equations (5.10) and (5.11) the sediment transport is given by:

$$s_{ti} = \sqrt{g \Delta (D_m)^3} \frac{8}{1 - \varepsilon} \left[\mu \left(\frac{Q_i}{C B \Delta D_m} \right)^{2/3} - 0.047 \right]^{3/2} \quad (5.12)$$

And the annual sediment load is computed as follows:

$$s_t = \int s_{ti} dt \quad (5.13)$$

Thus, using Equation (5.12) and (5.13) one specified annual sediment load can be determined.

In the present assessment, it was decided to impose the annual sediment load in the gravel reach and the volume of deposition (volume "V") produced by the subsidence rate; the difference between both gives the annual sediment load in the sandy reach. Furthermore, the values reported in Table 4.4 were used and the following parameters were considered constant:

| | | | |
|---------------|----------|----------|---|
| B_d | : 100 m | C : | : 55 m ^{1/2} /s (Sloff and Barnavelde, 1996) |
| D_{50} | : 2.6 mm | Δ | : 1.65 |
| ε | : 0.40 | | |

The deposition width was considered equal to the main channel width because the analysis is based on annual load and the D_{50} equal to 2.6 mm because allows as to compare directly the slope for different sediment loads. Finally, the discharge was split into two components when its value was higher than the bank-full discharge (≈ 1250 m³/s); one component conveyed by the floodplain and the other by the main channel. It was assumed that the floodplain conveys the 50% of the difference between the

The above assumptions allow to estimate lead the slope as unique variable in the system of equations, so the appropriate value to compute the target sediment load can be achieved. Figure 5.12 shows the results of the analysis, where the relation between sediment load in the gravel reach and the bed slope in the sandy reach is presented for two subsidence rates. As the reader can notice, in Figure 5.12 there is hardly any difference between both curves and indeed they are not representative for Meuse River. This suggests that the slope is not sensitive indicator for the downstream fining of sediments in the case of the Meuse River.

A better approach would be to consider not only the effect of the subsidence on the sediment load downstream, but also to take into account the reduction in D_{50} . The bigger the subsidence, the smaller D_{50} becomes in the downstream reach.

Finally, a remark should be made regarding the predicted versus the observed slope. As can be observed in Figure 5.12 the predicted slope is much smaller than the observed slope of 0.1 m/km. This is due to the limited applicability of the MPM sediment load predictor. As was shown in Section 4.3, the measured sediment loads are much smaller than the predicted ones. This is equivalent to the small slopes predicted here. An improved sediment transport predictor would give a better prediction of the downstream river slope.

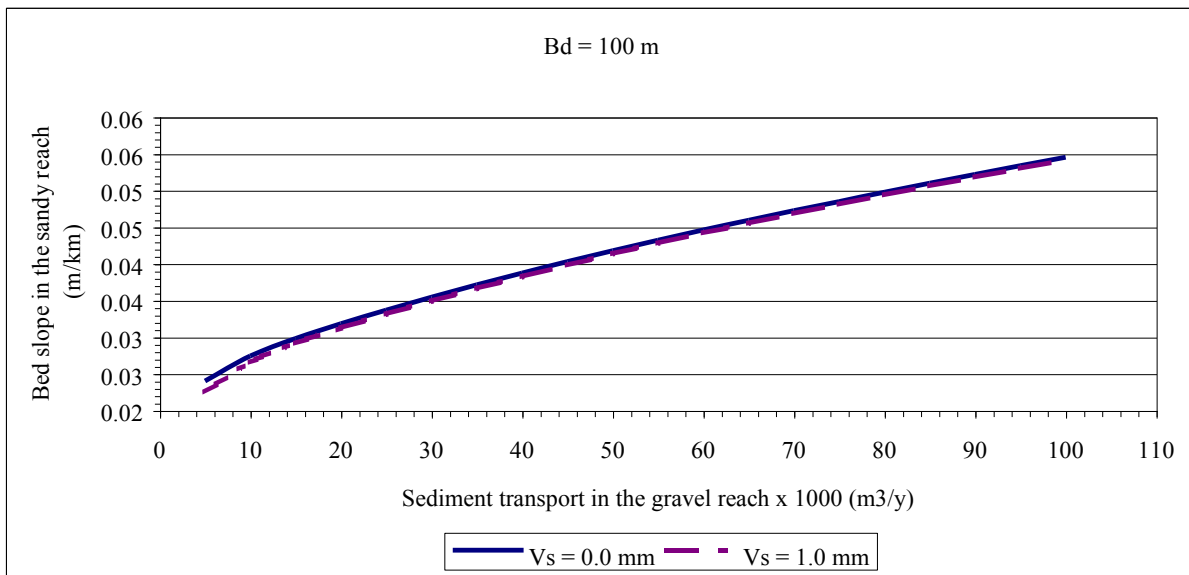


Figure 5.12 Relation between sediment load and bed slope in the sandy reach.

Chapter 6

Numerical simulation of the downstream fining of sediments

6.1 Introduction

In the previous chapter separate assessments of the different potential causes were carried out. This chapter presents an assessment in which the process of abrasion, break down, subsidence and selective transport are combined via a numerical model. Initially, the criteria to select the model are introduced and subsequently a description of the selected model is given. Next, the results of the simulations as well as of a sensitivity analysis in which one input parameter is changed systematically are presented. Finally the model is used to assess the effect of the training of the Meuse River in the 19th century.

6.2 Selection of the numerical model

To carry out numerical simulations in principle two models were available: SOBEK Graded and Acronym5. Delft Hydraulics and RIZA develop SOBEK Graded, while Acronym5 is software developed by Cui and Parker (1998). The main characteristics of each model are listed in Table 6.1.

Table 6.1
Characteristics of the models.

| Parameter | SOBEK Graded | Acronym5 |
|--|--------------------------|---|
| Temporal variations | Unsteady state | Steady state |
| Abrasion | Not considered | Considered |
| Subsidence | Not considered | Considered |
| Selective transport | Hiding factor in MPM | Parker (1990) approach |
| Scheme | 3 layers | 3 layers |
| Bed level changes | Aggrading Degradation | Aggrading only |
| Sediment predictor | Meyer, Peter & Müller | Parker (surface based) Engelund-Hansen |
| Discharge | Hydrograph | Constant |
| Length of the model | Full length | Subsidence reach |
| Grain size distribution (gravel reach) | Complete | Complete |
| Grain size distribution (sandy reach) | Complete | One diameter |
| Depositional pattern | 1-Dimensional | 1-Dimensional |

According to Table 6.1, Acronym5 considers the three processes involved in the downstream fining of sediments, notably abrasion, subsidence and selective transport. However, it does not consider the temporal variations in the equations ($\partial/\partial t$ terms are neglected) and therefore it computes long-term steady profiles (“equilibrium profiles”) which is important for a good appreciation of the influence that subsidence has the fining of sediments. On the other hand, SOBEK Graded is a robust program and it is able to handle unsteady situations but it does not consider abrasion of particles and subsidence. Moreover, since SOBEK Graded is a robust program, the demand of reliable information is high.

In the previous chapters it has been shown that the available information may not be representative of the field conditions and that there is no sediment transport predictor adequate to compute sediment load in the Meuse River. In addition in SOBEK Graded abrasion and subsidence are still missing. Therefore it is not advisable to use a model like SOBEK Graded, it was preferred to use a simplified model like Acronym5, in which the three important parameters for the downstream fining are already considered. Hence, Acronym5 was used to carry out the numerical simulations. An disadvantage of this approach was that to some extent a black-box model had to be used. No changes were made in Acronym5, although some serious limitations are present.

6.3 The selected numerical model

Cui and Parker (1998) developed the model Acronym5 and it could be obtained from Internet. The model uses the complete gravel size distribution ($D_j \geq 2.0$ mm) along the gravel reach and this size distribution may vary in downstream direction in response to abrasion, subsidence and selective transport. On the other hand, only one diameter is used to represent the sandy reach.

The set of equations presented in Section 3.9 are used in the model, but only the long-term profile is considered and therefore the time dependent terms are not included. The model accounts for the different grains size distribution of the surface layer, bed-load and substratum as well as for the abrasion of gravel into sand and silt. In particular, the model assumes that gravel abrades to silt until a certain cut-off size (D_c) is reached, at which the gravel spontaneously “breaks down” to sand of a single size. The silt produced by the abrasion process is treated as wash load.

Furthermore, the surface based sediment transport predictor per grain size of Parker (1990) (see Appendix 2) and the transfer function of Toro-Escobar et al (1996) are used in the gravel reach. This transfer function gives a relation between the percentage of the interface layer, bed-load and the surface layer for each grain size. Cui et al (1996) has used this function to simulate downstream fining with satisfactory results. The transfer function reads as follows:

$$p_{j0} = 0.7 f_j + 0.3 p_j \quad (6.1)$$

See section 3.6 for an explanation of the different symbols.

The resistance relation for the gravel reach is assumed to be of the standard Keulegan type whilst the sediment transport and resistance law for the sandy reach are that of Engelund-Hansen. The subsidence rate is assumed to be constant in space, the base level is also assumed to be constant and the sand is represented by only one diameter. The sand is not allowed to abrade.

Finally, the channel width is B_c and valley width is B_v , both taken to be constant and identical for both gravel and sand reaches. The stream is assumed to have some sinuosity (\check{S}), which is also taken to be constant and identical for both reaches. A constant flow (bank-full discharge) is maintained for a fraction of time “ T ” of any given year; the channel otherwise is dry.

Considering all this simplifications and assumptions, the Exner equation reads as follows:

$$\frac{B_v}{\check{S} B_c} (1-\varepsilon) \left(\frac{\partial z_o}{\partial t} + V_s \right) = \frac{\partial s_b}{\partial x} - 2\beta^* s_b \quad (6.2)$$

where V_s is the subsidence rate.

Acronym5 allows for three types of gravel-sand transitions: 1) the gravel can run out (gravel transport drops to zero); 2) all the gravel can reach the cut-off size and break to sand or 3) the sand can overwhelm the gravel. This last type of transition occurs when the capacity condition for sand

transport is reached before the gravel transport has dropped to zero and thus leaves a residual load of gravel in the sand-bed reach that is typically a very small fraction of the sand load. Further details on the model and on the equations can be found in Sinha and Parker (1996), Parker & Cui (1998) and Cui & Parker (1998).

To apply Acronym5 in the Meuse River an important remark should be considered. In Equation (6.2) the terms B_v and B_c are used; this is because the model assumes that if the entire basin were subjected to subsidence, but the compensating aggradation is restricted to the channel only, in time the channel would become higher than the floodplain. So, in the model the channel is assumed to shift or avulse so as to spread the deposits over the floodplain and consequently the effective width of deposition is included by means of using B_v different from B_c .

In the case of the Meuse River, the situation is slightly different and the meandering process is responsible for the spreading of the coarse sediments over a width different than the main channel width (as was discussed in Chapter 5). Nevertheless, the valley width can be considered equivalent to the deposition width ($B_v = B_d$) and the model is still applicable. If this is assumed Equation (6.2) can be rewritten as follows:

$$\frac{B_d}{I S B} (1-\varepsilon) \left(\frac{\partial z_o}{\partial t} + V_s \right) = \frac{\partial s}{\partial x} - 2\beta^* s \quad (6.3)$$

6.4 Results of the simulation

Hereafter, the model schematisation and the results of the simulation using Acronym5 are presented. The results obtained in this section are used subsequently in the sensitivity analysis of the different parameters.

6.4.1 Model schematisation

Since Acronym5 does not simulate differential vertical movements, only the subsidence area of the Roer Graben Rift system has been taken into consideration, that is, only from km 45 onwards has been modelled. Figure 6.1 shows schematically the model used.

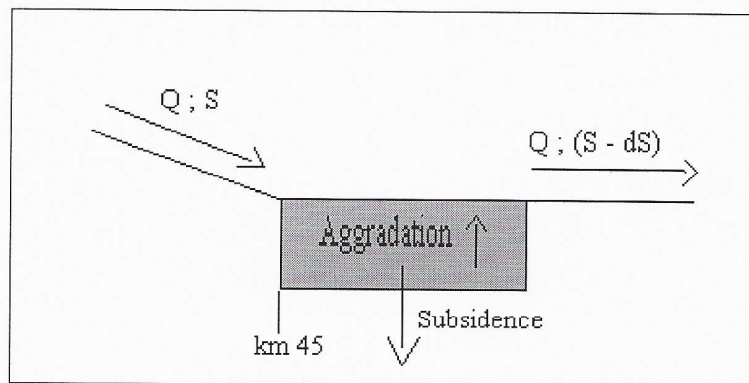


Figure 6.1. Scheme of the model used in the simulations.

The discharge considered during the simulations was the bank-full discharge, which is approximately $1250 \text{ m}^3/\text{s}$; this discharge, according to Table 4.4, happens about 1% of the time ($I = 1.0\%$). The sediment load entering at kilometre 45 were estimated from Wilbers (1996) (see Figure 4.11), and corresponds to about $36 \times 10^3 \text{ m}^3/\text{y}$. This amount of sediment was divided in gravel ($D_j > 2.0 \text{ mm}$) and sand according to the percentage found in Wilkens and Lambeek (1997); 80% and 20% respectively.

The subsidence rate considered was the average of the values that has been reported in Table 2.1 between kilometres 45.0 and 102.5; this average is 0.5 millimetres per year. Schröder (1994) reports abrasion coefficient for different gravel, for sandstone he reports $4 \times 10^{-5} \text{ m}^{-1}$ but for sandstone consisting of fine grains he reports $1.5 \times 10^{-6} \text{ m}^{-1}$. Since there is no information about these grain sizes in the Meuse deposits an average value was used ($\beta^* = 2 \times 10^{-5} \text{ m}^{-1}$).

The sinuosity of the Meuse was set at 1.46 (Paulissen, 1973) and the main channel width at 100 metres. For the deposition width a value of 650 metres was selected. The grain size cut-off, below which break down occurs, was set at 4.8 mm, following the results of Section 4.5. The bed porosity was estimated in 0.40. Finally, due to limitation of the model the sand diameter in the sandy reach was set at 2.0 mm instead of the better estimate of 2.6 millimetres.

6.4.2 Results of the simulation

Results of the application of the model are presented in Figure 6.2. In this the gravel-sand transition occurs at km 98, which is nearly the middle of the defined transition zone (km 90 to km 105). In this simulation the median diameter obtained by the model fairly agrees the behaviour of the field and average values. The gravel-sand transition occurs because the gravel load drops to almost zero allowing the sand to “overwhelm” the remaining gravel particles.

Important is the fact that the field values shown in the figure were obtained by the relation $D_m = 1.52D_{50}$ mentioned in Section 4.6. Remarkable is the gradual variation of the D_m in the gravel reach due to abrasion. The D_m in the sandy reach is equal to 2.0 mm due to limitations of the program.

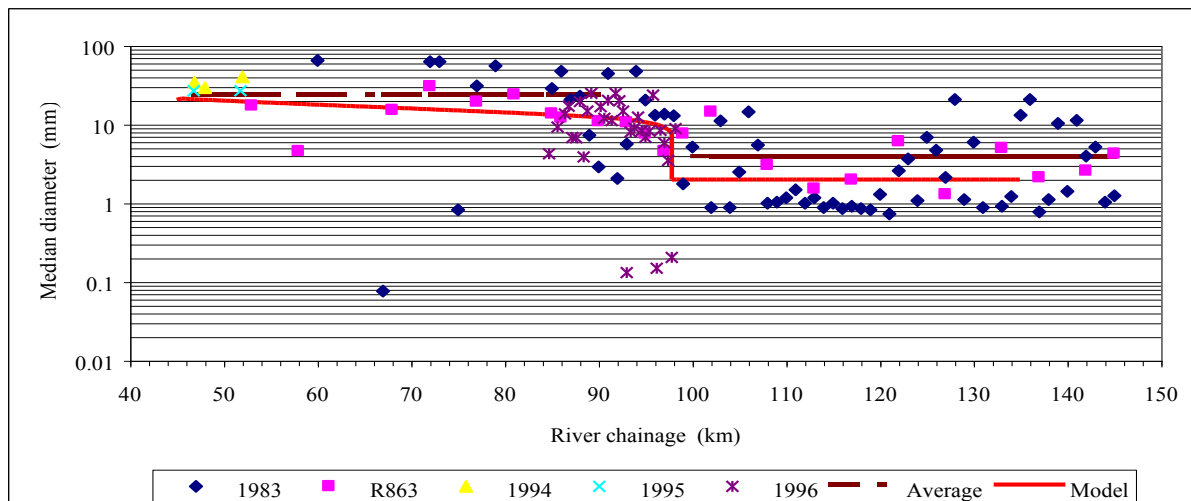


Figure 6.2 Variation of the median diameter of the substratum according to the simulation.

The Figures 6.3 to 6.5 give more information about the model results. In Figure 6.3 the water surface, bed level and Froude number are presented. The computed bed levels, and therefore water levels, do not match with the observed values, especially upstream from the gravel-sand transition. This may be caused because the model does not take into account the differential subsidence of the Roer Graben and therefore may only produce perfect concave profiles. In this Figure 6.3, there is a discontinuity in both water surface and bed level, which represents an internal boundary condition (the shock condition) for the formation of the gravel-sand transition. These discontinuities have been foreseen by Cui and Parker (1998) and interested readers are referred to the original source for a complete description of the shock condition. The Froude number is always lower than 1 and therefore there is no change in flow regime.

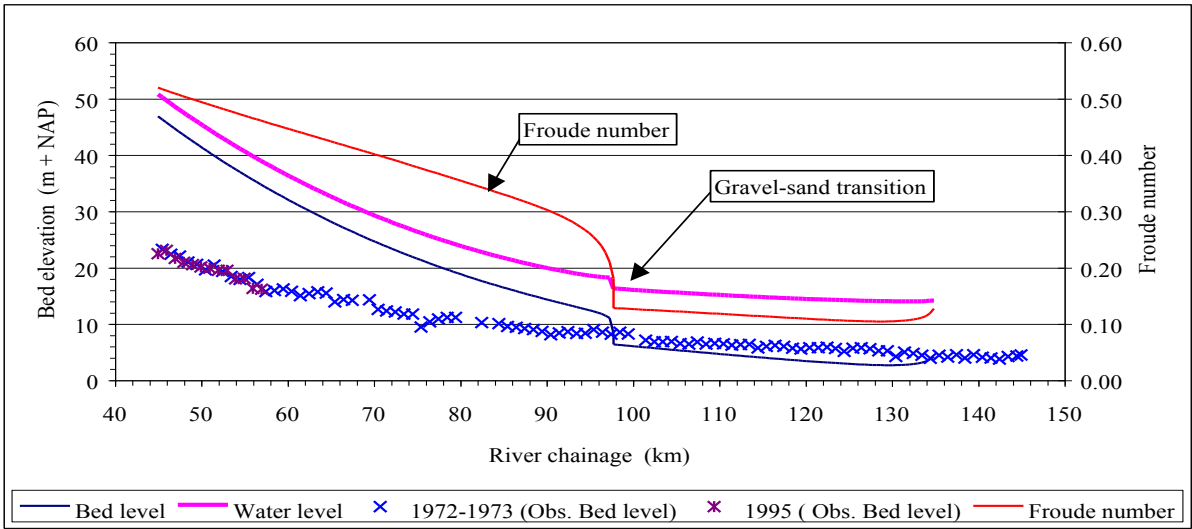


Figure 6.3 Water surface, bed elevation and Froude number computed.

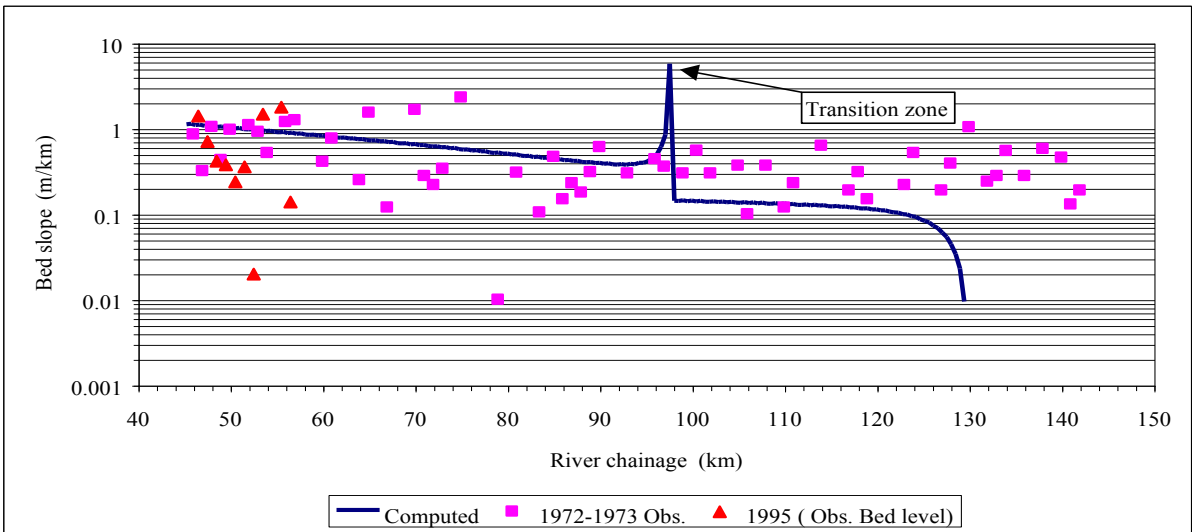


Figure 6.4 Channel bed slope (in m/km).

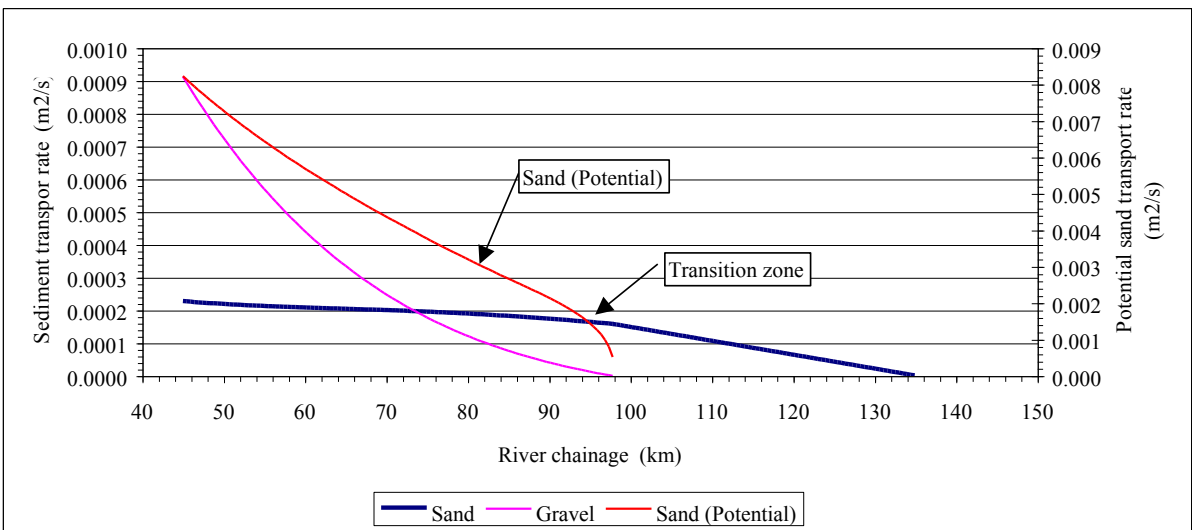


Figure 6.5 Gravel and sand transport rates (in m^2/s).

In Figure 6.4 the computed bed slope is presented. The peak in this figure is caused by the small shear stress at the gravel-sand transition. The sudden drop in slope at the end of the simulated reach is caused by the concave profile computed by the model.

Finally, Figure 6.5 shows the sediment transport rates. It is important to mention that in this Figure the sand transport is decreasing because it is deposited in the gravel pores and by the action of the subsidence. In order to represent accurately the sand transport differential subsidence rates have to be included in Acronym5 in the case of the Meuse River because downstream of km 104 there is hardly any vertical tectonic movements taking place (see Table 2.1). The results of the model in this reach are not appropriate for comparison with the available field data.

6.5 Sensitivity analysis

A sensitivity analysis was carried out in order to see the influence of each parameter in the model results. In the different tests one parameter was changed systematically, while the other ones were kept constant and equal to the values reported in Section 6.4.

The values tested in each one of the cases are:

- Subsidence rate: 0.0 mm/y; 0.1 mm/y and 1.0 mm/y;
- Sediment load: $45 \times 10^3 \text{ m}^3/\text{y}$ (+25%) and $27 \times 10^3 \text{ m}^3/\text{y}$ (-25%);
- Deposition width: 500 m; 750 m and 1000 m;
- Abrasion coefficient: 0.0 m^{-1} ; $1.0 \times 10^{-5} \text{ m}^{-1}$ and $3.0 \times 10^{-5} \text{ m}^{-1}$;
- Hiding exponent: 0; 0.1 and 0.5.
- Water discharge: $500 \text{ m}^3/\text{s}$ and $2000 \text{ m}^3/\text{s}$.

Figures 6.6 to 6.11 show the results of the sensitivity analysis; whereby the emphasis is on the location of the transition.

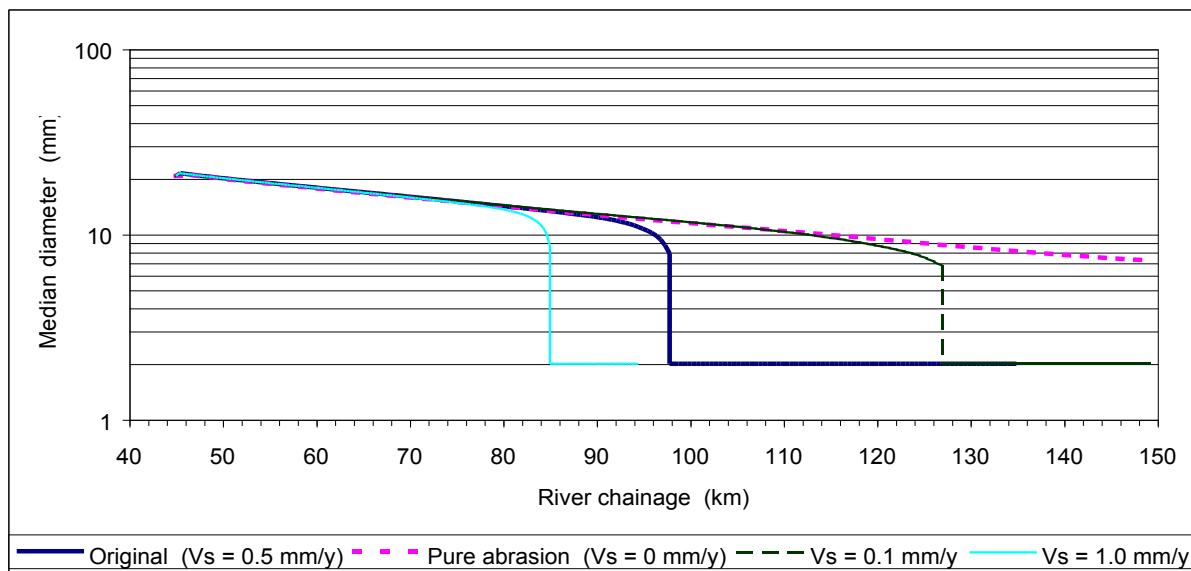


Figure 6.6 Effects on the D_m (substratum) due to variation in subsidence rate.

In Figure 6.6 it is possible to observe the effect of the subsidence rate; with higher values of V_s the transition point changes in upstream direction while the median diameter at the transition increases moderately. Conversely, when the subsidence rate is lower the transition moves in downstream direction, but the rate of change in location and in D_m is higher than the case of higher subsidence values. In the extreme case of pure abrasion ($V_s = 0$) there is no gravel-sand transition in the area of

interest. This case can also be used to see the effect of the abrasion in the reduction of the grain diameter. Over 100 km the median diameter reduces from 20 to 7 mm, which correspond to a reduction in volume of 90%, only 10% of the volume remains.

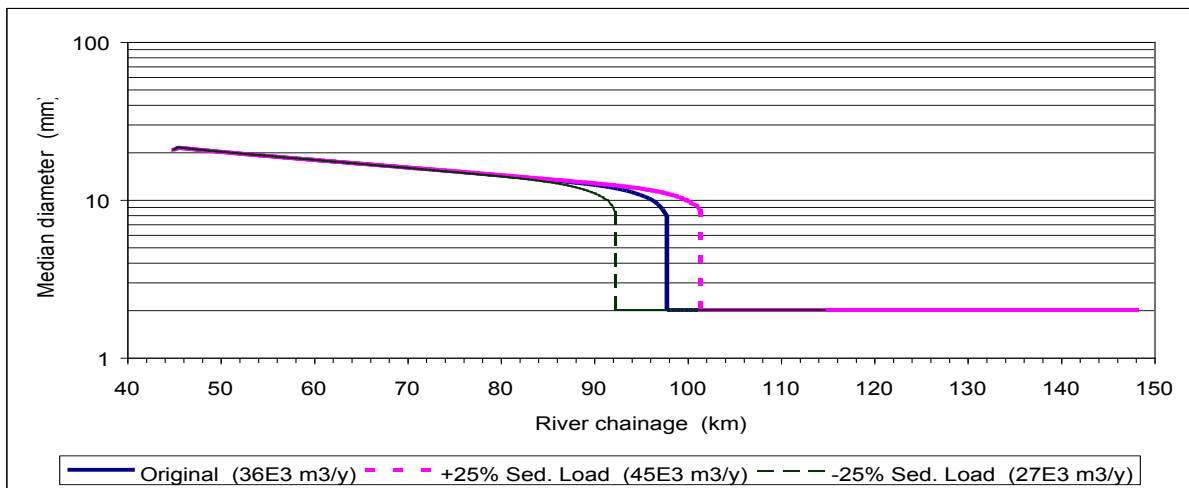


Figure 6.7 Variation on the D_m (substratum) due to changes in sediment load.

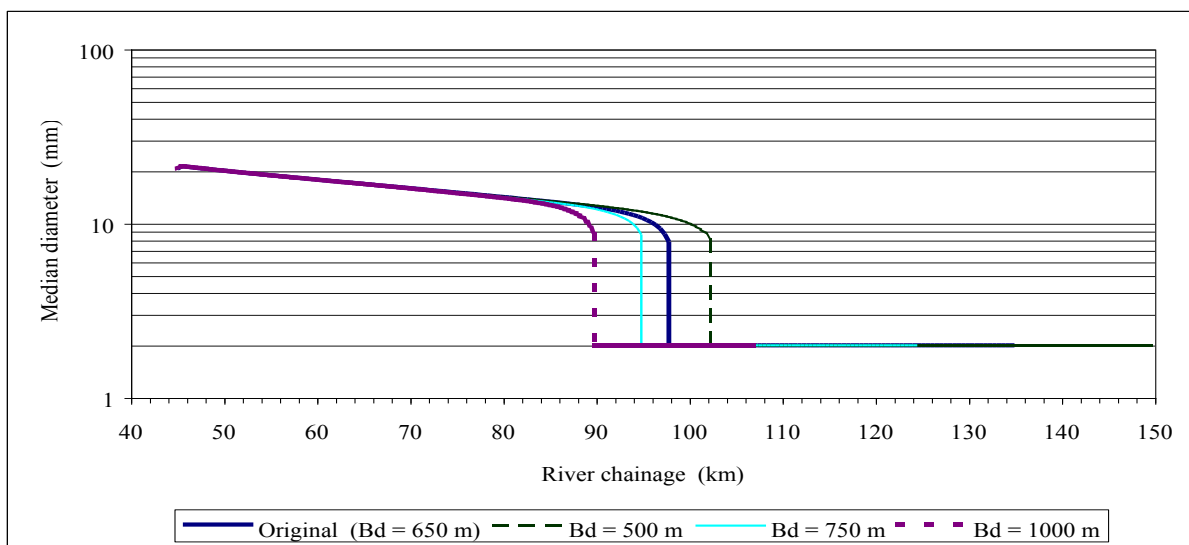
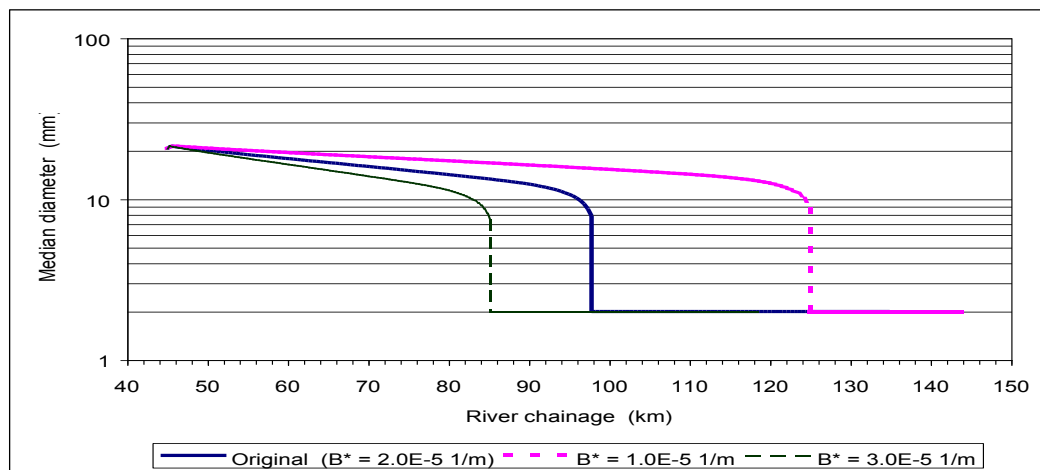


Figure 6.8 Influence of the deposition width in the values of D_m (substratum).



Variation of D_m (substratum) for different abrasion coefficient (β^*).

Figure 6.9

The effect of the changes in sediment load can be observed in Figure 6.7. In general terms, the shape of the curves is the same. Only the location of the gravel-sand transition changes slightly. Even though the increment in sediment load is appreciable ($\pm 25\%$) the transition is arrested within the zone defined (km 90 to km 105). This suggests that the location of the transition is not sensitive to the changes in total value of sediment load.

The deposition width (Figure 6.8) has a slight effect in the reduction of grain diameter. However, it affects the position of the transition, in fact, if the deposition width is narrowed the transition location is displaced in downstream.

Figure 6.9 shows results for changes in abrasion coefficient and it is possible to see that using lower values of β^* the transition points shifts in downstream direction. In the case of pure subsidence (not in the figure), all the available sand is deposited in between gravel grains and there is no sand left at the transition point and therefore it cannot form. This confirms that although abrasion does not explain completely the presence of the transition, it plays an important role. It provides sand to fill the voids between the gravel particles and thus allows the formation of a transition.

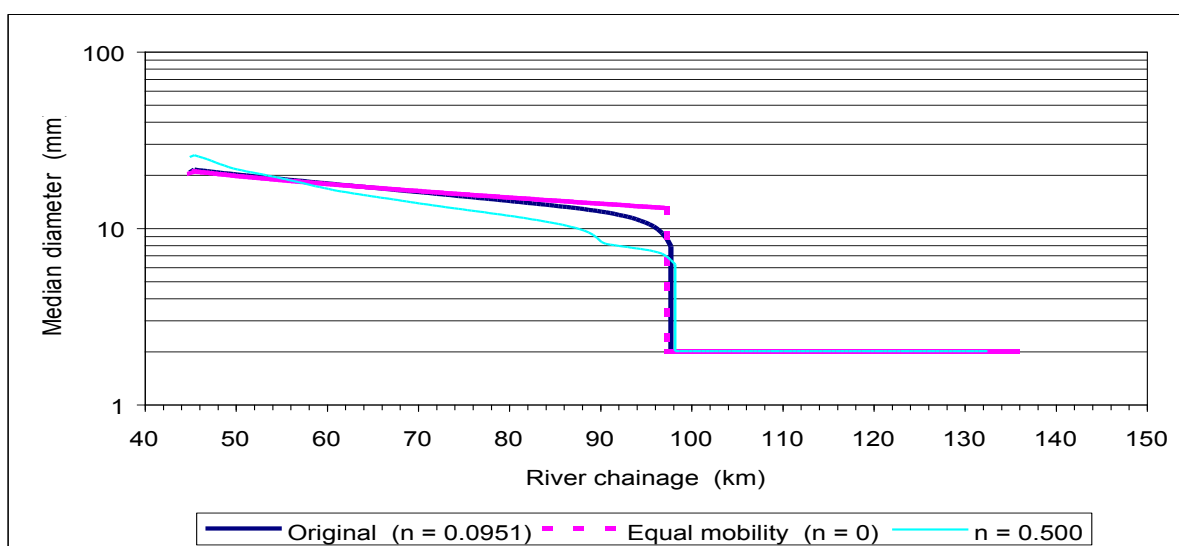


Figure 6.10 Changes in D_m due to changes in the hiding exponent (η) of the surface based sediment predictor of Parker (1990).

The hiding exponent in the surface based sediment transport predictor proposed by Parker (1990) (see Appendix 2) has an influence in the values of D_m (Figure 6.10). In perfect equal mobility (value of $\eta=0$), the diameter at the transition point is higher and the transition is sharper. Approaching pure selective transport (value of $\eta=1$) there are changes in the curve shape and this reflects the differential behaviour of each grain size. At the transition point the D_m is lower due to the fact that strong selective transport occurred.

According to Figure 6.11 the model Acronym5 is not sensible to changes in the water discharge; which is a strange characteristic for a morphological model.

Finally, in all the cases tested with the exception of the cases of pure abrasion and pure subsidence, the transition was formed due the fact that the gravel load drops to almost zero allowing the sand to overwhelm the remaining gravel particles. Moreover, the cut-off diameter was not reached in any of the simulation. Thus, break down did not occur.

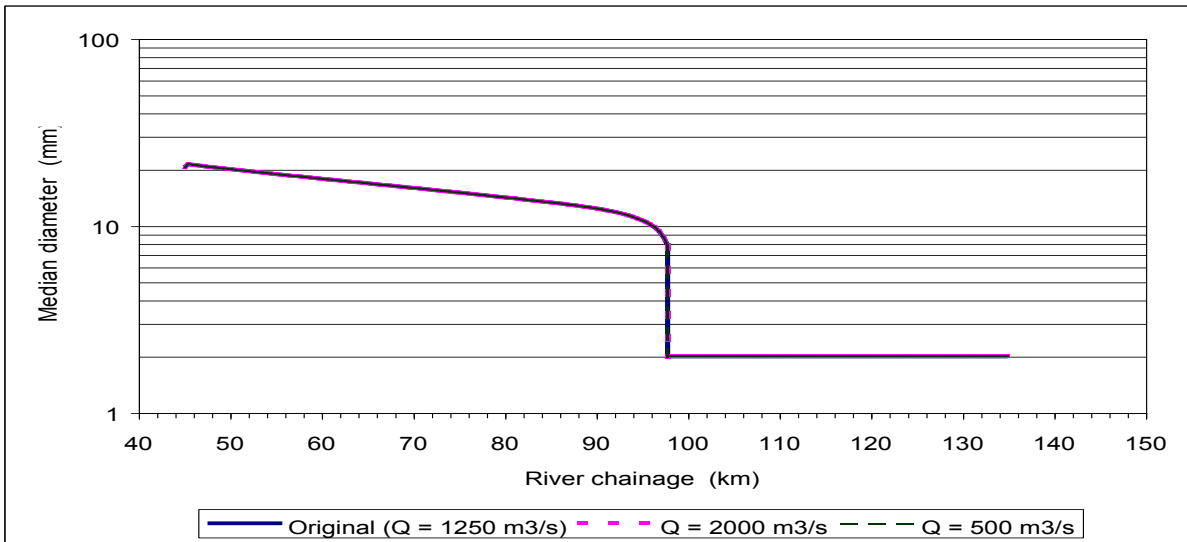


Figure 6.11 Sensitivity of the model to changes in the water discharge.

6.6 Effect of river training in the 19th century

The results presented in section 6.4 were obtained using a deposition width of 650 metres, which was probably the situation when the Meuse River was a free system. However, during the last two centuries the river has been trained and currently the planform of the river is fixed. This makes that the deposition width nowadays is similar to the main channel width, which is 100 metres approximately. Figure 6.12 presents the variation of the D_m in downstream direction for the case of a deposition width equal to 100 metres.

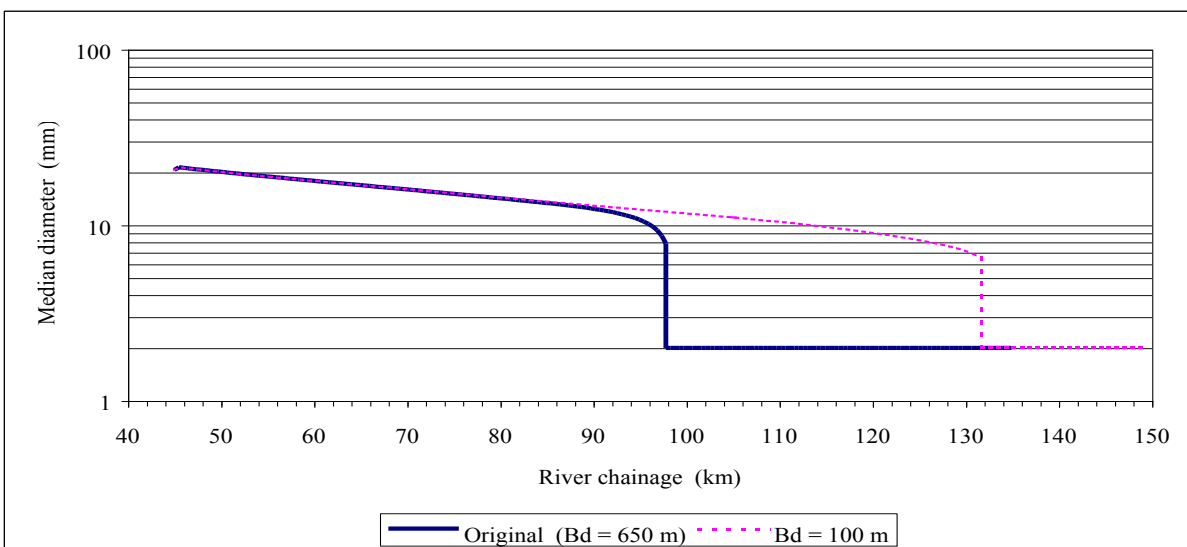


Figure 6.12 Variation of the D_m (substratum) for the current conditions of the deposition width ($B_d = 100$ metres).

This simulation suggests that the gravel-sand transition in the Meuse River is probably moving in downstream direction due to the narrowing of the deposition width. This movement is probably taking place very slowly and because of many human interference in the river is difficult to detect in the field.

Chapter 7

Discussion and implications of the results

7.1 Introduction

This chapter contains a discussion of the possible causes of fining mentioned in the previous chapters as well as its implications for the future data collection and mathematical modelling of the morphological behaviour of the Meuse River. In order to give a better description the chapter is divided into different sections, each of these dealing with a separate topic.

7.2 Limitations of the available field data

◆ *Bed material characteristics*

The analysis of the field data reveals that there is an appreciable variability of the bed material characteristics. These characteristics are varying in space and in time. The variability in space is amongst others caused by armouring (in vertical direction), by lateral sorting and by longitudinal sorting. Probably the latter variation occurs at the length scale of bends. Variability in time has two main causes. The passage of flood, which causes instability of the armour layer, generates much sediment and affects the armour layer composition. The second cause is the delayed response of the river system to human interference. This reflects that the river cannot be considered in “equilibrium condition”; most probably this condition of non-equilibrium is the result of the many training works and other human interference with the system (see Section 2.6) carried out in the Meuse since the 19th century. Moreover, there might be also changes in lithology that introduce additional difficulties to the bed material characterisation. Therefore, to characterise the Meuse River by means of simple statistical parameters is probably too simple and might not represent the real conditions of the river. Nevertheless, the changes in the average value of the bed material and the bed slope show that fairly sudden transitions are present. Table 7.1 shows the characteristics of these transition.

Table 7.1
Characteristic of the transitions in the Meuse River.

| Parameter | Location (km) | Values |
|-------------------------|---------------|------------------------|
| Slope | 60 – 80 | From 0.48 to 0.10 m/km |
| Grain size (D_{50}) | 90 – 105 | From 16 to 2.6 mm |

Finally, the development, in downstream direction, of a bimodal composition in the bed material of the Meuse River was confirmed. This bimodal composition is especially appreciable in the gravel-sand transition zone (km 90 to 105) and it is likely to be produced by the break down of particles. The results suggest that the diameter at which the particles are breaking is about 5 millimetres; this diameter though depends on the lithology of the bed material. Further studies into this aspect are needed.

◆ *Sediment transport process*

Sediment transport rates in the Meuse River are difficult to predict and the application of an existing sediment predictor can rise considerable inaccuracy. According to the results of Section 4.3, the Parker & Klingeman predictor might be used to forecast the sediment load when the armour layer is

present and MPM or Graf & Suzka predictor once the armour layer has been mobilised. Nevertheless, an appropriated sediment transport predictor for the Meuse River must take into account the presence of the armour layer and especially should be able to distinguish whether the armour layer has been mobilised by the previous conditions; i.e. it should take into consideration the “history” of the sediment transport process. Moreover, the use of a hiding coefficient and the full grain size distribution of the bed material composition are advisable. Finally, preferably the sediment predictor should be applicable to both reaches: gravel-bed and sandy-bed reach. There is an urgent need for the development of such a predictor. Some field data are available for the derivation of such a predictor, and additional data will be collected.

7.3 On the cause of the downstream fining in the Meuse River

According to Table 5.1 there are five possible causes for the gravel-sand transition in the Meuse River, notably: 1) abrasion of particles, 2) break down, 3) subsidence and selective transport, 4) ancient Meuse deposits and 5) the Roer River. In this study abrasion, break down and the combined action of subsidence and selective transport were studied. The two latter causes, the ancient deposits and the Roer River, are likely to be of minor importance for the case of the Meuse River although due to limitations in the available information and in time they were not explored extensively.

Looking at the abrasion process, the principal rock in the Meuse River deposits is sandstone. Solely, abrasion does not explain the sudden transition to a sand bed river; it produces a reduction of the grain diameter that is less than 1 millimetre over 15 kilometres. However, since sandstone is the principal rock, the product of its abrasion is mainly sand. Therefore the sand content in downstream direction increases, a situation that can be observed in Figure 4.7. Furthermore, the simulation results suggest that although abrasion is not governing the gravel-sand transition, the provision of sand by abrasion is important and helps in the development of the transition. On the other hand, break down of particles is probably the dominant process in the development of the bimodal composition of the bed material, but field evidences should be collected in order to verify this hypothesis.

The vertical tectonic movements (uplift and subsidence) within the basin play an important role in the long-term morphological behaviour of the Meuse River. The uplift process in the South Limburg block is likely to encourage an incision of the river bed and probably the current Meuse terraces are the product of this incision. Conversely, the subsidence in the Roer Graben provides a depositional environment and induces that the coarse fraction can be settled due to the selective transport of particles. If deposition and subsidence rates were in equilibrium, the bed level would not change in time but downstream fining would still occur.

According to Ikeda and Iseya (1987, 1988) there is a threshold point in the mobility of sediment mixtures. Figure 7.1 shows the results of the experiments carried out in the large flume of the Environmental Research Center of the University of Tsukuba using sand and gravel mixtures (Ikeda and Iseya, 1988). In this figure it is possible to observe that when the threshold in mobility is reached, there is a sudden change in bed slope. The fabric of the bed also changes from congested (or armoured) to a smooth (or sandy) and consequently the gravel-sand transition is formed. Moreover, downstream of the threshold point typical bed forms are formed and they produce that most of the remaining gravel grains are buried beneath the sand-bed as Ikeda & Iseya (1988) and Kodama et al (1993) already reported.

This threshold point could be related to the percentage of fine material present in the sediments and the process of filling up the voids between coarse grains. In Figure 7.1 the critical point is reached when the sand content is in the order of 50% but this value depends on the characteristics of the river and should be considered as an indication rather than an exact point. Before the voids are filled by fine material, there is grain to grain contact between the coarse particles and therefore they act together and produce a gravel bed river. However, when there is enough fine material deposited between the coarse grains, the contact between gravel particles is lost and at this moment, each coarse

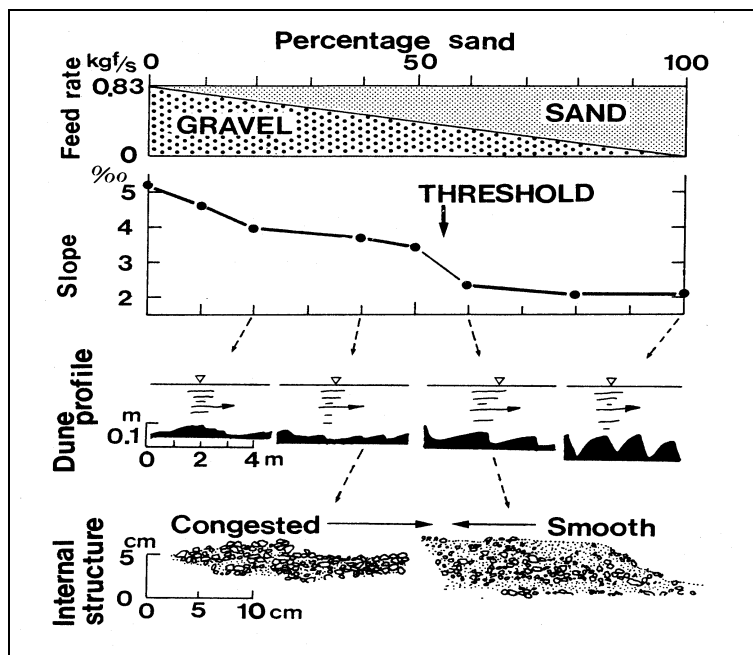


Figure 7.1 Changes in mobility, dune profiles and sedimentary structures as functions of the sand: gravel ratio of bed-load.
Source: Ikeda and Iseya (1988).

grain starts to act individually. This situation produces that the river bed structure changes from one in which there is fine material between a fabric of coarse grains to one in which there are gravel particles inside of a fine material layer; that is, from a gravel bed to a sandy bed.

In the Meuse River the gravel-sand transition occurs between kilometres 90 and 105 and according to Figure 4.7 in this reach the sand content of the bed material is in the order of the mentioned threshold point. The sand content in the studied case is reached by the combined action of two processes. The first one is the selective transport of particles, which is induced by the subsidence within the Roer Graben. This selective transport produces that coarser particles are preferentially settled. Consequently, the gravel content of the bed material is decreasing in downstream direction as well as the sediment load of gravel particles; the latter can be observed in Figure 6.5. The second process is the abrasion of sandstone, which produces sand; either by abrasion itself or by break down of the particles. Summarising, the gravel-sand transition in the Meuse River is the result of the combined action of selective transport (induced by subsidence) and the abrasion of particles.

According to the experiments of Ikeda and Iseya (1987, 1988) the transition of the bed slope should also be located near the transition in grain diameter. However, according to Figure 4.11 this does not happen in the Meuse River: the transition of the slope takes place between kilometre 60 and 80, that is upstream the transition in the grain size. If however only the surveys of 1909 and 1916 are considered (see Figure 7.2), it is possible to see that the change of the bed slope used to be located near the transition of the grain size. The present location of the bed slope transition is probably the result of the many human interferences that have taken place since the middle of the 19th century.

Another possible explanation for the present location of transition in bed slope might be the sediment transport itself. Since during the most part of the year there is no transport of gravel, the bed slope can be related to the transport of sand (assuming uniform flow) and therefore the transition of the bed slope is displaced towards the upstream direction.

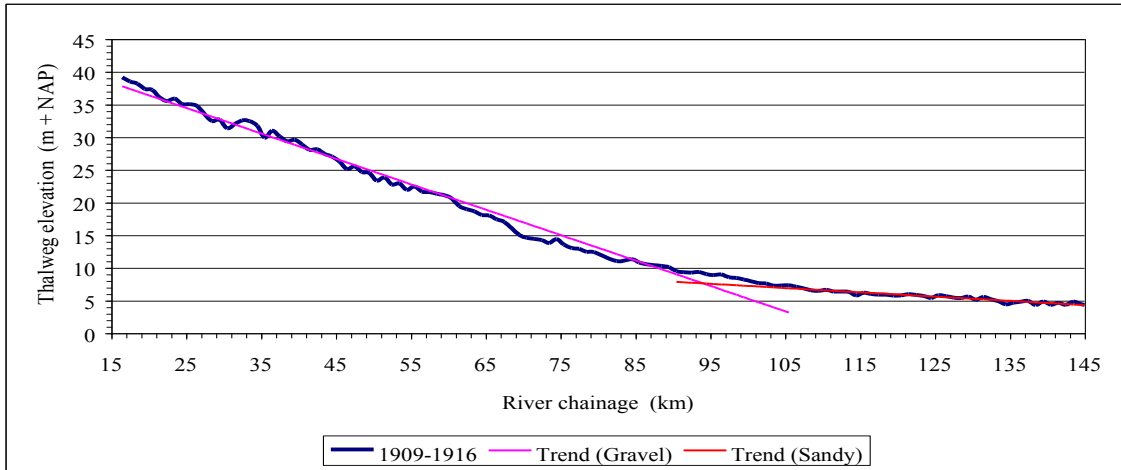
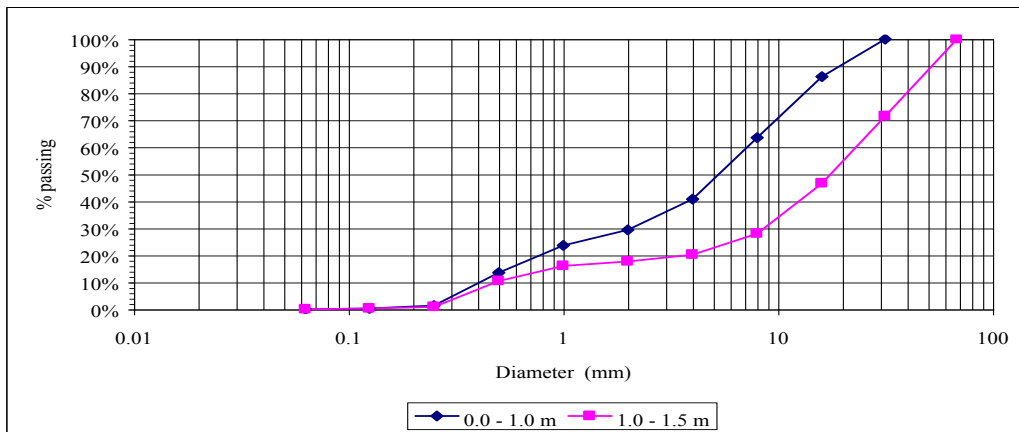


Figure 7.2 Trend of the bed slope at the beginning of the 19th century.

One additional remark in gravel-sand transition of the Meuse River, is the possibility that the remaining gravel particles are buried beneath the sandy bed. This can be detected by taking samples from deeper layers of the river bed. Figure 7.3 shows granulometric curves at two locations in the transition zone. In this figure the deeper layers have coarser material, which is in agreement with the type of transition and the burial of the gravel fractions.

A. At km 94.6



B. At km 97.4

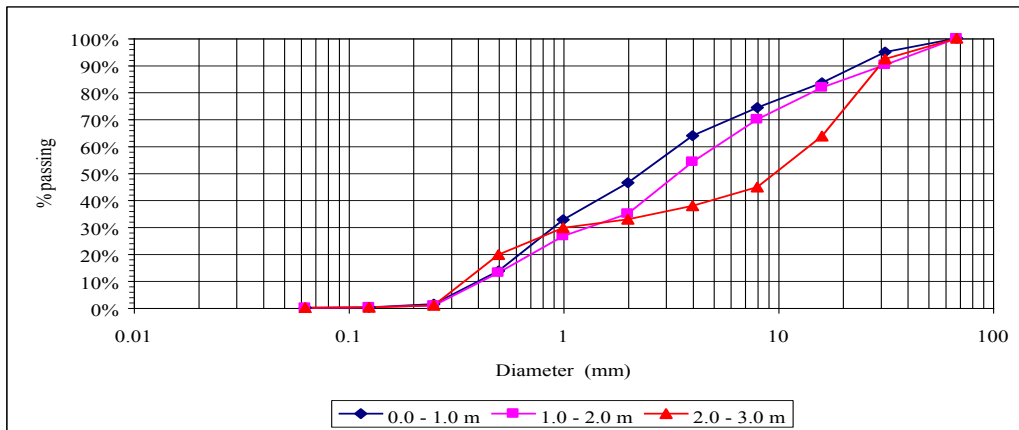


Figure 7.3 Grain size distributions of the substratum at different depths.
Data source: Fugro Comp. (1996).

◆ *Deposition width*

The width over which deposition is taking place in the subsiding reach was shown to be an important factor in the overall process of the downstream fining. However, its consideration depends on the time scale of the problem; in the case of long-term profiles the deposition width should be considered as the width over which the river has been meandering. This width depends on factors like the meandering process, bank erosion rates, and soil type among others. The simplified approach of Section 5.3 and the numerical simulations in Chapter 6 using Acronym5 suggest that in the case of the Meuse River, the representative deposition width is 650 meters. Probably though a more complicated picture should be drawn. During the meandering process the channel is mostly present in a narrow band around the valley axis. Occasionally the meandering extends farther away from this axis. This implies that in the floodplain areas away from the axis conditions are different. There also finer material is stored, and hence these far-away reaches contribute less to the preferential setting of the coarser sediments. The value of 650 meters should therefore be considered as the result of a weighting procedure of probability of occurrence of a channel and the effectiveness of the selective transport.

Finally, the results using a deposition width of 100 metres indicate that due to fixation of the planform the gravel-sand transition would shift in downstream direction. This shifting in position could be the explanation of why the field data suggest that the gravel-sand transition is between km 90 and 105. Perhaps in the past, the transition was arrested near km 90 but since the Meuse River has been trained and its planform fixed, the transition may have moved slowly towards a more downstream location, which could be at this moment, near km 105. This dynamic process is likely to be happening and explains the scatter in the data. Unfortunately at this moment, there is no morphological time scale to predict how long the shifting process would take. Simulation with SOBEK Graded would however provide additional insight into this phenomena.

7.4 On the used numerical model (Acronym5)

The numerical model used, Acronym5, is a useful tool in the modelling of the gravel-sand transition. However, it can be improved in order to handle more complicated situations and to get better results. The shock condition used to describe the gravel-sand transition should be improved in order to avoid discontinuities in the water and bed levels at the point of transition, this is specially important in the case of the water level. The possibility of differential tectonic movement (uplift and subsidence) should also be included making the model able to handle complex basins, like the Meuse basin. This point will make the model stronger and it will also allow for a better understanding of the role that differential tectonic movements have in the downstream fining of sediments.

Furthermore, according to 4.3.5 the use of only one representative discharge for both gravel-bed and sandy-bed reaches is not correct. The use of a smaller representative discharge in the sandy-bed reach would lead to higher values of slope and therefore better results for the case of the Meuse River. Additionally, an important issue is the apparent insensitivity that the results of the model have to changes in the water discharge, specially the variation of the D_m in downstream direction. It is expected that changing the discharge also the process of fining will also change, but apparently this is not the case. Further studies in this subject are needed.

In addition, in the particular case of the Meuse River, the applicability of the sediment transport predictors is questionable and consequently, the use of a specific formula may lead to misinterpretations.

Finally, time dependant variables could also be included in the model and this will allow to use a better description of the hydrology and to reproduce in a better way the sediment transport process.

7.5 Implications for collection of field data

The implications of the results obtained in this study can be summarised into two groups: first, field data collection and its analysis; and second, morphological modelling of the river.

◆ Bed material characterisation

- A. During the process of collecting samples, special care should be taken to differentiate between the armour layer and the substratum material. At present this is done in the sampling of the Common Meuse. In the past (e.g. Rijkswaterstaat, 1983) this was not sufficiently done.
- B. According to the data used in this study, additional samples of the armour layer and substratum composition are needed, especially from kilometre 50 to 88 and from kilometre 100 to 150.
- C. In the process of collecting samples, separate description of the right bank, middle of the river as well as left bank should be done.
- D. Petrographical description (including the rock shape) of the sediments along the Meuse River is important for a better description of the abrasion process, this can be done from the samples taken to describe the armour layer and substratum material.
- E. It is advisable to do a complete geological reconnaissance along the Meuse in order to study whether lithology may have influence on the gravel-sand transition.
- F. Finally, the use of the bucket sampling method in the Meuse River is not advisable for collecting samples.

◆ Sediment transport rates

- A. The field measurement of sediment load should be done more frequently. It is advisable to do sampling not only during flood condition but also before and after the flood. In particular, after a large flood, substantial quantities of sediments are still transported at lower discharges.
- B. The grain size distribution as well as the petrology of the sediments collected should be analysed. This will yield additional insight into the abrasion process and will help in future model calibrations.
- C. The amount of sampling points of the sediment load should be extended in the future, because the river shows a large variation in sediment load, not only in time but also in space.
- D. The network of sampling point could be extended using hydrophones or similar devices. Although these devices give mainly qualitative results, even these qualitative results are quite useful.

◆ Field data interpretation

- A. When interpreting field data, it is important to keep in mind that the Meuse River is never in “equilibrium condition” and consequently there are variations in space and in time. During the last two centuries there have been many human interference in the system and therefore the river is still in process of adaptation.

- B. The same holds for the effect of subsidence. Sediment is stored in the subsiding zone, and hence the continuity equation is more complicated than in other rivers. This holds also per fraction.
- C. Additionally, during the process of interpretation the combination of the different sources of information (geology, sediment load, petrology, etc) is a key element; because the evolution of the Meuse basin is the result of many different processes. The present study has shown how these different sources of information can be combined to yield additional insight.

7.6 Implication for the morphological modelling of the Meuse River

- ◆ In morphological modelling of the Meuse River is not advisable to use parameters that are sensitive to the bimodal composition of the bed material like the D_{50} .
- ◆ It is necessary to derive an adequate sediment transport predictor for the Meuse River. This predictor should preferably be per grain fraction and it should be able to take the “history” of sediment transport process into account. A proper calibration versus field data is a must.
- ◆ In the modelling of the Meuse River an adequate description of the sediment transport process should be incorporated. The model should be able to distinguish whether the armour layer has been mobilised or not.
- ◆ The deposition width to be considered in the model should be according to the time scale of the problem in consideration. Presently the channel width appears to be an appropriate measure.
- ◆ Incorporation of abrasion process in modelling the Meuse River is important, since abrasion is helping in the formation of the gravel-sand transition.
- ◆ Incorporation of differential vertical movement (subsidence and uplift) in modelling the Meuse is also important. These tectonic movements encourage either the incision of the river or the necessary environment to settle the coarse fractions of the bed-load material.
- ◆ Acronym5 seems to be a useful tool in modelling gravel-sand transition. However, there are some aspects of the model (as already mentioned) which can be improved in order to do it a more powerful tool.
- ◆ As an alternative, SOBEK Graded can be extended to include the effect of abrasion and the effect of subsidence. Probably SOBEK Graded is more attractive than Acronym5 as it is suited for unsteady transient conditions.
- ◆ Finally it should be realised that a complete calibration of a numerical model of the Meuse River on historical data will never be possible. Too many uncertainties and limitations of available data preclude this. It seems preferable to concentrate on a model that predicts the present conditions at an accepted level.

Chapter 8

Conclusions and recommendations

8.1 Conclusions

In this study the available information on the geological conditions and the river characteristics of the Meuse River were assessed and analysed in an attempt to understand the occurrence of a transition from a gravel-bed to a sand-bed river. The following conclusions can be drawn from this study:

On the transition of bed material characteristics and slope

- The Meuse River can be characterised as a gravel-bed river upstream of km 90 and as a sand-bed river downstream of km 105. Hence a gravel-sand transition occurs in the Meuse River between approximately the kilometres 90 and 105. In this transition the D_{50} of the substratum material changes from about 16 mm to about 2.6 mm.
- There is also a pronounced and fairly sharp reduction in the bed slope. This slope changes from about 0.48 m/km to about 0.10 m/km and this transition happens around kilometre 70. In the early 20th century this transition was located near km 90 as well, but due to human interference the change in slope has travelled in upstream direction.
- The gravel-sand transition takes place fairly smoothly. Gradually the sand content increases in downstream direction. The transition is also gradual because lateral sorting effects play a role as well, and these obscure the processes involved.
- Different explanations are possible for this transition from gravel bed to sandy bed: 1) abrasion of particles; 2) break down of grains; 3) subsidence inducing selective transport; 4) ancient Meuse deposits and 5) the Roer River. The transition in the Meuse River is probably caused by a combination of abrasion and break down and subsidence.
- This is because of the preferential deposition of coarse material in the subsiding reach, less coarse material is transported downstream. The above conditions, together with the abrasion process of the sandstone, allow that the sand content to increase in downstream direction and a threshold point is reached, where the river start to behave like a sand bed river. The abrasion process provides, together with the sediments entering the zone, the necessary quantity of sand to reach the critical value in the sand content.
- The assumed deposition width plays a major role in that assessment. There is however only limited understanding of the concept of deposition width as used in this study. This deposition width is much larger than the channel width, and although some support is available for this assumption, more studies are needed to clarify the concept and to make a good choice of the deposition width based on the meandering characteristics of the river and the lateral sorting on point bars.
- The gravel-sand transition is likely to be moving in downstream direction due to the river training works that the Meuse River has suffered in the past.

On the bed material characteristics of the Meuse River

- There is a large variability both in space (lateral, vertical and longitudinal direction) and probably in time, of the particle distribution of the bed material in the Meuse River. The variability is linked to the physical processes in the Meuse River. Also the transient phenomena induced by human interference in the system since the 19th century might be important in this respect.
- The bed material in the Meuse River shows a development of a bimodal grain size distribution of the substratum material. This bimodal composition shows a gap between diameters of 1 and 5 millimetres approximately.
- Such bimodal distributions can better be represented by D_m rather than by D_{50} . The ratio D_m/D_{50} can reach very high values for bimodal distributions.
- Although quite some progress in the understanding of the underlying processes, also via this study, there is still not sufficient data and insight to fully characterise the bed material characteristics of the Meuse River. More studies are should be carried out in the future.

On sediment transport in the Meuse River

- Sediment transport processes in the Meuse River are quite complicated and difficult to understand because of 1) the occurrence of an armour layer in the Common Meuse; 2) the poorly understood effect of floods on the armour layer, 3) the occurrence of a transition from a gravel-bed to a sand-bed river near Roermond; 5) the effect of human interference which has induced transient phenomena and 6) the limited availability of field data on bed material and sediment transport.
- The set of available data on bed material and sediment transport is growing but only slowly, because of the dependency on the occurrence of floods.
- The available data on sediment transport show quite some scatter. This is not so much due to inaccuracies in the measurements but rather to the physical processes which cause that at the same discharges quite different sediment transport rates might occur depending on the previous conditions.
- There is no sediment transport that can, with a reasonable accuracy, predict the sediment transport in the Meuse River. There is an urgent need for the development of such a predictor. Such a predictor should be based on the available sediment transport data, but conceptually should also take the complicated physical phenomena into account.
- Preferably the sediment transport predictor to be developed should be applicable to both the gravel-bed and the sand-bed reach.
- Sediment transport in the gravel-bed reach and in the sandy-bed reach are taking place at different discharges. Most sediment in the sandy-bed reach is taking place at lower discharges than in the gravel-bed reach. This suggests that the full hydrograph should be used in modelling and not one dominant discharge.

On the numerical modelling of the morphology of the Meuse River

- In this study several methods were used to assess the occurrence of a transition, ranging from simple arithmetics to a complicated numerical model developed by Cui and Parker (1998).
- The numerical model used here includes abrasion, break down, subsidence and selective sorting. The model is quite useful in understanding the causes of the transition in the Meuse River.
- The applied model is also limited in its possibilities. Major disadvantages are: 1) the use of one representative discharge which leads to a too small slope in the sandy-bed reach; 2) the way the deposition width is included in the model; 3) the occurrence of a shock at the transition of gravel-bed to sandy-bed reach, and some other aspects.
- The applied model cannot simulate transient phenomena either. Hence it might be considered to extent the capabilities of SOBEK Graded to study the transition in more detail and to simulate also the transient phenomena introduced by human interference with the river system since the 19th century.

8.2 Recommendations

The recommendations that can be made on the basis of the conclusions arrived at in this study can be listed as follows:

Collection of field data

- There is a clear need for additional data collection in the Meuse River. Much more good information is needed on the bed material characteristics and on sediment transport in the Meuse River. Every opportunity that arises to collect data on sediment transport should be used, because of the few floods that usually occur.
- The sampling procedure to be use in the Meuse must distinguish between armour layer and substratum material. This implies that bucket sampling as used in the reach upstream of barrages is not a suitable technique.
- Preferably the local slope should be measured during the sediment transport measurements. This is relatively easy for the steeper gravel-bed reach. This is helpful for the further elaboration of the sediment transport data.
- In processing bed material data it is not recommended to use of sensitive parameters to bimodal compositions like the D_{50} in modelling the Meuse River.

Modelling of the Meuse River

- It is advisable to incorporate in the morphological modelling of the Meuse River the abrasion process and the differential tectonic movements (uplift and subsidence).
- The downstream fining should be studied with a model that incorporates the time-dependent parameters of the equations in order to investigate its contribution. In such a model also the effect of human interference with the system, notably the river training that has fixed the river planform and has reduced the deposition width can be studied. An obvious choice for the

modelling system to be used is SOBEK Graded but this has to be extended with abrasion, break down and subsidence. Such a model study will also provide insight into the time scale of adaptation of the river to human induced changes.

- A sediment transport predictor should be developed for the Meuse River that gives an adequate description of the sediment transport phenomena, including the effect of the “history” of the flow, and which is suited to the existing sediment transport data.

Additional studies

- A special field study is needed to investigate the importance of abrasion and of break down. In this study information on the bed material composition in terms of size, petrological and mineralogical composition, particle shape and roundness should be collected.
- An additional study is needed to improve the understanding of the deposition width. This study should incorporate deposition and lateral sorting on point bars and the effect of meandering and bank erosion rates should be included. Where available also field data on floodplain composition should be used. Additional data collection might be required and possible numerical modelling, e.g. with Delft 2D/3D MOR and Graded might be included.

Bibliography

- ABBOTT, M. B. and Cunge, J. A. (1982). Engineering applications of computational hydraulics. Vol. 1. Pitman advance publishing program. United Kingdom.
- ABBOTT, P. L. and Peterson G. L. (1978). "Effects of abrasion durability on conglomerate clast populations: examples from cretaceous and eocene conglomerates of the San Diego area, California". J. Sediment. Petrol., 48(1), 31-42.
- ALONSO, A. and Garzón, G. (1994). "Quaternary evolution of a meandering gravel bed river in central Spain". Terra Nova, Vol. 6, 465-475.
- ASHIDA, K. and Michiue, M. (1971). "An investigation of river bed degradation downstream of a dam". Proc. of the XIV Congr. of IAHR, Paris, C301-C309.
- ARMANINI, A. (1991). "Longitudinal sorting in unsteady flow". Proc. of the XXIV Congr. of IAHR, Madrid, A463-A470.
- ARMANINI, A. and Arnoldi, S. (1994). "River aggradation of non-uniform grain-size: analytical approach". International workshop on floods and inundation related to large earth movements. IAHR. October 4-7, Trent, Italy. A3.1-A3.12.
- ARMANINI, A. (1995). "Non-uniform sediment transport: dynamics of the active layer". J. Hydr. Res., IAHR, 33(5), 611-622.
- BATTEY M. H. and Pring, A. (1997). Mineralogy for students. Third edition, Longman. England.
- BAYAZIT, M. (1977). "Stability of channels beds by armoring". J. Hydr. Div., ASCE, 103(7), 1119-1120. Discussion of Little and Mayer (1976).
- BHALLAMUDI, S. M. and Chaudry, M. H. (1991). "Numerical modeling of aggradation and degradation in alluvial channels. J. Hydr. Engr., ASCE, 117(9), 1145-1164.
- BEREZOWSKY, M. and Jiménez, A. A. (1994). "A simplified method to simulate the time evolution of the river bed armoring process". J. Hydr. Res., IAHR, 32(4), 517-533.
- BLATT, H., Middleton, G. and Murray, R. (1972). Origin of sedimentary rocks. Prentice-Hall. U.S.A.
- BORA, D. K., Alonso, C. V. and Prasad, S. N. (1982a). "Routing graded sediments in streams: formulations". J. Hydr. Div., ASCE, 108(12), 1486- 1503.
- BORA, D. K., Alonso, C. V and Prasad, S. N. (1982b). "Routing graded sediments in streams: applications". J. Hydr. Div., ASCE, 108(12), 1505- 1517.
- BORA, D. K. (1988). "Armoring and sorting simulation in alluvial rivers". J. Hydr. Eng., ASCE, 114(3), 344-347. Discussion of Karim and Holly (1986).
- BORA, D. K. (1989). "Scour-depth prediction under armoring conditions". J. Hydr. Eng., ASCE, 115(10), 1421-1425.
- BRADLEY, W. (1970). "Effect of weathering on abrasion of granitic gravel, Colorado River (Texas). Geol. Soc. Am. Bull., Vol. 81, 61-80.
- BREUKEL, R. M. A., Silva, W., Vuuren, W. E. van, Botterweg, J. and Venema, R. (1992). The Meuse River. Past, present and future. Rijkswaterstaat, RIZA, nota 91.052. Arnhem, The Netherlands. (In Dutch)
- BRIDGE, J. S. (1992). "A revised model for water flow, sediment transport, bed topography and grain size sorting in natural river bends". Water Resour. Res., 28(4), 999-1013.

- CAMELBEECK, T. and Meghraoui, M. (1996). "Large earthquakes in Northern Europe more likely than once thought". *EOS*, 77(42), 405-416.
- CAMELBEECK, T. and Meghraoui, M. (In press). "Geological and geophysical evidence for large palaeo-earthquakes with surface faulting in the Roer Graben (Northwest Europe). *Geophys. J. Int.*
- CHANG, H. H. (1994). "Selection of gravel-transport formula for stream modelling". *J. Hydr. Eng., ASCE*, 120(5), 646-651.
- CHIEW, Y. M. (1991). "Bed features in non uniform sediments". *J. Hydr. Eng., ASCE*, 117(1), 116-120.
- CHIN, C. O., Melville, B. W., and Raudkivi, A. J. (1994). "Streambed armoring". *J. Hydr. Eng., ASCE*, 120(8), 899-918.
- CODEL, R. B., Abt, S. R., Johnson, T. and Ruff, J. (1990). "Estimation of flow through and over armored slopes". *J. Hydr. Div., ASCE*, 116(10), 1252-1269.
- COMPTON, R. R. (1985). *Geology in the field*. John Wiley & Sons, Inc. U.S.A.
- CORREIRA, L. R. P., Krishnappan, B. G. and Graf, W. H. (1992). "Fully coupled unsteady mobile boundary flow model". *J. Hydr. Eng., ASCE*, 118(3), 476-494.
- CUI, Y., Parker, G. and Paola, C. (1996). "Numerical simulation of aggradation and downstream fining". *J. Hydr. Res., IAHR*, 34(2), 185-204.
- CUI, Y. and Parker, G. (1997). "A quasi-normal simulation of aggradation and downstream fining with shock fitting". *Intl. J. Sedim. Res.*, 12(2), 68-82.
- CUI, Y. and Parker, G. (1998). "The arrested gravel front: stable gravel-sand transitions in rivers. Part 2: General numerical solution". *J. Hydr. Res., IAHR*, 36(2), 159-182.
- CUNGE, J. A., Holly, F. M. Jr. and Verwey, A. (1980). *Practical Aspects of computational river hydraulics*. Pitman Advance Publishing program. London, U. K.
- DEIGAARD, R. and Fredsøe, J. (1978). "Longitudinal grain sorting by current in alluvial streams". *Nordic Hydrology*, Vol. 9, 7-16.
- DEIGAARD, R. (1980). Longitudinal and transverse sorting of grain sizes in alluvial rivers. Series paper No. 26. Institute of Hydrodynamics and Hydraulic Engineering, Technical University of Denmark. Denmark.
- DENNIS, J. G. (1972). *Structural geology*. John Willey & Sons, Inc. U. S. A.
- DE SITTER, L. U. (1964). *Structural geology*. Second edition. McGraw Hill, Inc. U. S. A.
- DIETRICH, W. E., Kirchner, J. W., Ikeda, H. and Iseya F. (1989). "Sediment supply and the development of the coarse surface layer in gravel-bedded rivers". *Nature*, Vol. 340, July, 215-217.
- DI SILVIO, G. and Peviani, M. (1991). "Long term equilibrium profile of mountain rivers". Proc. of the XXIV Congr. of IAHR, Madrid, A501-A510.
- DI SILVIO, G. and Marion, A. (1997). "Transfer function for the deposition of poorly sorted gravel in response to streambed aggradation". *J. Hydr. Res., IAHR*, 35(4), 563-566.
- DUIZENDSTRA, H. D., Kos, T. J. M. en Hal, L. W. J. (1994). *Bodemtransportmetingen in de Grensmaas vanaf bruggen: eerste testmetingen*. Rijkswaterstaat RIZA, werdocument 94.059X. Nederland.
- DUIZENDSTRA, H. D. and Flokstra, C. (1997). *Graded sediments in SOBEK*. Continued research 1995-1996. RIZA & Delft Hydraulics, research report Q2128. The Netherlands.

- EDELMAN, C. H. et Van Baren, F. A. (1935). La pétrographie des sables de la Meuse Néerlandaise. Mededelingen Landbouwhoogeschool 39. Wageningen, Nederland.
- FAESSEN, E. L. J. H. (1993). De morfodynamiek van de Maas: een analyse van historische kaarten. Instituut voor Ruimtelijk Onderzoek, Rapport GEOPRO 1993.02 Faculeit Ruimtelijke Wetenschappen, Vakgroep Fysische Geografie, Universiteit Utrecht. Nederland.
- FERGUSON, R. I., Hoey, T. B., Wathen, S. J., Werritty, A. and Sambrook Smith, G. H. (1995). "Downstream fining of river gravels: an integrated field, lab and modelling study". Fourth international workshop on gravel-bed rivers and the environment. Gold Bar, WA., USA.
- FERGUSON, R. I., Hoey, T. B., Wathen, S. J. and Werritty, A. (1996). "Field evidence for rapid downstream fining of river gravels through selective transport". *Geology*, 24(2), 179-182.
- FRIPP, J. B., Diplas, P. (1993). "Surface sampling in gravel streams". *J. Hydr. Eng., ASCE*, 119(4), 473-490.
- FUGRO INGENIEURSBUREAU B.V. (1996). Resultaten van the laboratoriumonderzoek, Project Zand-Maas. Ref. H-0895/01/Vde/SvD. Nederland.
- GARCIA, M. and Parker, G. (1991). "Entrainment of bed sediments into suspension". *J. Hydr. Eng., ASCE*, 117(4), 414-435.
- GARDE, R. J., Al-Shaikh Ali, K. and Diette, S. (1977). "Armoring process in degrading streams". *J. Hydr. Div., ASCE*, 103(9), 1091-1095.
- GELUK, M. C., Duin, E. J. Th., Duser, M., Rijkers, R. H. B., van den Berg, M. W. and Rooijen, P. van. (1994). "Stratigraphy and tectonics of the Roer Valley Graben". *Geologie en Mijnbouw*, 73(2-4), 129-141.
- GERRETSEN, J. H. (1968). Materiaaltransport door de Maas. Rijkswaterstaat, Directie Limburg, Afdeling Studiedienst Maas, Nota 68.8.
- GERRETSEN, J. H. (1972). Bed levels of the Meuse River. Rijkswaterstaat, Directie Limburg, Afdeling Studiendienst Mass.
- GILLULY, J., Waters, A. C. and Woodford, A. O. (1959). Principles of Geology. Second edition. W. H. Freeman & Company. U. S. A.
- GÖLZ, E. und Tipper, M. (1985). "Korngrößen, abried und erosion am Oberrhein". *DGM 29 H.4*, 115-122.
- GÖLZ, E. (1986). "Das rezente Rheingeschiebe; herkunft, transport und ablagerung". *Z. dt. Geol. Ges.*, 137, 587-611.
- GÖLZ, E. (1990). "Suspended sediment and bed load problems of the upper Rhine". *CATENA-An Interdisciplinary Journal of Soil Science-Hydrology-Geomorphology*, Vol. 17, 127-140.
- GÖLZ, E., Schröter, M. and Mikoš, M. (1995). "Fluvial abrasion of broken quartzite used as a substitute for natural bed load". *Proc. VI Intl. Symp. on River Sedimentation*, New Delhi, 387-395.
- HASSAN, M. A. and Church, M. (1994). "Vertical mixing of coarse particles in gravel bed rivers: a kinematic model". *Water Resour. Res.*, 30(4), 1173-1185.
- HELLERT, P. L. and Paola, C. (1992). "The large-scale dynamics of grain-size variation in alluvial basins, 2: Application to syntectonic conglomerate". *Basin Research*, Vol. 4, 91-102.
- HELMER, W., Klaassen, G. J. and Silva, W. (1991). Future for a gravel bed river. Rijkswaterstaat, RIZA, nota 91.0007. Arnhem, The Netherlands. (In Dutch)
- HEY, R. D., Bathurst, J. C. and Thorne, C. R. (1982). Gravel-bed rivers. Fluvial processes, engineering and management. John Wiley & Sons. U.S.A.

- HOEY, T. B. and Ferguson, R. (1994). "Numerical simulation of downstream fining by selective transport in gravel bed rivers: model development and illustration". *Water Resour. Res.*, 30(7), 2251-2260.
- HOEY, T. B. and Ferguson, R. (1997). "Controls of strength and rate of downstream fining above a river base level". *Water Resour. Res.*, 33(11), 2601-2608.
- HOLLY, F. M. Jr. and Rahuel, J. L. (1990a) "New numerical/physical framework for mobile-bed modelling. Part I: numerical and physical principles". *J. Hydr. Res., IAHR*, 28(4), 401-416.
- HOLLY, F. M. Jr. and Rahuel, J. L. (1990b) "New numerical/physical framework for mobile-bed modelling. Part II: test applications". *J. Hydr. Res., IAHR*, 28(5), 545-564.
- HOTCHKISS, R. H. and Parker, G. (1991). "Shock fitting of aggradation profiles due to backwater". *J. Hydr. Eng., ASCE*, 117(9), 1129-1144.
- HSU, S. M. and Holly, F. M. Jr. (1992). "Conceptual bed-load transport model and verification for sediment mixtures". *J. Hydr. Eng., ASCE*, 118(8), 1135-1152.
- IKEDA, H. and Iseya, F. (?). "On the length of dunes in the lower Teshio river". *Transactions of the Japanese Geomorphological Union*, 2(2), 231-238.
- IKEDA, H. (1970). "On the longitudinal profiles of the Asake, Mitaki and Utsube rivers, Mie prefecture". *Geographical Review of Japan*, 43(3), 148-159. (In Japanese, abstract in English).
- IKEDA, H. (1973). "A study on the formation of sand bars in a experimental flume". *Geographical Review of Japan*, 46(7), 435-451. (In Japanese, abstract in English).
- IKEDA, H. (1975). "On the bed configuration in alluvial channels; their types and conditions of formation with reference to bars". *Geographical Review of Japan*, 48(10), 712-730. (In Japanese, abstract in English).
- IKEDA, H. and Iseya, F. (1987). "Thresholds in the mobility of sediments mixtures". *International Geomorphology 1986, Part I*. Edited by V. Gardiner. John Wiley & Sons Ltd, 561-570.
- IKEDA, H. and Iseya, F. (1988). Experimental study of heterogeneous sediment transport. *Environ. Res. Center Papers, University of Tsukuba*, No. 12, 50p.
- IKEDA, S. and Nishimura, T. (1985). "Bed topography in bends of sand-silt rivers". *J. Hydr. Eng., ASCE*, 111(11), 1397-1411.
- IKEDA, S. and Nishimura, T. (1986). "Flow and bed profile in meandering sand-silt rivers". *J. Hydr. Eng., ASCE*, 112(7), 562-579.
- INMAN, D. L. (1949). "Sorting of sediments in the light of fluid mechanics". *J. Sedim. Petrology*, 19(2), 51-70.
- ISEYA, F. (1984). An Experimental study of dune development and its effect on sediment suspension. *Environ. Res. Center Papers, University of Tsukuba*, No. 5, 56p.
- ISEYA, F. and Ikeda, H. (1987). "Pulsations in bedload transport rates induced by a longitudinal sediment sorting: a flume study using sand and gravel mixtures". *Geogr. Ann.* 69A(1), 15-27.
- JAIN, S. C. and Park, I. (1989). "Guide for estimating riverbed degradation". *J. Hydr. Eng., ASCE*, 115(3), 356-366.
- JAIN, S. C. (1990). "Armor or pavement". *J. Hydr. Eng., ASCE*, 116(3), 436-440.
- JANSEN, P. Ph., van Bendegom, L., van den Berg, J., de Vries, M. and Zanen A. (1994). *Principles of river engineering: the non-tidal alluvial rivers*. Delftse Uitgevers Maatschappij. The Netherlands.

- KARIM, M. F. and Holly, F. M. Jr. (1986). "Armoring and sorting simulation in alluvial rivers". *J. Hydr. Eng., ASCE*, 112(8), 705-715.
- KAWAI, S. and Julien, P. Y. (1996). "Point bar deposits in narrow sharp bends". *J. Hydr. Res., IAHR*, 34(2), 205-218.
- KELLERHALS, R. and Church, M. (1977). "Stability of channel beds by armoring". *J. Hydr. Div., ASCE*, 103(7), 826-827. Discussion of Little and Mayer (1976).
- KHIN Ni Ni Thein. (1989). One-dimensional morphological modelling of graded sediments. Delft Hydraulics, Report Q697, The Netherlands.
- KLAASSEN, G. J. (1986). Morphology of armoured river beds. Experiments with flood waves. Delft Hydraulics, Report M2056, The Netherlands.
- KLAASSEN, G. J., Ribberink, J. S. and de Ruiter, J. C. C. (1988). On sediment transport of mixtures. Delft Hydraulics, Publication No. 394, The Netherlands.
- KLAASSEN, G. J. (1990). Armoured rivers during floods (literature survey). Delft Hydraulics, TOW Rivers, Report Q790, The Netherlands.
- KODAMA, Y. and Inokuchi, M. (1986). "Change in the sedimentary fabric of surface deposits along the lower course of the River Watarase". *Bulletin of the Environ. Res. Center, University of Tsukuba*, No. 10, 67-79. (In Japanese).
- KODAMA, Y. (1990). "Rate of broken round in the river bed gravels of the Azusa and the Sagae". *Bulletin of the Environ. Res. Center, University of Tsukuba*, No. 14, 109-114. (In Japanese).
- KODAMA, Y. (1992). "Effect of abrasion on downstream gravel-size reduction in the Watarase River, Japan: field work and laboratory experiment". *Environ. Res. Center Papers, University of Tsukuba*, 15, 88p.
- KODAMA, Y., Sharoni, S., Ikeda, H. and Iijima, H. (1993). "Large flume experiment on gravel particle entrainment in sandy bed rivers". *Bulletin of the Environ. Res. Center, University of Tsukuba*, No. 17, 1-18. (In Japanese).
- KODAMA, Y. (1994a). "Downstream changes in the lithology and grain size of fluvial gravels, the Watarase River, Japan: evidence of the role of abrasion in downstream fining". *J. Sedimentary Research, SEPM*, A64(1), 68-75.
- KODAMA, Y. (1994b). "Experimental study of abrasion and its role in producing downstream fining in gravel-bed rivers". *J. Sedimentary Research, SEPM*, A64(1), 76-85.
- KODAMA, Y. (1994c). "Geographical channel slope change in the lower Watarase River caused by thresholds in gravel and sand mobility". *Geographical Review of Japan*, 67A(5), 311-324. (In Japanese, abstract in English).
- KOMAR, P. D. (1987). "Selective grain entrainment by a current from a bed of mixed sizes: a reanalysis". *J. Sedim. Petrology*, 57(2), 203-211.
- KOMAR, P. D. and Carling, P. A. (1991). "Grain sorting in gravel-bed streams and the choice of particle sizes for flow-competence evaluations". *Sedimentology*, Vol. 38, 489-502.
- KRAMER, J. de. (1997). Oevererosie in de Grensmaas in het heden, verleden en de toekomst. Faculteit Ruimtelijke Wetenschappen, Vakgroep Fysische Geografie, Universiteit Utrecht. Nederland.
- KRUMBEIN, W. C. (1941). "The effects of abrasion on the size, shape and roundness of rock fragments". *J. Geol.*, Vol. 49, 482-520.

- KUENEN, P. H. (1956). "Experimental abrasion of pebbles: 2. Rolling by current". *J. Geol.*, Vol. 64, 336-368.
- KUHNLE, R. A. (1993). "Incipient motion of sand-gravel sediment mixtures". *J. Hydr. Eng., ASCE*, 119(12), 1400-1415.
- LAGUZZI, M. (1994). Modelling of sediment mixtures. Delft Hydraulics, Report Q1660, The Netherlands.
- LANE, S. N., Richards, K. S. and Chandler J. H. (1995). "Morphological estimation of the time-integrated bed load transport rate". *Water Resour. Res.*, 31(3), 761-772.
- LARONNE, J. B. and Carson, M. A. (1976). "Interrelationships between bed morphology and bed-material transport for a small, gravel-bed channel". *Sedimentology*, Vol. 23, 67-85.
- LENAU, C. W. and Hjelmfelt, A. T. (1992). "River bed degradation due to abrupt outfall lowering". *J. Hydr. Eng., ASCE*, 118(6), 918-933.
- LISLE, T. E., Iseya, F. and Ikeda, H. (1993). "Response of a channel with alternate bars to a decrease in supply of mixed-size bed load: a flume experiment". *Water Resour. Res.*, 29(11), 3623-3629.
- LISLE, T. E., Pizzuto, J. E., Ikeda, H., Iseya, F. and Kodama, Y. (1997). "Evolution of a sediment wave in an experimental channel". *Water Resour. Res.*, 33(8), 1971-1981.
- LITTLE, W. C. and Mayer, P. G. (1976). "Stability of channel beds by armoring". *J. Hydr. Div., ASCE*, 102(11), 1647-1661.
- LIU, B. Y., Ashida, K. and Egashira, S. (1991). "Sediment sorting and its simulation model in meander streams". *Proc. of the XXIV Congr. of IAHR, Madrid*, A451-A460.
- LOW, H. S. (1989). "Effect of sediment density on bed-load transport". *J. Hydr. Eng., ASCE*, 115(1), 124-138.
- LUKOVAC-BARBALIC, S. (1989). Data assessment and modelling approach for the River Meuse between Ampsin-Neuville and Borgharen. MSc. Thesis: International Institute for Hydraulic and Environmental Engineering (IHE), Delft. The Netherlands.
- LUTGENS, F. K. and Tarbuck, E. J. (1996). *Foundations of earth science*. Prentice-Hall Inc. U.S.A.
- LYN, A. D. (1987). "Unsteady sediment-transport modeling". *J. Hydr. Engr., ASCE*, 113(1), 1-15.
- MENENDEZ, A. N. (1997). "Sedimentologic modeling selection based on study scale". *J. Hydr. Eng., ASCE*, 113(10), 922-925.
- MIALL, A. D. (1996). *The geology of fluvial deposits. Sedimentary facies, basin analysis, and petroleum geology*. Springer, Italy.
- MICHA, J. C. and Borlee, M. C. (1989). "Recent historical changes on the Belgian Meuse". In: Petts, G.E., *Historical changes*.
- MIKOŠ, M. (1993). "Fluvial abrasion of gravel sediments". *Versuchsanstalt für Wasserbau, Hydrologie und Glaziologie der Eidgenössischen. Mitteilungen* 123. Technischen Hochschule Zürich.
- MIKOŠ, M. (1994). "The downstream fining of gravel-bed sediments in the Alpine Rhine River". *Lecture notes in Earth Science*, Vol. 52; *Dynamics and geomorphology of mountain rivers*. P. Ergenzinger, K. H. Schmidt (Eds.). Springer-Verlag. Heidelberg, Germany. 93-108.
- MINISTRY of Public Works. (1985). *The Belgian dams. Verviers*. Ministry of Public Works, Service de Barrages. Belgium. 55 pp.

- MOL, J. (1990). The heavy mineral composition of the lower terraces and the floodplain of the Meuse in northern Limburg. Faculty of Earth Sciences, Free University. Amsterdam, The Netherlands.
- MOSS, A. J. (1972). "Technique for assessment of particle breakage in natural and artificial environments". *J. Sedim. Petrology*, 42(3), 725-728.
- ODGAARD, J. (1984). "Grain-size distribution of river-bed armor layers". *J. Hydr. Eng., ASCE*, 110(10), 1479-1484.
- PACHECO-CEBALLOS, R. (1992). "Bed-load coefficients". *J. Hydr. Eng., ASCE*, 118(10), 1436-1442.
- PAOLA, C. (1986). "Subsidence and gravel transport in alluvial basins". In: *Frontiers in sedimentology geology*. Kleinsphn, K. L. and Paola, C. (Editors). New Perspectives in Basin Analysis. Springer-Verlag. U.S.A.
- PAOLA, C. Hellert, P. L. and Angevine, C. L. (1992). "The large-scale dynamics of grain-size variation in alluvial basins, 1: Theory". *Basin Research*, Vol. 4, 73-90.
- PAOLA, C. and Seal, R. (1995). "Grain size patchiness as a cause of selective deposition and downstream fining". *Water Resour. Res.*, 31(5), 1395-1407.
- PARK, I. and Jain, S. C. (1987). "Numerical simulation of degradation of alluvial channel beds". *J. Hydr. Eng., ASCE*, 113(7), 845-859.
- PARKER, G., Dhamotharan, S. and Stefan, H. (1982). "Model experiments on mobile, paved gravel bed streams". *Water Resour. Res.*, 18(5), 1395-1408.
- PARKER, G., and Klingeman, P. C. (1982). "On why bed streams are paved". *Water Resour. Res.*, 18(5), 1409-1423.
- PARKER, G., Klingeman, P. C. and McLean, D. G. (1982). "Bedload and size distribution in paved gravel-bed streams". *J. Hydr. Div., ASCE*, 108(4), 544-571.
- PARKER, G. and Andrews, E. D. (1985). "Sorting of bed load sediment by flow in Meander bends". *Water Resour. Res.*, 21(9), 1361-1373.
- PARKER, G. (1989). "Downstream variation of grain size in gravel rivers: abrasion versus selective sorting". *International workshop on fluvial hydraulics of mountain regions*. IAHR. October 3-6, Trent, Italy. C1-C11.
- PARKER, G. (1990). "Surface-based bedload transport relation for gravel rivers". *J. Hydr. Res., IAHR*, 28(4), 417-436.
- PARKER, G. and Sutherland, A. J. (1990). "Fluvial armor". *J. Hydr. Res., IAHR*, 28(5), 529-544.
- PARKER, G. (1991a). "Selective sorting and abrasion of river gravel. I Theory". *J. Hydr. Eng., ASCE*, 117(2), 131-149.
- PARKER, G. (1991b). "Selective sorting and abrasion of river gravel. II Applications". *J. Hydr. Eng., ASCE*, 117(2), 150-177.
- PARKER, G. (1991c). Some random notes on grain sorting. *Grain Sorting Seminar, ASCONA, Switzerland*, October 21-26, 1991.
- PARKER, G. and Cui, Y. (1998). "The arrested gravel front: stable gravel-sand transitions in rivers. Part 1: Simplified analytical solution". *J. Hydr. Res. IAHR*, 36(1), 75-100.
- PAULISSEN, P. (1973). *De morfologie en de kwartairstratigrafie van de maasvallei in Belgisch Limburg*. *Verhandelingen van de Koninklijke Vlaamse Academie voor Wetenschappen, Letteren en Schone Kunsten van België*. Jaargang XXXV, Nr. 127. België.

- PIZZUTO, J. E. (1995). "Downstream fining in a network of gravel-bedded rivers". *Water Resour. Res.*, 31(3), 753-759.
- PLUMLEY, W. J. (1948). "Black Hills terrace gravels: a study in sediment transport". *J. Geol.*, Vol. 56, 526-577.
- POSEY, C. (1977). "Stability of channels by armoring". *J. Hydr. Div., ASCE*, 103(9), 1118-1119. Discussion of Little and Mayer (1976).
- POWELL, D. M. and Ashworth P. J. (1995). "Spatial pattern of flow competence and bed load transport in a divided gravel bed river". *Water Resour. Res.*, 31(3), 741-752.
- PRESS, F. and Siever, R. (1978). *Earth*. Second edition. W. H. Freeman & Company. U. S.A.
- PRESS, F. and Siever, R. (1996). *Understanding Earth*. Third edition. W. H. Freeman & Company. U. S.A.
- RAHUEL, J. L., Holly, F. M., Chollet, J. P., Belleudy, P. J. and Yang, G. (1989). "Modeling of riverbed evolution for bedload sediment mixtures". *J. Hydr. Eng., ASCE*, 115(11), 1521-1542.
- RANA, S. A., Simons, F. B. and Mahmood, K. (1973). "Analysis of sediment sorting in alluvial channels". *J. Hydr. Div., ASCE*, 99(11), 1967-1981.
- RAUDKIVI, A. J. and Ettema, R. (1982). "Stability of armour layers in rivers". *J. Hydr. Div., ASCE*, 108(9), 1047-1057.
- REID, I. and Laronne, J. B. (1995). "Bed load sediment transport in an ephemeral stream and a comparison with seasonal and perennial counterparts". *Water Resour. Res.*, 31(3), 773-781.
- RIBBERINK, J. S. (1987). *Mathematical modelling of one-dimensional morphological changes in rivers with non-uniform sediment*. Communications on Hydraulic and Geotechnical Engineering, Report 87-2. Delft University of Technology, Faculty of Civil Engineering. The Netherlands
- RIJKS GEOLOGISCHE DIENST. Geologische kaart van Zuid-Limburg en omgeving. Afzetting van de Maas, schaal 1:50000. Nederland.
- RIJKS GEOLOGISCHE DIENST. Geologische kaart van Zuid-Limburg en omgeving. Oppervlaktekaart, schaal 1:50000. Nederland.
- RIJKS GEOLOGISCHE DIENST. Geologische kaart van Zuid-Limburg en omgeving. Pré-Kwartair, schaal 1:50000. Nederland.
- RIJKS GEOLOGISCHE DIENST. Geologische kaart van Zuid-Limburg en omgeving. Paleozoïcum, schaal 1:50000. Nederland.
- RIJKSWATERSTAAT. (1983). *Zeefkrommen Maasbodem*. Rijkswaterstaat, Directie Limburg. Nederland.
- RIJKSWATERSTAAT. (1995). *Verruimen zomerbed van de rivier de Maas. Tussen Gennep en Grave in het kader van het project zandmaas*. Bestek BDW 5098. Bijlage C, Grondgegevens. Rijkswaterstaat Directie Limburg. Nederland.
- SAIEDI, S. (1997). "Coupled modeling of alluvial flows". *J. Hydr. Eng., ASCE*, 123(5), 440-446.
- SAMBROOK SMITH, G. H. and Ferguson, R. I. (1995). "The gravel-sand transition along river channels". *J. Sedimentary Res.*, A65(2), 423-430.
- SATOFUKA, Y., Ashida, K. and Egashira, S. (1991). "Variation of sediment discharge in braided channels". *Proc. of the XXIV Congr. of IAHR, Madrid*, A41-A450.
- SCHMIT, J. C., Rubin, D. M. and Ikeda, H. (1993). "Flume simulation of recirculating flow and sedimentation". *Water Resour. Res.*, 29(8), 2925-2939.

- SCHRÖTER, M. (1994). Regularización y control de ríos. Instituto de Hidráulica, Hidrología e Ingeniería Sanitaria. Universidad de Piura, Perú.
- SCHRÖTER, M. (1995). Vergleichende untersuchung des abriebverhaltens von gebrochenem material (Taususquarzit). Angefertigt am Institut für Geologie und Paläontologie der Universität Stuttgart.
- SCHUMM, S. A. and Stevens, M. A. (1973). "Abrasion in place: a mechanism for rounding and size reduction of coarse sediments in rivers". *Geology*, Vol. 1, 37-40.
- SEAL, R. and Paola, C. (1995). "Observations of downstream fining on the North Fork Toutle river near Mount St. Helens, Washington". *Water Resour. Res.* 31(5), 1409-1419.
- SEAL, R., Toro-Escobar, C., Cui, Y., Paola, C., Parker, G., Southard, J. B. and Wilcock, P. R. (1995). "Downstream fining by selective deposition: theory, laboratory, and field observations". Fourth international workshop on gravel-bed rivers. Gold Bar, WA., USA.
- SEAL, R., Paola, C., Parker, G., Southard, J. B. and Wilcock, P. R. (1997). "Experiments on downstream fining of gravel: I. Narrow-channel runs". *J. Hydr. Eng., ASCE*, 123(10), 874-884.
- SEKINE, M. and Parker, G. (1992). "Bed-load transport on transverse slope. I" *J. Hydr. Eng., ASCE*, 118(4), 513-535.
- SHEN, H. W. and Lu, J. "Development and prediction of bed armoring". (1983). *J. Hydr. Eng., ASCE*, 109(4), 611- 629.
- SIEBEN, A. (1993). Hydraulics and morphology of mountain rivers: a literature survey. Communications on Hydraulic and Geotechnical Engineering, Report 93-4. Delft University of Technology, Faculty of Civil Engineering. The Netherlands.
- SIEBEN, A. (1994). Notes on the mathematical modelling of alluvial mountain rivers. Communications on Hydraulic and Geotechnical Engineering, Report 94-3. Delft University of Technology, Faculty of Civil Engineering. The Netherlands.
- SIEBEN, A. and Sloff, C. J. (1994). "Analysis of a 2-DH mathematical model for mountain rivers with graded sediment". International workshop on floods and inundation related to large earth movements. IAHR. October 4-7, Trent, Italy. A3.1-A3.12.
- SIEBEN, A. (1996). One-dimensional models for mountain-river morphology. Communications on Hydraulic and Geotechnical Engineering, Report 96-2. Delft University of Technology, Faculty of Civil Engineering. The Netherlands.
- SIEBEN, A. (1997). Modelling of hydraulics and morphology in mountain rivers. Communications on Hydraulic and Geotechnical Engineering, Report 97-3. Delft University of Technology, Faculty of Civil Engineering. The Netherlands.
- SINHA, S. K. and Parker, G. (1996). "Causes of concavity in longitudinal profiles of rivers". *Water Resour. Res.*, 32(5), 1417-1428.
- SLOFF, C. J. and Barneveld H. J. (1996). Morfologisch model Zandmaas. Waterloopkundig laboratorium, Rapport Q 2066. Nederland.
- SUSUKI, K. (1993). "Grain sorting of sediments". *J. Hydrosoci. and Hydr. Eng., JSCE*, Spec. issue, No. SI-2, Fluvial Hydraulics, 57-77.
- SORBER, A. and De Vaan, G. (1995). Ruimtelijke variatie van de sedimentaire structuur en textuur van de bedding van de Grensmaas (stuw Borgharen, km. 15.5 – Maaseik, km52.7). Interuniversitair Centrum voor Geo-ecologisch Onderzoek, Rapport ICG 95/3. Universiteit Utrecht. Nederland.

- SWAMEE, P. K. and Ojha, C. S. (1991). "Bed-load and suspended-load transport of nonuniform sediments". *J. Hydr. Eng., ASCE*, 117(6), 774-787.
- THERZAGHI, K., Peck, R. B. and Mesri, G. (1996). *Soil mechanics in engineering practice*. Third edition. John Wiley & Sons, Inc. New York, U.S.A.
- THIJSSSEN Drilling Company. (1995). *Grondonderzoek Grensmaas traject Borgharen – Uikhoven*. Werk nr. 95060. Rijkswaterstaat directie Limburg. Maastricht, Nederland.
- THORNE, C. R., Bathurst, J. C. and Hey, R. D. (1987). *Sediment transport in gravel-bed rivers*. John Wiley & Sons. U.S.A.
- TÖRNQVIST, T. E. (1993a). *Fluvial sedimentary geology and chronology of the Holocene Rhine-Meuse delta, The Netherlands*. Netherlands Geographical Studies, No. 166. Utrecht, The Netherlands.
- TÖRNQVIST, T. E. (1993b). "Holocene alternation of meandering and anastomosing fluvial systems in the Rhine-Meuse delta (Central Netherlands) controlled by sea level rise and subsoil erodibility". *J. Sedim. Petrology*, 63(4), 683-693.
- TÖRNQVIST, T. E., Van Ree, M. H. M. and Faessen, E. L. J. H. (1993). "Longitudinal facies architectural changes of a middle Holocene anastomosing distributary system (Rhine-Meuse delta, The Netherlands)". In: C. R. Fielding (Editor), *Current research in fluvial sedimentology*. *Sediment. Geol.*, Vol. 85, 203-219.
- TÖRNQVIST, T. E. (1994). "Middle and late Holocene avulsion history of the River Rhine (Rhine-Meuse delta, The Netherlands)". *Geology*, Vol. 22, 711-714.
- TORO-ESCOBAR, C. M., Parker, G. and Paola, C. (1996). "Transfer function for the deposition of poorly sorted gravel in response to streambed aggradation". *J. Hydr. Res., IHAR*, 34(1), 35-53.
- TSUJIMOTO, T. (1992). "Armouring, pavement and longitudinally alternate sorting." *Proc. Fifth Int. Symp. on River Sedimentation, Karlsruhe*, 653-662.
- TROUTMAN, B. (1980). "A stochastic model for particle sorting and related phenomena". *Water Resour. Res.*, 16(1), 65-76.
- VAN DEN BERG, M. W. (1994). "Neotectonics of the Roer Valley rift system. Style and rate of crustal deformation inferred from syn-tectonic sedimentation". *Geologie en Mijnbouw*, 73(2-4), 143-156.
- VAN DEN BERG, M. W., Groenewoud, W., Lorenz, G. K., Lubberts, P. J., Brus, D. J. and Kroonenberg S. B. (1994). "Patterns and velocities of recent crustal movements in the Ducht part of the Roer Valley rift system". *Geologie en Mijnbouw*, 73(2-4), 157-168.
- VAN DEN BERG, M. W. (1996). *Fluvial sequences of the Maas: a 10 Ma record of neotectonics and climatic change at various time-scales*. PhD. thesis, University of Wageningen. The Netherlands.
- VANDENBERGHE, J., Kasse, C., Bohncke, S. and Kozarski, S. (1994). "Climatic related river activity at the Weichselian-Holocene transition: a comparative study of the Warta and Maas rivers". *Terra Nova*, Vol. 6, 476-485.
- VAN DIJK, G. J., Berendsen, H. J. A. and Roeleveld, W. (1991). "Holocene water level development in The Netherlands's river area; implications for sea-level reconstruction". *Geologie en Mijnbouw*, Vol. 70, 311-326.
- VAN MANEN, G. R., Omneweer, J. G. en Van Den Berg, J.H. (1994). *Ruimtelijke variatie van de sedimentaire structuur en textuur van de bedding van de Grensmaas (stuw Borgharen, km 15.5 – Maaseik, km 52.7)*. Report GEOPRO 1994.04. Faculteit Ruimtelijke Wetenschappen, Vakgroep Fysische Geografie, Universiteit Utrecht. Nederland.
- VAN STRAATEN, L. M. J. U. (1946). *Grondonderzoek in Zuid-Limburg*; Proefschrift. Leiden, Nederland.
- VRIES, M. de. (1975). "A morphological time-scale for rivers". *Proc. of the XVI Congr. of IAHR, São Paulo*.

(also Delft Hydr. Lab. Publ. No.147).

WATERLOOPKUNDIG Laboratorium. (1981). Morfologische verschijnselen Grensmaas. Rapport R863. Nederland.

WATERLOOPKUNDIG Laboratorium. (1994). Onderzoek watersnood Maas. Deelrapporten 4, 5 en 6. Ministerie van Verkeer en Waterstaat. Nederland.

WATHEN, S. J., Ferguson, R. I., Hoey, T. B. and Werritty, A. (1995). "Unequal mobility of gravel and sand in weakly bimodal river sediments". *Water Resour. Res.*, 31(8), 2087-2096.

WEERTS, H. J. T. and Bierkens, M. F. P. (1993). "Geostatistical analysis of overbank deposits of anastomosing and meandering fluvial systems; Rhine-Meuse delta, The Netherlands". In: C. R. Fielding (Editor), *Current research in fluvial sedimentology*. *Sediment. Geol.*, Vol. 85, 221-232.

WILBERS, A. (1996). De Grensmaas over de jaren. Een onderzoek naar de morfologische veranderingen in de bedding van de Grensmaas over de periode 1978 tot en met 1995. Faculeit Ruimtelijke Wetenschappen, Vakgroep Fysische Geografie, Universiteit Utrecht. Nederland

WILCOCK, P. R. (1997). "The components of fractional transport rate". *Water Resour. Res.*, 33(1), 247-258.

WILCOCK, P. and McArdeil B. W. (1997). "Partial transport of a sand/gravel sediment". *Water Resour. Res.*, 33(1), 235-245.

WILKENS, D. H. and Lambeek, J. J. P. (1997). Bodemtransportmetingen Grensmaas. Delft Hydraulics, Rapport Q2354. Nederland.

WOLCOTT, J. (1988). "Nonfluvial control of bimodal grain-size distributions in river-bed gravels". *J. Sedim. Petrology*, 58(6), 979-984.

WÖRMAN, A. (1992). "Incipient motion during static armoring". *J. Hydr. Eng., ASCE*, 118(3), 496-501.

YATSU, E. (1955). "On the longitudinal profile of the graded river". *Transaction, American Geophysical Union*, 36(4), 655-663.

YEH, K. C., Li, S. J. and Chen, W. L. (1995). "Modeling non uniform sediment fluvial process by characteristic method". *J. Hydr. Eng., ASCE*, 121(2), 159-170.

YEN, C. L. and Lee, J. Y. (1992). "Aggradation-degradation process in alluvial channels". *J. Hydr. Eng., ASCE*, 118(12), 1651-1669.

YEN, C. L. and Lee, K. T. (1995). "Bed topography and sediment sorting in channel bend with unsteady flow". *J. Hydr. Eng., ASCE*, 121(8), 591-599.

ZAGWIJN, W. H. (1986). Nederland in het Holoceen. Rijks Geologische Dienst. Haarlem, Nederland.

ZAGWIJN, W. H. (1989). "The Netherlands during the Tertiary and the Quaternary: a case history of coastal lowland evolution". *Geologie en Mijnbouw*, Vol. 68, 107-120.

APPENDIX 1
Mathematical description of
the abrasion process

Appendix I
Mathematical description of the abrasion process

See:

Parker, G. (1991a). "Selective sorting and abrasion of river gravel. I Theory". J. Hydr. Eng., ASCE, 117(2), 131-149.

[https://doi.org/10.1061/\(ASCE\)0733-9429\(1991\)117:2\(131\)](https://doi.org/10.1061/(ASCE)0733-9429(1991)117:2(131))

APPENDIX 2
Some sediment predictors for
mixtures of sediments

1. Meyer-Peter and Müller sediment predictor formula.
 (whit hiding factor of Egiazaroff modified by Ashida and Michiue)

$$\frac{s_j}{f_j \sqrt{\Delta g D_j^3}} = 13.3 (\tau'_j - \xi_j 0.047)^{3/2}$$

$$\tau'_j = \frac{\mu R i}{\Delta D_j} \quad \text{Grain shear stress}$$

$$\mu = \left(\frac{C}{C_g} \right)^{3/2} \quad \text{Ripple factor}$$

$$C_g = 18 \log_{10} \left(\frac{12R}{D_{90}} \right) \quad \text{Grain roughness}$$

$$\xi_j = \left[\frac{\log_{10}(19)}{\log_{10} \left(19 \frac{D_j}{D_{mf}} \right)} \right]^2 \quad \frac{D_j}{D_{mf}} \geq 0.4 \quad \text{hiding factor}$$

$$\xi_j = 0.85 \frac{D_{mf}}{D_j} \quad \frac{D_j}{D_{mf}} < 0.4$$

$$D_{mf} = \Sigma f_j D_j \quad \text{Geometric mean diameter of the sediment load}$$

C : Chézy coefficient;
 R : hydraulic radius; and

2. Ackers and White sediment predictor formula.

$$G_j = \frac{s_j h}{f_j (\Delta+1) q D_j} \left(\frac{u_*}{u} \right)^{n_j} \quad \text{Dimensionless transport rate}$$

$$G_j = C_j \left(\frac{F_{grj}}{A_j} \frac{1}{\sqrt{\xi_j}} - 1 \right)^{m_j}$$

$$u_* = \sqrt{g R i} \quad \text{Shear velocity}$$

$$F_{gr} = \frac{(u_*)^n}{\sqrt{g \Delta D_j}} \left[\frac{u}{\sqrt{32} \log_{10} \left(\frac{10 R}{D_j} \right)} \right]^{1-n} \quad \text{Mobility number}$$

$$\xi_j = \left(0.4 \sqrt{\frac{D_{mf}}{D_j}} + 0.06 \right)^2 \quad \text{Day's hiding factor}$$

$$D_o = D_j \left(\frac{\Delta g}{v^2} \right)^{1/3}$$

$$D_{gr} = D_{35} \left(\frac{\Delta g}{v^2} \right)^{1/3}$$

$$1 \leq D_{gr} \leq 60$$

$$D_{gr} > 60$$

$$n_j = 1.0 - 0.56 \log_{10}(D_o)$$

$$n_j = 0.00$$

$$m_j = \frac{9.66}{D_o} + 1.34$$

$$m_j = 1.50$$

$$\log_{10}(C_j) = 2.86 \log_{10}(D_o) - (\log_{10}(D_o))^2 - 3.53$$

$$C_j = 0.025$$

$$A_j = \frac{0.23}{\sqrt{D_o}} + 0.14$$

$$A_j = 0.17$$

3. Surface based bed-load transport (Parker, 1990).

$$\frac{\Delta g s_{bj}}{\left(\frac{\tau}{\rho}\right)^{3/2} p_j} = 0.00218G(\chi) \quad \text{Dimensionless bed-load transport}$$

$$G(\chi) = 5,474 \left(1 - \frac{0.853}{\chi}\right)^{4.5} \quad \chi > 1.59$$

$$G(\chi) = e^{[14.2(\chi - 1) - 9.28(\chi - 1)^2]} \quad 1 \leq \chi \leq 1.59$$

$$G(\chi) = \chi^{14.2} \quad 1 < \chi$$

$$\chi = w \varphi_{op} \xi_j \quad \text{Dummy variable}$$

$$w = 1 + \frac{\sigma_\phi}{\sigma_{\phi_0}} (w_0 - 1) \quad \text{Straining parameter}$$

(σ_{ϕ_0} and w_0 ; see figure below)

$$\varphi_{op} = \frac{\tau_{*j}}{\tau_{*ij}} \quad \text{Dimensionless shear stress}$$

($\tau_{*ij} = 0.0386$)

$$\tau_{*j} = \frac{\tau}{\rho \Delta g D_{mp}} \quad \text{Dimensionless Shields stress}$$

($\tau = \rho g R_i$)

$$\xi_j = \alpha \left(\frac{D_j}{D_{mp}}\right)^{-\eta} \quad \text{Hiding factor}$$

($\alpha = 1.048$ and $\eta = 0.0951$ for Oak Creek data)

$$f_j = \frac{S_{bj}}{S_b} = \frac{S_{bj}}{\sum S_{bj}}$$

$$D_{mp} = \sum p_j D_j$$

- D_{mp} : mean geometric diameter of the surface layer;
- w_o : parameter (see figure below);
- σ_ϕ : standard deviation of surface size distribution on ϕ -scale
- σ_{ϕ_o} : parameter (see figure below).

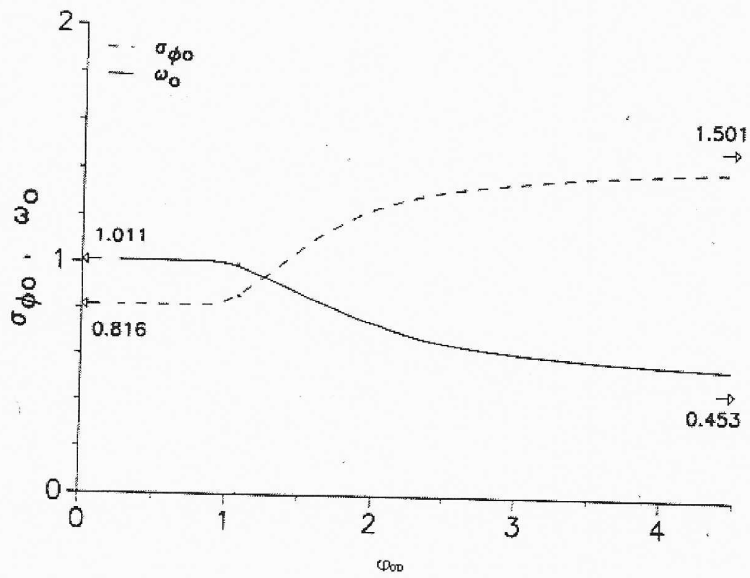
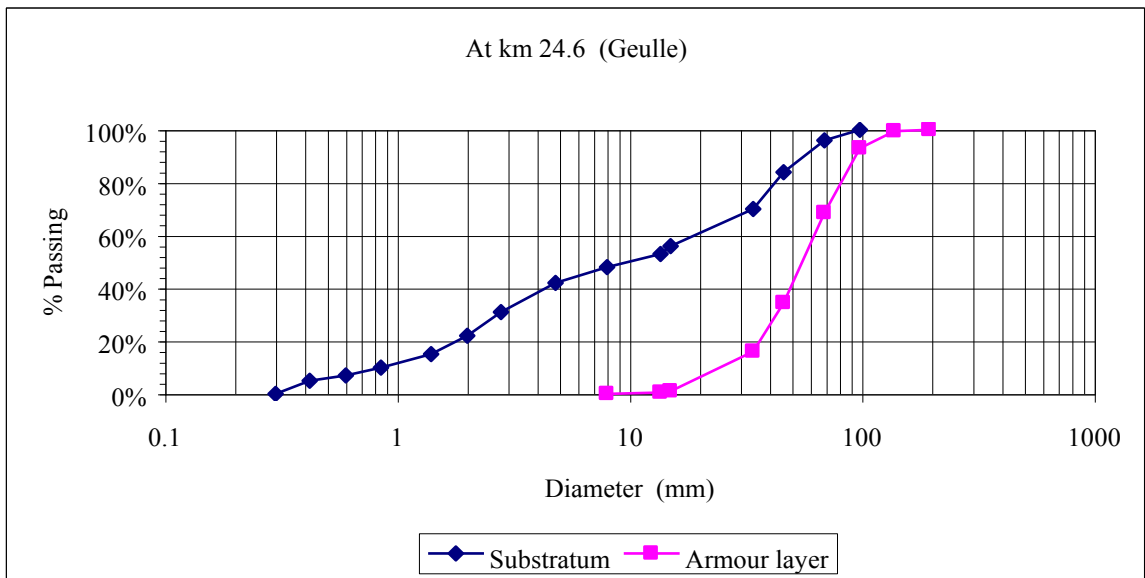
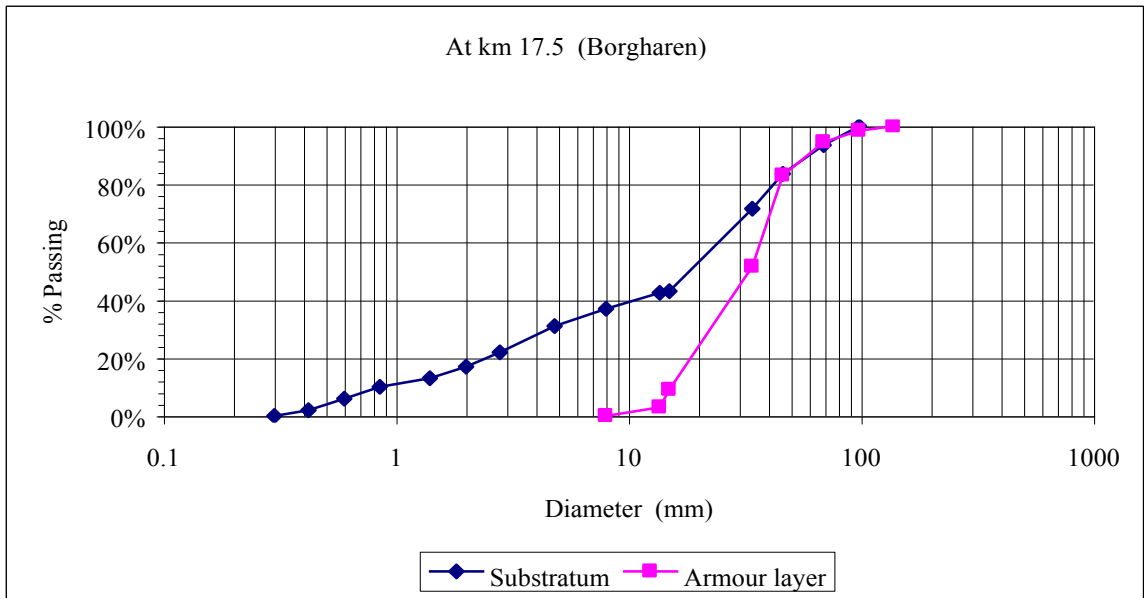
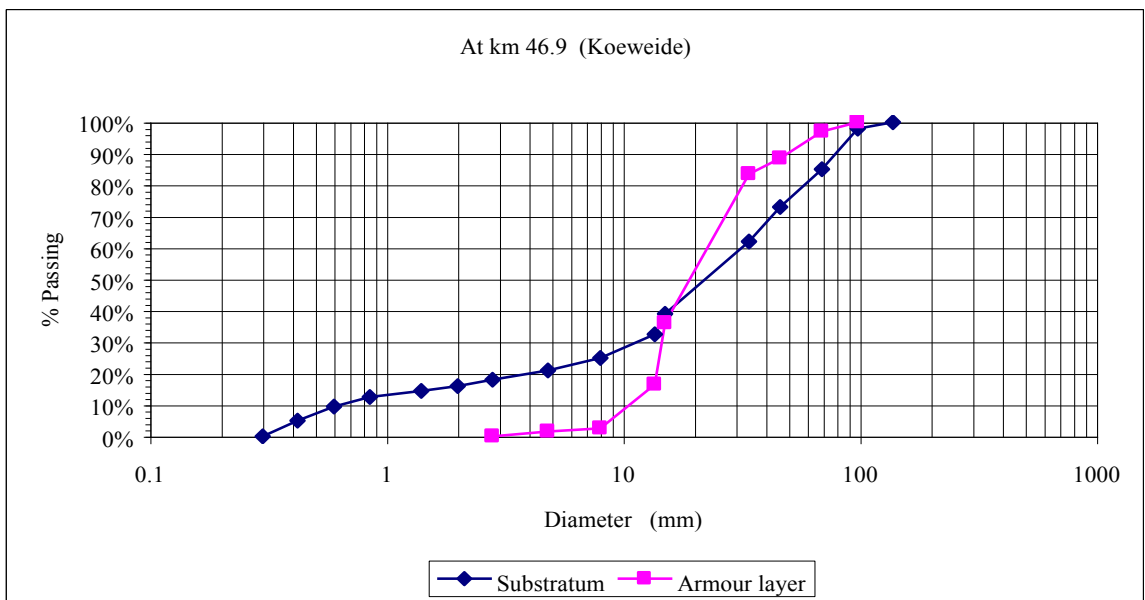
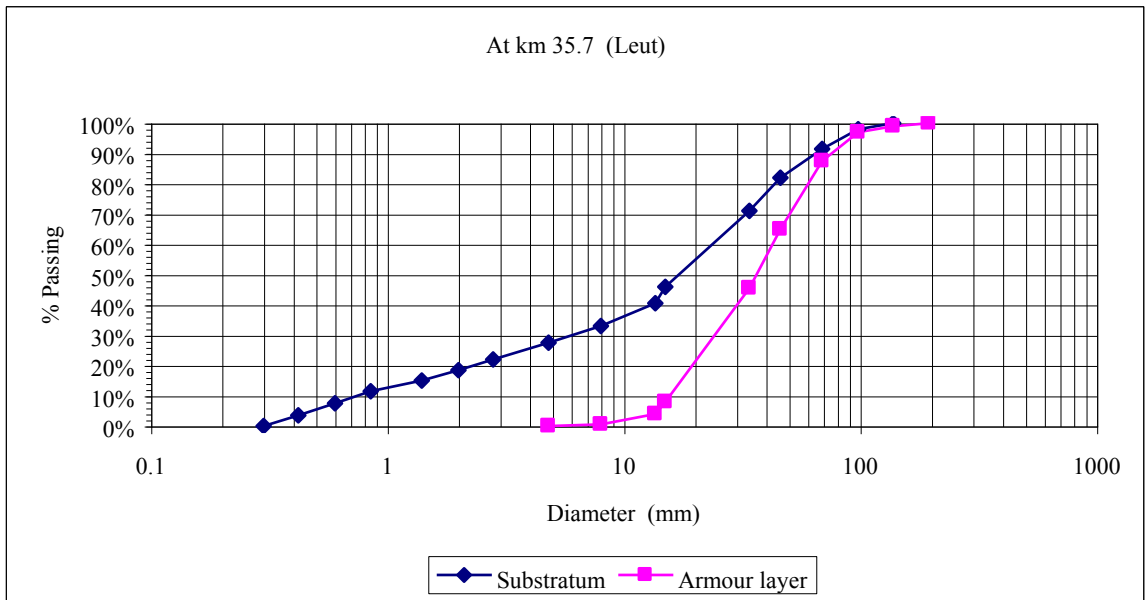
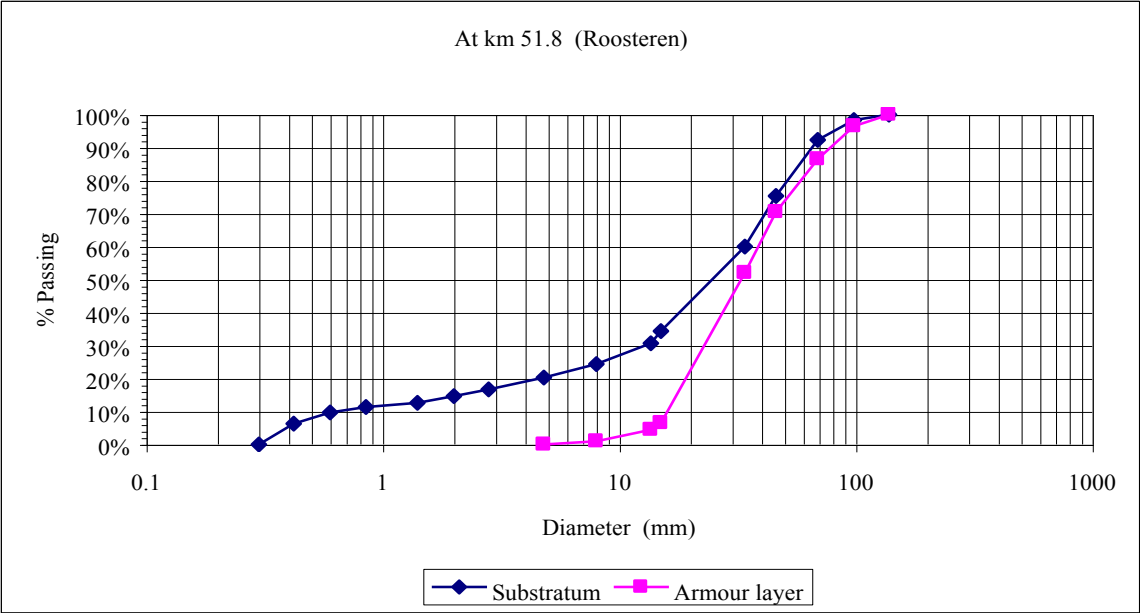


Figure. Plots of w_o and σ_{ϕ_o} versus ϕ_{op} .
Source: Parker (1990).

APPENDIX 3
Armour layer and substratum composition







APPENDIX 4
Bimodal composition of the bed material

